IEA
SOLAR R&D

INTERNATIONAL ENERGY AGENCY

programme
to develop and test
solar heating
and cooling systems

TASK IV-Development of an Insolation
Handbook and Instrument Package

DOE/NBM--2005488

DE82 005488

MASTER

# AN INTRODUCTION TO METEOROLOGICAL MEASUREMENTS AND DATA HANDLING FOR SOLAR-ENERGY APPLICATIONS

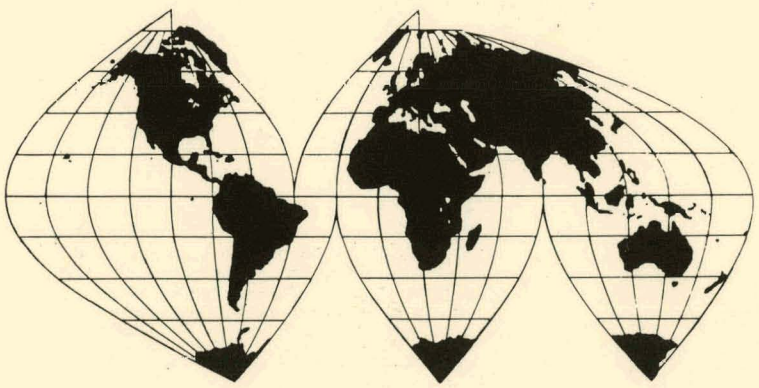



JANUARY 1980

## DISCLAIMER

# AN INTRODUCTION TO METEOROLOGICAL MEASUREMENTS AND DATA HANDLING FOR SOLAR ENERGY APPLICATIONS

International Energy Agency

Programme to Develop and Test Solar Heating and Cooling Systems

TASK IV



January 1980

# PREFACE

Recognizing a need for a coordinated approach to resolve energy problems, certain members of the Organization for Economic Cooperation and Development (OECD) met in September 1974 and agreed to develop an International Energy Program. The International Energy Agency (IEA) was established within the OECD to administer, monitor and execute this International Energy Program.

In July 1975, Solar Heating and Cooling was selected as one of the sixteen technology fields for multilateral cooperation. Five project areas, called tasks, were identified for cooperative activities within the IEA Program to Develop and Test Solar Heating and Cooling Systems. Recognizing the importance of resource information, two of the five tasks within the program were designated as meteorological support tasks for solar heating and cooling research and applications. The five tasks and the respective operating agents (lead country responsible for the task) are:

I. Investigation of the Performance of Solar Heating and Cooling Systems – Denmark.

II. Coordination of R & D on Solar Heating and Cooling Components – Japan.

III. Performance Testing of Solar Collectors – Germany.

IV. Development of an Insolation Handbook and Instrument Package – United States.

V. Use of Existing Meteorological Information for Solar Energy Application – Sweden.

This report is one of two products of Task IV.

The objective of Task IV was to obtain improved basic resource information for the design and operation of solar heating and cooling systems through a better understanding of the required insolation (solar radiation) and related weather data, and through improved techniques for measurement and evaluation of such data.

At the February 1976 initial experts meeting in Norrköping, Sweden, the participants developed the objective statement into two subtasks:

1. An Insolation Handbook

2. A Portable Meteorological Instrument Package.

This handbook is the product of the first subtask. The objective of this handbook is to provide a basis for a dialogue between solar scientists and meteorologists. Introducing the solar scientist to solar radiation and related meteorological data enables him to better express his scientific and engineering needs to the meteorologist; and introducing the meteorologist to the special solar radiation and meteorological data applications of the solar scientist enables him to better meet the needs of the solar energy community.

To achieve the objective, papers have been contributed by members of the task and by invited guest solar scientists and meteorologists. These contributions have received peer review within the solar energy engineering and meteorological professions. Every effort has been made to serve not only the solar heating and cooling reasearch and applications data requirements but also the general solar energy community's meteorological data needs.

M. R. Riches, Chairman
Task IV

## ACKNOWLEDGEMENTS

Many individuals within the IEA and outside the IEA have contributed significantly to this Handbook. It is impossible to name them all. Therefore, on behalf of Task IV participants, I express sincere appreciation for your efforts and thank you for your contributions.

I would like to recognize E. A. Carter and his staff at the Kenneth E. Johnson Environmental and Energy Center of The University of Alabama in Huntsville for coordinating the final drafts and the reviews. Without their efforts no handbook could have been produced.

I would also like to acknowledge T. K. Won and E. J. Truhlar of the Canadian Atmospheric Environment Service for arranging and managing the final editing. This effort has turned a collection of excellent papers into a useful handbook.

I extend a special thank you to the authors and the Task participants. I know that much of your effort was an additional burden placed on top of an already demanding work load.

M. R. Riches

## Contributing Organization and Experts

### Participants

The Government of Belgium

The National Research Council of Canada

The Commission of the European Communities

The Kernforschungsanlage, Jülich, Germany

The Consiglio Nazionale delle Ricerche, Italy

The Stichting Energionderzoek Centrum, Nederland

The Ministerio de Industria (Centro de Estudios de la Energia), Spain

The Office Federal de l'Economie Energetique, Switzerland

The United States Department of Energy

### National Contact Persons

Belgium
Dr. D. Crommelynck
Institute Royal Meteorologique
Avenue Circulaire 3
1180 Bruxelles

Canada
Mr. T. K. Won
Climatological Service Division
Atmospheric Environment Service, DOE
4905 Dufferin Street
Toronto, Ontario M3H 5T4

European Commission
Dr. E. Aranovich
European Commission
Joint Research Center Euratom
Ispra, Italy

Germany (Federal Republic)
Dr. F. A. Peuser
Projektleitung Energieforschung
Kernforschungsanlage Julich GmbH
Postfach 1913
D-5170 Jülich

Italy
Professor R. Visintin
Universitia degli Studi de Calabria
Dipartimento de Fisica
Cosenza

Netherlands
Dr. M. H. De Wit
University of Technology
Department of Architecture, Building and Planning
P.O. box 513
5600 MB Eindhoven

Spain
Mr. L. Nadal
Inst. Nacional de Technica Aerospacial
Torrejon de Ardoz
Madrid

Switzerland
Dr. P. Valko
Swiss Meteorological Institute
Krahbuhlstrasse 58
CH-8044 Zurich

United Kingdom
Mr. B. R. May
U. K. Meteorological Office
Room T21
Met. 01 Eastern Road
Bracknell, Berkshire RG12 2UR

United States of America (Operating Agent)
Mr. M. R. Riches
U. S. Department of Energy
Office of Energy Research
ER-14
Mail Stop J309
Washington, DC 20545

**Invited Guest Scientists**

Dr. M. Bruck
Solar Energy Division
Austrian Solar and Space Agency
Garnisongosse 7
A-1180 Wien
Austria

Mr. R. Dogniaux
Institute Royal Meteorologique de Belgique
3 Avenue Circulaire
B-1108 Brussels
Belgium

Mr. J. R. Latimer
Atmospheric Environment Service
4905 Dufferin Street
Downsview, Ontario
Canada M3H ST4

Dr. H. Lund
Thermal Insulation Laboratory
Technical University of Denmark
Building 118
DK-2800 Lyngby
Denmark

Dr. C. Gandino
EEC Meteorological Observatory
I-21020-Ispra
Italy

Dr. K. Dehne
Meteorologisches Deutscher Wetterdienst
Observatorium Hamburg
Frahmredder 95
D-2000 Hamburg 65
Germany

Dr. J. W. Gruter
KFA - IKP
PB 1913
D-517 Jülich
Germany

Dr. H. Karl
Institut for Theorie der Electroteknik
Breitscheidstrasse 3
D-7000 Stuttgart
Germany

Dr. F. Vivona
Instituto de Fisica dell'Atmosfera
Consiglio Nazionale Richerche
Progetto Energetica
Via Nizza 128
00198 Roma
Italy

Dr. T. Sunami
Solar Energy Division
Sunshine Project Promotion Headquarters MITI
1-3-1 Kasumigaseki
Chiyoda-ku, Tokyo
Japan

Dr. L. Dahlgren
Weine Josefsson
SMHI Box 923
S-601 19 Norrköping
Fack, Sweden

Dr. B. Leckner
Department of Energy Conversion
Chalmers University of Technology
S-402 Gotcborg
Sweden

Mr. A. J. Frantzen
Royal Netherlands Meteorological Inst.
Wilhelmina 10, DeBilt
The Netherlands

CONTENTS

## LIST OF FIGURES

## LIST OF TABLES

CHAPTER 1

# THE SOLAR ENERGY SCIENTIST AND HIS METEOROLOGICAL DATA NEEDS

M. R. Riches
Office of Energy Research
United States Department of Energy
Washington, D. C. 20545
The United States of America

## 1.1 The Problem and Objective

Assessing the solar radiation resource for solar energy applications is a multifaceted problem. The basic questions that must be answered to solve this problem are:

- Who are the end users and what meteorological parameters must be measured for them?
- What must be the data quality to meet user requirements (where quality includes accuracy, precision, and frequency of measurements, coupled with their geographic distribution and format of presentation)?
- What alternatives to measurement exist?
- What data are available and can these data be developed into a quality data set?

These questions overlap, and must be considered together. But the key to assessing solar energy potential is identification of the user community and—above all—its needs.

The objective of this section is to identify the user, define the meteorological parameters that must be measured, and introduce the quality requirements of the user. Subsequent sections and chapters of this Handbook will address (a) statistical analysis of the data, (b) geographic distribution, (c) format presentation, (d) alternatives to measurement, and (e) existing data sources.

## 1.2 The User

The solar radiation data user community can be classified in many ways: e.g., solar electrical and solar thermal systems, concentration ratio, or other application specific schemes. An example of solar thermal systems is provided in Figure 1-1, where solar thermal applications are classified according to temperature requirements for end use. The temperature requirements specify the concentration ratio: the latter is used to specify the solar radiation sensor requirements.

The classification scheme selected here divides the user community into two basic groups:

- The Researcher, and
- The Designer.

The Researcher is interested primarily in advanced solar energy applications and works at obtaining a better understanding of the physical and biological relationships between the applications and solar radiation. This includes the design of new systems and the adoption of known technologies for new applications in terms of use and geographic location. It should be noted that many of the solar energy researcher's basic data needs will be similar to those of other Earth scientists.

The Designers of solar energy systems are defined as those who plan, design and operate solar energy systems in settings other than a Research and Dev-

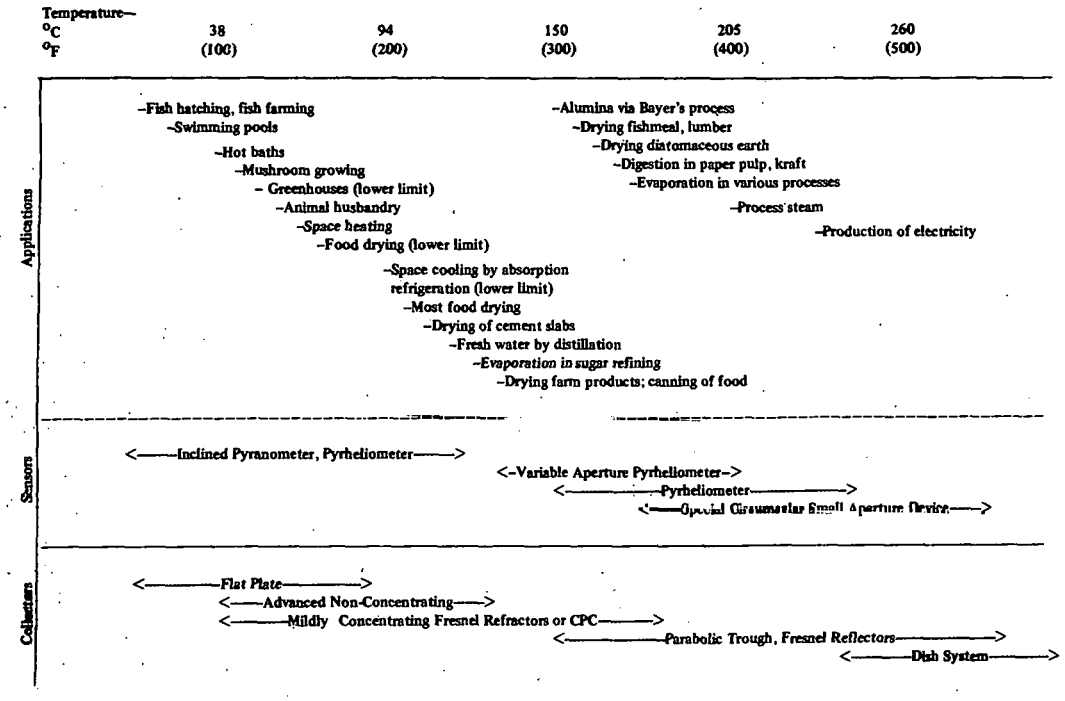


*Figure 1-1 Required temperatures for various solar thermal applications (After Hoffman and Rapp, 1976)*

elopment (R & D) mode. This group includes a wide range of engineers, chemists, biologists, as well as system owners, bankers, insurance agents.

### 1.3 Data Needs

The basic meteorological data required for solar energy applications are relatively few: air temperature, dew point (or relative humidity), wind velocity, and appropriate solar radiation data. For research and design activities, data requirements for solar energy applications are summarized in Table 1-1a and Table 1-1b. Specific network suggestions for meteorological measurements related to the users are discussed in the Appendix to this chapter. The specifications for a portable meteorological package proposed by IEA Task IV are shown in Table 1-2 (see references).

The Researcher requires sample, short-term, detailed data sets of the highest accuracy. These data include spectral content of the diffuse, direct, and reflected solar radiation as well as detailed, collateral knowledge of the atmosphere including hazard information. This information may then be used to predict a system component performance, to analyze the actual performance, to investigate optimization schemes, and to develop simplified models (both atmospheric and system design). Additionally, the research data base provides a limited data base (geographically) for future unanticipated uses.

The Designer requires limited research data, synoptic scale data sets, and data estimation and extension techniques. The Designer generally uses products of the Researcher, the national weather services and private data sources. Here the specific data include global, direct and non-horizontal solar radiation data, the principal meteorological parameters, and hazard information (hail, snow and wind loads, lightning, etc.). The Designer then may use this information to optimize and evaluate systems, to perform market analyses, and to plan monitoring sites for large scale applications. His principal concern is that these data are of the quality required for specific applications. That particular quality ranges from on-site and near-research quality for large applications to validated solar radiation models and collateral meteorological data for solar domestic heating, hot water, and cooling applications.

Table 1-1a

Solar Radiation Data Requirements for Research

| Research Activity | Data Required |
|---|---|
| **Solar Heating and Cooling of Buildings; and Agricultural and Industrial Process Heat Systems** | |
| • Active Systems (e.g., Flat Plate and Evacuated Tubes) and Passive Systems | Several typical and extreme sample, short term detailed data sets of high quality non-horizontal (including vertical surfaces) and direct beam solar radiation data, IR, UV, albedo and other spectral data for heat loss, materials reliability and selective surface studies; sample micrometeorological studies to assess special design problems and unique solar applications, sample data at short time intervals (1 min) for special systems studies, detail atmospheric data. |
| • Active Concentrating Systems | As above; sample circumsolar data for CPC[1], Fresnel lens, etc., systems studies. |
| **Photovoltaic Applications** | |
| • Non-Concentrating Systems | As for solar heating and cooling with more stress on spectral information, including spectral diffuse and direct. |
| • Concentrating | As above, with more stress on direct beam data including spectral circumsolar information. |
| **Solar Thermal Electric Systems** | |
| • Distributed Systems (e.g., water pumping) | As solar heating and cooling, with stress on direct beam and circumsolar data. |
| • Large Scale Power Systems | As above. |
| **Biomass Production (e.g., plantations)** | Spectral quality of total radiation in sample climate regions for systems modeling. |

[1] Compound Parabolic Collector

Table 1-1b

Solar Radiation Data Requirements for Design Applications

| Design Activity | Data Required |
|---|---|
| **Solar Heating and Cooling of Buildings; and Agricultural and Industrial Process Heat Systems** | |
| • Active and Passive Systems | The same research data set; models to extend global, direct and non-horizontal data; synoptic scale global, direct, and non-horizontal measured data; meteorological data such as temperature, dew point, wind speed and direction, hail frequency, lightning frequency, etc.; standard year data sets; data atlas including monthly means, frequency statistics, etc., including solar and other meteorological variables; data at hourly intervals. |
| • Active Concentrating Systems | As above; circumsolar data included in model data sets, atlas and standard year data summaries, increased stress on direct beam. |
| • Site Specific Application (Active) | For large scale or unique systems, special site specific data and specially tailored data sets, such as cloud frequency data, seasonal measured data to test applicability of models (highly project specific). |
| Photovoltaic Applications | As solar heating and cooling, more stress on spectral in data included in summaries; site specific data at large scale power plants for design refinement. |
| Solar Thermal Electric Systems | Same as solar heating and cooling with increased need for direct beam solar radiation data; site specific data for large scale power plants. |
| Biomass Production | As for photovoltaic applications. |

### 1.4 Summary of User Data Requirements

By dividing the solar energy community into these two groups–Researcher and Designer–it can be seen that meteorological data requirements for solar energy are similar to the needs for most other geo-scientists. Increased awareness of the requirements, initiation or modification of research programs, and some additions to the existing meteorological networks will be necessary to respond to the requirements. By increasing the dialogue between meteorologist and solar engineers these changes can be achieved and at the same time the solar engineer can be provided with the skills required for special site specific studies.

Table 1-2

Final Specifications for a Portable Meteorological Instrument Package

| Item | Accuracy(1) | Precision(2) | Time of Integration |
|---|---|---|---|
| Direct (Normal Incidence) | ±5% or ±25 W $m^{-2}$(3) | 2% | 10 min continuous(4) |
| Global (Direct plus diffuse) | ±5% or ±25 W $m^{-2}$(3) | 2% | |
| Solar on Inclined Surface | ±5% or ±25 W $m^{-2}$(3) | 2% | |
| Incoming IR (Inclined) | ±10% or ±25 W $m^{-2}$(3) | 2% | |
| Output of an Inclined Solar Cell (Opt.) | ---------- | ---- | |
| Air Temperature | ±1.0°C(5) | ±0.5°C(5) | |
| Wind Speed | ±1 m $s^{-1}$ or ±5%(3) | ±0.5 m $s^{-1}$ | |
| Wind Direction | ±10° | ±5° | |
| Humidity (Opt.) | ---------- | ---- | |

1 Mean values when in absolute units related to a standard
2 Reproducability of the instrument
3 Whichever is the largest
4 Other integration times optional
5 Higher accuracy or precision optional

Notes:
- Recording method optional
- Record: Date, time, station identity, electronic calibration reference
- Battery takeover for clock, no other power specifications
- Final data output in SI units (from computer processing or possible unit itself)
- Must have a "jack" for on-station data readout equipment

## PART 2

# HANDBOOK USER GUIDELINES

### 1.5 Purpose

Part 2 of this introduction is to guide the reader to related portions of the handbook. Because individual topics have been addressed by different authors, similar general topics may be described in more detail in different chapters, but this may not be readily apparent to the reader. Also some topics are treated in detail for the atmospheric scientist which may be beyond the needs of the engineer and user of the information. This guide portion is intended to help the engineer select the topics for specific applications.

### 1.6 Sun, Earth and Atmosphere

Chapter 2 contains a comprehensive description of the sun-earth relationship which is useful in understanding the variation between local time and solar time and the radiation available for various collector types (flat plate and concentrating) and collector orientation. Applications of the principles may be found in Chapter 3, Section 3.5 and Chapter 4, Section 4.5. The atmospheric effects on the radiation available are described in Chapter 3; specific details of turbidity and precipitable water, in Chapter 8. The methods of measuring the atmospheric variables related to solar energy are described in Chapter 10.

### 1.7 Types of Radiation

The types of solar radiation measurement methods including all spectral ranges, are discussed in Chapter 4, i.e., global (horizontal), direct (suntracking), diffuse (sky radiation) and radiation available to typical flat-plate collectors at various orientations and locations. Spectral characteristics are defined in Chapter 2 and discussed in detail, including measurement techniques, in Chapter 5. Infrared radiation (wavelength approximately 1 to 100 micrometers, $\mu$m) is introduced in Figure 2-7. Chapter 6 describes loss of heat in infrared wavelengths to night sky. Circumsolar diffuse radiation (the forward scattering of the sunlight in the atmosphere resulting in the bright glare within about a 5 deg conical angle around the disc of the sun) and its relation to solar concentrators, is described in Chapter 7. Applications of solar radiation to collecting solar energy are described by Patel (1979).

### 1.8 Relationship of Clouds and Available Solar Radiation

Clouds and their accompanying weather are the most significant atmospheric phenomena restricting the availability of solar radiation at the surface of the earth. There is certainly a relationship between cloud observations and solar radiation measurements, but due to variations in cloud types, amounts and heights, a close relationship has been elusive. Therefore, the duration of sunshine derived from cloud observations provides only a rough estimate of solar radiation (see Chapter 10, Section 10.5.1). The measurement of the duration of sunshine is more closely related to the solar energy available. Chapter 9 treats the instruments for measuring the duration of sunshine; Chapter 8 addresses statistically the effect of short period fluctuations of sunshine on the useable solar energy and Chapter 10 provides a mathematical means of estimating solar radiation from the ratio of sunshine received to that available.

### 1.9 Albedo or Reflectance

The albedo or reflectance of natural and man-made surfaces is discussed in Chapter 3, Section 3.6. Appendix II, Table 3, provides specific ground reflectance values for various surfaces.

## 1.10 Units and Symbols

The Task IV endorses the units and symbols proposed in *Solar Energy* (Beckman, 1978) and a partial list is shown here in Tables 1-3, 1-4, 1-5 and 1-6. All authors may not have used these symbols in their manuscripts. Conversions to these recommended symbols and units were made or are indicated where possible.

## 1.11 Condensed Glossary

A condensed glossary of some of the most common terms used in the applications of solar energy are included in Appendix I-B to this chapter.

## 1.12 Bibliography

A bibliography of general purpose books and reports for solar energy applications follows the references to this chapter. The membership of Task IV of IEA contributed to this bibliography so that books from most countries would be included. The list, of course, is not complete and is intended as examples of books which may lead to additional references. The IEA assumes no responsibility for the completeness or usefulness of the information nor does it endorse any of the books.

Table 1-3

Recommended Symbols for Radiation Quantities

| Preferred Name | Symbol* Solar Energy | Unit Solar Energy |
|---|---|---|
| radiant energy | Q | J |
| radiant flux | $\Phi$ | W |
| radiant flux density | $\phi$ | $W\,m^{-2}$ |
| irradiance | E | $W\,m^{-2}$ |
| radiosity or radiant exitance | M | $W\,m^{-2}$ |
| radiant emissive power or radiant self-exitance | $M_s$ | $W\,m^{-2}$ |
| radiant intensity or radiance | L | $W\,m^{-2}\,sr^{-1}$ |
| irradiation or radiant exposure | H | $J\,m^{-2}$ |
| Solar Radiation on Insolation | | |
| global irradiance or solar flux density | G | $W\,m^{-2}$ |
| beam irradiance | $G_b$ | $W\,m^{-2}$ |
| diffuse irradiance | $G_d$ | $W\,m^{-2}$ |
| global irradiation | H | $J\,m^{-2}$ |
| beam irradiation | $H_b$ | $J\,m^{-2}$ |
| diffuse irradiation | $H_d$ | $J\,m^{-2}$ |
| Atmospheric Radiation | | |
| irradiance | $\phi$ | $W\,m^{-2}$ |
| radiosity | $\phi$ | $W\,m^{-2}$ |
| exchange | $\phi_N$ | $W\,m^{-2}$ |

*Subscript s - solar (or short wave); subscript t - thermal (or long wave); subscript b - beam (direct); subscript d - diffuse (scattered); subscript N - net radiation (global and terrestrial).

Table 1-4

Recommended Symbols* for Radiation by Materials

The emission, absorption, reflection and transmission of radiation by materials are described in terms of quantities where suffixes, either *"ance"* or *"ivity"*, have been used to distinguish between different approaches to the definition of the phenomena. But each discipline appears to attach a different definition to each suffix.

Here the suffix *"ance"* is used for the four dimensionless quantities defined as follows:

emittance $\varepsilon = \frac{E}{E_b}$ (or $\frac{M_s}{M_{sb}}$);

reflectance $\rho = \frac{\phi}{\phi_i}$;

absorptance $\alpha = \frac{\phi'}{\phi_i}$;

transmittance $\tau = \frac{\phi_t}{\phi_i}$,

where $E$ and $\phi$ are the radiant flux densities that are involved in the particular process. As these are the quantities that are measured for most surfaces used in solar equipment, it is sufficient to recommend these names.

The use of $\alpha$ for absorptance and diffusivity is common, as is the use of $\rho$ for reflectance and density of matter. Neither case should cause confusion.

*Subscript s = solar; subscript b = beam; subscript i = incident.

Table 1-5

Recommended Subscripts

| Subscripts | Definition |
|---|---|
| a | ambient |
| b | black body |
| b | beam (direct) |
| d | diffuse (scattered) |
| h | horizontal |
| i | incident |
| n | normal |
| o | outside atmosphere |
| r | reflected |
| s | solar |
| sc | solar constant |
| ss | sunrise (sunset) |
| t* | total |
| t, th | thermal |
| u | useful |
| λ | spectral |

*The need for a subscript for total radiation is not great as the recommendation suggests that global irradiance, i.e., the sum of beam and diffuse irradiance, be unsubscribed.

Beckman (1978)

Table 1-6

Additional Symbols Used in This Handbook

| Symbol | Definition | Units |
|---|---|---|
| $I$ | Normal incident beam irradiance | W $m^{-2}$ |
| $\Theta$ | Zenith angle | deg |
| $90 - \Theta$ | Elevation angle | deg |
| $i$ | Angle of incidence | deg |
| $\phi$ | Latitude | deg |
| $\omega$ | Hour angle | deg |
| $\delta$ | Declination angle | deg |
| $\gamma$ | Solar azimuth angle | deg |
| $\psi$ | Azimuth angle of inclined surface | deg |
| $s$ | Slope of inclined surface | |
| $w$ | Precipitable water | cm |
| $\beta$ | Ångström turbidity coefficient ($\beta = 0.935\ B$) | |
| $B$ | Schüepp turbidity coefficient | |

## References


Beckman, W. A., et al. 1978. "Technical Notc, Units and Symbols in Solar Energy." *Solar Energy*. No. 21, pp. 65-68. Pergamon Press, Ltd.

Hoffman, A. A. J. and Rapp, D. 1976. *A Classification of Solar Energy Techniques and Uses by Temperature Range.* Unpublished report to the United States Energy Research and Development Administration (now U. S. Department of Energy).

International Energy Agency. *The International Energy Agency Portable Meteorological and Solar Radiation Instrument Package and Solar Radiation Instrument Package Guidelines: Their Demonstration – A Final Report by Task IV.* International Energy Agency. Program to Develop and Test Solar Heating and Cooling Systems. (To be published.)

Patel, A. M. 1979. *Examples of Solar Radiation Data and Applications for Solar System Design.* UAH Technical Note 79-2. The University of Alabama in Huntsville.


## Bibliography


Anderson, G. and Riordan, M. *The Solar Home Book (Heating, Cooling and Designing With the Sun).* Cheshire Books, Harrisville, NH, U. S. A.

Battelle Centre de Recherche de Genève. 1976. *Etude relative à l'utilisation de l'énergie solaire pour la production d'électricité dans les Alpes, Rapport de synthèse pour la Commission Fédérale de la Conception global de l'energie.* Battelle, Bern, Switzerland. p. 45.

Battelle Centre de Recherche de Geneve. 1976. *Etude relative a l'utilisation de l'energie solaire pour la production d'electricite dans les Alpes, Annexes techniques pour la Commission Federale de la conception globale de l'energie.* Battelle, Bern, Switzerland. p. 133.

Beckman, W. A., Klein, S. A. and Duffie, J. A. 1977. *Solar Heating Design by the F-Chart Method.* John A. Wiley & Sons. Inc.

Braunlich, G. 1975. *Moglichkieten zur Nutzung der Sonnenenergie in Oesterreich, Grundlagen, Forsuhungszentrum Graz, ifu Veroffentlichung.*

Building Services Research and Information Association. *Heat and Power from the Sun - an Annotated Bibliography.* Building Services Research and Information Association, Bracknell, United Kingdom.

Caratsch, M. 1976. *Heizen mit Sonnenenergie.* Techn. Rd. Sulzer 4, 1976. p. 151-157.

Curtis, E. J. W. *Solar Energy Applications in Architecture.* Medical Architecture Research Unit. Department of Environmental Design, Polytechnic of North Holloway Road, London N7.

Duffie, J. A. and Beckman, W. A. 1974. *Solar Energy Thermal Processes*. John A. Wiley & Sons, Inc.

Duppenthaler, A. 1977. *Die Berechnung des Bruttowärmeertrages von Solarkollektoren. Part I and II.* Internal Report TM-IN-670, Swiss Federal Institute for Reactor Research, Wurenlinger, pp. 34-55.

Faist, M. A., et al. 1978. *Application de l'énergie solaire aux bâtiments.* SIA, EPF-Lausanne, Genève, Switzerland.

Howell, D. *Your Solar Energy Home.* Oxford: Pergamon Press. (United Kingdom)

Howell, Yvonne and Berry, Justin A. *Engineers' Guide to Solar Energy.* Solar Energy Information Services, P. O. Box 204, San Mateo, California 94401, U. S. A.

Institution of Heating and Ventilating Engineers. *The IHVE Guide A6 (Solar Data) Published by the Institution of Heating and Ventilating Engineers.* 49 Cadogan Square, London, SW1X OJB., U. K.

Kesselring, P. and Duppenthaler, Al. 1979. *The Layout of Solar Hot Water Systems, Using Statistical Meteo- and Heat Demand Data.* Reprint, p. 6, ISES Congress, Atlanta, GA, U.S. A., May June, 1979.

McCartney, Kevin. 1978. *Practical Solar Heating.* United Kingdom: Prism Press.

McVeigh, J. C. and Schumacher, D. C. 1978. *Going Solar.* Natural Energy Association, Kingston-Upon-Thames, U. K.

Rist, M. Dr. 1979. *Direkte und Indirekte Nutzung der Sonnenergie in der Landwirtschft.* Premier Symposium sur la recherche et le développment en énergy solaire en Suisse organisé par l'école polytechnique fédéral de Lausanne, Switzerland, pp. 1-7.

Robotti, A. 1977. *L'impigeo dell'energia solare.* UTET, Torino, Italy.

Sabady, P. 1977. *The Solar House.* Newnes-Butterworths, Borough Green, Sevenoaks, Kent, U. K.

Santarini, E. 1977. *It Clima Come Elemento Di Progetto Nella Edilzia.* Liguori, Napoli, Italy.

Schmid, CH. H. 1977. *Die Nutzbare Wärme von Flachkollektoren.* IV, Symposium SSES, Biel, 21.1.1977, p. 176-191.

SOLOREX Corp. *The SOLAREX Guide to Solar Electricity.* SOLOREX Corp., U. S. A.

Zogg, M. 1977. *Warmwasserbereitung mit Sonnenenergy.* Blaue TR-Reihe, Heft 128, Technische Rundschau, Bern, Switzerland, p. 92.

Appendix I-A

# GENERAL AND RESEARCH METEOROLOGICAL MEASUREMENTS FOR SOLAR ENERGY APPLICATIONS

**Prepared for**

**The World Meteorological Organization**
**Geneva, Switzerland**
**October 1978**

**M. R. Riches**

## 1-A.1 General Network Measurements

### The Parameters -

The conventional meteorological data to supplement solar radiation data required for solar energy applications are relatively few, vis., air temperature, dew point (or relative humidity) and wind velocity, are required. Hourly values, which are taken at most principal meteorological stations, satisfy this need. The solar radiation parameters required are listed in Table A-1; including their priorities, measurement frequencies, and accuracies. The precision in all cases, is suggested to be ±2%.

It is recommended that the sunshine duration be recorded in hundredths of an hour electronically. These measurements should be referred to the World Meteorological Organization standard—the Campbell-Stokes Sunshine Recorder.

It is also recommended that direct solar radiation at normal incidence be measured rather than calculated from diffuse radiation measurements. The method selected depends primarily on sensor costs and maintainability. At present, the diffuse radiation measurement is less costly and requires less routine attention, but the absolute accuracy is lower than measurements of direct radiation at normal incidence. The relative accuracy, however, may be higher because diffusometers require less routine attention than pyrheliometers.

### The Spatial Density -

At national meteorological stations, it is recommended that solar radiation parameters be included as part of the "standard" meteorological measurements. In other words, the solar energy network should be a routine part of the regular national program of meteorological observations. Special exceptions include large-scale systems in areas of the world where no meteorological data yet exist but where solar energy applications are likely to be developed.

The suggested network density is such that station-to-station spatial correlation of data be at least 0.7 (0.9 is easily achievable in homogeneous regions) for corresponding mean *monthly* values of daily totals of global solar radiation. The station spacing suggested here is intended as a guide to network planning. Analysis may be required by individual nations to determine their most suitable spatial distribution. Except for regions with strong gradients (such as coastal and mountainous areas), this requirement is probably reached with stations on a 500 km grid (Pivovarova, 1978). To better define the station spacing additional research is required. For solar energy applications areas with strong gradients may be sufficiently defined as those with "short-term" mobile stations, whose length of time on station will be a function of the dynamics of the microclimate being assessed.

Table A-1

Solar Radiation Parameters for a General Network

| Item | Priority | Frequency | Accuracy |
|---|---|---|---|
| Global radiation | 1 | hourly integrals(1) | ±5% or ±25 W $m^{-2}$(3) |
| Sunshine duration | 1 | hourly | ±10% |
| Direct or diffuse radiation (5° aperture pyrheliometer or shade ring) | 2 | hourly integrals(2) | ±5% or ±25 W $m^{-2}$(3) |
| Global radiation on inclined surface(2) (foreground should be neutral such as grid of black slates 2 m X 2 m X 5 cm) | 3 | hourly integrals(1) | ±10% 200 W $m^{-2}$<br>±50% 100-200 W $m^{-2}$ |

Priority: 1 = required; 2 = recommended; 3 = desired.

(1) If digital recording equipment is used 10 min (or less), integrals should be collected for quality control and engineering analysis; if strip chart recorders are used, the chart recorder speed and chart width should be such that 10 min integrals can be computed to desired accuracy. (Electrically sensitive paper or other suitable chart recorder system should be used so that 10 min integrals can be obtained by automatic chart reading devices.) The time reference desired is that the solar radiation integrals match meteorological data, i.e., local standard time. However, if true solar time is used, meteorological data must be interpolated to this base. It is recommended that the meteorological service provide the interpolations rather than have the engineer make his own. If 10 min integrals (or less) are used this problem essentially disappears.

(2) Station latitude +15° for heating season and −15° for cooling season. (Note: may be omitted in tropics.)

(3) Whichever is the larger.

**Data Storage and Analysis -**

The meteorological data should be stored so that original records are available for future analysis, i.e., data correction and special research studies.

In general, solar energy applications require data summaries other than the standard mean monthly maps, and tables, etc., which are normally provided by climatologists. Various statistical analyses are desired, which should include power spectra of radiation fluctuations; the runs of hours or days above or below given energy levels; correlations between solar radiation variables and temperature, dew point; meteorological hazards; frequency tables of temperature versus dew point. It is recommended that meteorological services be aware of these (and other) user needs, and store data in a format such that the desired statistics can be derived. For example, if original strip charts are stored, data can be digitized/computer-processed by almost any user at future times.

## 1-A.2 Research Network Measurements -

### The Parameters -

A program of measurements for research dealing with solar energy applications is recommended in Table A-2. This list includes measurements that are related to solar energy research and design applications.

As a first approximation, it should be noted that the priority 1 (necessary) parameters can be measured with current sensors. Every effort should be made, however, to improve and refine measurement capabilities at research facilities.

Spectral data can be taken with colored glass domes on pyranometers with standard interference filters on pyrheliometers. Again, this is the first approximation. The number of filters used should be sufficient to define photoactive spectral regions characteristic of photovoltaic cells, photochemical reactions and photosynthesis. High-accuracy, high-resolution spectrometers need be used only at a few selected research sites around the world.

### Spatial Density -

The spatial density of the research network should be sufficient to have one station in each climatic zone of a country, as specified by a broad climate classification system, e.g., Köppen (1931). Additionally, these sites should be placed so that they serve a broad range of users. It is also recommended that both atmospheric scientists and energy scientists coordinate their plans when selecting potential stations for research purposes.

### Data Storage and Analysis -

Original data should be stored in one-min integrals for five years. This, of course, is an arbitrary specification. The first data set stored in this way can be analyzed in great detail so that future storage involving research network information can be determined. Analyses will also impact on the general network, e.g., to specify recording frequencies, to suggest new or modified measurements. Solar energy related research projects that can be served by this research data base are too numerous to discuss here, but projects should include model development, advanced sensor development, special short-term data samples, special calibration and consultation services.

## 1-A.3 Conclusions

The national weather services should easily meet general and research solar radiation and meteorological data needs of the solar energy community because they are not being asked to provide data for site-specific solar applications. By providing a general solar radiation climatology and a few research data sets, most user needs can be satisfied. Recommended measurement programs should be started as soon as possible, since the usefulness of the data is directly related to its length of record.

## References

Pivovarova, Z. I. 1978. *On the Accuracy of Solar Radiation Data, Network Observations, and Network Density*. Unpublished presentation, Geneva, World Meteorological Organization, October 1978.

Köppen, W. 1931. *Grundriss der Klimakunde*. Berlin: Water de Gruyter and Co.

## Table A-2

## Solar Radiation Parameters for Research Purposes

| Item | Priority | User* | Frequency | Application |
|---|---|---|---|---|
| Global Radiation | (1) | 1,2,3 | 1-min integrals | non-concentrating devices, model development, climatology. |
| Sunshine Duration | (1) | 1,2,3 | % per hour | |
| Direct Radiation | (1) | 1,2,3 | 1-min integrals | concentrating devices |
| Diffuse Radiation | (1) | 1,2,3 | 1-min integrals | |
| Global Radiation on Arbitrary Surfaces** | (1) | 1,2,3 | 1-min integrals | device design, building design. |
| Albedo | (1) | 3,2,1 | 1-min integrals | model development |
| Infrared (IR) Down | (1) | 1,2,3 | 1-min integrals | device design, cooling to night sky |
| Infrared (IR) Up | (1) | 1,2,3 | 1-min integrals | |
| Ultraviolet (UV) | (1) | 1,2,3 | 1-min integrals | material degradation |
| Spectral (direct, diffuse, albedo) | (2) (1 for PV) | 1,2,3 | 1-min integrals | photovoltaic design, photochemical processes, photosynthesis |
| Turbidity | (1) | 3,2,1 | 1-min integrals | model development, climatology |
| Tracking Pyranometer | (2) | 2,3,1 | 1-min integrals | mildly concentrating device design |
| Solar Cell Device (horizontal, direct, tilted) | — | 1 | 1-min integrals | determination of utility |
| Angular Distribution of Diffuse Radiation | (3) | 2,3,1 | 1-min integrals | model development, system design |
| Circumsolar Radiation | (3) | 2,3,1 | 1-min integrals | highly concentrating system design, model development |
| Air Temperature | (1) | 1,2,3 | 1-min integrals | |
| Dew Point | (1) | 1,2,3 | | |
| Wind Speed | (1) | 1,2,3 | | climatology, device design |
| Wind Direction | (1) | 1,2,3 | | |
| Atmospheric Pressure | (1) | 3,2,1 | hourly | |
| Cloud Cover*** | (1) | 3,2,1 | hourly, 10-min during special studies | model development |
| Weather | (1) | 3,2 | as appropriate | |
| Precipitation | (1) | 3,2,1 | 10-min samples | |
| Snow Cover | (1) | 3,2,1 | as appropriate | climatology, model development |
| Snow Depth | (1) | 3,2,1 | as appropriate | |
| Precipital Water | (1) | 3 | hourly | |
| Dust Fall | (2) | 2,3 | daily | special applications |
| Soil Temperature | (2) | 2,3 | daily mean value | biomass production |
| Soil Humidity | (2) | 2,3 | daily mean value | biomass production |

Priority:
1. Necessary
2. Recommended
3.Desired

User:
1. Designer
2. Solar Researcher
3. Atmospheric Scientist

Assumptions:
• Accuracy is state-of-the-art

*Sequence indicates a use rate if different than 1,2,3 or 2,3. Initial user is the most frequent user. **To include sensors tilted at Lat. facing South (or North) with neutral albedo, Lat.±15%, and vertical South, North, East and West. ***Recommend all sky camera or television camera (can be digitized directly) be used to monitor clouds as well as observer reports.

## Appendix I-B

# GLOSSARY

*Absorption* -

The process in which incident radiant energy is retained by a substance. A further process always results from absorption: i.e., the irreversible conversion of the absorbed radiation into some other form of energy within and according to the nature of the absorbing medium. The absorbing medium itself may emit radiation, but only after an energy conversion has occurred.

*Air Mass, m,* -

The path length of radiation through the atmosphere, considering the vertical path at sea level as unity. Thus, at sea level, m = 1 when the sun is at the zenith (i.e., directly overhead), and m = 2 for a zenith angle ($\Theta$, the angle subtended by the zenith and the line of sight to the sun) of 60°. Except for very large zenith angles ($m > 3$, where the atmospheric refraction becomes significant) $m = \sec \Theta$.

*Albedo* -

Ratio of the radiation reflected by a surface to that incident on it.

*Angle of Incidence, i,* -

The angle at which a ray of energy impinges upon a surface, measured between the direction of propagation of the energy and the normal to the surface at the point of impingement, or incidence.

*Attenuation of Solar Radiation* -

Loss of energy suffered by a beam of radiant energy which traverses the earth's atmosphere. Losses are caused by scattering by air molecules, by selective absorption by certain molecules, and by absorption and scattering by aerosols.

*Circumsolar Radiation* -

Radiation scattered by the atmosphere into the area of the sky immediately adjacent to the sun. It produces the solar aureole, whose angular extent is directly related to the atmospheric turbidity, increasing with high turbidity.

*Diffuse Solar Radiation/Sky Radiation* -

Downward scattered and reflected solar radiation coming from the whole hemisphere with the exception of the solid angle subtended by the sun's disc.

*Direct Solar Radiation* -

Solar radiation coming from the solid angle of the sun's disc on a surface perpendicular to the axis of this cone, comprising mainly scattered and unreflected solar radiation.

*Extraterrestrial* -

Solar radiation received at the upper limit of the earth's atmosphere.

*Global Solar Radiation* -

The downward direct and diffuse solar radiation received on a horizontal surface.

*Radiation* -

Emission or transfer of energy in the form of electromagnetic waves or particles.

*Solar Constant* -

Amount of solar radiation incident, per unit area and time, on a surface which is normal to the solar beam at the outer limit of the atmosphere, the earth being at its mean distance from from the sun.

*Solar Radiation* -

Radiation emitted by the sun.

*Sunshine Hours* -

1. Hours between astronomical sunrise and sunset are the *astronomically possible* sunshine duration hours.

2. Hours between local sunrise and sunset with regard to the natural horizon at the station in question are the *effective possible* sunshine duration hours.

*Terrestrial Radiation* -

The radiation emitted by the planet Earth including its atmosphere.

*Total Radiation* -

Sum of solar and terrestrial radiation.

## CHAPTER 2

# THE SUN AND ITS RADIATION

**A. D. Watt**
**Watt Engineering Ltd.**
**Route 1, 2142 T-Road**
**Cedaredge, Colorado 81413**
**The United States of America**

### 2.1 The Sun as a Star

The sun is a typical main-sequence star of spectral class G. The majority of stars follow along the main sequence band relating visual magnitude and spectral class, shown in Figure 2-1. The sun's spectral class G means that its apparent surface temperature is in the 6,000 K region. By way of comparison, Betelgeuse, one of the super giants, has an effective surface temperature of only 3,500 K, while Spica has a surface temperature near 50,000 K.

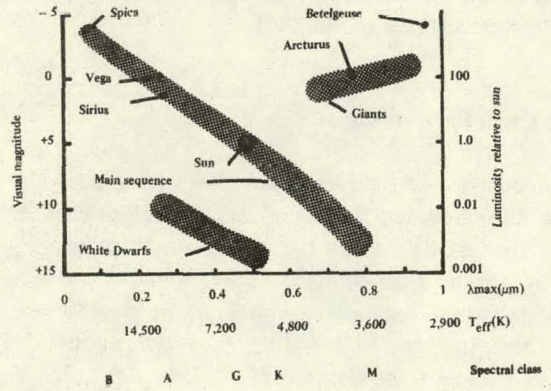


*Figure 2-1 H.R. Diagram - based on data from Wyatt (1964), and Akasofu and Chapman (1972), λ is wavelength in micrometers.*

The sun is located in one of the spiral arms (the Orion arm) of our galaxy, which is frequently referred to as the "Home Galaxy". The sun's mass is $2 \times 10^{30}$ kg and the radius of its visible disc is $6.96 \times 10^5$ km.

The temperature near the center of the sun is inferred to be extremely high; i.e., in the order of $1.5 \times 10^7$ K. Here the protons are believed to be converted into helium nuclei by thermonuclear reactions.

Each kilogram of hydrogen converted yields $6.3 \times 10^{14}$ Joules. Since the power radiated from the sun is the order of $3.8 \times 10^{26}$ W, the amount of hydrogen consumed per year would be about $1 \times 10^{-11}$ of the solar mass.

Most of the energy output from the sun is in the form of electromagnetic radiation centered near the visible portion of the spectrum. The heat energy generated in the central region is transferred outward by radiative and convection processes. The outer portion of the sun is defined as consisting of three layers, which, progressing outward, are: (1) the photosphere; (2) the chromosphere; and (3) the corona.

The photosphere is the most stable of the three. Most of the sun's electromagnetic radiation is from the photosphere, which therefore contributes to the stability of the solar constant. It is this portion of the sun that appears as a bright disc. This disc is not uniformly bright, as shown in Figure 2-2. This phenomenon, known as limb darkening, occurs because light from the limb comes from higher and cooler layers than the light from the center of the disc. The amount of decrease in radiance depends on the wavelength. The visible radiation from the sun appears to follow the relation:

$$R(r) \approx R(0)[\cos((\frac{r}{r_d})(\frac{\pi}{2}))]^{0.25} \quad (1)$$

where R(r) is the radiance at a distance from the center, R(0) is the radiance at the center and $r_d$ is the radius of the visible disc. When the entire spectrum is considered, the exponent would be reduced to near 0.1.

Above the photosphere the gas density decreases rapidly and the effective temperature increases until in the corona temperatures are of the order of $10^6$ K.

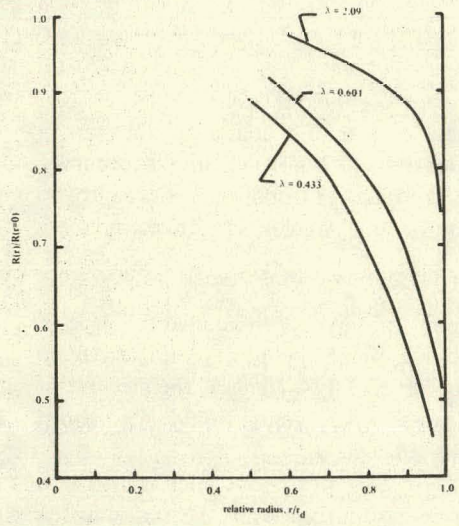


*Figure 2-2 Solar disc radiance based on data from Abbot (1908), λ is the wavelength in micrometers, R(r) is the surface radiance at a distance r from the center and $r_d$ is the radius of the visible disc. (See also, Pierce and Waddell, 1961).*

The corona is non-uniform, consisting of rays, plumes and arches (see Figure 2-3), structures which are closely associated with the sun's internal magnetic field. During disturbed periods the solar corona extends to as much as several solar radii from the surface of the sun. During very quiet sun conditions (low sunspot numbers) the corona decreases.

The chromosphere and the corona are more time variant than the photosphere. Their outputs are in the x-ray and extreme ultraviolet (UV) spectral regions, with intensities as much as ten times greater during solar sunspot maxima than during sunspot minima. A possible slight reduction in photosphere output with sunspot activity may, in effect, balance the x-ray and UV variation.

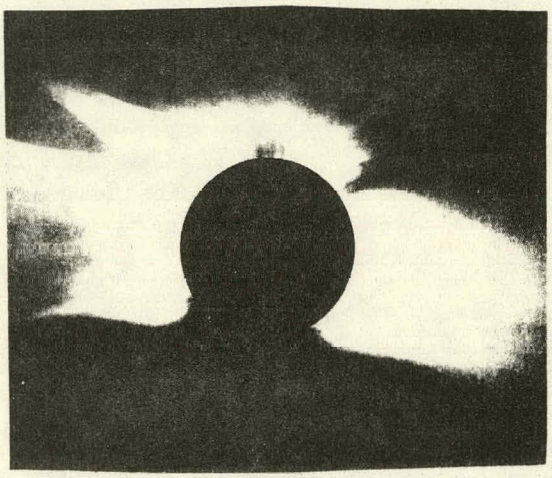

*Figure 2-3 The solar corona*

The number of sunspots observed on the sun's disc has changed with time. In the last century we have become accustomed to a relatively uniform cyclic behavior with a period of eleven years. Significant departure from this pattern was observed in the 17th century (see Figure 2-4).

## 2.2 Sun/Earth Relationships

A heliocentric, i.e., sun-centered view of the sun-earth's system is shown in Figure 2-5. The elliptical orbit of the earth around the sun results in the closest approach, perihelion, of $1.47 \times 10^{11}$ m, which occurs about January 3. Aphelion, the greatest distance from the sun, $1.52 \times 10^{11}$ m, occurs about July 5. At a mean solar distance of $1.495 \times 10^{11}$ m, one astronomical unit, the earth intercepts some $1.7 \times 10^{17}$ W. At this distance, the average solar flux outside the earth's atmosphere is defined as the solar constant. A great deal of effort has been expended in attempting to determine whether the solar constant is constant and what is its correct value.

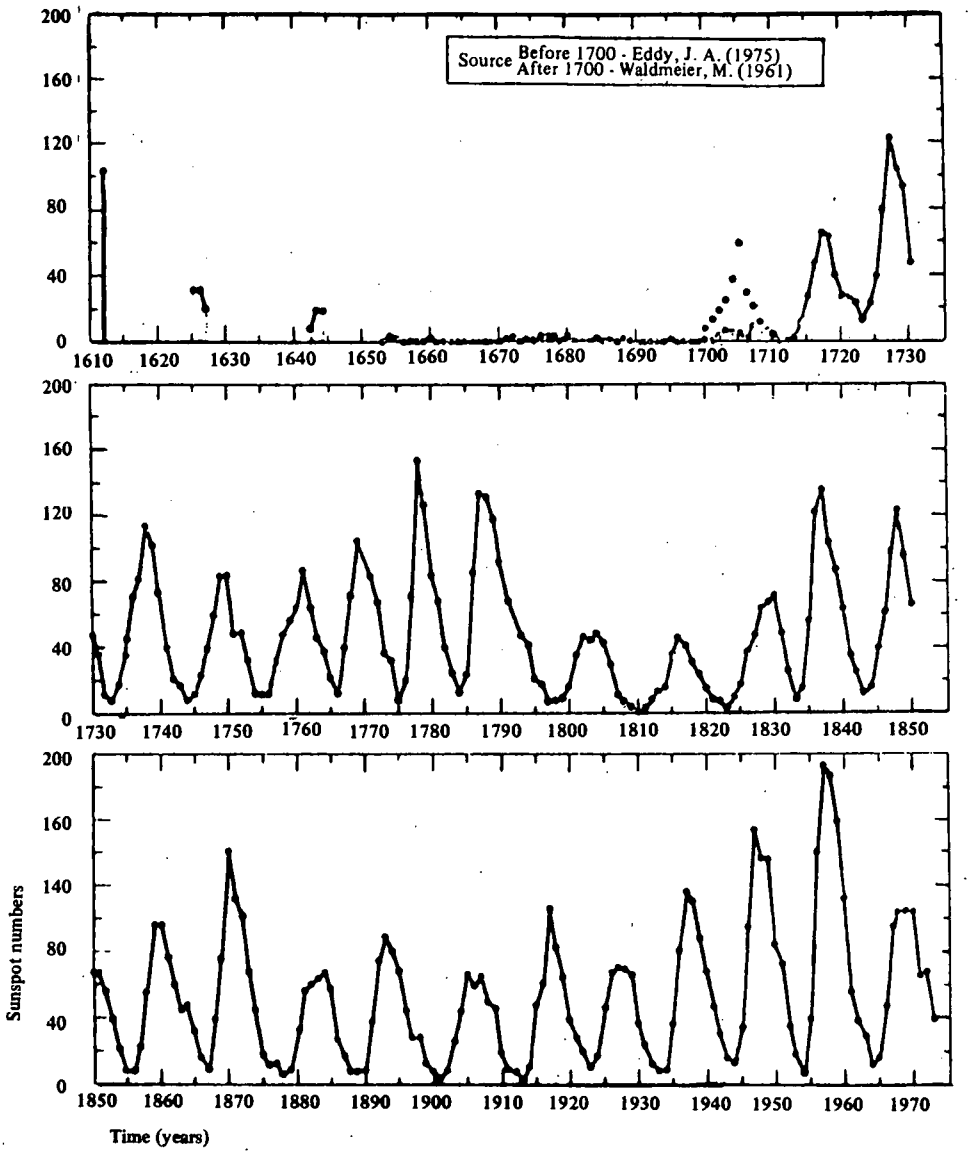


*Figure 2-4 Annual mean sunspot number*
*(From J. A. Eddy, 1975)*

There are several methods of measurement requiring atmospheric corrections to determine the solar constant, see Hoyt (1979). The fundamental (often referred to as long) method used by the Smithsonian Institution assumes the direct solar radiation is reduced from its solar constant value by an exponential function. This calculation uses a constant times an optical air mass "m" which at sea level is taken as equal to the secant of the zenith angle. This method is not valid for m larger than 3. This "long" method requires observations over several hours for the zenith angle to change so that a straight line through these measured values can be extrapolated to zero air mass, i.e., outside the atmosphere.

Some of the problems encountered include:

(1) Instrumental spectral response and absolute calibration accuracy. (See Fröhlich, 1973, and Fröhlich and Brusa, 1975.)

(2) Changes in atmospheric transmission during the 2 to 4 hours required for measurements.

(3) The amount to be added for unmeasured portions of the spectrum; about 3% for the region below 0.34 $\mu$m, and 2 or 3% above 2.5 $\mu$m.

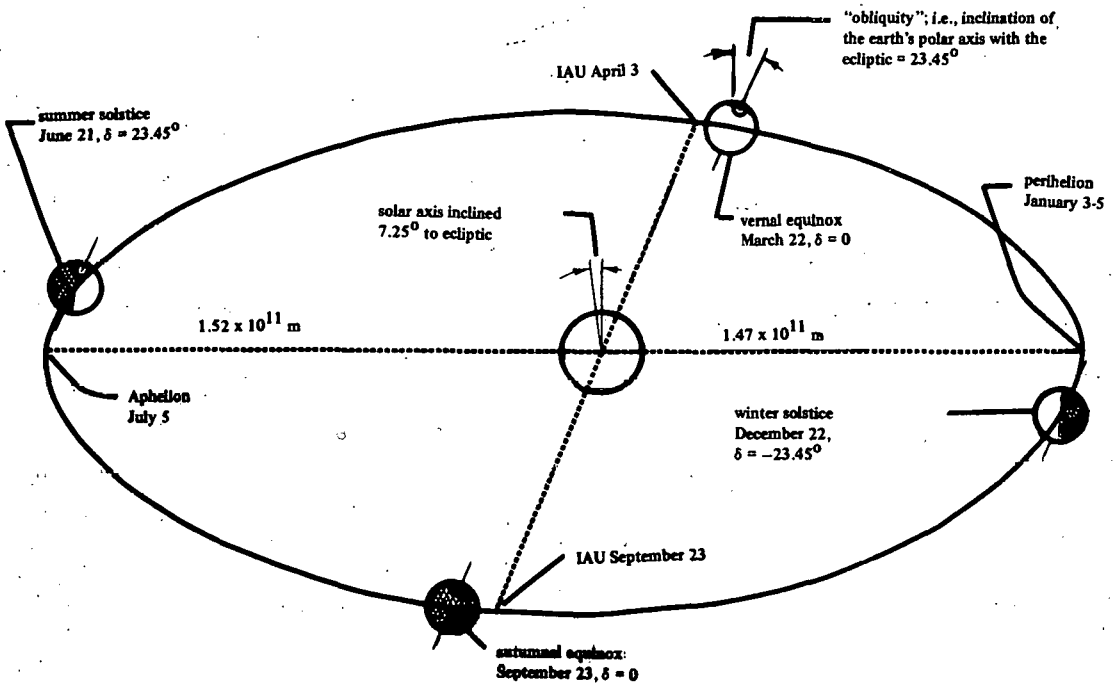


*Figure 2-5 Heliocentric view of the sun and the earth's orbit; i.e., the ecliptic plane which contains the sun and the earth. One Astronomical Unit (IAU) is the average sun-earth distance. δ is the declination. The dates may vary by a day or so.*

(4) Absorption is not linearly related to air mass passed through, and the layering of the atmosphere because of variations in the atmospheric moisture and dust.

To minimize the effects of changing atmospheric transmission, (item 2), the Smithsonian Institution developed the "short" method. This involves the determination of the brightness of the sky surrounding the sun, which is related to the scattering produced by the atmosphere at the time of observation. An empirical correction was then developed for the direct term. Although this permits a measurement to be made in a short period of time, it introduces other potential errors.

One of the major problems with measurements at the earth's surface is the amount to add for the spectral portions removed by the atmosphere. The solar spectrum varies a great deal in the ultraviolet and x-ray region.

As a result, the short wave correction factor will likely have varying errors as a function of solar activity or sunspot number. The long wave correction factor depends upon the amount of water vapor present in the atmosphere. The overall accuracy is dependent upon the accuracy with which the absorption due to water vapor, ozone, and carbon dioxide can be estimated.

It is known that the amount of visible radiation is reduced by darkening in the sunspot regions. Assuming that the remainder of the sun's disc had a constant output, it would appear that the solar constant would be reduced during periods of high sunspot number. On the other hand, it is known that the ultraviolet and x-ray radiation from the sun increase during periods of high solar activity, which would tend to increase the solar constant with increasing sunspot number. Because of these counteracting factors, it is not clear how the solar constant would change with varying sunspot number.

A precise value for the solar constant still appears elusive, as evidenced by the papers given at the workshop on the solar constant at Big Bear, California, in May 1975, (Zirin and Walter, 1975). When one

considers the effective change of that portion of the solar spectrum observed at the base of the atmosphere where most of the ultraviolet and x-ray radiation has been absorbed, it is unlikely that any significant change can be detected over a sunspot cycle in the remaining portion of the solar spectrum reaching the surface. This agrees with the results of an analysis performed by Hoyt (1979). The short-term fluctuations (day-to-day or month-to-month) are believed to be less than 0.25%. The long-term change of the solar constant (over a sunspot cycle) appears to be less than ±1%. A value of 1.365 kW $m^{-2}$ * is chosen for subsequent calculations.

The solar radiation spectrum at a distance of one astronomical unit, along with its integral, is shown in Figure 2-6. The solar constant is obtained by integrating the spectral distribution from essentially zero wavelength up to 1,000 $\mu$m. A more detailed spectral distribution on a log-log scale is shown in Figure 2-7. Tabulations of the solar spectrum irradiance are given by Labs and Neckel (1971),

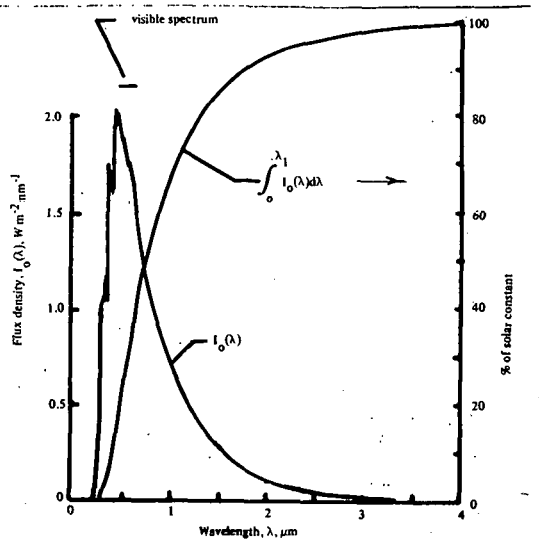


*Figure 2-6 Solar radiation spectrum at one astronomical unit, 1.495 X $10^{11}$. (Based on data from M. P. Thekaekara.)*

*See Chapter 3, Section 3.2. A value of 1.373 kW $m^{-2}$ for the solar constant has been adopted for this book. Calculations in this chapter should be increased by 0.008 to be consistent with the adopted solar constant.

and by Thekaekara (1974). From these tabulations it is seen that less than 0.02% of the radiant solar energy lies below a wavelength of 0.25 micrometers, and that less than 1% above 4 $\mu$m.

The inclination of the earth's equator to the ecliptic, which is known as the obliquity, is shown in Figure 2-5, along with the earth's elliptical orbit.* The earth's motion in its orbit produces the seasonal and geographic variations of the daily solar energy received on a horizontal surface outside the earth's atmosphere.

The variation in the sun-earth distance and the resulting solar intensity correction factor is shown in Figure 2-8 as a function of day of the year along with the variation in the sun's declination. The equations which can be used to calculate the solar declination and extraterrestrial flux are given in Table 2-1.

### 2.3 Solar Radiation (Direction-Time Effects)

The direct component of solar radiation on a clear day arrives within a cone of about $0.5^0$, since the sun's semi-diameter ranges from about $0.263^0$ (0.00458 rad) on July 5, to $0.271^0$ (0.00473 rad) on January 3.

The direction of arrival of the direct component of solar radiation is determined by celestial mechanics. The heliocentric view, Figure 2-5, shows that the closest approach occurs about January 3, at a distance of 0.98329 AU. The direction of arrival at the earth's surface is best seen switching to the geocentric; i.e., earth-centered and observer-centered views shown in Figure 2-9.

The geocentric view at the top of this figure shows the observer located at a latitude $\phi$ north of the equator and at a sun hour angle $\omega$ before noon. The solar declination is the angle between the sun's ray and the earth's equatorial plane.

*Current orbital values are: eccentricity, 0.0167 and obliquity, $23.45^\circ$.

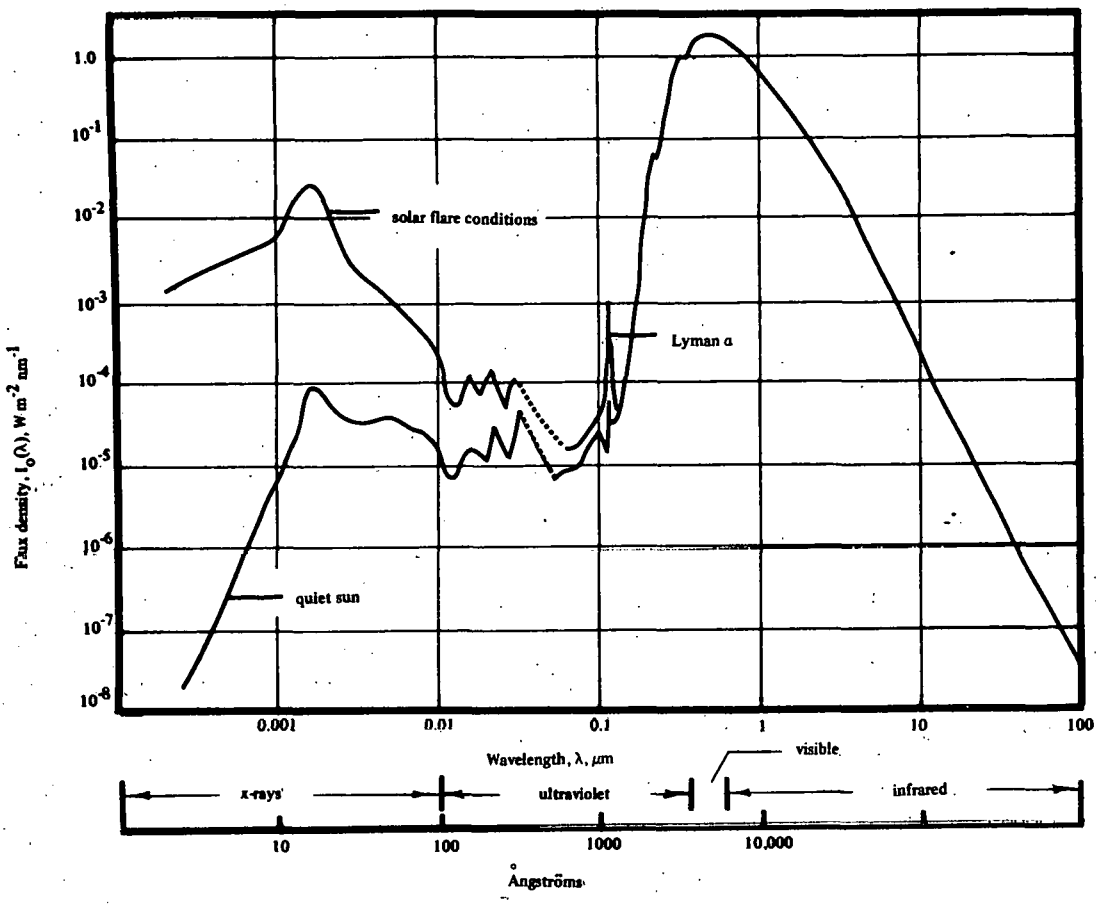


*Figure 2-7 Solar spectrum at one astronomical unit (Based on data from Smith and Gottlieb, 1974)*

The lower sketch shows an observer-centered view with the same relative position of the axis as in the geocentric view; i.e., the polar axis is parallel to the earth's axis. The north-south axis is along the line of the meridian of longitude shown in the top sketch, and the east-west line is tangent to the latitude circle at the point of observation. In this figure the hour angle $\omega$ is shown projected in the latitude plane, the declination lies in a plane parallel to the solar latitude; the latitude $\phi$, in the observer's longitude plane.

A more familiar and detailed observer-centered view is shown in Figure 2-10, where the axis system is rotated so as to place the zenith reference as an upward pointing, i.e., vertical line. The angles are still related in the same manner as in the preceding figure but are readily related to our normal reference frame where the zenith is overhead and the N-S and E-W lines are horizontal.

The solar azimuth angle, $\gamma$, shown in the horizontal plane, results from projecting the sun's ray onto the horizontal plane. The solar zenith angle, $\Theta$, and the elevation angle, $90 - \Theta$, are also indicated.

It is instructive to note that if $\delta$ is positive (spring and summer) the sun rises and sets north of the east-west direction. If $\delta$ is negative (fall and winter) the sun rises and sets in the southern half of the plane.

The relationships between the various angles described thus far are contained in the set of equations in Table 2-2.

The elliptical orbit of the earth around the sun produces a non-uniform solar time* as related to the uniform time used in the civil (Local Standard Time)

---

*Noon, solar time occurs when the sun's elevation angle is at its greatest (the sun lies in the longitude plane). At noon solar time a true north-south line may be determined from the shadow on a horizontal surface from a vertical object such as a plumb line.

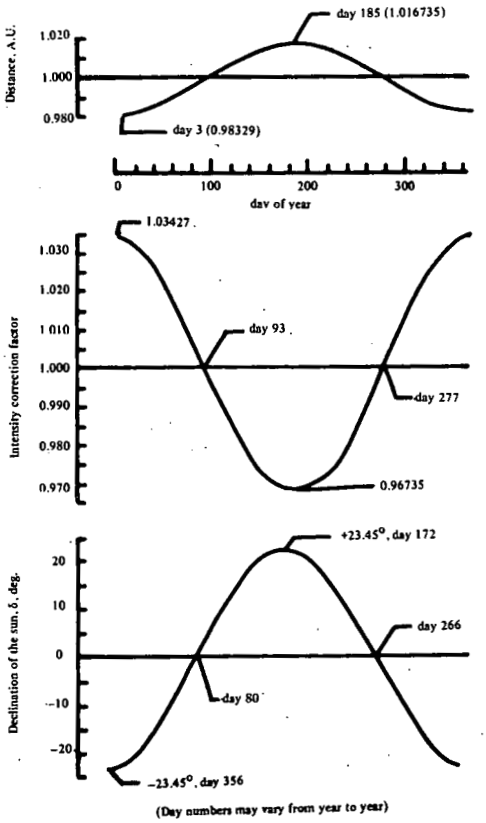


*Figure 2-8 Sun-earth distance, intensity correction factor and declination of the sun.*

systems. The differences in time between these systems for a location on a standard meridian are shown in Figure 2-11, and are given in minutes for each day of the year, along with the corresponding solar declination.

Approximate values for the equation of time are given in Table 2-3 along with a date to day of year conversion. The actual solar time in terms of Local Standard Time for an arbitrarily located observer was given in Eq. (5).

The times of sunrise and sunset, as well as hours of possible sunshine, are often useful for analyzing solar data or designing solar systems. These are given in the following set of equations.

Table 2-1

Equations for Solar Declination and Extraterrestrial Normal-Incidence Flux
(n is the number of this day of the year)

**DECLINATION**

$$\delta^\circ \approx 23.45 \sin[1.008(n - 80)]$$
$1 \leq n \leq 80$ (accuracy $\approx 0.59^\circ$ in February)

$$\delta^\circ \approx 23.45 \sin[0.965(n - 80)]$$
$81 \leq n \leq 266$ (accuracy $\approx 0.50^\circ$ in August)

$$\delta^\circ \approx -23.45 \sin[0.975(n - 266)]$$
$267 \leq n \leq 365$ (accuracy $\approx 0.45^\circ$ in October) (2)

An alternative expression with accuracy of $\approx 0.22^\circ$ for non-leap years is:

$$\delta^\circ \approx 0.36 - 22.96 \cos 0.9856\, n - 0.37 \cos(2 \times 0.9856\, n) - 0.15 \cos(3 \times 0.9856\, n) + 4.00 \sin 0.9^\circ \text{(2a)}$$

A simple approximation with accuracy of $\approx 1^\circ$ is:

$$\delta^\circ \approx 23.45 \cos(0.985\,(n - 81)) \quad (2b)$$

**FLUX**

A simple approximation is:

$$I_0 \approx 1.365\,\{1 + 0.033 \cos(0.985\,(n - 3))\},\ \text{kW m}^{-2} \quad (3)$$

*Accuracy calculations, private communication from Dr. Hans Lund

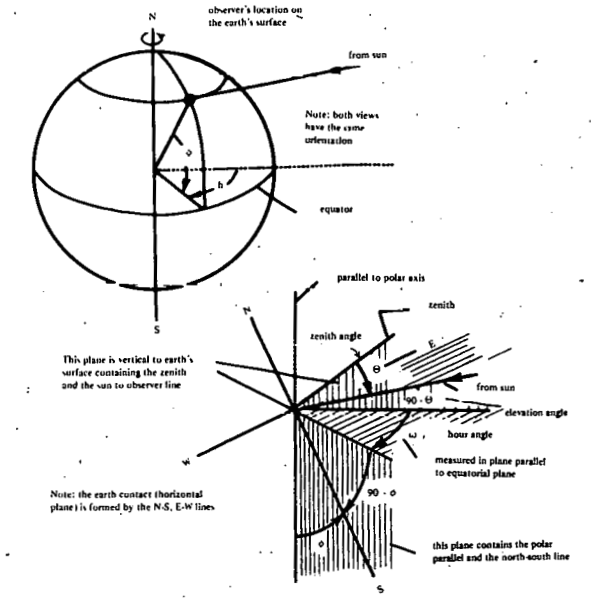


*Figure 2-9 Geocentric and observer-centric views showing pertinent angles involved. Note: north, south, east, west lines are tangent to the earth's surface.*

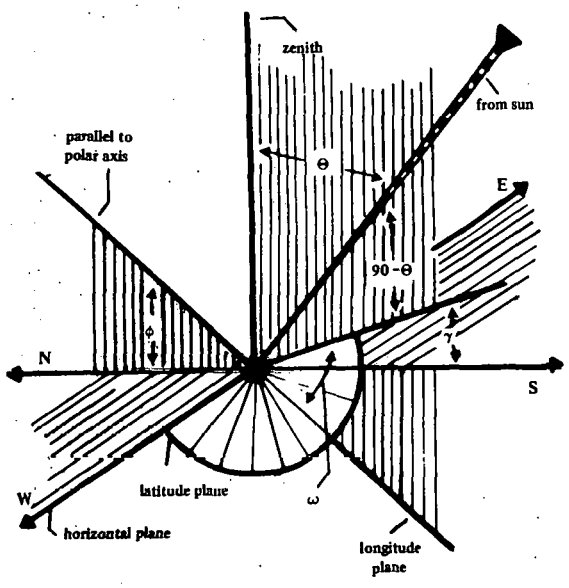


*Figure 2-10 Observer-centered view with zenith vertical and north-south/east-west plane horizontal. Note: latitude, $\phi$, in vertical plane containing N-S axis. Hour angle, $\omega$, in latitude plane is angle between the N-S zenith plane and plane containing the elevation angle, 90 − Θ, which is a vertical plane containing the sun line. Zenith angle, Θ, is in the same plane as 90 − Θ. Azimuthal angle, $\gamma$, is in the horizontal plane and gives the angle in this plane between the N-S; i.e., observer longitude plane and the plane containing the zenith and the sun line.*

Table 2-2

Solar Angle

**ZENITH AND ELEVATION**

$$\cos\Theta = \cos\phi\cos\delta\cos\omega + \sin\phi\sin\delta \quad (4)$$

where

Θ is the solar zenith angle,

$\phi$ is the latitude,

$\delta$ is the solar declination, see Eq. (2) or Figure 2-11,

$\omega$ is the hour angle (in deg) about noon,

$$\omega = 15 \times (12 - H_s),$$

note: $\omega$ is + before noon and − after noon, where $H_s$, the true solar time in hours (0 to 24) is given by the relation:

$$H_s = H_{smt} + (\tfrac{1}{60})E_{qt} \pm (\tfrac{1}{15})(L_{sm} - L_{ob})^* \quad (5)$$

where

$H_{smt}$ is Local Standard Time or Standard Meridian Time (0 to 24 hours),

$E_{qt}$ is the equation of time in minutes; see Figure 2-12 or Eq. (7),

$L_{sm}$ is the longitude (in deg) of the standard meridian** for the observer's time zone,

$L_{ob}$ is the longitude of the observer (in deg)

**AZIMUTH**

$$\sin(\gamma - 180) = \frac{\cos\delta\sin\omega}{\sin\Theta} \quad (6)$$

$$\cos\gamma = \frac{(\sin\delta - \sin\phi\cos\Theta)}{\cos\phi\sin\Theta} = \frac{(\sin\delta - \sin\phi\cos\Theta)}{\cos\phi\sin\Theta} \quad (6a)$$

*Use + for West longitude and − for East longitude locations

**Note: Standard meridians for time zones in degrees are 15 X the time zone number.

Sunrise-Sunset Times

- Solar Time -

$$H_{st,sr} = (\tfrac{1}{15}) \arccos(\tan\phi\tan\delta) - C \quad (8)$$

$$H_{st,ss} = 12 + (\tfrac{1}{15}) \arccos(-\tan\phi\tan\delta) + C$$

- Local Standard Time -

$$H_{smt,sr} = H_{st,sr} - \frac{E_{qt}}{60} + \frac{(L_{ob} - L_{sm})}{15} \quad (9)$$

- Hours of Possible Sunshine -

$$H_{ps} = (\tfrac{2}{15}) \arccos(-\tan\phi\tan\delta) + 2C \quad (10)$$

The exact times of sunrise and sunset include a correction, C. The basic equations without C are related to the geometric position of the center of the sun. Since sunrise is defined as the time at which the upper limb of the sun becomes visible, it is necessary to correct the sunrise time by two effects. First, the upper limb of the sun becomes visible before the center as it rises above the horizon; this amounts to 16 minutes of arc. Second the atmospheric refraction bends the sun's rays by as much as 36 minutes of arc. The sum of the effects is 52 minutes of arc which must be converted to units of time. Since 15° of arc in a latitude plane equals 1 h, the correction factor, C, is a constant equal to 52/(60)(15) = 0.0578 h. A further correction must be made which allows for the fact that the sun only rises perpendicular

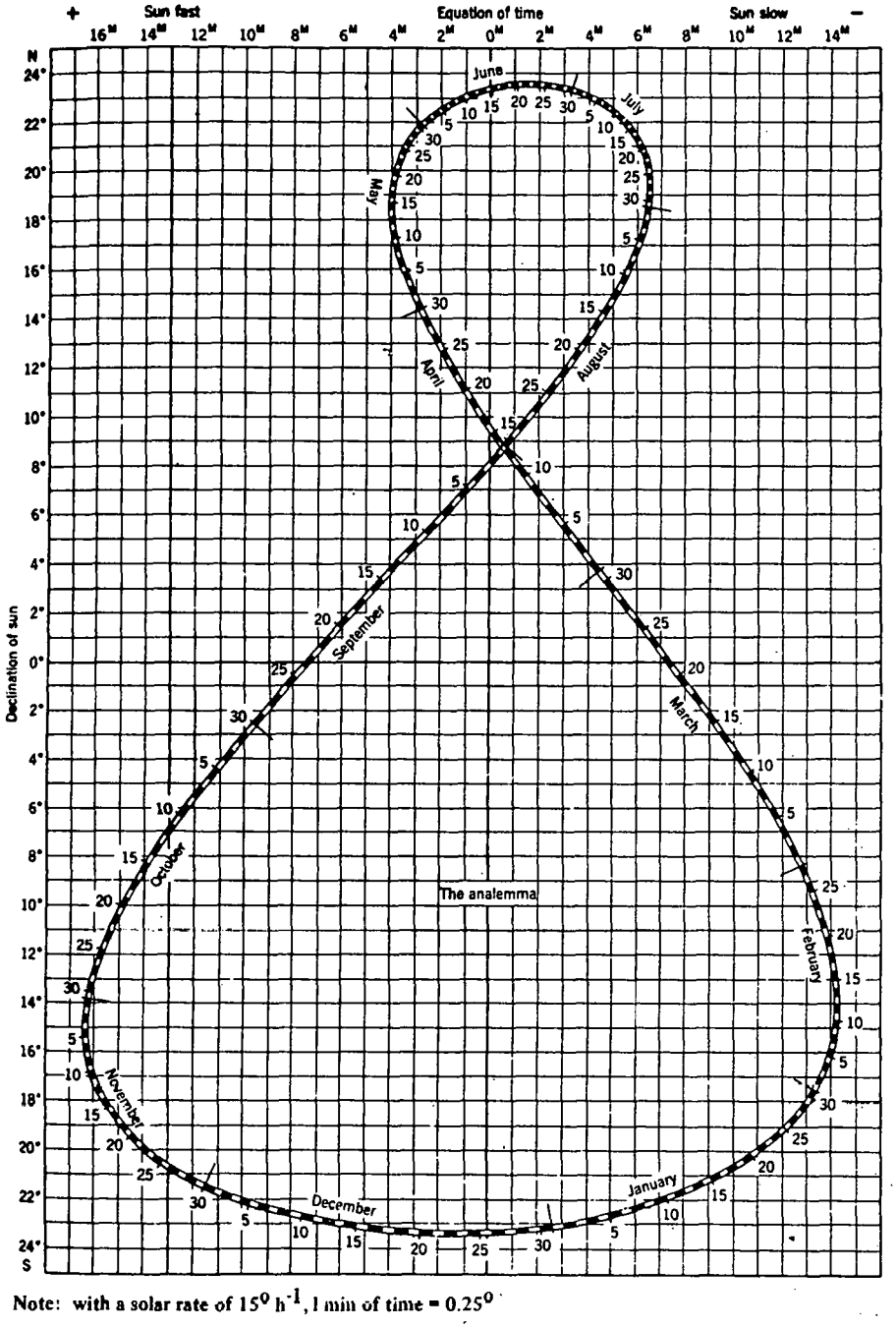


Note: with a solar rate of $15^{0}\ h^{-1}$, 1 min of time = $0.25^{0}$

*Figure 2-11 The analemma allows both the sun's declination and equation of time to be estimated for any day in the year. (From Strahler, 1960)*

Table 2-3

Date to Day of Year Conversions and Equation of Time Approximations

Date to day of year conversions

| Month | Date | Day (n) | Leap year day (n) |
|---|---|---|---|
| 1 | Jan. X | X | X |
| 2 | Feb. X | X + 31 | X + 31 |
| 3 | Mar. X | X + 59 | X + 60 |
| 4 | Apr. X | X + 90 | X + 91 |
| 5 | May X | X + 120 | X + 121 |
| 6 | Jun. X | X + 151 | X + 152 |
| 7 | Jul. X | X + 181 | X + 182 |
| 8 | Aug. X | X + 212 | X + 213 |
| 9 | Sep. X | X + 243 | X + 244 |
| 10 | Oct. X | X + 273 | X + 274 |
| 11 | Nov. X | X + 304 | X + 305 |
| 12 | Dec. X | X + 334 | X + 335 |

where X = day of the month
n = day of the year

Equation of time
(Correction in min, accuracy = 1 min)

$$E_{qt} \approx -14.2 \sin\left((n+7)\left(\frac{180}{111}\right)\right),\ n = 1 \text{ to } 106$$

$$\approx 4 \sin\left((n-106)\left(\frac{180}{59}\right)\right),\ n = 107 \text{ to } 166$$

$$\approx -6.5 \sin\left((n-166)\left(\frac{180}{80}\right)\right),\ n = 167 \text{ to } 246$$

$$\approx 16.4 \sin\left((n-247)\left(\frac{180}{113}\right)\right),\ n = 247 \text{ to } 365 \qquad (7)$$

to the horizon near the equator. The resulting "just visible sun" correction is given by the following equation:

Correction for semi-diameter and refraction in hours,

$$C = \frac{0.0578}{\cos\phi \sin(\text{arc } \cos(\tan\phi \tan\delta))}. \qquad (11)$$

For refraction only the constant is 0.04. The entire correction is shown in Figure 2-12.

It is interesting to note that the total hours of possible sunshine given in Eq. (10), if integrated (without C) over the year, yields an average of 12 h per day for every location on the earth. With C added, hours of average daylight increase slightly with latitude.

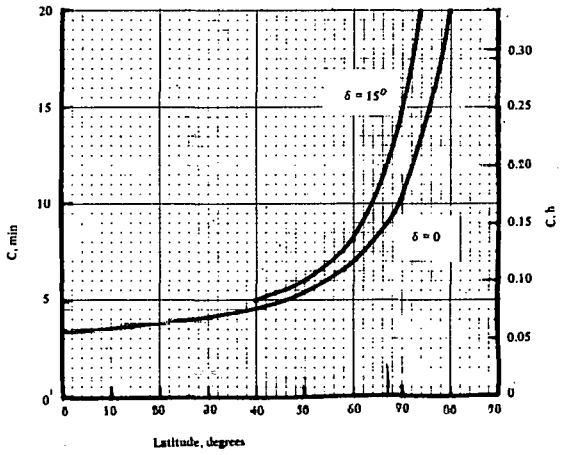


*Figure 2-12 Sunrise-sunset time correction, C*

Figure 2-13 is a diagram for 35°N latitude showing solar altitude and azimuth angles from the *Smithsonian Physical Tables* (1934). Diagrams for azimuth angles for the N latitudes are in the reference.

Example of Time and Angle Calculation

Location: Albuquerque, New Mexico
35°N, 106.5°W
December 1, 11:00 a.m. MST
(day 335)

1. What is the solar time?

The standard meridian is 105°. From Figure 2-11 the equation of time is: $E_{qt}$ = 11.3 min.

Using Eq. (5)

$$H_s = H_{smt} + E_{qt}/60 + (L_{sm} - L_{ob})/15$$

$$= 11.00 + 0.188 + (105 - 106.5)/15$$

$$= 11.088 \text{ h}$$

12 - 11.088 = 0.912 h before solar noon.

2. What is the sunrise time on December 1?

From Figure 2-12, C = 0.08 h, and from Eq. (8) the solar sunrise time is 7.05 - C = 6.97 h. From Eq. (9) the local standard time is:

$$H_{smt} = H_s = E_{qt}/60 + (L_{ob} - L_{sm})/15$$

$$= 6.97 - 0.188 + (106.5 - 105)/15$$

$$= 6.882 \text{ h}$$

$$= 6 \text{ h}, 53 \text{ min Local Standard Time.}$$

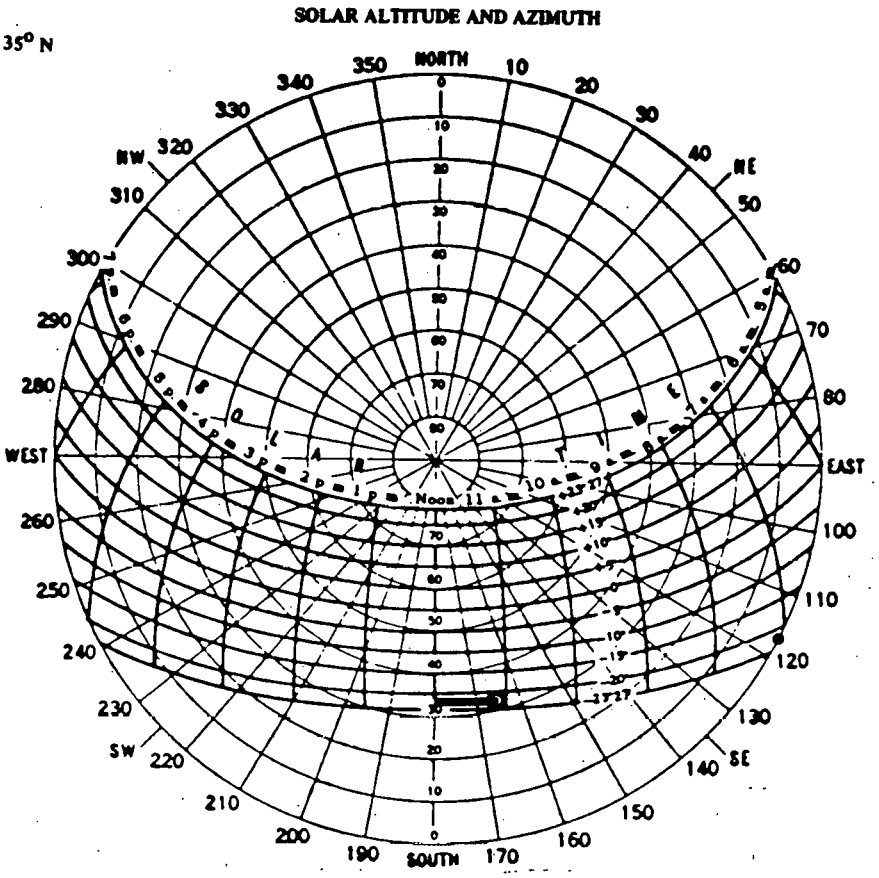


| Declination | Approximate dates |
|---|---|
| +23°27' | June 22 |
| +20° | May 21, July 24 |
| +15° | May 1, August 12 |
| +10° | April 16, August 28 |
| + 5° | April 3, September 10 |
| 0° | March 21, September 23 |
| - 5° | March 8, October 6 |
| -10° | February 23, October 20 |
| -15° | February 9, November 3 |
| -20° | January 21, November 22 |
| -23°27' | December 22 |

*Figure 2-13 Plan view showing solar elevation and azimuth angles (From the Smithsonian Physical Tables, 1934)*

**References**


Abbot, C. G. and Fowle, F. E. 1908. *Ann. Smithsonian Ap. Obs.* 2.

Akasofu, S. -I. and Chapman, S. 1972. *Solar Terrestrial Physics.* Oxford Claredon Press.

Eddy, J. A. 1975. "The Last 500 Years of the Sun", *Proceedings of The Cal. Tech. Solar Constant Workshop,* Big Bear Observatory, 19-21 May, 1975.

Eddy, J. A. 1977. "The Case of the Missing Sunspots". *Scientific American.* May 1977, pp. 80-92.

Frohlich, C. 1973. " The Relation Between the IPS now in use and Smithsonian Scale 1913, Ångstrom Scale and Absolute Scale." *Proceedings of Symposium on Solar Radiation*; Smithsonian Institution, November 1973, pp. 61-78.

Frohlich, C. and Brusa, R. W. 1975. "Measurement of the Solar Constant, A Critical Review." *The Cal. Tech. Solar Constant Workshop,* Big Bear Observatory, 19-21 May, 1975, pp. 111-126.

Hoyt, D. V. 1979. "The Smithsonian Astrophysical Observatory Solar Constant Program." *Reviews of Geophysics and Space Physics,* Vol. 17, No. 3, pp. 427-458, May 1979.

Labs, D. and Neckel, H. 1971. *Solar Physics.* No. 19, p. 3.

Pierce, A. K. and Waddell, J. H. 1961. "Analysis of Limb Darkening Observations", *Memoirs of the Royal Astronomical Society*. London. Vol. 68, pp. 89-112.

Smith, E. vP. and Gottlieb, D. M. 1974. "Solar Flux and its Variation". *NASA Preprint No. X-901-74-156, Proceedings of the Symposium on Possible Relationships Between Solar Activity and Meteorological Phenomena,* Goddard Space Flight Center, Nov. 7-8, 1973.

Strahler, A. N. 1963. *The Earth Sciences.* New York: Harper and Row.

Thekaekara, M. P. 1974. "Extraterrestrial Solar Spectrum, 3000-6100 Å, at 1 Å Intervals". *Applied Optics.* Vol 13, No. 3, pp. 518-522.

Wyatt, S. P. 1964. *Principals of Astronomy.* Allyn & Bacon, Inc.

Waldmeier, M. 1961. *The Sunspot Activity in the Years 1610-1960.* Zurich: Schulthess & Co.

Zirin, H. and Walter, J. (editors). 1975. *Proceedings of the Workshop: 'The Solar Constant and the Earth's Atmosphere'*, Cal. Tech., Big Bear Observatory, May 19-21, 1975, NSF Grant, DES 75-16101, BBSO No. 0149.


**Bibliography**


Abbot, C. G. 1922. "Results of the Measurements of the Intensity of Solar Radiation." *Annals of the Astrophysical Observatory of the Smithsonian Institute.* Vol. 4, Ch. IV, pp. 193-195.

Blanco, V. M. and McCuskey, S. W. 1961. *Basic Physics of the Solar System.* Addison-Wesley Publishing Co.

Duffie, J. A. and Beckman, W. A. 1974. *Solar Energy Thermal Processes.* New York: John Wiley & Sons.

Fritz, S. 1951. "Solar Radiant Energy and its Modifications by the Earth and its Atmosphere." *Compendium of Meteorology.* pp. 13-33.

Marvin, C. F. 1925. "On the Question of Day-to-Day Fluctuations in the Derived Value of the Solar Constant." *Monthly Weather Review.* Vol. 53, No. 7.

Sellers, W. D. 1965. *Physical Climatology*. Chicago: University of Chicago Press.

U. S. Government. *The American Ephemeris and Nautical Almanac*. Washington, D. C.: U. S. Government Printing Office.

Valley, S. L. 1965. *Handbook of Geophysical and Space Environments*. New York: McGraw Hill Book Co.

White, O. R. (editor). 1977. *The Solar Output and Its Variation*. Colorado Assoiated University Press.

Willson, R. C. 1973. "New Radiometric Technique and Solar Constant Measurements." *Solar Energy*. No. 14, p. 203.

CHAPTER 3

# SOLAR RADIATION AND ATMOSPHERIC INTERACTION

**Bo Leckner**
**Department of Energy Conversion**
**Chalmers University of Technology**
**S-71296 Goteborg**
**Sweden**

## 3.1 Introduction and Definitions

The quantity needed in solar energy applications is the radiant flux incident on a collecting surface. This flux consists of direct solar radiation, diffuse sky radiation, and reflected radiation from the surroundings.

The estimation of the amount of incident energy requires two types of information, geometrical and physical. Well-defined geometrical parameters relate the collecting surface with the sun and with its surrounding surfaces as "seen" from the collecting surface.

The physical information is the subject of the present chapter which deals with the quantity and characteristics of the solar radiation outside the atmosphere, its interaction with atmospheric constituents, and the reflective properties of surrounding surfaces. The path of the solar rays is expressed relative to the vertical path through the atmosphere by means of the relative air mass. In this context the air mass, m, becomes a purely geometrical quantity,

$$m = \frac{1}{\cos \Theta} \qquad (1)$$

where $\Theta$ is the solar zenith angle, with good accuracy for $z < 80°$. (However, in accurate calculations at larger zenith angles, this simple expression has to be modified because m depends on the composition of the atmosphere and refraction.)

The terms used to describe radiation in meteorology, heat transfer engineering, radiometry, etc., differ considerably. It is therefore necessary to state clearly the meaning of certain expressions, occurring in the present text. Essentially, the *U. S. A. Standard Nomenclature and Definitions for Illuminating Engineers, Illuminating Engineering Society,* (1967) is followed:

The terms radiation, irradiation, transmission, reflection and absorption describe processes.

The terms used to describe quantities are:

(Radiant) *flux* or *radiant power* $\Phi$ -
energy per unit time [W]

*Exitance* (M) -
the radiant flux leaving a surface per unit surface area [$W\ m^{-2}$]

*Irradiance* (E) -
the radiant flux incident upon a surface per unit surface area [$W\ m^{-2}$]

*Intensity* -
the radiant flux leaving a source per unit solid angle [$W\ sr^{-1}$]

*Radiance* (L) -
the radiant flux leaving or arriving at a surface in a given direction per unit solid angle and per unit of surface area projected orthogonal to that direction [$W\ m^{-2} sr^{-1}$]

Some terms used to describe properties:

*Reflectance* -
the ratio of the radiant flux reflected from a surface to that incident upon it [$\rho = \frac{\phi_r}{\phi_i}$] *

*Absorptance* -
the ratio of the radiant flux absorbed by a surface to that incident upon it [$\alpha = \frac{\phi_a}{\phi_i}$] *

*Spectral* -
contained within a small wavelength interval centered at a particular wavelength [$\lambda$]

*Total* -
usually means wavelength integrated

### 3.2 Character of Extraterrestrial Solar Radiation

The solar power (energy per unit time) incident on a unit surface element, oriented normal to the sun's rays outside the atmosphere of the earth at the mean sun-earth distance, is called the solar constant.

A value, often quoted in the solar energy literature, is 1.353 ± 0.021 kw $m^{-2}$ (Thekaekara, 1973) at mean sun-earth distance. Recently, a careful analysis of published results has lead to 1.3710 ± 0.0048 kW $m^{-2}$ with a 0.95 confidence interval (Crommelynck, 1977). The difference between the two values is principally due to the radiation scales on which the measuring instruments are calibrated. (The International Pyrheliometric Scale, IPS 1956, in the former case and an Absolute Scale in the latter case, the difference between the two scales being about 2%). A small seasonal variation owing to the ellipticity of the orbit of the earth amounts to -3.3% at aphelion and +3.4% at perihelion. (The reviewers have agreed that the value 1.373 kW $m^{-2}$ on Absolute Scale, given by White (1977), is the accepted value for the solar constant, or in recent terminology, the solar parameter.)

*See Table 1-4, page 1-8

The spectral distribution of extraterrestrial solar irradiance, expressed as average values over narrow spectral intervals, has been published by Thekaekara (1973). In some parts of the spectrum, the uncertainty in the spectral values is considerably greater than that in the integrated solar constant value. The distribution follows approximately the Planck distribution of a blackbody at 5760 K but deviates in some spectral regions due to variations in opacity of the sun's atmosphere. The part of the extraterrestrial spectrum shown in Figure 3-1a contributes about 99% of the solar constant. Due to absorption and scattering in the earth's atmosphere, the energy reaching the ground is always less than the extraterrestrial amount.

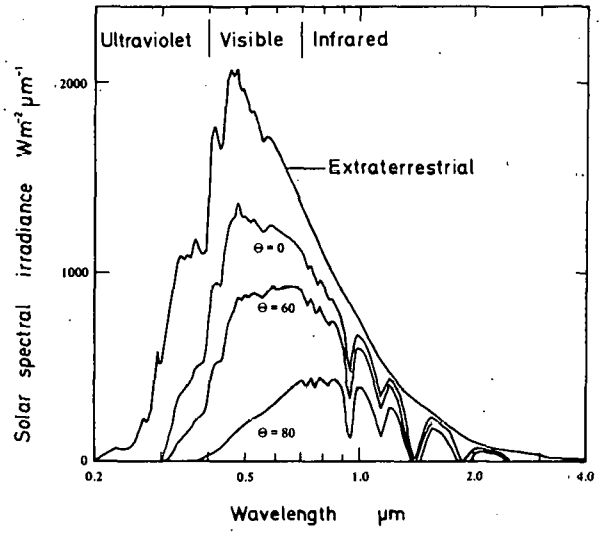


*Figure 3-1a The extraterrestrial spectral irradiance (Thekaekara, 1973) compared with the direct spectral irradiance at a surface normal to the beam at ground level, calculated with data from Leckner (1978) and vertical amounts of ozone 0.3 $cm_{STP}$, water vapor 1.0 g $cm^{-2}$. Turbidity coefficient $\beta = 0.1$ and $\alpha = 1.3$.*

### 3.3 Absorption by Atmospheric Constituents

The absorption of a beam of solar radiation along a path through the atmosphere is given theoretically by Bouguer's law:

$$E_\lambda = E_{o\lambda} \exp(-\Sigma_i k_{\lambda i} a_i m) \qquad (2)$$

where

$\downarrow E_{o\lambda}$ is the extraterrestrial irradiance at wavelength $\lambda$

$\downarrow E_{\lambda}$ is the irradiance at the end of a path of length m air masses

$a_i$ is the amount of the absorbing medium, i, integrated along a vertical column through the atmosphere. The total amount of this medium along the path is $a_i m$

$k_{\lambda i}$ is the absorption coefficient at wavelength $\lambda$ of this medium, i.

Among the atmospheric constituents that absorb in the solar spectrum are the following:

- Ozone whose electronic transitions give rise to a series of absorption bands that prevents practically all solar radiation with wavelengths shorter than 0.3 $\mu$m from reaching the ground. The absorption decreases with increasing wavelength, allowing some solar radiation to pass through the atmosphere at about 0.3 $\mu$m. At about 0.35 $\mu$m the ozone absorption is negligible. Another ozone absorption band system extends from about 0.4 to about 0.8 $\mu$m with its largest absorption coefficients around 0.6 $\mu$m.

- Water vapor whose vibration-rotation transitions give rise to absorption in a number of wavelength regions, appearing as bands centered at 0.72, 0.81, 0.94, 1.1, 1.38, 1.87, 2.7 and 3.2 $\mu$m. The bands actually consist of a fine structure whose lines have absorption coefficients varying rapidly with wavelength.

- Uniformly mixed gases, such as $CO_2$, $NO_2$, CO, $O_2$, and $CH_4$ absorb in narrow bands. Their contribution to absorption is small and often neglected.

- Particles suspended in the atmosphere, dust, haze and clouds attenuate the solar beam by scattering, but also by absorption to some extent. The quantitative importance of particle absorption is not well known, but probably is significant only in the wavelength region beyond 2 $\mu$m. The particle absorption is often treated together with scattering under the term *extinction*.

A rigorous evaluation of the absorption according to Eq. (2) would be extremely time consuming due to the complex line structure of most absorption bands. Band models are used instead, expressing effective absorption coefficients for narrow spectral intervals. In Leckner (1978) such effective absorption coefficients are listed for the spectral intervals given in Thekaekara's tabulation of extraterrestrial spectral irradiance. Eq. (2) is then valid using effective absorption coefficients of water vapor and uniformly mixed gases, i.e., $f(k_{\lambda H_2O} a_{H_2O})$ and $f(k_{\lambda g} a_g)$, respectively. From Figure 3-1b it can be seen that the principal contributions to absorption result from ozone in the ultraviolet and from water vapor in the infrared range. The small contributions from the uniformly mixed gases is partly overlapped by the water vapor bands.

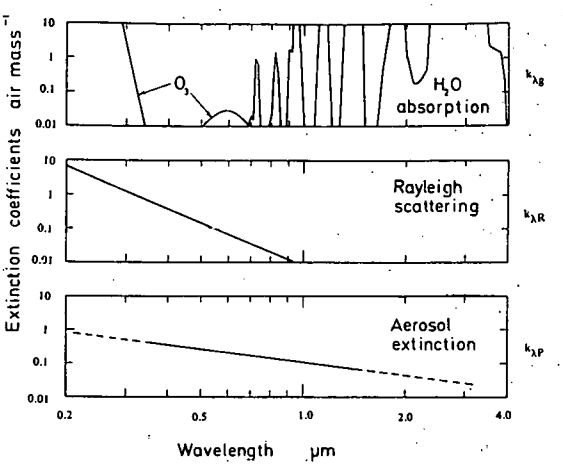


*Figure 3-1b Effective extinction coefficients of a vertical path through the atmosphere. Data as in Figure 3-1a.*

The vertical amounts of water vapor and ozone vary with time and location. Using average water vapor values published in, e.g., Schüepp (1966), one can make a first estimate of the absorption.

This estimate is sufficient for many purposes, since the incremental absorption owing to variations in amount around an average value is quite small, e.g., even a tenfold increase in the amount

of water vapor results in only about a 5% decrease in the total direct irradiance. The variations due to changes in the amount of ozone are even smaller. The practical consequences in the total (wave-length integrated) direct irradiance are illustrated in Figure 3-2, to be further explained below.

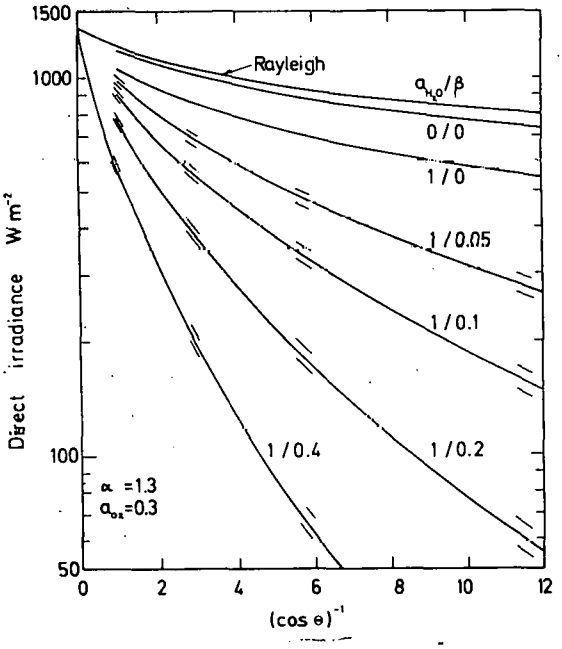


*Figure 3-2 Calculated total direct irradiances at a perpendicular surface as a function of air mass for various atmospheric conditions. Data as in Figure 3-1a. The influence of half or double amounts of water vapor is indicated by the thin lines.*

Representations of the total atmospheric absorptance of each absorbing medium treated separately should be interpreted with care. Absorption and scattering overlap each other to some extent as shown in Figure 3-1b. Thus, total quantities are preferably expressed in the form of a measure of total extinction such as turbidity or transmission factor, which includes absorption as well as scattering.

### 3.4 Scattering by Atmospheric Constituents

The energy removed from the direct solar beam by absorption is converted into internal energy of the absorbing medium. The energy removed by scattering, on the other hand, is redistributed in all directions without changes in wavelength. Consequently, two aspects of scattering are important: attenuation of the direct beam and spatial distribution of the scattered radiation.

Particles suspended in the air as well as the air molecules themselves have the ability to scatter. The attenuation follows Bouguer's law, Eq. (2). It can be shown theoretically that the scattering coefficients to be used with the absorption terms in Eq. (2) can be approximated by:

$$k_{\lambda s} = \text{const}\ \lambda^{-a} \qquad (3)$$

Constant in this equation is proportional to the amount of scattering matter.

Since the number of molecules in a vertical column of the atmosphere is known, the molecular or Rayleigh scattering is well defined by:

$$K_{\lambda R} = 0.008735\ \lambda^{-4.08}\rho/\rho_o \qquad (4)$$

where $\rho_o$ is the air density at 273 K and 1013 mb. The term $\rho/\rho_o$ is a correction for other ground-level conditions. The aerosol particles originate from a number of different sources. They consist mainly of dust emanating from the ground, water and ice particles arising through condensation nuclei of hygroscopic salts on which water is condensed to a larger or smaller extent, and, finally, of locally important man-made air pollution. To the variation in chemical composition can be added large variations in size, size distribution, and vertical amount. If minor complications are disregarded, the constant in Eq. (3) can be said to depend on the amount of particles, whereas the wavelength-exponent $a$ varies with their size distribution. Aerosols composed predominately of very small particles tend to have an $a$ approaching the molecular limit of 4. Distributions dominated by very large particles like those in fog or cloud lead to wavelength exponents $\approx 0$. Between these extreme limits, the majority of aerosols have values in the range $1 < a < 2$.

All the alternating factors normally are not known from ground level. Therefore, the aerosol scattering (or rather extinction) coefficient is evaluated from measurements for a given path through the atmos-

phere. An account of the measurement technique traditionally used is given in the *IGY Instruction Manual* (1958). Such measurements as well as calculations are based on Eq. (3):

$$K_{\lambda p} = \beta\lambda^{-\alpha} \tag{5}$$

where $\beta$ is called the turbidity coefficient. When $\alpha = 1.3$, this is Ångström's expression. Ångström (1961) and Volz (1955) concluded after numerous measurements in the visible spectral region that $\alpha \approx 1.3$ is a reasonable average value, although a considerable variation in the range $0.5 \lesssim \alpha \lesssim 2$ was observed. Eq. (5) is useful as a computational model of aerosol extinction. However, if the equation is employed to obtain $\beta$ from measurements assuming $\alpha = 1.3$, a "virtual" variation in $\beta$ may result if the aerosol corresponds to a wavelength exponent $\alpha \neq 1.3$ at the occasion when the measurements are made. Eqs. (4) and (5) are plotted in Figure 3-1b.

The incident beam is scattered in all directions from a scattering particle, with back and forward directions dominating. In molecular scattering the back and forward fractions scattered are equal. For scattering from larger particles the forward-scattered fraction is much larger than the back-scattered fraction, while the intensity of scattered radiation tends to be strongly peaked forward in directions close to that of the original beam. As a consequence of the angular distribution of scattered radiation, the radiance of the resultant sky radiation is unevenly distributed over the sky, having its largest values in the vicinity of the sun and its smallest in the part of the sky opposite the sun. Only in a very dense medium, such as cloud or fog, does multiple scattering even out the spatial distribution. Thus, the radiance distribution of an overcast sky is more regular than that of the clear sky and is given by the Moon-Spencer formula, where L is the luminance and $\Theta$ is the zenith angle.

$$L(\Theta) = \frac{L(\Theta = 0)(1 + 2\cos\Theta)}{3} .$$

This equation gives the approximate radiance distribution of the cloudy sky. The radiance distribution of a clear sky may be gained from the numerous luminance measurements. (*CIE*, 1973 and Tonne and Normann, 1960).

### 3.5 Resultant Solar Radiation at the Ground

The resultant solar radiation at the ground is expressed as direct, diffuse, and global radiation.

The flux of radiant energy at a unit surface element at the ground, expressed in W $m^{-2}$, is an ambiguous quantity, unless the inclination of the receiving surface element is specified. Measurements are usually made with horizontal surfaces or surfaces normal to the sun, whereas solar energy devices may have any orientation.

#### 3.5.1 Direct (beam) Radiation

The direct solar irradiance arrives at a receiving surface from the geometrical disc of the sun. The direct irradiance related to an actual surface is:

$$\downarrow G_{bi} = G_b \cos i \tag{6}$$

where i is the angle of incidence to the surface normal. For a horizontal surface $i = \Theta$ the solar zenith angle.

The magnitude of the direct irradiance depends on the attenuation in the atmosphere. With absorption and scattering coefficients from Leckner (1978) the total direct irradiance is calculated by summing over all wavelength intervals $\Delta\lambda$

$$G_b = \sum G_{b\lambda}\Delta\lambda \tag{7}$$

for various assumed atmospheric conditions, Figure 3-2. The uppermost curve in the diagram corresponds to the attenuation of pure Rayleigh scattering and the second curve to the additional influence of ozone and the uniformly mixed permanent gases. These artificial atmospheres are both referred to in the literature as "the dry and perfectly clean atmosphere". The third curve shows the effect of adding water vapor. The remaining curves represent real atmospheres with various aerosol contents expressed by the turbidity coefficient $\beta$ according to Eq. (5). The relatively small importance of half or double amounts of water vapor is indicated by the thin lines on both sides of the curves.

Unfortunately, the amount of aerosol is usually not known, so that the diagram can only serve as an approximate aid for correlating with standard measurements. The purpose of measurements is usually to define standard conditions with a seasonal variation for a certain location. An interesting example of this is the data on direct irradiance given in the *ASHRAE Handbook of Fundamentals* (1972), which, although correlated empirically, do fit into Figure 3-2.

Another way of expressing the attenuation of the atmosphere is by means of the turbidity factor, T, defined as:

$$G_b = G_{bo} \exp(-TK(m)m) \qquad (8)$$

where $G_{bo}$ is the solar constant. K(m) is the wavelength-integrated absorption coefficient of the dry and perfectly clean atmosphere. Internationally agreed-upon values of K(m) are listed in *I.G.Y. Instruction Manual* (1958). T is equal to one for the dry and clean atmosphere and thus expresses the number of such atmospheres that corresponds to a real atmosphere. The turbidity factor has been related to the effective absorption coefficient, K, in an effort to obtain a measure of turbidity that is independent of air mass. Only then is T a real measure of the atmospheric condition. This has not been completely successful since there is a small dependence on air mass for constant atmospheric conditions (at air mass 2 the variation is less than 0.25). The turbidity factor deals with the entire attenuation of the direct beam whereas the turbidity coefficient involves only the aerosol extinction. Details on definitions and measurement techniques used to T and $\beta$ are found in *I.G.Y. Instruction Manual* (1958).

A simple measure of the attenuation of direct radiation, specially intended for solar energy application does not exist. The above-mentioned methods are useful, but they suffer from certain drawbacks, some of which are pointed out in *I.G.Y. Instruction Manual* (1958). Also, to establish seasonal average values of turbidity, an internationally accepted recommendation concerning the selection of atmospheric conditions suitable for measurements should be made. It is evident that the presently used "standard" values depend somewhat on the observer's subjective choice on the occasions suitable for measurements.

In this Handbook, Chapter 8 and Appendix II prefer the Schüepp turbidity coefficient, B, whereas in the present chapter the Ångström turbidity coefficient, $\beta$, is used for convenience. The relationship between the two coefficients is approximately

$$\beta = 0.935B.$$

They are measured in different ways, however.

The above discussion deals with the (most important) case of direct irradiance unaffected by clouds. The attenuation by clouds ranges from the slight influence of fairly transparent cirrus clouds to total extinction of thicker cloud layers. These cases have to be treated with direct measurements and statistical methods. Some examples are given in the section treating global radiation.

### 3.5.2 Diffuse Radiation

The irradiance of the solar radiation scattered from the sky onto a receiving surface is called "diffuse radiation" or "sky radiation". If the radiation from all directions is integrated over the sky, the following equation describes the diffuse radiation as "seen" from the receiving surface:

$$G_d = \int_0^{2\pi} d\psi \int_0^{\Theta'(\psi)} L(\Theta,\psi) \cos i \sin\Theta \, d\Theta \qquad (9)$$

Here

$\Theta,\psi$ define the position in a hemispherical sky; $\Theta$ is the angle from zenith and $\psi$ is the azimuth angle;

i is the angle of incidence subtended at the receiving surface, from the surface normal to a position in the sky at $(\Theta,\psi)$;

$\Theta'(\psi)$ defines the horizon as seen from the receiving surface. In the ideal case of a horizontal surface and an unobstructed horizon, $\Theta'(\psi) = \pi/2$;

$L(\Theta,\psi)$ is the radiance of the sky at $(\Theta,\psi)$. Due to the angular distribution of scattered radiation, the radiance varies over the sky, having its largest values near the sun and

its smallest in the part of the sky opposite the sun.

When the diffuse sky radiation is received on a horizontal surface from a hemispherical sky, only the total quantity need to be considered. On the other hand, when parts of the sky are obstructed either by surrounding structures or by an inclined receiving surface, the radiance distribution may be important. The surface turned towards the sun will receive a larger part of the total sky radiation than the surface turned away from it. The irradiation on inclined surfaces will be treated in detail in Chapter 4. Here, it is sufficient to mention that the isotropic sky approximation, $L(\Theta,\psi)$ = constant, is often justified in view of its small importance relative to the contribution from direct radiation. Then Eq. (9) can be solved for sky irradiance at a surface inclined at an angle $a$ to the horizontal plane having an otherwise free horizon yielding

$$G_d = \frac{G_{dh}(1 + \cos a)}{2} \qquad (10)$$

where $G_{dh} = \pi L$ is the sky irradiance at a horizontal surface.

The magnitude of diffuse sky radiation depends on solar elevation, the amount and type of aerosol and cloud. It is also influenced by the albedo of the ground, since reflected radiation from the earth's surface is back-scattered from the atmosphere to some extent. The clear sky diffuse irradiance at a horizontal surface may be estimated, assuming that a fraction, $\kappa$, of the energy lost from the direct beam by scattering is effectively scattered downwards:

$$G_{dh} = \kappa(G_{bg} - G_b)\cos\Theta \qquad (11)$$

where $G_{bg}$ is the direct irradiance, if subjected only to gaseous absorption, Figure 3-3. With $\kappa \approx 0.5$ this equation has been found to fit some long-term experimental data (Leckner, 1978).

Measurements by Valko (1966) show the general trend of diffuse radiation from a sky partly covered by clouds: a small increase with cloudiness until a cloud cover of three to four tenths, then a strong increase with a maximum of about four times the corresponding clear sky value at a cloudiness around eight tenths. The sky radiation from the completely covered sky is usually lower than that of a clear sky.

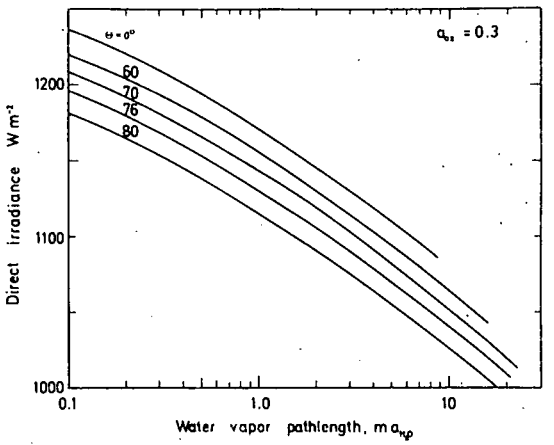


*Figure 3-3 Calculated total direct irradiance in a fictitious, purely absorbing atmosphere, expressed as a function of water vapor pathlength $m \cdot a_{H_2O}$ for various zenith angles $\Theta$. Calculated with data from Leckner (1978) and an ozone amount of 0.3 $cm_{STP}$. The influence of a change in ozone amount is negligible.*

Only in case of middle clouds (altostratus, altocumulus ~ 2500-6000 m) are higher values observed. It is obvious that the maximum depends on the contribution of scattered (or "reflected") radiation from the bright side of the clouds. When the sky is completely covered this effect vanishes. This scattering is particularly noticeable from cloud edges near the sun. Contributions from such reflections give extremely high irradiances of short duration, which are typically illustrated in actual recordings (Meinel and Meinel, 1976). It is also evident from the measurements by Valko that a "clear sky" may be covered by a few tenths of clouds, especially if the clouds are far from the sun.

### 3.5.3 Global Radiation

Global radiation is the sum of the direct and diffuse radiation from the sky. It is usually defined for a horizontal receiving surface, exposed to a hemispherical sky

$$G = G_b \cos\Theta + G_{dh} \qquad (12)$$

G is the quantity measured at meteorological stations.

In solar energy applications, the global irradiance at a surface of any defined orientation and surrounding is of interest:

$$G = G_b \cos i + G_d + R \qquad (13)$$

where R is the reflected radiation from the surroundings incident on the receiving surface. In this case the global radiation depends not only on meteorological conditions but also on the location and the orientation of the receiving surface; however, the denomination *global radiation* is maintained rather than *total radiation*, since the word *total* is commonly used with the meaning of "wavelength-integrated".

In order to transform global radiation data measured on a horizontal surface to that on an inclined surface, a separate estimate of the direct or the diffuse component is required. Furthermore, the reflected component must be determined.

When the amount of global radiation available during a period of time is evaluated, the problem associated with clouds can not be avoided in most climates. Here, measurements and correlations of measurements are used. The intended application and the type of data available determine the way in which the global radiation data are handled. Some approaches will be briefly exemplified:

- Daily global radiation (or sometimes monthly mean daily global radiation) $\bar{G}$ relative to the corresponding amount outside the atmosphere $\bar{G}_o$ is expressed as a function of the duration of sunshine $\bar{S}$ relative to the corresponding possible duration of sunshine $\bar{S}_o$ with a relationship such as

$$\frac{\bar{G}}{\bar{G}_o} = a + b\frac{\bar{S}}{\bar{S}_o} \qquad (14)$$

where a and b are coefficients to be determined (see Chapter 10, Tables 10-2 and 10-3). Examples of applications are given by Ångström (1957) and Exell (1976). Formulas of this kind, often with refinements, are employed for climatological studies of the geographical distribution of global radiation, since the places where the duration of sunshine is registered are more common than those where radiation measurements are made. The information given by this climatological description is mostly qualitative for solar energy applications. However, with some approximation, it can also be used for calculations as indicated below.

- The monthly mean value of relative daily global radiation characterizes somewhat the monthly variation of relative daily global radiation $\bar{G}/\bar{G}_o$ plotted in a cumulative frequency diagram, Figure 3-4; this has been shown by Liu and Jordan (1960) and in an equivalent way using $\bar{S}/\bar{S}_o$ by Schüepp (1966). Liu and Jordan also present an empirical relationship between diffuse and global radiation and a method of calculating average hourly values which are symmetrically distributed about noon. In another paper (Liu and Jordan, 1963) these authors show how to calculate global irradiance at inclined surfaces and how to predict the long-term performance of flat-plate solar collectors. Their work was to some extent dependent on the data available at that time. With more data, refinements and developments along similar lines are possible. It is important to notice, however, that the smoothed values given are not sufficient for studying the dynamic behavior of solar energy systems. If the dynamic behavior is significant, erroneous estimates of the amount of collected energy may result.

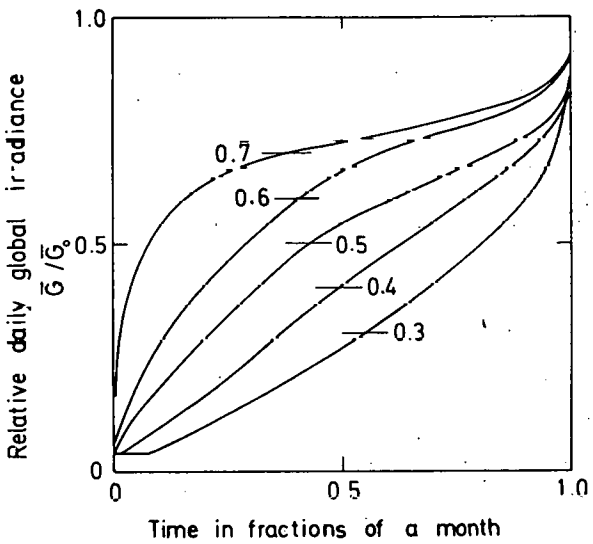


*Figure 3-4 Generalized cumulative frequency diagram for relative daily global irradiance at a horizontal surface according to Liu and Jordan (1960). Monthly average values are shown on each curve.*

- Hourly values or instantaneous radiation measurements at the solar energy collector are, of course, the best source of accurate information. Hourly values together with other relevant meteorological data, such as air temperature, have been used in simulations of thermal solar energy systems, Klein et al (1976). An interesting approach using Fourier transforms of the instantaneous solar input and of the system response is mentioned by Meinel and Meinel (1976).

More work on the accuracy and usefulness of simplified methods is desirable.

### 3.5.4 Spectral Quality

The simple spectral model mentioned above (Leckner, 1978) expresses the direct irradiance at a surface normal to the beam by means of Eqs. (2), (4) and (5):

$$G_{b\lambda} = G_{bo\lambda}\exp[-(k_{\lambda oz}a_{oz} + f(k_{\lambda H_2O}a_{H_2O}) + f(k_{\lambda g}a_g) + k_{\lambda R} + k_{\lambda p})m] \quad (15)$$

and the clear sky diffuse irradiance on a horizontal surface is obtained from Eq. (11):

$$G_{dh\lambda} = \kappa[G_{bo\lambda}\exp(-(k_{\lambda oz}a_{oz} + f(k_{\lambda H_2O}a_{H_2O}) + f(k_{\lambda g}a_g))m) - G_{b\lambda}]\cos\Theta \quad (16)$$

The corresponding spectral global irradiance on a horizontal surface is

$$G_\lambda = G_{b\lambda}\cos\Theta + G_{dh\lambda} \quad (17)$$

Some calculations have been made in which it was assumed that the aerosol extinction follows Eq. (5) with $\alpha = 1.3$ over the entire spectral region for solar zenith angles $\Theta = 0$, 60 and 80°. Results are expressed in Figure 3-5 as the fraction of total irradiance below a certain wavelength. As expected, the direct irradiance loses more energy in the short wavelength region at greater solar zenith angles (see also Figure 3-1a). The wavelength corresponding to an irradiance fraction of 50%, the mean energy wavelength, also becomes larger. The spectral distribution of global radiation, however, is fairly constant and can be approximately represented by one curve. This is due to a balance between the radiation back-scattered into space in the short-wave region and

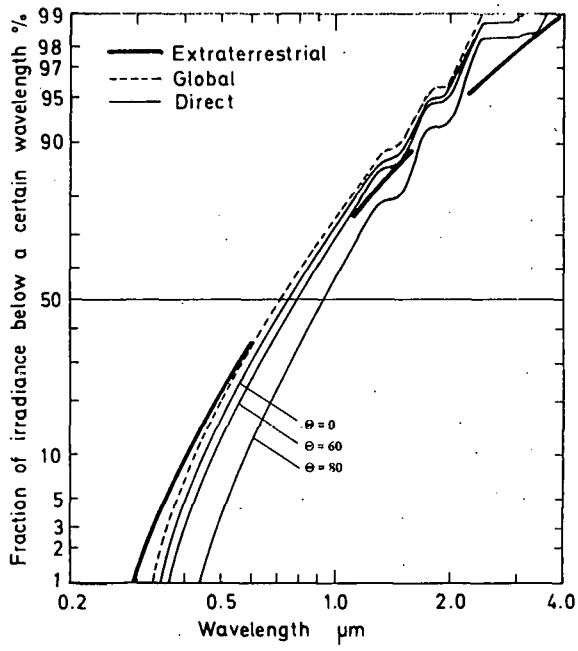


*Figure 3-5 Fraction of the total irradiance below a certain wavelength. Extraterrestrial curve according to Thekaekara (1973). Remaining curves calculated from data in Leckner (1978) and Figure 3-1a and 3-1b.*

the absorption by water vapor in the long-wave region. The balance is well maintained under all normal atmospheric conditions. Figure 3-6 illustrates this in the form of spectral global irradiances normalized with that at 0.5 μm. Figure 3-5 shows that 98 to 99% of the total global or direct radiation is below 2.3 μm.

The above calculation was made for amounts of ozone of $a_{oz} = 0.3$ $cm_{STP}$, $a_{H_2O} = 1$ g $cm^{-2}$, and a turbidity of $\beta = 0.1$ but is qualitatively true for other normal atmospheric conditions also.

## 3.6 Surface Reflection

### 3.6.1 Definitions and General Character

There are two types of reflection important for solar energy applications: specular (mirror) reflection and diffuse reflection. The geometrical relationships for specular reflection are found in the optical literature or, as applied to solar energy, in Meinel and Meinel (1976). In the present section, specular reflection is mentioned only as a special case; diffuse reflection is therefore emphasize.

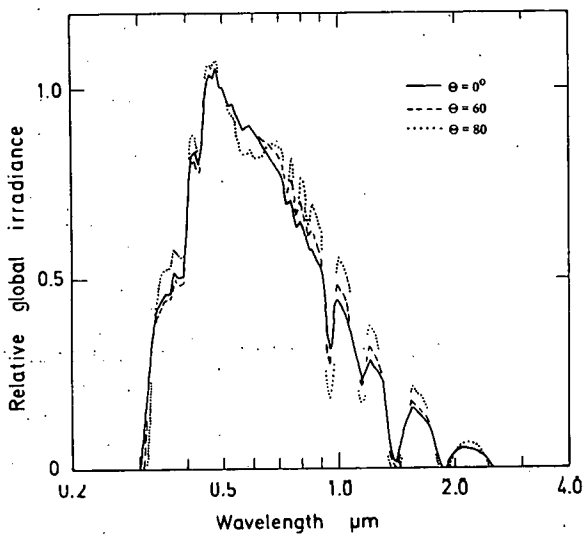


*Figure 3-6 Relative global spectral irradiance at various zenith angles, normalized at a wavelength of 0.5 μm. Calculated with data from Leckner (1978) and Figure 3-1a and 3-1b.*

The intensity of radiation reflected from a perfectly diffuse reflector is proportional to the cosine of the angle to the surface normal. This is a consequence of Lambert's cosine law. Since the projected area of the reflecting surface also varies with the cosine of the same angle, the radiance of such a surface is independent of the viewing angle. (On visual observation, the surface appears equally bright from all viewing angles.) The distribution, but not necessarily the magnitude, of the reflected flux at the perfectly diffuse reflector.

The reflection from real surfaces may approach either the ideal specular or diffuse limit, but very often has an intermediate distribution (see Figure 3-7). The directional distribution of the reflected flux depends not only on the surface material, but also on the surface condition (roughness, purity and temperature) and the directional distribution of the incident flux.

The ideal, spectrally independent surface is called a *grey surface.* In practice, few surfaces approach this since significant spectral variations often occur depending on the surface characteristics and its material composition.

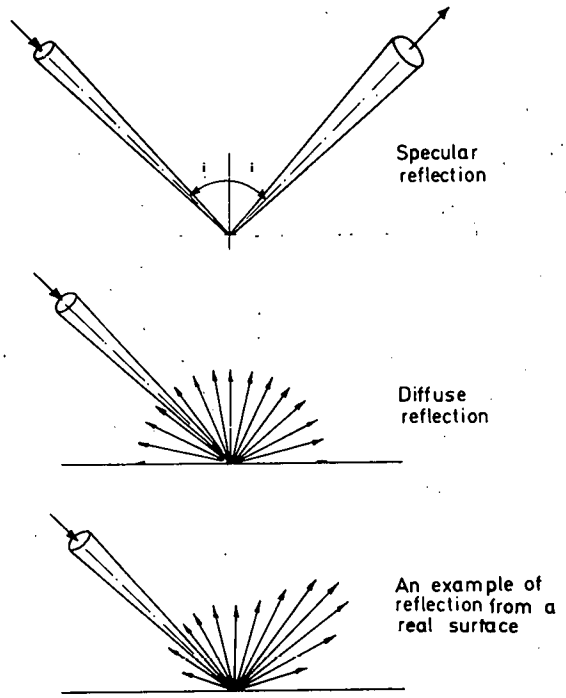


*Figure 3-7 Examples of directional distribution of the radiance of reflected radiation from an incident beam. The figures show the plane of incidence.*

The reflection from optically smooth (the degree of surface roughness is much less than the wavelength of the radiation) and clean surfaces can be predicted by electromagnetic theory. Metal surfaces are good reflectors and tend to be specular reflectors, while non-metals are not as good and tend to be diffuse reflectors. Some influencing factors may be listed:

- many types of surface reflect all the incident radiation when the angle of incidence is large
- small scale roughness has a diffusing effect
- impurities, oxide coatings or layers and deliberately applied layers may change the reflecting characteristics completely. It should be noted that thin layers, e.g., of paint or even metals, may be partly transparent, so that a combined effect of the layer and the original surface occurs. Thickness, absorption capacity of the layer and wavelength of the incident radiation are also important parameters.

It is difficult to give a general description of the reflection properties of all surfaces, as illustrated by the extensive compilation of measurements on radiant surface properties presented by Touloukian (1972).

The ratio between reflected and incident flux is called reflectance. The total reflectance is defined as

$$\rho = \frac{\int_0^\infty \rho_\lambda G_\lambda d\lambda}{G} \qquad (18)$$

It can be seen from the integral in Eq. (18) that the total reflectance is affected by the wavelength distribution of the irradiance G, if a certain wavelength variation in $\rho_\lambda$ is assumed . In the special case when G is the global solar irradiance, $\rho$ is called the solar reflectance or albedo. Since the spectral distribution of the global radiation is practically invariable, the total solar reflectance is not influenced by wavelength variations in the irradiance once the integration has been carried out. If the reflecting surface is not even and diffusely reflecting, however, the solar reflectance will depend on the directional distribution of the incident global flux and consequently on the state of the sky and the position of the sun. The directional distribution of the reflected flux is also influenced and deviates from the constant radiance distribution implicitly assumed.

Thus, for refined calculations more exact measurements of reflection are needed. This subject is treated in detail in the heat transfer literature (see, e.g., Seigel and Howell, 1972). Some definitions are given below:

- The bidirectional reflectance. The incident flux is contained within a solid angle $d\Omega_i$ at a position defined by the angular coordinates $\Theta_i$, $\psi_i$, and the reflected flux is contained within $d\Omega_r$ at $\Theta_r$, $\psi_r$ (see Figure 3-8).

- The hemispherical-directional reflectance. The incident radiation is integrated over the hemisphere, and the reflected flux is observed within a solid angle $d\Omega_r$ at $\Theta_r$, $\psi_r$.

- The directional-hemispherical reflectance. The incident flux is contained within a solid angle $d\Omega_i$ at $\Theta_i$, $\psi_i$, and the reflected radiance is integrated over the hemisphere.

The bidirectional reflectance depends on surface conditions and the four angles $\Theta_i$, $\psi_i$, $\Theta_r$, $\psi_r$, whereas the other reflectances only depend on two angles. The solar reflectance, on the other hand, is assumed independent of angles.

In calculations, the simplest possible measure of reflection, the total solar reflectance, is preferred. However, one should be aware of possible deviations from the assumptions of diffuse radiation incorporated in this parameter.

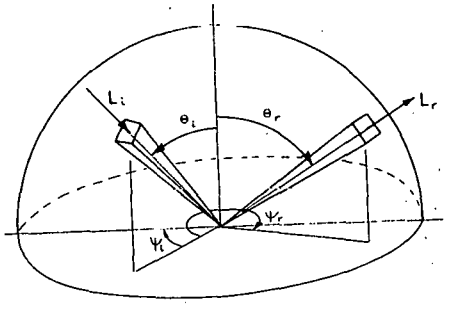


*Figure 3-8 Geometry showing an incident beam of radiance $L_i$, and reflected beam of radiance $L_r$, for the definition of directional reflectances.*

### 3.6.2 Albedo of Natural Surfaces

A survey of measurements of the total albedo of natural surfaces is given by Kondratyev (1972) who represents the albedo either as a function of the state of the surface and solar elevation or as daily, monthly and seasonal mean values.

Table 3-1 compiled by Bartman (1967) and quoted by Kondratyev (1972), illustrates the character of the reflection from natural surfaces well and explains the reasons for variations in the albedo. Table 3, Appendix II provides specific ground reflectance values for various surfaces.

### 3.6.3 Reflectance From Man-Made Surfaces

*Man-made* implies that the surfaces are selected and prepared to fulfill a certain duty. Some examples are:

- Specular surfaces (mirror surfaces) are usually metals or metallic coatings on smooth substrates. Transparent coatings of various kinds are applied. Maintenance of high, specular reflection presents practical problems; degradation by oxidation, abrasion, dirt, etc., must be considered.

- Black surfaces are used to increase the absorption of incident radiation, i.e., the reflectance should be as small as possible. The thickness of the black layer and its surface roughness influence the reflection properties.

- Selective surfaces should be black in the solar spectral region but highly reflecting (i.e., poor emitters) in the infrared region $> 3$ $\mu$m in order to avoid thermal losses from the collecting surface. Selective surfaces are treated by Meinel and Meinel (1976).

- Diffusely reflecting (and absorbing) surfaces are used in many measuring instruments. Deviations from the diffuse property, often at large angles of incidence, lead to a *cosine error* in the instrument.

- Coatings are important for all the above-mentioned surfaces.

A compilation of measurements on coating is found in Volume 9 of *Thermophysical Properties of Matter* (Touloukian, 1972).

### 3.6.4 Implications for Solar Energy

The example given below is illustrative of Eq. (13) and shows how the magnitude of the reflected flux incident on an inclined plane collector surface may be calculated by using the diffuse approximation.

Table 3-1

Reflectance of Natural Surfaces

| SURFACE | SPECTRAL CHARACTERISTICS | ANGULAR DISTRIBUTION OF REFLECTANCE | TOTAL REFLECTANCE |
|---|---|---|---|
| Soils & Rocks | 1. Increasing to 1 $\mu$m<br>2. Decreasing above 2 $\mu$m<br>3. Moisture decreases reflectance | 1. Backscattering and forward scattering<br>2. Sand has large forward scattering<br>3. Loam has small forward scattering | 1. 5-45%<br>2. Moisture decreases reflectance by 5-25%<br>3. Smooth surfaces have higher reflectance<br>4. Diurnal variation, maximum reflectance for small sun angles |
| Vegetation | 1. Small (below 0.5 $\mu$m)<br>2. A small maximum bump between 0.5 and 0.55 $\mu$m<br>3. Chlorophyll absorption at 0.68 $\mu$m<br>4. Sharp increase at 0.7 $\mu$m<br>5. Decrease above 2 $\mu$m<br>6. Depends on growing season | 1. Backscattering<br>2. Small forward scattering | 1. 5-25%<br>2. Diurnal effects, maximum reflectance for angles<br>3. Marked annual variation |
| Water Basins | 1. Maximum in range 0.5-0.7 $\mu$m<br>2. Depends on turbidity and wave height | 1. Large back and forward scattering | 1. Small reflectance<br>2. Diurnal variation maximum for small sun angles<br>3. Depends on turbidity and wave height |
| Snow & Ice | 1. Decreases slightly with increasing wave length<br>2. Large variability depending on purity, wetness, physical condition | 1. Diffuse component plus specular component<br>2. Specular component increases with increasing angle of incidence | 1. Variable, 25-80%<br>2. 84% in Antarctic<br>3. 74% Ross Sea ice<br>4. 30-40% White Sea ice |

According to Eq. (10), a fraction, $F_{c-s} = (1 + \cos a)/2$, of the hemispherical isotropic sky radiation (index s) reaches the collector surface (index c). (See Chapter 8 for additional information.) Assume that the surrondings "seen" by the collector surface consist of a single diffusely reflecting surface (index i), which extends to the horizon. The albedo of the surface is $\rho_i$. If $G_i$ is the global irradiance at surface i, the reflected exitance is $\rho_i G_i$. A fraction, $F_{c-i}$, of this reflected radiation reaches the collector surface. Thus, the entire diffuse irradiance from sky and surroundings at the collector surface is

$$G_{dc} = G_{dh}F_{c-s} + \rho_i G_i F_{c-i} \qquad (19)$$

where $F_{c-s} + F_{c-i} = 1$ since an entire hemisphere is "seen" from the plane collector surface.

In a more complicated situation, the sky fraction and the fractions of n reflecting surfaces can be determined in the same way.

$$G_{dc} = G_{dh}F_{c-s} + \sum_{i=1}^{n} \rho_i G_i F_{c-i} \qquad (20)$$

The fractions, $F_{c-s}$ and $F_{c-i}$, are called angle factors or configuration factors; values of these evaluated for standard configurations are listed in, e.g., Siegel and Howell (1972), who also give methods of calculating the interreflections between diffuse surfaces or between combinations of ideal diffuse and specular surfaces.

Kondratyev (1969) presents some data on global irradiation at inclined surfaces that can be used to compare with calculated results using the relationships given in this chapter.

Sought: The global irradiance, $G_{s\psi}$, at an inclined surface relative to the corresponding irradiance at a horizontal surface G as a function of the angle of inclination $a$.

Given: Surface azimuth from sun $\psi = 0$. Clear sky.

a) March 23, 1959: $\Theta = 62°$, $\rho = 0.45$ (wet granular snow).

b) July 31, 1959: $\Theta = 62°$, $\rho = 0.20$ (summer conditions).

Assumed: Atmospheric conditions: $\beta = 0.07$ and $a_{H_2O} = 1.0$ g cm$^{-2}$.

Calculations: Eqs. (13) and (19) give

$$G_{s\psi} = G_b \cos(\Theta - a) + G_{dh}(1 + \cos a)/2 + \rho G(1 - \cos a)/2$$

Eq. (12) gives

$$G = G_b \cos\Theta + G_{dh}$$

and Eq. (11) gives

$$G_{dh} = 0.5(G_{bg} - G_b)\cos\Theta$$

From Figure 3-2, $G_b = 750$ W m$^{-2}$ and Figure 3-3, $G_{bg} = 1130$ W m$^{-2}$. Result: Figure 3-9.

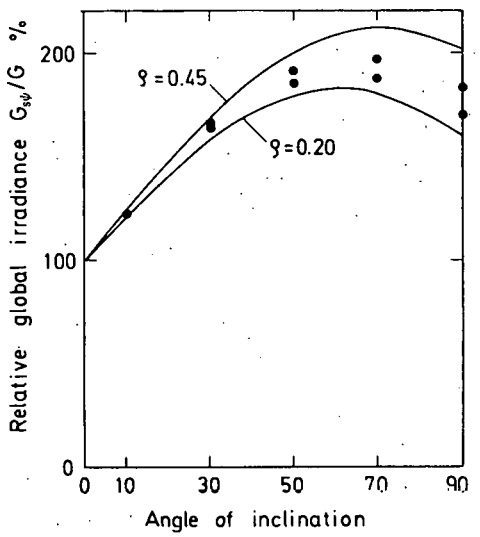


*Figure 3-9 Relative global irradiances at a surface inclined at an angle a and oriented towards the sun. Solar zenith angle $\Theta = 62°$. Albedo of surroundings $\rho = 0.45$ or $\rho = 0.20$. Full lines are measurements (Kondratyev, 1969). Points are calculated values.*

Discussion: The calculated results are as good as one could expect considering the simple method of calculation and the assumptions made. The essential errors are contained in the diffuse approximation. The diffuse-sky approximation leads to an underestimate of the contribution from sky radiation when the surface is inclined towards the sun (when $a$ approaches $\Theta$). The strong forward scattering of the

wet granular March snow also contributes to an underestimate, which increases with the reflected contribution, whereas the reflected radiation of the summer case is probably fairly diffuse. Figure 3-9 illustrates the reason for using the diffuse approximation in many practical calculations: the error, although large in comparison with the magnitudes of the sky and reflected radiation, is not serious relative to the global radiation, in which the direct radiation component is the most significant. A similar method and other examples for calculating the solar radiation received on inclined surfaces are given in Chapter 4, Sections 4.5.4 and 4.5.5, Chapter 8, Section 8.5, and *International Energy Agency Solar Heating and Cooling Program, Task V.*

**References**


Ångström, A. 1957. "On the Computation of Global Radiation from Records of Sunshine". *Arkiv. for Fysik*, No. 2, pp. 471-479.

Ångström, A. 1961. "Techniques of Determining the Turbidity of the Atmosphere." *Tellus*, No. 13, pp. 214-223.

ASHRAE. 1972. *Handbook of Fundamentals.* Chapter 22. American Society of Heating, Refrigeration and Air-Conditioning Engineers, New York.

CIE. 1973. "Standardization of Luminance Distributions on Clear Skies." CIE, No. 22.

Crommelynck, D. 1977. "Value of the Solar Constant Deduced from the Measurements made After 1960." Proceedings of the "Symposium on Radiation in the Atmosphere." Garmisch-Partenkirchen, August 1976. *Science Press.*

Exell, R. H. B. 1976. "The Solar Radiation Climate of Thailand." *Solar Energy*. No. 18, pp. 349-354.

*IGY Instruction Manual.* Part VI. 1958. "Radiation Measurements and Instruments." Pergamon Press, London.

Illuminating Engineering Society. 1967. "USA Standard Nomenclature and Definitions for Illuminating Engineers." *USAS* Z7. Illuminating Engineering Society, New York.

Klein, S. A., Beckman, W. A. and Duffie, J. A. 1976. "A Design Procedure for Solar Heating Systems." *Solar Energy*. No. 18, pp. 113-127.

Kondratyev, K. Ya. 1969. *Radiation in the Atmosphere."* New York: Academic Press.

Kondratyev, K. Ya. 1972. *Radiation Processes in the Atmosphere.* World Meteorological Organization. WMO- No. 309.

Leckner, B. 1977. "The Spectral Distribution of Solar Radiation at the Earth's Surface." *Solar Energy*. No. 19.

Liu, B. Y. H. and Jordan, R. C. 1960. "The Interrelationship and Characteristic Distribution of Direct, Diffuse and Total Solar Radiation." *Solar Energy*. No. 4, pp. 1-19.

Liu, B. Y. H. and Jordan, R. C. 1963. "The Long-Term Average Performance of Flat-Plate Solar-Energy Collectors." *Solar Energy*. No. 7, pp. 53-74.

Meinel, A. B. and Meinel, N. P. 1976. *Applied Solar Energy: An Introduction.* Reading, Mass.: Addison-Wesley Publishing Co.

Schüepp, W. 1966. *Solar Radiation.* N. Robinson, ed. Amsterdam: Elsevier Publishing Co.

Siegel, R. and Howell, J. R. 1972. *Thermal Radiation Heat Transfer.* New York: McGraw Hill.

Thekaekara, M. P. 1973. "Solar Energy Outside the Earth's Atmosphere." *Solar Energy*. No. 14, pp. 109-127.

Tonne, F. and Normann, W. 1960. "Die Berechnung der Sonnenwärmestrahlung auf Senkrechte und Beliebig Genieigte Flächen unter Berücksichtigung Meteorologischer Messungen." *Z. für Meteorologie.* No. 14. pp. 166-179.

Touloukian, Y. S., ed. 1972. *Thermophysical Properties.* Vol. 7, 8 and 9. New York: IFI/Plenum.

Valko, P. 1966. "Die Himmelsstrahlung in ihrer Beziehung zu Verschiendenen Parametern." *Arch. Met. Geoph. Biokl.* No. 14, pp. 336-359.

Volz, F. 1955. "Atmospheric Turbidity and its Spectral Extinction." *Geofisica Pura e Applicata.* No. 31, pp. 199-223.

White, O. R., ed. 1977. *The Solar Output and Its Variation.* Colorado Associated University Press.

**Bibliography***

Elssaser, M. with Culbertson, M. 1960. "Atmospheric Radiation Tables, Meteorological Monographs." *American Meteorological Society.* Vol. 4, No. 23, 43 pp.

Fraser, R. S. 1975. "Degree of Interdependence Among Atmospheric Optical Thicknesses in Spectral Bands Between 0.36-2.1." *Journal of Applied Meteorology.* Vol. 14, pp. 1187-1196.

Gates, D. M. and Harrop, W. J. 1963. "Infrared Transmission of the Atmosphere to Solar Radiation." *Applied Optics.* Vol. 2, No. 9, pp. 887-898.

Goody, R. M. 1964. *Atmospheric Radiation: Theoretical Basis.* Oxford Press.

Goody, R. M. and Robinson, G. D. 1951. "Radiation in the Troposphere and Lower Stratosphere." *Quarterly Journal of the Royal Meteorological Society.* Vol. 77, pp. 151-187.

Tomasi, C., Guzzi, R. and Vittori, O. 1974. "A Search for the e-Effect in the Atmospheric Water Vapor Continuum." *Journal of the Atmospheric Sciences.* Vol. 31, No. 1, pp. 255-260.

*Provided by:
Rudolfo Guzzi
Microfisica Dell'Atmosfera C.N.R.
Via De' Castagnoli
1 - 40126 Bologna
Italia

CHAPTER 4

# SOLAR RADIATION MEASUREMENT METHODS

J. R. Latimer
Atmospheric Environment Service
4905 Dufferin Street
Downsview, Ontario, Canada

## 4.1 General Discussion

### 4.1.1 Site Requirements Related to Solar Energy Applications

Keeping in mind that radiation data recorded at particular sites, for example, urban areas or demonstration structures, are often non-representative, it appears essential that judicious consideration should be given to site selection at the outset. Most studies acknowledge the substantial spatial and temporal variabilities of solar radiation regimes, and the observational and analytical limitations that restrict satisfactory evaluation of these variabilities. These difficulties interfere with the establishment of reliable long-term statistics and design criteria. Much of the macroscale (>100 km) character of radiation fields may be attributed to meteorological controls. For example, the marked difference of cloud regimes between maritime and continental areas is a major source of macroscale variability. At the mesoscale (~ 10-100 km) the dominant influences are generally topographical in origin. The siting of observing stations presents a challenge to those responsible for determining the essential character of the solar energy resource. Therefore, a number of useful site selection criteria follow below.

The site selected for a radiation instrument should be as free as possible from any obstructions, and at the same time, should be readily accessible for inspection. It is of particular importance that the site be free from obstructions in the azimuth from northeast through south to northwest (Northern Hemisphere). If practicable, a radiation instrument should be located so that (1) a shadow will not be cast on it at any time, (2) it is not in proximity to light-colored walls or other objects likely to reflect sunlight on it, and (3) it is not exposed to artificial radiation sources. If it is at all possible, the site should be chosen so that any obstruction in the azimuth range between earliest sunrise and latest sunset should have an elevation not exceeding 5°.

When measuring radiation on inclined surfaces, particular attention must be paid to the character of the section of topography "viewed" by the instrument. The albedo of the topography will have a nominal value with marked seasonal as well as diurnal components. The albedo of most surfaces increases with increasing solar zenith angle. During winter, a new snow cover may have an albedo exceeding 80%. In general, the terrain "viewed" should be uniform in character so that marked spatial variations of albedo close to the instrument location can be avoided. The sensor should view the same field as the collector device when measurements are taken at the site of application.

An excellent method of obtaining a survey record of an observation site is by means of a (horizon) camera which exposes azimuthal and elevation grid lines on the negative. A series of exposures should be made to identify the angular elevation and azimuth of terrain features and obstructions. If a survey camera is not available, the angular outline of obscuring objects may be mapped by means of a theodolite. Periodic surveys are useful to indicate seasonal changes, and to indicate significant changes caused by new obstructions. Site documentation should include altitude of observing station above mean sea level, height of instruments above station level, and geographical coordinates. It is also useful to have a site

plan, drawn to scale, showing the location of the radiation instruments, recording equipment and connecting cables, topographic features and contours, the direction of true north.

Probably the most important single consideration is the accessibility of instruments for daily inspection. It is most desirable that instrumentation be inspected daily, and more often when possible.

### 4.1.2 Instrument Considerations

Selection of the proper instruments is dependent upon the requirements and resources available. A list of instrument manufacturers is included in Appendix I and some details of instruments are discussed later.

### 4.1.3 Installation Considerations

Radiation instruments installed out-of-doors for continuous use should always be securely fastened to their intended mounting platforms. Precautions should always be taken to avoid subjecting radiation instruments to mechanical shock or vibration during installations. The structure on which instruments are mounted should be sufficiently rigid to prevent movement in windy weather.

Pyranometers should be fastened down using the holes provided in their baseplates. First the instrument is oriented so that the emerging leads or cable connection will be shaded during high sun periods, thus minimizing heating of the electrical connections. The pyranometer should then be secured lightly with screws or bolts; leveled by means of leveling screws and the attached spirit level, then fastened by tightening the retaining screws, taking care that the level setting is not disturbed.

Shading devices employed with pyranometers for measuring diffuse solar radiation, and equatorial drive systems employed with pyrheliometers for measuring direct solar radiation should be installed according to manufacturers' instructions. Such equipment usually requires adjustment over a period of time to achieve proper tracking.

The cable employed to connect a radiation instrument to a recording system should be twin copper conductor and waterproofed (A. W. G. No. 16 is suitable). The cable should be fastened down securely to minimize motion during windy weather. Whenever possible, cables should be placed underground when the recording system is located some distance away. It is generally advisable to use shielded cable in order to minimize electrical interference. With thermoelectric devices, care must be exercised to obtain a permanent copper-to-copper bond between connections prior to soldering. All exposed junctions must be weatherproofed. After identification of circuit polarity, cables should be connected to recording systems in accordance with relevant manufacturers' instructions. Particular care must be exercised when terminating cable shields to avoid ground loop currents.

### 4.1.4 Routine Maintenance

The exposed optical components of radiation instruments should be cleaned regularly during the daily inspection period. Components (e.g., glass hemispheres) should be wiped clean and dry. If frozen snow, glazed frost, hoar frost or rime ice is present the deposits should be very gently removed. If local pollution or sand forms a deposit, cleaning should be carried out carefully, preferably after blowing off most of the loose material or after wetting it a little, in order to prevent scratching the surface. Such abrasive action can appreciably alter the original optical properties of the material.

The level of each sensor should be checked, and desiccators recharged with active material if necessary. Any shading device for measuring diffuse radiation and equatorial drives should be reset. Recording equipment should be inspected and maintained according to relevant manufacturer's instructions.

### 4.1.5 Sensor Characteristics

#### 4.1.5.1 Variation of Response with Angle of Incidence

The dependencies of the directional response of the sensor on the elevation and azimuth of the solar radiation beam received are usually known as the Lambert cosine response and the azimuth response, respectively. Ideally the response of the receiver is proportional to the cosine of the zenith angle of the radiation received and is constant at all azi-

muth angles. For pyranometers it is convenient to assess the percentage error relative to the sun's elevation of 10° on a clear day. Integral errors caused by departure from ideal response of the sensor should not exceed 5 to 7% for pyranometers (WMO, 1968).

#### 4.1.5.2 Temperature Response

Many radiation sensors exhibit a change in response with variation in ambient temperature. Some instruments are equipped with built-in temperature compensation circuits in an effort to minimize this effect over a wide temperature range. The temperature variation of the instrument response may be measured in a temperature-controlled chamber. A temperature coefficient should then be used to apply a suitable correction to the radiation data.

#### 4.1.5.3 Linearity

Throughout the normal range of response of a sensor the output signal should be proportional to the radiation received. The response of radiation instruments should be within ±2% of being linear (WMO, 1968).

#### 4.1.5.4 Spectral Response

Errors caused by departure from the required spectral response of the sensor should not exceed ±2% over the range of interest (WMO, 1968). Instruments which have thermoelectric sensors that are coated with suitable materials, e.g., Parson's Black or 3M Velvet Black, and also have selected optical grade components usually present no spectral response problem. Photo detectors, however, usually exhibit large variations of spectral response and have not been used successfully to measure radiant flux over a wide spectral range.

#### 4.1.5.5 Response Time

Radiation sensors should have first-order response, non-oscillatory or critically damped characteristics. In such cases, the response time is called the time constant and corresponds to the elapsed time required for the output signal to be reduced to 1/e or 36.8% of its initial value. The time constant of radiation sensors should be less than 1 min since, as a rule, it is necessary to wait up to 5 times this amount of time to obtain a "steady state" signal during calibration. Fast response instruments (time constant less than 1 s) are seldom necessary for most solar energy applications.

### 4.1.6 Electronic Integration and Averaging Techniques

There are a variety of ways by which the signals from radiation instruments are recorded. One common method is by means of a potentiometric strip-chart recorder. Multi-channel recorders are available if several sensors are required. Chart recorders are useful for their detailed permanent record, and as a means of quality controlling the data. More recently it has become the vogue to employ multi-channel automatic data-logging systems, either measuring instantaneous values or using electric integration. When instantaneous readings are recorded, the time interval over which the series extends, and the number of data values making up the measurement, should be large enough to ensure that the mean derived yields a representative value for the time interval. Electronic integration is a useful method of obtaining a mean value for a selected time interval. Usually 10 min is about the shortest interval required for most solar energy applications. A useful system should allow integration to be selected for 10-, 30- and 60-min periods. Data loggers usually record on magnetic or paper tape with subsequent processing and quality control by computer.

## 4.2 Global Solar Radiation

### 4.2.1 Definition

The solar radiation received from a solid angle $2\pi$ on a horizontal surface is referred to as global solar radiation. This includes both direct solar radiation received from the solid angle of the sun's disc and radiation that has been scattered or diffusely reflected in traversing the atmosphere.

### 4.2.2 Sensor – Pyranometer

The instrument measuring solar radiation from a solid angle $2\pi$ on a plane surface is called a pyranometer. The manufacturer of pyranometers usually makes use of thermoelectric, photoelectric, pyroelectric or bimetallic elements as receivers. Since

pyranometers are exposed continually under all weather conditions they must be robust in design and resist the effects of humid air. The receiver should be hermetically sealed inside its casing or the casing must be removable so that condensed moisture can be removed. When the receiver is not permanently sealed a desiccator is usually fitted into the base of the instrument. The properties of pyranometers which are of concern when evaluating the accuracy and quality of radiation measurements are: sensitivity stability, response time, cosine response, azimuth response, linearity, temperature response and spectral response. A number of the more common forms of pyranometers are discussed below.

#### 4.2.2.1 Thermopile Receivers

Most of the pyranometers now available are contained in this category. The thermopile is usually constructed of individually welded thermoelements or a wire-bound-plated element. The hot-junction receivers of the themopile are coated with a suitable black paint, such as Parson's Optical Black or 3M Velvet Black, while the cold-junction receivers are either painted white or are close to a heat sink. The receiving surface is then covered by one or two concentric hemispheres of optical-grade glass.

The characteristics of a number of well-known pyranometers are given in Table 4-1. The manufacturer's name is included in parentheses under the model designation. Some pyranometers are now available with temperature-compensation circuits. Filter hemispheres are available for the Eppley PSP (precision spectral pyranometer).

#### 4.2.2.2 Solar Cells

A number of pyranometers are constructed with silicon photovoltaic solar cells. Although the accuracy obtainable is not high, it may be adequate for many uses in integrating over periods of a day or longer. Inaccuracies in the measurements result from several undesirable characteristics of silicon cells. First, the cells respond selectively with wavelength of the incident solar radiation. The response is negligibly small at wavelengths shorter than 0.40 $\mu$m. Because of the surface characteristics of silicon solar cells, their response deviates strongly from the ideal cosine law. Silicon solar cells are normally used in the short circuit mode.

A number of nominal characteristics of solar cell pyranometers are given below (* = no data):

| | |
|---|---|
| Response (mA/W $m^{-2}$) | 0.025 |
| Stability (%/yr) | * |
| Response Time (1/e,ms) | 1 |
| Cosine Error (% at 10° solar elevation) | -50 |
| Azimuth Error (% at 10° solar elevation) | ±2 |
| Non-linearity (%) | ±2 |
| Temperature Dependence (%/°C) | 0.04 to 0.1 |
| Impedance ($\Omega$) | 10 |

*(Note: cosine error of a bare cell may be considerably improved by mounting it below a contoured plastic diffuser.)*

#### 4.2.2.3 Bimetallic Pyranometer

This pyranometer depends on the differential motion of bimetallic strips for the response to solar radiation. Several configurations have been developed but the principle is similar in all. One horizontal strip is blackened and exposed to the sun while another strip is similarly exposed but painted white or chromed. Sometimes two whitened or chromed strips are exposed. These are connected in opposition so that, ideally, identical temperature changes in both black and white strips will result in no response. However, absorbed solar radiation will cause the black strip to be warmer than the white and its increased curvature will result in the motion of a recording pen. The whole mechanism, with a completely self-contained clock-driven recorder, is enclosed in a weather-resistant case with the sensitive elements exposed under a plastic or glass hemisphere. The self-contained instrument is also known as a pyranograph (actinograph).

The time constant of pyranographs is large (about 5 min) and their usefulness in recording short-term values of radiation is therefore limited. Because of its distortion with temperature the blackened strip cannot remain flat, a fact which makes the calibration factor a function of both the azimuth and elevation angle of the incident radiation. The calibration factor is also a function of the incident energy, and can change by as much as 20% over the normal diurnal range. Generally, an actinograph maintained in good condition should be regarded as having an accuracy of not better than ±10%.

Table 4-1

Characteristics of Pyranometers

| Characteristics (* = no data) \ Pyranometers | Moll-Gorczynski (Kipp & Zonen) | Eppley 180° 50j (Eplab) | Eppley 180° 10j (Eplab) | Eppley PSP (Eplab) | Eppley Black & White (Eplab) | Dirmhirn-Sauberer (Philipp Schenk) | Model SR-75 (Spectrolab) |
|---|---|---|---|---|---|---|---|
| Response (mV/W $m^{-2}$) | 0.01 | 0.004 | 0.01 | 0.007 | 0.01 | 0.003 | 0.008 |
| Stability (%/yr) | ±2 | * | * | ±2 | * | * | * |
| Response time (1/e,s) | 5 | 5 | 8 | 1 | 3 | 6 | <2 |
| Cosine error (% at 10° solar elevation) | +7 | -7 | -7 | -5 | -7 | -7 | -5 |
| Azimuth error (% at 10° solar elevation) | +7 | ±5 | +5 | +2 | +5 | +5 | ±2 |
| Non-linearity (%) | ±2 | * | * | ±1 | ±1 | * | ±1 |
| *Temperature dependence:* | | | | | | | |
| - Uncompensated (%/°C) | -0.2 | -0.13 | -0.13 | * | * | -0.04 | * |
| - Compensated (% from -20 to +40°C) | * | ±2 | ±2 | ±1 | ±1.5 | * | ±2 |
| Impedance (Ω) | | | | | | | |
| - Uncompensated | 10 | 40 | 100 | * | * | 5 | * |
| - Compensated | * | 350 | 350 | 300 | 300 | * | 500 |

### 4.2.3 Care of Pyranometers

The quality of global solar radiation data depends to a large measure on the daily care given to the pyranometer and associated equipment. Pyranometers should be given a daily inspection. The glass covers (hemispheres) must be kept clean of dew, frost, ice, snow and pollution. This can usually be effected by wiping clear and clean with a soft cloth. Frozen snow, glazed frost, hoar frost or rime can usually be removed with a warmed cloth. If moisture deposits form on the inside surfaces of the hemispheres, they should be very carefully removed and wiped clean and dry. The desiccant should also be recharged.

The level of pyranometers should be checked frequently, and radiation shields, cables and connections inspected. Any problems encountered and actions taken should be entered in the station log book.

Recording equipment must be inspected daily and maintained in proper working order. This must include a time check and adjustment to True Solar Time when necessary. Periodic standardization and calibration of the equipment should also be undertaken to ensure proper quality control of data collection.

### 4.2.4 Sample Data

Two samples of data are given here for Toronto. The first sample (Table 4-5), gives the hourly totals and daily total of the global solar radiation measured on a typically clear day. The second sample (Table 4-6) gives data for an overcast (cloudy) day with no direct sunshine. The data are plotted in Figures 4-1 (curve 5) and at the half hour values of Local Apparent Time (LAT). At this location on 26 May, the daily total extraterrestrial solar radiation on a horizontal surface was 40.73 MJ $m^{-2}$ assuming an extraterrestrial solar irradiance of 1370 W $m^{-2}$. The daily total solar energy available on a horizontal surface on 26 May, a clear day, was 29.66 MJ $m^{-2}$, while on 12 June, a cloudy day, it was only 9.16 MJ $m^{-2}$; the ratio of surface to extraterrestrial daily total global solar radiation is 0.728 and 0.21, respectively. It is very apparent that the higher total energy yield on the clear day is provided by the direct components (29.66 - 3.56 = 26.10 MJ $m^{-2}$). The global solar radiation reaches peak values

during the hours ending at 1200 and 1300 LAT, with almost equal values recorded for each solar hour before and after solar noon.

## 4.3 Direct Solar Radiation

### 4.3.1 Definition

The solar radiation received from the solid angle of the sun's disc on a surface perpendicular to the axis of the solid angle is called direct solar radiation.

### 4.3.2 Sensor

The instrument measuring direct solar radiation is called the pyrheliometer. The manufacturer of pyrheliometers usually makes use of thermoelectric, photoelectric, pyroelectric or bimetallic elements as receivers. The receiver is placed at one end of a tube with the other end open to receive the radiation. The dimensions of the receiver, tube and opening define the opening angle or aperture of the pyrheliometer. Apertures generally range from 4 to 12°, with 5 to 6° being the most common. Since the sun's disc subtends an angle of approximately 0.5° it is evident that pyrheliometers measure a significant amount of circumsolar radiation.

#### 4.3.2.1 Sensors for Non-Continuous Measurements

Many pyrheliometers are not sufficiently robust in design to warrant continuous outdoor use. This is particularly true if the receiver is not sealed against moisture infiltration. Four well-known pyrheliometers and their characteristics are listed in Table 4-2. Other types are available which, because of space limitation, are not included.

The pyrheliometers mentioned are usually operated by hand for recording a series of essentially instantaneous values during good weather. The Abbot silver-disc pyrheliometer and the Ångström compensation pyrheliometer have been used from 1956 as reference standards for the International Pyrheliometric Scale. The Kendall practical absolute cavity radiometer (PACRAD), along with a select group of other instruments, are the basis of a new World Radiation Reference. None of the above are suitable for continuous measurement out-of-doors.

#### 4.3.2.2 All-Weather Sensors for Continuous Measurements

Pyrheliometers which are exposed continually in all weather must be robust in design and resist the

Table 4-2

Characteristics of Pyrheliometers

| Pyrheliometers / Characteristics: nominal (* = no data) | Abbot Silver-disk (Talbert Instrument 6) | Ångström Electrical Compensation (Eplab, SMHI - Sweden) | Linke-Feussner (Kipp & Zonen) | Kendall Absolute Radiometer (Eplab, Technical Measurements, Inc.) |
|---|---|---|---|---|
| Sensor type | silver disk with mercury thermometer | maganin strips with thermocouples | Moll thermopile | cavity with thermopile |
| Aperture | circular: 6° | rectangular: 5° X 10° | circular: 10° | circular: 5° |
| Response | 200 W $m^{-2}$ $C^{-1}$ | 5000 W $m^{-2}$ $A^{-1}$ | 50 W $m^{-2}$ $mV^{-1}$ | 1000 W $m^{-2}$ $mV^{-1}$ |
| Response time (1/e) | > 2 min | 10 s | 10 s | 10 s |
| Temperature dependence | N/A | N/A | 0.002/°C | N/A |
| Impedance | N/A | N/A | 100 Ω | * |

effects of humid air. The receiver must be hermetically sealed inside its case or the case must be fitted with a desiccator.

The pyrheliometer must always be maintained pointing at the sun. This is usually accomplished by a motor-driven equatorial system or by an automatic sun tracker. Such equipment must be able to operate in all weather and extremes of temperature encountered at the site.

A typical well-known pyrheliometer suitable for continuous measurements out-of-doors is the Eppley normal incidence pyrheliometer (NIP). The manufacturer also has available a motor-driven equatorial system which will mount three pyrheliometers. An Eppley NIP is mentioned here as a typical instrument of this type, although other suitable instruments are available from other manufacturers.

The Eppley NIP is a thermopile instrument with built-in temperature compensation. The receiver is hermetically sealed in an atmosphere of dry air by means of a quartz window covering the aperture.

Characteristics of Eppley
Normal Incidence Pyrheliometer

| | |
|---|---|
| Response | 0.007 MV/W $m^{-2}$ |
| Stability | <1%/yr |
| Response time (1/e) | 4s |
| Temperature dependence | |
| -30 to +40°C | ±1% |
| Impedance | 200 Ω |

#### 4.3.3 Daily Care

Pyrheliometers should be given the same attention afforded pyranometers. The exposed optical components must be cleaned regularly during the daily inspection period. In addition, the sun-tracking system must be adjusted so that the diopter scale indicates that the pyrheliometer is pointing in the correct direction. Care and maintenance of the sun-tracking system should be carried out according to the manufacturer's recommendations.

#### 4.3.4 Sample Data

Referring to Tables 4-5 and 4-6, and Figures 4-1 and 4-2 (column 8 and curve 7, respectively), the daily total direct component on 26 May, 1977 (clear day), was 40.5 MJ $m^{-2}$ while on 12 June (cloudy day) it was zero. A solar-tracking surface, normal to the solar beam, had a daily total direct component (on the first day) 55% greater than that on a horizontal surface, a very significant increase in available energy. However, on the cloudy (second) day, no direct component was received, only the diffuse. At high sun elevations (1200 and 1300 LAT) the ratio of the direct to the corresponding extra-terrestrial components (4.932 MJ $m^{-2}$) is 0.698 and 0.695, respectively, or almost 70% of that available outside the atmosphere.

### 4.4 Diffuse Solar Radiation

#### 4.4.1 Definition

Diffuse solar (or sky) radiation is the downward solar radiation as received on a horizontal surface from a solid angle of $2\pi$ with the exception of the solid angle subtended by the sun's disc.

#### 4.2.2 Sensor

The sensor for measuring diffuse solar radiation is the pyranometer, which is equipped with a special shading or occulting device to exclude the direct component. Such an arrangement is sometimes called a diffusograph. When both direct and global solar radiation are measured by separate instruments the diffuse component may be found by calculation.

##### 4.4.2.1 Measurement by Diffusograph

The diffusograph should be installed according to the manufacturer's instructions. The plane of the shadow band must be set parallel to the equatorial plane by inclining the band in the north-south plane at an angle $\phi$ from the south (in the Northern Hemisphere), where $\phi$ is the latitude of the site. The center of the band must be moved periodically along a line parallel to the polar axis as the declination of the sun changes so that the pyranometer may be shaded from the direct solar radiation. After the initial installation of a diffusograph the plane of the shadow band must be adjusted over a period of 3 or 4 sunny days to ensure that the entire glass dome of the pyranometer lies entirely in shade. The frequency with which the band must be moved because of

changes in the solar declination is a function of the size of the pyranometer, the width of the band, and the rate of change of declination.

For most locations an adjustment of the position of the shadow band once each day is desirable, except perhaps near the solstices when once every 2 or 3 days is usually sufficient. Of course it is difficult to adjust the band during cloudy conditions when no shadow is cast. This difficulty can be overcome by establishing a scale on the polar axis of adjustment (marked in degrees of declination). The solar declination can then be found for any day of the year from a Nautical Almanac, other astronomical tables or a computer program and the band adjusted accordingly.

Use of the shadow band necessitates applying a correction to the data for that part of the diffuse radiation which is obstructed by the band. The problem of correcting data should be approached both theoretically and experimentally, although neither approach is entirely satisfactory because the diffuse radiation varies over the dome of the sky.

Assuming that the radiation intensity, L, is uniform over an isotropically diffuse hemisphere, that the pyranometer receiver absorbs according to the cosine law, and that there is no reflected contribution from the shadow band, then the radiation from the whole hemisphere is $G_d = \pi L$. The fraction of the diffuse radiation screened off by the shadow band is given by:

$$\Delta G_d = \frac{2w}{\pi r}\cos^3\delta(\psi_o \sin\phi\sin\delta + \cos\phi\cos\delta\sin\psi_o)$$

where w is the width of the shadow band, r is its radius, $\delta$ is the solar declination, $\phi$ is the latitude of the installation, and $\psi_o$ is the azimuth angle of the sun at sunset. The correction factor to be applied to the diffusograph measurements is $1/(1 - \Delta G_d)$ and depends on the three constants r, w and $\phi$ and the two variables $\delta$ and $\psi_o$. For example, the Eppley diffusograph has the dimensions w = 76 mm and r = 307 mm. Table 4-3 has been prepared for the 16th calendar day of the month with an additional 4% additive correction incorporated to account for the effects of non-isotropic distribution of the radiance over the sky. It should be realized that these corrections are approximations for a particular design of diffusograph and for general sky conditions. They must not be viewed as a substitute for corrections derived for a specific instrument at a given location.

The correction for clear-sky conditions may also be determined experimentally by comparing the diffuse radiation as measured when the shadow band is in it normal position with that measured with the shadow band temporarily replaced by a shadow disc. The disc should be large enough to ensure that the glass hemisphere is completely shaded at all solar zenith angles. An appropriate shadow disc should subtend an angle at the sensor of approximately 6°. This is accomplished by maintaining the distance between the sensor and disc at ten times the diameter of the disc. For overcast conditions

Table 4-3

Shadow Band Correction Factors for the Eppley Diffusograph
(with w = 76 mm, r = 307 mm)

| Lat.°N | JAN | FEB | MAR | APR | MAY | JUN | JUL | AUG | SEP | OCT | NOV | DEC |
|---|---|---|---|---|---|---|---|---|---|---|---|---|
| 0 | 1.17 | 1.21 | 1.24 | 1.22 | 1.19 | 1.16 | 1.17 | 1.20 | 1.23 | 1.21 | 1.19 | 1.16 |
| 10 | 1.15 | 1.19 | 1.23 | 1.23 | 1.20 | 1.18 | 1.19 | 1.21 | 1.23 | 1.20 | 1.16 | 1.14 |
| 20 | 1.13 | 1.16 | 1.21 | 1.23 | 1.21 | 1.19 | 1.20 | 1.21 | 1.22 | 1.18 | 1.14 | 1.12 |
| 30 | 1.11 | 1.14 | 1.19 | 1.22 | 1.21 | 1.20 | 1.21 | 1.21 | 1.20 | 1.15 | 1.12 | 1.10 |
| 40 | 1.09 | 1.12 | 1.17 | 1.20 | 1.21 | 1.20 | 1.21 | 1.21 | 1.18 | 1.13 | 1.10 | 1.08 |
| 50 | 1.07 | 1.10 | 1.14 | 1.18 | 1.20 | 1.20 | 1.20 | 1.19 | 1.15 | 1.11 | 1.08 | 1.06 |
| 60 | 1.05 | 1.07 | 1.11 | 1.15 | 1.19 | 1.20 | 1.19 | 1.17 | 1.13 | 1.09 | 1.06 | 1.04 |
| 70 | ----- | 1.05 | 1.08 | 1.13 | 1.18 | 1.21 | 1.19 | 1.14 | 1.11 | 1.06 | 1.04 | ----- |
| 80 | ----- | ----- | 1.06 | 1.11 | 1.19 | 1.22 | 1.20 | 1.14 | 1.09 | 1.04 | ----- | ----- |
| 90 | ----- | ----- | 1.05 | 1.11 | 1.20 | 1.23 | 1.21 | 1.15 | 1.07 | ----- | ----- | ----- |

the shadow band in place over the pyranometer should be compared with simultaneous measurements of global solar radiation. These procedures should be repeated under various atmospheric conditions to give reliable correction factors.

#### 4.4.2.2 Calculations from Global and Direct Measurements

The global solar radiation can be written as $G = G_b + G_d$ where $G_b$ is the vertical component of direct solar radiation and $G_d$ is the diffuse solar component. Furthermore, $G_b = I \cdot \cos\Theta$, where I is the direct component and $\Theta$ is the solar zenith angle. Therefore the diffuse component of solar radiation can be expressed as $G_d = G - I \cos\Theta$, allowing the diffuse solar radiation to be calculated from measurements of global and direct solar radiation. In addition, the solar zenith angle, $\Theta$, must be computed for the midpoint of the time interval over which K and I are integrated (e.g., hourly radiation totals of K and I are assigned to the appropriate half hour). Of course, when L = O, i.e., when the sun is not visible, $G_d$ approaches G, and no further computation is required.

### 4.4.3 Sample Data

Referring to Tables 4.5 and 4.6, and Figures 4-1 and 4-2 (column 2 and curve 1, respectively), the daily total diffuse solar radiation increased from 3.56 MJ $m^{-2}$ on 26 May (clear day) to 9.27 MJ $m^{-2}$ on 12 June (cloudy day). The shadow band correction factor given in Table 4-3 has been applied to the data. The correction factor for June is evidently too large since the diffuse component after correction is greater than the global component by about 1% averaged over the day. Hence, at latitude 43°48'N the shadow band correction factor should be revised from 1.20 to 1.19 for this particular day. In fact, the hourly sums and daily totals of diffuse and global solar radiation should be the same since no direct radiation was received during the day. In practice, however, instrumental errors will often result in small differences, some of which may yield a diffuse reading higher than the global.

## 4.5 Solar Radiation on an Inclined Surface

### 4.5.1 Definition

The solar radiation on an inclined surface includes the direct, diffuse and reflected solar radiation received from a solid angle of $2\pi$ on a plane surface of any inclination and azimuth orientation. Examples of inclined surfaces are north-, east-, south- and west-facing walls of buildings, or a flat plate solar collector facing south inclined at 60°.

### 4.5.2 Measurements With Pyranometers

Measurements of solar radiation on inclined surfaces are readily made by means of pyranometer. However, a number of precautions should be observed. Particular attention must be paid to the orientation of the instrument so that the required angles of inclination and azimuth are attained. When the receiving surface of a pyranometer is inclined to the horizontal a number of its response characteristics may change.

Some pyranometers are equipped with radiation shields which reduce heating of the body of the instrument by direct sunlight. This desired shading effect is modified to some extent when the pyranometer is inclined, and may require the addition of a supplementary shade to prevent overheating.

Inclined pyranometers also show a change in response as compared to response in the horizontal position. This is believed to result mainly from a change in the heat transfer between the surface of the thermopile and the glass hemisphere. Several studies which have reported data on this effect are given in Table 4-4a with selected results. It should be noted that the figures by Norris (1974) for an inclination of 90° could not be confirmed by other authors.

More recently investigations of the tilt effect of Dehne (1978) using diffuse radiation yields almost the same data for the EPSP as published by Latimer (1970). But for the KZP it can be seen that the

Table 4-4a

Response of Inclined Pyranometers Normalized to Horizontal
(Eppley Precision Spectral Pyranometer = EPSP; Eppley Black & White = EBW;
Kipp & Zonen Pyranometer = KZP)

| Experimental Study (see refer.) | Pyranometer | Angle of Inclination (re: horizontal) 30° | 45° | 60° | 90° | 180° |
|---|---|---|---|---|---|---|
| Latimer (1970) | EPSP | 0.994 | 0.992 | 0.991 | 0.992 | 0.988 |
| | EBW | 0.998 | 0.995 | 0.993 | 0.991 | 0.986 |
| | KZP | 0.997 | 0.996 | 0.995 | 0.993 | 0.989 |
| Norris (1974) | EPSP | 1.005 | 1.012 | 1.02 | 1.11 | 1.01 |
| | KZP | 1.015 | 1.02 | 1.02 | 1.10 | 0.98 |
| Flowers (1977) | EPSP | 1.006 | 1.007 | 1.002 | 1.005 | |
| | EBW | 0.990 | 0.984 | 0.978 | 0.975 | |
| | KZP | 0.992 | 0.993 | 0.995 | 0.998 | |

effect depends both on the level of irradiance and on the orientation of the thermopile in accordance with physical considerations. Table 4-4b shows the relative response for 450 W $m^{-2}$ and 1400 W $m^{-2}$ as well as for the orientations of thermopile strips parallel and perpendicular to the tilt axis.

In practice for a high level of irradiance ($\approx$ 1000 W $m^{-2}$) and for a favored position of thermopile (strips parallel to the tilt axis) a deviation of ~2% from the untilted case should be taken into account. For the new KZP-Type CM10 the tilt effect is as small as for the EPSP.

It should be emphasized that the change in sensitivity by tilting is systematic and therefore correctable, in principle, by software.

### 4.5.3. Special Site Criteria

Pyranometers measuring on inclined surfaces receive a component of solar radiation reflected from

Table 4-4b

Response of Inclined Pyranometer (Type KZP CM5 /00692)
Normalized to Horizontal. (After Dehne, 1978)

| | | Angle of Inclination (re: horizontal) 30° | 60° | 90° | 180° |
|---|---|---|---|---|---|
| 450 W $m^{-2}$ | 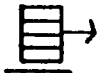 | 0.996 | 0.989 | 0.988 | 0.999 |
| |  | 0.993 | 0.986 | 0.981 | 0.996 |
| 1400 W $m^{-2}$ |  | 0.990 | 0.978 | 0.975 | 0.999 |
| |  | 0.979 | 0.960 | 0.957 | 0.997 |

the terrain adjacent to the instrument. The reflecting terrain should be uniform, e.g., a grass surface (with the possibility of snow cover in winter). Whatever the surface chosen, its mean albedo (and diurnal and seasonal variations) should be measured periodically. Furthermore, when a pyranometer is being used as part of a collector evaluation/research program, it must have the same view as the solar device concerned.

### 4.5.4 Calculation

Principal attention is given here to describing the method used to calculate the solar radiation incident on non-horizontal surfaces. Kondratyev (1969) has provided the basic equations for calculating the radiation incident on inclined surfaces given the energy incident on a horizontal surface.

The direct solar radiation incident on a slope $G_{bs}$ can be calculated from its horizontal value using

$$G_{bs} = \frac{G_b \cdot \cos i}{\cos\Theta} \tag{1}$$

where $G_b = G - G_d$ is the direct solar component on a horizontal surface, i is the angle of incidence of the sun's rays on the slope, and $\Theta$ is the solar zenith angle.

In addition

$$\cos i = \cos a \cdot \cos\Theta + \sin a \cdot \sin\Theta \cdot \cos(\psi - \psi_s) \tag{2}$$

$$\cos\psi = \frac{\sin\phi \cdot \cos\Theta - \sin\delta}{\cos\phi \cdot \sin\Theta} \tag{3}$$

$$\cos\Theta = \sin\phi \cdot \sin\delta + \cos\phi \cdot \cos\delta \cdot \cos\omega \tag{4}$$

where $a$ is the inclination of the slope, $\psi$ is the azimuth of the sun, $\psi_s$ is the azimuth or aspect of the slope, $\delta$ is the solar declination, and $\omega$ is the hour angle.

The preceding equations rely completely on the geometrical relationships between the sun and the horizontal and inclined surfaces, so that no assumptions or simplifications are involved. However, since the denominator in Eq. (1) will tend towards zero near sunrise and sunset, excessively high estimates of direct radiation on the slope can result. To avoid this problem, calculations should cover a period commencing at the full hour following sunrise and ending at the full hour preceding sunset. For the intervening hours each hourly radiation total should be assigned to the appropriate half hour of LAT.

The diffuse radiation on the slope may be calculated using:

$$G_{ds} = \frac{G_d(1.0 + \cos a)}{2} + \frac{G \cdot \rho(1.0 - \cos a)}{2} \tag{5}$$

where $G_d$ is the diffuse solar radiation on a horizontal surface and $\rho$ is the albedo of the surface. In Eq. (5) the first expression on the right-hand side is the diffuse sky radiation; and the second, the radiation reflected by the adjacent surface, $G_d$, is assumed to be distributed isotropically. Such an assumption is simplistic since the distribution of the diffuse sky radiation is highly variable, being primarily influenced by the position of both the sun and cloud in the sky.

Finally, the total radiation incident on the slope is specified by

$$G_s = G_{bs} + G_{ds}. \tag{6}$$

The basic equations described above assume a knowledge of the direct and diffuse components, but such data are not commonly available.

Table 4-7 presents sample results from calculations using the technique.

### 4.5.5 Sample Data and Application to Solar Energy

Tables 4-5 and 4-6 (columns 3, 4, and 5) and Figures 4-1 and 4-2 (curves 2, 3, and 4) give samples of solar radiation measured on south-facing surfaces inclined at 30°, 60° and 90° to the horizontal for 26 May (clear day) and 12 June (cloudy day). Although on the clear day the slope which in inclined at 30° received the maximum radiation (compared to all other measurements) between approximately 1000 and 1500 LAT, the daily total is slightly less than that for a horizontal surface. On the cloudy day the global radiation on a horizontal surface exceeds the radiation on an inclined surface during all hours of the day. Long-term data of this type are very useful in determining the optimum slope and aspect of a surface at a site for maximum solar energy utilization during different periods of a

year, or on an annual basis. The data in Tables 4-5 and 4-6 cannot be easily compared with those in Table 4-7, since the former were measured on individual days, while the latter were computed as mean values for 9 years of data.

For a description of other procedures used to calculate solar radiation on inclined surfaces see Chapter 3, Section 3.6.4; Chapter 8, Section 8.5; *IEA Solar Heating and Cooling Program, Task V*; and the report of Carter and Patel (1979).

Table 4-5

Solar Radiation (MJ $m^{-2}$)

Toronto MRS Lat. 43°48'N Long. 79°33'W 192 m (MSL)

26 May 1977

| Hour Ending (LAT) (1) | Diffuse (2) | 30° Inclined (3) | 60° Inclined (4) | 90° Inclined (5) | Global (6) | Reflected (7) | Direct (8) |
|---|---|---|---|---|---|---|---|
| 0400 | 0.000 | 0.000 | 0.000 | 0.000 | 0.000 | 0.000 | 0.000 |
| 0500 | 0.014 | 0.018 | 0.019 | 0.016 | 0.029 | 0.002 | 0.163 |
| 0600 | 0.114 | 0.150 | 0.145 | 0.159 | 0.396 | 0.099 | 1.781 |
| 0700 | 0.201 | 0.733 | 0.270 | 0.315 | 1.044 | 0.256 | 2.548 |
| 0800 | 0.295 | 1.567 | 1.028 | 0.466 | 1.745 | 0.394 | 2.885 |
| 0900 | 0.315 | 2.363 | 1.839 | 0.878 | 2.385 | 0.486 | 3.129 |
| 1000 | 0.330 | 3.042 | 2.468 | 1.305 | 2.917 | 0.541 | 3.269 |
| 1100 | 0.341 | 3.531 | 2.939 | 1.629 | 3.302 | 0.569 | 3.349 |
| 1200 | 0.317 | 3.812 | 3.197 | 1.800 | 3.531 | 0.591 | 3.443 |
| 1300 | 0.307 | 3.740 | 3.128 | 1.755 | 3.488 | 0.608 | 3.429 |
| 1400 | 0.307 | 3.498 | 2.905 | 1.606 | 3.305 | 0.601 | 3.381 |
| 1500 | 0.272 | 3.024 | 2.443 | 1.273 | 2.955 | 0.566 | 3.356 |
| 1600 | 0.248 | 2.333 | 1.789 | 0.830 | 2.428 | 0.501 | 3.243 |
| 1700 | 0.223 | 1.537 | 1.016 | 0.442 | 1.785 | 0.396 | 3.022 |
| 1800 | 0.200 | 0.696 | 0.344 | 0.328 | 1.062 | 0.242 | 2.496 |
| 1900 | 0.128 | 0.153 | 0.161 | 0.182 | 0.410 | 0.093 | 1.552 |
| 2000 | 0.019 | 0.022 | 0.024 | 0.024 | 0.037 | 0.004 | 0.200 |
| 2100 | 0.000 | 0.000 | 0.000 | 0.000 | 0.000 | 0.000 | 0.000 |
| Total | 3.56 | 28.870 | 22.530 | 12.330 | 29.660 | 5.770 | 40.500 |
| Mean | 0.198 | 1.604 | 1.252 | 0.685 | 1.648 | 0.320 | 2.250 |

Table 4-6

Solar Radiation (MJ $m^{-2}$)

Toronto MRS Lat. 43°48'N Long. 79°33'W 192 m (MSL)

12 June 1977

| Hour Ending (LAT) (1) | Diffuse (2) | 30° Inclined (3) | 60° Inclined (4) | 90° Inclined (5) | Global (6) | Reflected (7) | Direct (8) |
|---|---|---|---|---|---|---|---|
| 0400 | 0.000 | 0.002 | 0.003 | 0.001 | 0.001 | 0.000 | 0.000 |
| 0500 | 0.006 | 0.014 | 0.012 | 0.007 | 0.013 | 0.008 | 0.000 |
| 0600 | 0.074 | 0.078 | 0.067 | 0.047 | 0.083 | 0.022 | 0.000 |
| 0700 | 0.197 | 0.181 | 0.145 | 0.101 | 0.202 | 0.047 | 0.000 |
| 0800 | 0.398 | 0.358 | 0.287 | 0.200 | 0.395 | 0.086 | 0.000 |
| 0900 | 0.417 | 0.376 | 0.305 | 0.215 | 0.413 | 0.089 | 0.000 |
| 1000 | 0.514 | 0.452 | 0.359 | 0.250 | 0.507 | 0.107 | 0.000 |
| 1100 | 0.707 | 0.627 | 0.502 | 0.352 | 0.693 | 0.144 | 0.000 |
| 1200 | 1.200 | 1.031 | 0.808 | 0.564 | 1.168 | 0.243 | 0.000 |
| 1300 | 1.627 | 1.423 | 1.120 | 0.779 | 1.590 | 0.327 | 0.000 |
| 1400 | 1.458 | 1.312 | 1.048 | 0.733 | 1.434 | 0.294 | 0.000 |
| 1500 | 1.119 | 0.965 | 0.756 | 0.527 | 1.095 | 0.228 | 0.000 |
| 1600 | 0.861 | 0.788 | 0.642 | 0.458 | 0.846 | 0.168 | 0.000 |
| 1700 | 0.469 | 0.433 | 0.351 | 0.249 | 0.468 | 0.097 | 0.000 |
| 1800 | 0.134 | 0.134 | 0.112 | 0.081 | 0.142 | 0.032 | 0.000 |
| 1900 | 0.110 | 0.106 | 0.085 | 0.057 | 0.117 | 0.028 | 0.000 |
| 2000 | 0.014 | 0.020 | 0.018 | 0.011 | 0.023 | 0.008 | 0.000 |
| 2100 | 0.000 | 0.001 | 0.001 | 0.001 | 0.001 | 0.000 | 0.000 |
| Total | 9.270 | 8.270 | 6.600 | 4.620 | 9.160 | 1.930 | 0.000 |
| Mean | 0.515 | 0.460 | 0.367 | 0.257 | 0.509 | 0.107 | 0.000 |

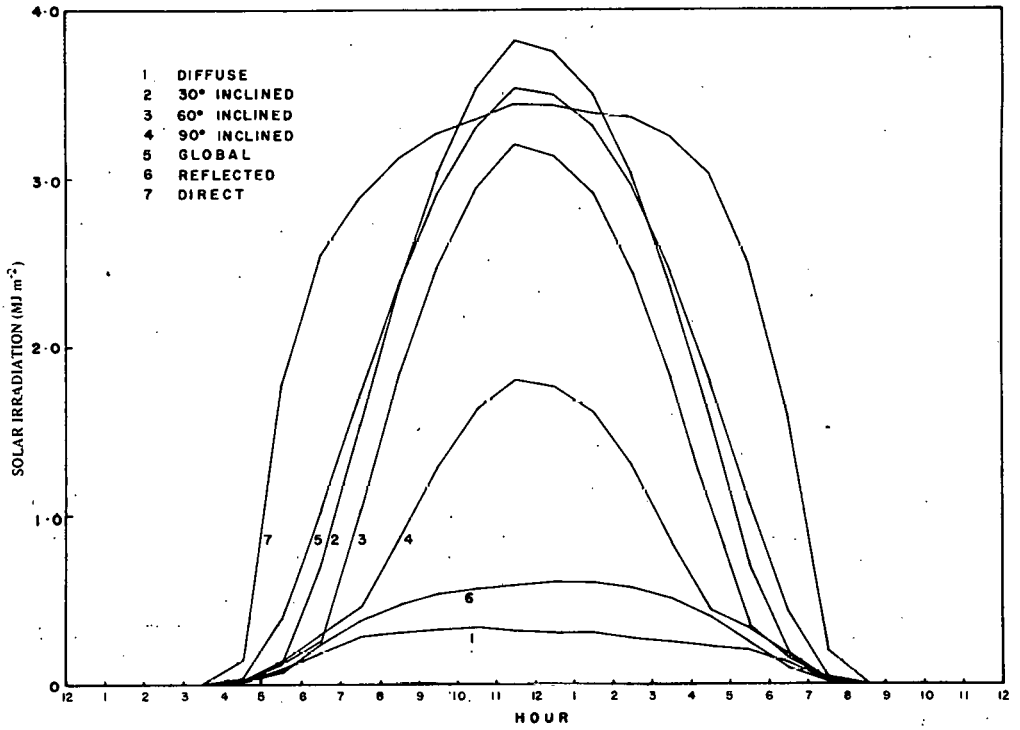


*Figure 4-1 Information from Table 4-5, Toronto, 26 May 1977*

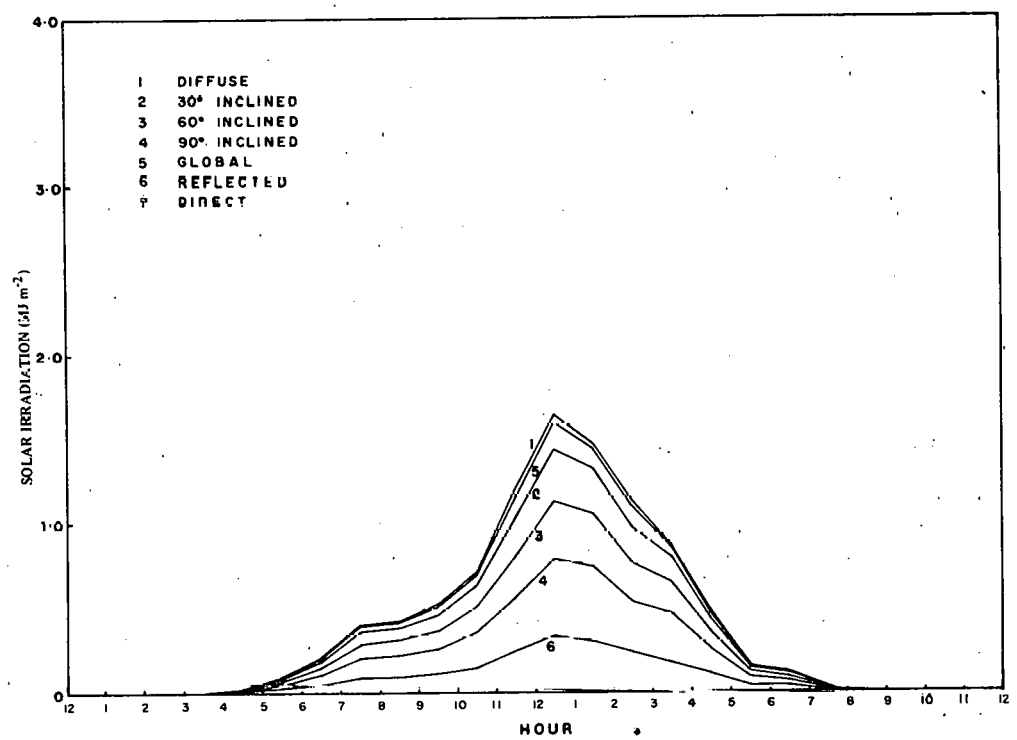


*Figure 4-2 Information from Table 4-6, Toronto, 12 June 1977*

Table 4-7

Toronto MRS Ontario

Mean Monthly Values of Daily Solar Radiation on Inclined Surfaces

($MJ\ m^{-2}\ Day^{-1}$)

MAY

| SLOPE (DEG.) | DIR | DIF | ASPECT | REF | TOTAL | DIR | DIF | ASPECT | REF | TOTAL | DIR | DIF | ASPECT | REF | TOTAL | DIR | DIF | ASPECT | REF | TOTAL |
|---|---|---|---|---|---|---|---|---|---|---|---|---|---|---|---|---|---|---|---|---|
| | | | 180 | | | | | 135 | | | | | 90 | | | | | 45 | | |
| 10 | 9.92 | 8.71 | | 0.04 | 18.66 | 10.03 | 8.71 | | 0.04 | 18.78 | 10.40 | 8.71 | | 0.04 | 19.14 | 10.76 | 8.71 | | 0.04 | 19.50 |
| 20 | 8.96 | 8.51 | | 0.15 | 17.62 | 9.21 | 8.51 | | 0.15 | 17.86 | 10.01 | 8.51 | | 0.15 | 18.66 | 10.69 | 8.51 | | 0.15 | 19.34 |
| 30 | 7.74 | 8.19 | | 0.32 | 16.25 | 8.14 | 8.19 | | 0.32 | 16.65 | 9.47 | 8.19 | | 0.32 | 17.98 | 10.40 | 8.19 | | 0.32 | 18.91 |
| 40 | 6.27 | 7.75 | | 0.57 | 14.59 | 6.96 | 7.75 | | 0.57 | 15.28 | 8.83 | 7.75 | | 0.57 | 17.15 | 9.85 | 7.75 | | 0.57 | 18.16 |
| 50 | 4.62 | 7.21 | | 0.86 | 12.69 | 5.81 | 7.21 | | 0.86 | 13.89 | 8.14 | 7.21 | | 0.86 | 16.22 | 9.13 | 7.21 | | 0.86 | 17.20 |
| 60 | 2.82 | 6.58 | | 1.21 | 10.61 | 4.83 | 6.58 | | 1.21 | 12.62 | 7.36 | 6.58 | | 1.21 | 15.17 | 8.19 | 6.58 | | 1.21 | 15.90 |
| 70 | 1.38 | 5.89 | | 1.59 | 8.86 | 4.02 | 5.89 | | 1.59 | 11.50 | 6.54 | 5.89 | | 1.59 | 14.02 | 7.13 | 5.89 | | 1.59 | 14.61 |
| 80 | 0.95 | 5.15 | | 2.00 | 8.09 | 3.32 | 5.15 | | 2.00 | 10.47 | 5.66 | 5.15 | | 2.00 | 12.80 | 5.95 | 5.15 | | 2.00 | 13.09 |
| 90 | 0.68 | 4.39 | | 2.42 | 7.49 | 2.70 | 4.39 | | 2.42 | 9.51 | 4.78 | 4.39 | | 2.42 | 11.59 | 4.68 | 4.39 | | 2.42 | 11.49 |
| | | | ASPECT | | 0 | | | ASPECT | | -45 | | | ASPECT | | -90 | | | ASPECT | | -135 |
| 10 | 10.91 | 8.71 | | 0.04 | 19.86 | 10.82 | 8.71 | | 0.04 | 19.56 | 10.49 | 8.71 | | 0.04 | 19.23 | 10.10 | 8.71 | | 0.04 | 18.84 |
| 20 | 10.93 | 8.51 | | 0.15 | 19.58 | 10.81 | 8.51 | | 0.15 | 19.47 | 10.19 | 8.51 | | 0.15 | 18.84 | 9.34 | 8.51 | | 0.15 | 17.99 |
| 30 | 10.66 | 8.19 | | 0.32 | 19.17 | 10.57 | 8.19 | | 0.32 | 19.08 | 9.72 | 8.19 | | 0.32 | 18.23 | 8.33 | 8.19 | | 0.32 | 16.84 |
| 40 | 10.08 | 7.75 | | 0.57 | 18.40 | 10.06 | 7.75 | | 0.57 | 18.37 | 9.12 | 7.75 | | 0.57 | 17.44 | 7.19 | 7.75 | | 0.57 | 15.51 |
| 50 | 9.20 | 7.21 | | 0.86 | 17.27 | 9.37 | 7.21 | | 0.86 | 17.44 | 8.47 | 7.21 | | 0.66 | 16.54 | 6.07 | 7.21 | | 0.86 | 14.14 |
| 60 | 8.04 | 6.58 | | 1.21 | 15.83 | 8.45 | 6.58 | | 1.21 | 16.24 | 7.72 | 6.58 | | 1.21 | 15.51 | 5.08 | 6.58 | | 1.21 | 12.87 |
| 70 | 6.69 | 5.89 | | 1.59 | 14.17 | 7.39 | 5.89 | | 1.59 | 14.86 | 6.86 | 5.89 | | 1.59 | 14.34 | 4.24 | 5.89 | | 1.59 | 11.72 |
| 80 | 5.19 | 5.15 | | 2.00 | 12.34 | 6.19 | 5.15 | | 2.00 | 13.34 | 5.96 | 5.15 | | 2.00 | 13.11 | 3.52 | 5.15 | | 2.00 | 10.67 |
| 90 | 3.53 | 4.39 | | 2.42 | 10.33 | 4.90 | 4.39 | | 2.42 | 11.71 | 5.05 | 4.39 | | 2.42 | 11.86 | 2.86 | 4.39 | | 2.42 | 9.67 |

JUNE

| | | | ASPECT | | 180 | | | ASPECT | | 135 | | | ASPECT | | 90 | | | ASPECT | | 45 |
|---|---|---|---|---|---|---|---|---|---|---|---|---|---|---|---|---|---|---|---|---|
| 10 | 10.48 | 9.92 | | 0.04 | 20.44 | 10.53 | 9.92 | | 0.04 | 20.49 | 10.73 | 9.92 | | 0.04 | 20.69 | 10.96 | 9.92 | | 0.04 | 20.92 |
| 20 | 9.69 | 9.69 | | 0.16 | 19.54 | 9.79 | 9.69 | | 0.16 | 19.64 | 10.28 | 9.69 | | 0.16 | 20.13 | 10.73 | 9.69 | | 0.16 | 20.58 |
| 30 | 8.61 | 9.32 | | 0.35 | 18.28 | 8.78 | 9.32 | | 0.35 | 18.46 | 9.88 | 9.32 | | 0.35 | 19.34 | 10.26 | 9.32 | | 0.35 | 19.94 |
| 40 | 7.27 | 8.82 | | 0.61 | 16.70 | 7.57 | 8.82 | | 0.61 | 17.01 | 8.94 | 8.82 | | 0.61 | 18.38 | 9.55 | 8.82 | | 0.61 | 18.98 |
| 50 | 5.70 | 8.21 | | 0.94 | 14.85 | 6.33 | 8.21 | | 0.94 | 15.48 | 8.15 | 8.21 | | 0.94 | 17.30 | 8.71 | 8.21 | | 0.94 | 17.85 |
| 60 | 3.96 | 7.49 | | 1.31 | 12.77 | 5.24 | 7.49 | | 1.31 | 14.04 | 7.30 | 7.49 | | 1.31 | 16.11 | 7.66 | 7.49 | | 1.31 | 16.47 |
| 70 | 2.14 | 6.71 | | 1.72 | 10.56 | 4.31 | 6.71 | | 1.72 | 12.74 | 6.39 | 6.71 | | 1.72 | 14.82 | 6.51 | 6.71 | | 1.72 | 14.94 |
| 80 | 1.32 | 5.86 | | 2.16 | 9.35 | 3.53 | 5.86 | | 2.16 | 11.56 | 5.48 | 5.86 | | 2.16 | 13.51 | 5.30 | 5.86 | | 2.16 | 13.32 |
| 90 | 0.94 | 5.00 | | 2.62 | 8.56 | 2.88 | 5.00 | | 2.62 | 10.49 | 4.58 | 5.00 | | 2.62 | 12.19 | 4.05 | 5.00 | | 2.62 | 11.66 |
| | | | ASPECT | | 0 | | | ASPECT | | -45 | | | ASPECT | | -90 | | | ASPECT | | -135 |
| 10 | 11.06 | 9.92 | | 0.04 | 21.04 | 11.04 | 9.92 | | 0.04 | 21.00 | 10.84 | 9.92 | | 0.04 | 20.80 | 10.61 | 9.92 | | 0.04 | 20.56 |
| 20 | 10.89 | 9.69 | | 0.16 | 20.74 | 10.88 | 9.69 | | 0.16 | 20.73 | 10.49 | 9.89 | | 0.16 | 20.34 | 9.94 | 9.69 | | 0.16 | 19.79 |
| 30 | 10.40 | 9.32 | | 0.35 | 20.08 | 10.49 | 9.32 | | 0.35 | 20.16 | 9.97 | 9.32 | | 0.35 | 19.65 | 9.00 | 9.32 | | 0.35 | 18.67 |
| 40 | 9.65 | 8.82 | | 0.61 | 19.09 | 9.83 | 8.82 | | 0.81 | 19.27 | 9.32 | 8.82 | | 0.61 | 18.76 | 7.85 | 8.82 | | 0.61 | 17.29 |
| 50 | 8.61 | 8.21 | | 0.94 | 17.75 | 9.03 | 8.21 | | 0.94 | 18.17 | 8.58 | 8.21 | | 0.94 | 17.72 | 6.65 | 8.21 | | 0.94 | 15.80 |
| 60 | 7.30 | 7.49 | | 1.31 | 16.10 | 8.01 | 7.49 | | 1.31 | 16.81 | 7.74 | 7.49 | | 1.31 | 16.54 | 5.55 | 7.49 | | 1.31 | 14.36 |
| 70 | 5.89 | 6.71 | | 1.72 | 14.31 | 6.86 | 6.71 | | 1.72 | 15.29 | 6.81 | 6.71 | | 1.72 | 15.24 | 4.58 | 6.71 | | 1.72 | 13.01 |
| 80 | 4.31 | 5.88 | | 2.16 | 12.34 | 5.63 | 5.86 | | 2.16 | 13.65 | 5.85 | 5.86 | | 2.16 | 13.88 | 3.74 | 5.86 | | 2.16 | 11.77 |
| 90 | 2.69 | 5.00 | | 2.62 | 10.30 | 4.33 | 5.00 | | 2.62 | 11.94 | 4.88 | 5.00 | | 2.82 | 12.50 | 3.03 | 5.00 | | 2.62 | 10.64 |

Hay, 1977

**References**


Carter, E. A., Greenbaum, S. A. and Patel, A. M. 1976. *Listing of Solar Radiation Measuring Equipment and Glossary*. Center for Environmental and Energy Studies. The University of Alabama in Huntsville. Reprinted as *Catalog of Solar Radiation Measuring Equipment*. (ORO/5362-1), Carter, E. A., Breithaupt, W. G. and Patel, A. M. Contract No. EG-77-S-05-5362, April 1977.

Carter, E. A. and Patel, A. M. 1979. *Evaluation of Methods of Calculating Solar Radiation on an Inclined Surface*. Johnson Environmental and Energy Center, The University of Alabama in Huntsville. Contract No. EG-77-C-02-4494.

Coulson, K. L. 1975. *Solar and Terrestrial Radiation*. New York: Academic Press.

Flowers, E. J. 1977. *Test and Evaluation of the Performance of Solar Radiation Sensors at Inclination from the Horizontal Under Laboratory and Field Conditions*. DSE/1041-1, EX-76-A-29-1041, NOAA/ERL.

Hay, J. E., 1977. *An Analysis of Solar Radiation Data for Selected Locations in Canada*. Climatological Studies No. 32, Canadian Atmospheric Environment Service, Downsview, Ontario. pp. 158.

*I. G. Y. Instruction Manual*. 1958. "Radiation Instruments and Measurements." Part VI, London.

Kondratyev, K. Y. 1969. *Radiation in the Atmosphere*. New York: Academic Press.

Kondratyev, K. Y. and Fedorova, M. P. 1976. "Radiation Regime on Inclined Surfaces." *Proceedings of WMO-UNESCO Symposium on Solar Energy*. Geneva.

Latimer, J. R. 1979. "Investigation of Solar Radiation Instruments at the National Atmospheric Radiation Centre." *Conference International Solar Energy Society*. Melbourne.

Latimer, J. R. 1972. "Radiation Measurements." *Technical Manual Series No. 2, International Field Year Great Lakes*. IHD, Information Canada, Ottowa.

Norris, D. J. 1974. "Calibration of Pyranometers on Inclined and Inverted Positions." *Solar Energy*. No. 16. pp. 53-55.

World Meteorological Organization. 1968. *Guide to Meteorological Instruments and Observing Practices*. Chapter 9, 3rd Edition. Geneva.

CHAPTER 5

# SPECTRAL IRRADIANCE MEASUREMENTS OF NATURAL SOURCES

D. Crommelynck
Royal Meteorological Institute of Belgium
3 Avenue Circulaire
B-1180 Brussels
Belgium

and

J. R. Latimer
Atmospheric Environment Service
4905 Dufferin Street
Downsview, Ontario,
Canada

## 5.1 Introduction

The global irradiance on a horizontal surface and its direct and diffuse components are generally well known, while the energy absorbed by a black solar collector can be measured relatively easily. However, there are some sensing or solar energy processes which are spectrally selective, including human vision, photosynthetic sensitivity of plants, photoelectric conversion, and the ageing of materials. The variations in time and space of the spectral distributions of natural sources are not well understood, certainly not from a climatological point of view.

The phototropic behavior of plants, the erythemal effects of sunlight on the human skin and the physics of photoelectric conversion are important and their fields of application are well known.

Plants possess specific spectral sensitivities and photomorphogenic activities, which, although differing from species to species, appear to be sensitive to certain wavelengths.

The study of plant biology with respect to the radiation environment in greenhouses (Dogniaux and Nisen, 1975) is not easy, because the incident spectral energy field is generally not well known or defined. The absorption spectra of *in vitro* chlorophyllian pigments is given for several plants in Figure 5-1.

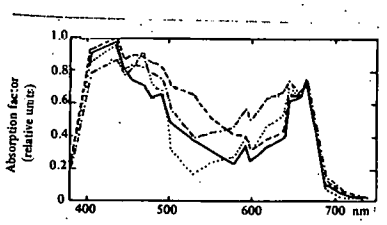


*Figure 5-1 In vitro absorption of the chlorophyllian pigments of four ornamental plants (Dodillet, 1961)*

If a mean of these curves is multiplied by the spectral distribution of natural light expressed in quanta per wavelength, the specific spectral irradiance is obtained (Figure 5-2). However, an actual curve for a plant varies with its real absorption coefficient and with the spectrum of the incident light. Human skin, as well as plant matter, is sensitive to radiation. Figure 5-3 shows the relative spectral sensitivity of human skin for five ozone thicknesses.

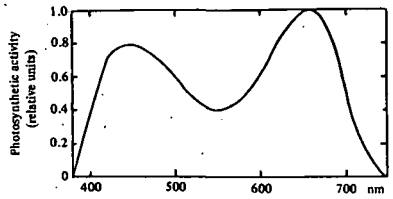


*Figure 5-2 Mean specific spectral photosynthetic irradiance (Dodillet, 1961).*

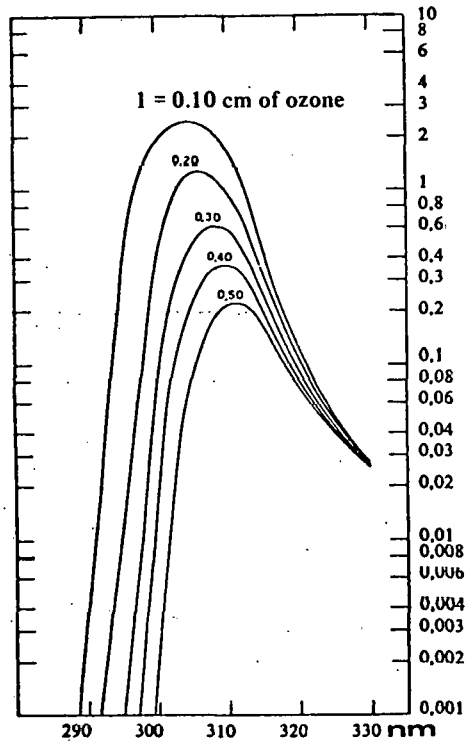


*Figure 5-3 Distribution of the specific erythermal spectral irradiance of the global solar radiation on a horizontal surface (altitude: sea level; sun elevation; 45°; very bright, clear sky) (Dogniaux, 1954)*

Plastics are also sensitive to radiation. Reticulation and chain breaking occur due to UV radiation resulting in loss of elasticity and mechanical resistance. These effects are often accompanied by photo-oxidation and color changes. When the radiation has a shorter wavelength than that required for bondage, the effects are proportional to the number of available quanta. The spectral distribution of the incident light must be known to evaluate the electrical energy which can be obtained with the use of specific photo-electric conversion devices.

The spectral variations are mainly due to the sun's elevation, and the variations in the atmospheric total ozone, water vapor and aerosol content and cloud cover. (Dogniaux, 1970; Guzzi et al, 1972, Kok, 1972; and Vittori et al, 1974.)

Spectral radiation can be catagorized according to source in a similar manner as global radiation:

1. direct spectral radiation from the sun measured on a plane normal to the incident rays;

2. global spectral radiation (from sun and sky);

3. diffuse spectral radiation (from sky only);

4. reflected spectral radiation (from the ground).

The global and diffuse spectral radiation values are usually measured on a horizontal plane unless otherwise specified.

These four streams of solar energy are not only a function of the location and time of observation but also of the wavelength. If one is not cautious in data gathering, the observational data are quickly overwhelming.

A general strategy is a prerequisite for the observation method used as well as for the data reduction and presentation.

Three approaches are possible:

1. To observe the whole spectrum continuously, the amount of data to be stored and reduced will thus be important.

2. To observe continuously a limited number of wavelengths, chosen so that the spectrum can be reconstructed whenever needed with reasonable accuracy.

3. To observe the whole spectrum for typical atmospheric situations and to derive from these a classification of the corresponding spectral distributions. Although the author prefers a combination of the second and third approaches, it must be recognized that the first is equally valid, and may be the simplest.

## 5.2 Measurement Techniques and Problems

### 5.2.1 Instrumentation for Spectral Measurement

Spectral observations can be obtained in several ways. The *spectrometer* senses a complete spectrum instantaneously. However, photographic or optical recording is needed. The *monochromator* records a spectrum, but requires some time to scan the useful wavelength range. A *series of sensors with filters* can be used for continuous observations.

In each case, a series of requirements must be met. In general, the source will not be uniformly distributed over the sky. This indicates that the instrumentation should obey the Lambert's law (cosine response) as close as possible because corrections can not be made.

Since spectral irradiance varies with time, the output signal should be linearized. Finally, and most importantly, the absolute spectral sensitivity of the observation system must be known.

If the linearity and the cosine law requirements are not sufficient, it is obvious that "calibration" in the strictest sense of the word is of no help (Crommelynck, 1977).

### 5.2.2 Preliminary Definitions

#### 5.2.2.1 The Source

The spectral irradiance on a flat surface due to a radiation source can be described by its relative $\mathscr{S}(\lambda)$ or absolute $S(\lambda)$ spectral distribution, where $\lambda$ is wavelength. The relationship between these distributions defines the factor s:

$$S(\lambda) = s \cdot \mathscr{S}(\lambda) \qquad (1)$$

The maximum value of $\mathscr{S}(\lambda)$ is usually normalized to unity, and $S(\lambda)$ is expressed in W $m^{-2}$ per unit wavelength interval.* The spectral irradiance is a differential quantity with respect to wavelength: $S(\lambda) = dS/d\lambda$. The integration of the absolute spectral irradiance over its complete spectral domain gives the total incident radiation irradiance S:

$$\int_\lambda S(\lambda)d\lambda = s\int_\lambda \mathscr{S}(\lambda)d\lambda = S \qquad (2)$$

#### 5.2.2.2 The Sensor

Assuming, that the field of view of the considered sensor is hemispherical and that the Lambert law and the linearity of response conditions are satisfied, the sensor is also characterized by its relative $\mathscr{D}(\lambda)$ or absolute $D(\lambda)$ spectral sensitivity. This is the ratio of output signal (noted uniformly by V) relative to the incident energy per unit wavlength interval $W(\lambda)$ with

$$W(\lambda) = \frac{d\bar{W}}{d\lambda} \quad \text{and} \quad D(\lambda) = \frac{\bar{V}(\lambda)}{W(\lambda)} \qquad (3)$$

The relative and absolute spectral sensitivities are related by:

$$D(\lambda) = d\mathscr{D}(\lambda) \qquad (4)$$

$\mathscr{D}(\lambda)$ is usually normalized to unity at wavelength of maximum sensitivity. A sensor is linear when for the same wavelength $\lambda_a$:

$$[aW(\lambda_a) + bW(\lambda_a)]\ D(\lambda_a) = aV(\lambda_a) + bV(\lambda_a)$$

$$= (a + b)V(\lambda_a) \qquad (5)$$

For different wavelengths, the output is equal to the sum of the individual wavelength outputs.

### 5.2.3 Measurements with Spectrometers and Monochromators

When a source of an absolute spectral distribution $S(\lambda) \equiv W(\lambda)$ is observed with a sensor having the absolute sensitivity function $D(\lambda)$, the result at wavelength $\lambda_o$ is:

$$S(\lambda_o) \cdot D(\lambda_o) = s \cdot d \cdot \mathscr{S}(\lambda_o) \cdot \mathscr{D}(\lambda_o) = V(\lambda_o) \qquad (6)$$

It is assumed that the slit function is retangular and contained within $D(\lambda_o)$, which is acceptable as

*frequency or wavenumber intervals are often considered.

a simple first approximation. For accurate measurements, especially with sources having line structures, the calculations of Lempicki et al (1961) should be used.

If the spectral characteristic $D(\lambda)$ of the instrument is known, it is easy to find the spectral distribution $S(\lambda)$ by scanning the wavelength range. Since it is sometimes difficult to keep $D(\lambda)$ constant for relatively long periods, a continuous comparison with a standard lamp of known spectral irradiance is required. The total incident energy is given by:

$$S = s\int_{\lambda}\mathscr{S}(\lambda)d\lambda = \frac{1}{d}\int\frac{V(\lambda)}{\mathscr{D}(\lambda)}d\lambda \qquad (7)$$

and can be crosschecked by a direct measurement of S.

A spectrometer specially developed for use in the field is the QSM-2500 Quanta spectrometer (400 to 740 nm) manufactured by Techtum Instrument in Sweden.

### 5.2.4 Measurements with Selective Filter Sensors

#### 5.2.4.1 Use of a Single Sensor

Black-coated thermopiles or bolometric sensors are uniformly sensitive over a wide spectral range, and their measurements yield the total irradiance, however, most sensors have a limited spectral range. They can be equipped with band-pass or other filters, which restrict the sensitivity from $\lambda$ min to $\lambda$ max. In this case the measurements may be expressed by the relationship:

$$\int_{\lambda_{min}}^{\lambda_{max}} S(\lambda)\cdot D(\lambda)d\lambda = s\cdot d\cdot\int_{\lambda_{min}}^{\lambda_{max}}\mathscr{S}(\lambda)\mathscr{D}(\lambda)d\lambda = V \qquad (8).$$

From measurements of either the short-circuit amperage or the voltage across a known resistance, and having no information about the source, the only result obtained is the converted electrical power.

If only $D(\lambda) = d\mathscr{D}(\lambda)$ is known, the spectral distribution function of the source cannot be deduced from V. However, if the relative spectral irradiance of the source is also known, then it is possible to determine the factor s with Eqs. (1) and (2):

$$s = \frac{V}{d\int\mathscr{S}(\lambda)\mathscr{D}(\lambda)d\lambda} \qquad (9)$$

If the sensor is sensitive only in a small spectral bandwidth (due to the use of interference filters), and if the spectral sensitivity function is symmetric with respect to the central wavelength between $\lambda_1$ and $\lambda_2$, then the situation is different.

If the source can be described by a linear function between $\lambda_1$ and $\lambda_2$, then:

$$\mathscr{S}(\lambda) = a\lambda + b \qquad (10)$$

so that:

$$s\cdot d\int_{\lambda_1}^{\lambda_2}\mathscr{S}(\lambda)\mathscr{D}(\lambda)d\lambda = s\cdot d\,\mathscr{S}(\lambda_0)\mathscr{D}(\lambda_0)\Delta\lambda \qquad (11)$$

where $\Delta\lambda$ is given by:

$$\Delta\lambda = \frac{1}{\mathscr{D}(\lambda_0)}\int_{\lambda_1}^{\lambda_2}\mathscr{D}(\lambda)d\lambda \qquad (12)$$

and $\mathscr{D}(\lambda_0)$ is *the maximum* of $\mathscr{D}(\lambda)$ within $\lambda_1$, $\lambda_2$:

$$\mathscr{S}(\lambda_0) = \frac{V}{s\cdot d\cdot\mathscr{D}(\lambda_0)\Delta\lambda} \qquad (13)$$

$\mathscr{S}(\lambda_0)$ fixes one of the parameters a or b when the other is known.

If the source is described by some other non-linear function or contains spectral lines within the interval $\lambda_1$, $\lambda_2$ then Eqs. (11) and (13) are not applicable. Moreover, if this method is used as a first approximation, a complementary study is needed to evaluate the error which is introduced by $\Delta\lambda$. If the spectral sensitivity curve is not symmetric, similar errors are introduced. Unfortunately, this is often the case with interference filters mounted between the diffuser and detector.

Spectral pyranometers sensitive to the ultraviolet region (315, 350 to 400 nm) are available from Fleming Instruments Ltd.

#### 5.2.4.2 Measurements with Two Sensors (Both High Pass) by the Difference Method

Instead of using a single cell, two different high-pass filter cells can be used; the difference of their observed signals can then be calculated. Such a procedure generally introduces more errors, because

there is a small probability that the leading edges (cut-offs) of the filters are equal. This asymmetry negates the symmetry requirement of 5.2.4.1.

As the complexity of such a system becomes greater it will be more difficult to guarantee the results. Ageing of the spectral characteristics will probably not be similar. Finally, additional errors will appear due to the fact that the transmission is, in general not constant in the wavelength region where the contribution to the resulting signal must cancel by differencing.

#### 5.2.4.3 Measurements with n Sensors

If the symmetry requirement cannot be fulfilled for each individual sensor of n sensors but the spectral sensitivity $D_n(\lambda)$ of each is well known, it is possible to obtain a reasonable knowledge of the observed natural source $S(\lambda)$ by using a set of n spectral sensors to obtain a system of integral equations

$$\int S(\lambda)D_n(\lambda)d\lambda = V_n. \qquad (14)$$

The required number and kinds of sensor are chosen in accordance with the expected variation of the spectrum with $\lambda$.

### 5.2.5 General Considerations Relative to the Construction of Spectrally Sensitive Sensors.

If the spectral detector is chosen so that it gives a linear response (short-circuit current of a solar cell), the response of the sensor will give a correct cosine response if either an integrating sphere or an appropriate diffusing slab is placed in front of the detector. The total spectral sensitivity of the system will result from the combined characteristics of the diffuser (or integrating sphere), filter, lens between the diffuser and filter and the spectral sensitivity of the detector.

Some spectral pyranometers have a Schott glass hemisphere (WG7, GG14, 0G1, RG2, RG8) (Eppley, U. S. A.). Significant errors can be made with this type of instrument if a correction is not applied (Gulbrandsen, 1978).

If there is an interference filter, the spectral transmission is a function of the angle of incidence of the incoming light. If it is a normal, parallel beam, the transmission function will be relatively narrow and symmetrical. If the filter is placed directly behind the diffusing system, the transmission function will be broadened and no longer symmetric.

Since usually detectors are not uniformly sensitive in all wavelengths (except thermopiles), some residual asymmetry will be present even if a lens is placed in front of the interference filter. An accurate instrument should have a system to maintain a constant temperature of the detection components, and should use a redundant detector to reduce drifts and dark currents. For obvious reasons, the interference filter should not be placed on the outside surface of the system. It is often difficult to find an instrument which has high reliability under all conceivable weather conditions.

### 5.2.6 Comparison of Spectrally Sensitive Sensors

Once an observational network is installed, it is necessary to ensure that all the observations are compatible. Instrument intercomparisons and spectral calibrations are usually necessary. The intercomparisons with a standard sensor is sufficient, if the relative spectral sensitivities are identical.

With

$$D_n(\lambda) = d_n\mathscr{D}_n(\lambda),\ D_p(\lambda) = d_p\mathscr{D}_p(\lambda). \qquad (15)$$

that means:

$$\mathscr{D}_n(\lambda) \equiv \mathscr{D}_p(\lambda) \equiv \mathscr{D}(\lambda). \qquad (16)$$

Simultaneous measurements with different cells, having the same uniform irradiance source $S(\lambda)$, which may be arbitrary, give the following outputs:

$$d_n \int S(\lambda)\mathscr{D}(\lambda)d\lambda = V_n \qquad (17)$$

$$d_p \int S(\lambda)\mathscr{D}(\lambda)d\lambda = V_p \qquad (18)$$

so that:

$$d_n = \frac{V_n}{V_p} d_p \qquad (19)$$

If $\mathscr{D}_n(\lambda) \neq \mathscr{D}_p(\lambda)$, simultaneous measurements of a common source will provide $d_n$ as a function of $d_p$ only if the relative sensitivities $\mathscr{D}_n(\lambda)$ and $\mathscr{D}_p(n)$ as

well as the relative spectral distribution of the source $\mathscr{S}(\lambda)$ are known:

$$d_n = \frac{V_n}{V_p} dp \frac{\int \mathscr{S}(\lambda)\mathscr{D}_p(\lambda)d\lambda}{\int \mathscr{S}(\lambda)\mathscr{D}_n(\lambda)d\lambda} \quad (20)$$

These results are also valid for solar cells; care must be taken that the loading conditions of the electric circuit are similar and functionally defined. If the absolute spectral distribution $S(\lambda)$ is known, as well as $\mathscr{D}_n(\lambda)$ simultaneous measurements are useless because $d_n$ is:

$$d_n = V_n \frac{1}{\int S(\lambda)\mathscr{D}_n(\lambda)d\lambda} \quad (21)$$

### 5.2.7 Determination of Characteristics (Wyatt, 1978)

The characteristics of spectral detection systems must necessarily include and ensure:

1. *The linearity*, which should be normalized relative to a standard scale;

2. *The cosine response* for different incident directions;

3. *The absolute spectral sensitivity* function as well as the *thermal behavior* and *zero point* deviation (Gulbrandsen, 1978).

The first two characteristics can be checked with relative ease by the methods used for pyranometers; in principle they will not change with time.

The absolute spectral sensitivity is much more difficult to determine; it can be influenced by temperature, time and drift. Equipment for recalibration is expensive and probably cannot be justified except for the largest observational networks.

It is imperative that the user of an instrument know precisely what methods were used to calibrate it, what the standards were, and what degree of accuracy was obtained. Two categories of instruments can be considered.

#### 5.2.7.1 Spectrometers or Monochromators

The usual means of calibration is achieved with a standard lamp of well known spectral intensity distribution to determine the absolute spectral sensitivity. However, care must be taken and attention given to calibration stability, ageing, bandwidth or slit function and response time. As for filter sensors *of known relative spectral sensitivity* use is made of Eq. (21). The method proposed for filter sensors in 5.2.7.2 is also useful for calibrating spectrometers or monochromators.

#### 5.2.7.2 Sensors with Filters

For the calibration of sensors with filters when their relative spectral sensitivity is not known, the use of lamps or other broad-band spectral sources is inadequate. Monochromatic (lasers) or quasi-monochromatic variable or tunable sources should be used according to equation $D(\lambda_n) = V_n/S(\lambda_n)$.

The procedure is:

1. to stabilize the source for a certain wavelength;

2. to measure the spectral output power with an absolute radiometer or with a precisely calibrated or certified silicon cell (transfer standard);

3. to transform the non-uniform flux of the source into a *uniform* spectral irradiance via the careful use of an integration sphere (the precise knowledge of its spectral reflectance is required).

4. to irradiate the sensor and measure the output for a desired wavelength

5. to repeat this sequence for a series of wavelengths and to obtain the absolute spectral sensitivity function $D(\lambda)$.

It must be kept in mind that dye lasers do not always cover the desired range of wavelengths. To overcome this problem the relative spectral sensitivities must be determined and scaled in absolute units in accord with the results obtained by laser sources in conjunction with an absolute radiometer standard

or a silicon-cell transfer standard. This means that at least for one wavelength $D(\lambda_o) = V_o/S(\lambda_o)$ must be determined.

When sensors are installed for the first time in a network, they should be given special attention to ensure that their functioning is not affected by the weather. The procedure for determining $D(\lambda)$ should be repeated periodically so that effects of ageing can be detected.

Diffusing surfaces must be cleaned frequently because the blue end of the spectrum is particularly attenuated by dust or thin deposits of grease, especially when the outer surface is not polished.

## 5.3 Determination of the Specific Total and Spectral Irradiance of Spectrally Sensitive Phenomena

### 5.3.1 The Problem

For some applications it is not the spectral irradiance $S(\lambda)$ or the irradiance S which is of interest but rather the specific spectral irradiance $T(\lambda)$:

$$T(\lambda) = S(\lambda)D(\lambda) \tag{22}$$

or the total specific irradiance T:

$$T = \int S(\lambda)D(\lambda)d\lambda \tag{23}$$

since these are associated with spectrally sensitive effects.

For example, $D(\lambda)$ may be the relative spectral sensitivity or efficiency of the average human eye, the specific absorption spectrum of a plant (Figure 5-1), the spectral response of the human skin (Figure 5-3) or other selected spectral irradiance conversions suggested above and described in DIN5031 (1978). The units of these specific irradiances depend on the mechanism selected (lumen for vision, finsen or erythermal watts for skin effects, etc.)

### 5.3.2 The Measurement of the Specific Irradiance T

The best way to determine T is to use a sensor which has the same spectral sensitivity $D(\lambda)$ as the selected effect. If such a sensor does not exist, it can be constructed by combining either a flat-response detector of absolute sensitivity D (thermopile) or a spectral-sensitive detector of absolute sensitivity $D'(\lambda)$ (solar cell) with an *ad hoc* filter of spectral transmission $F(\lambda)$ or $F'(\lambda)$. Then $D(\lambda)$ becomes in the first case:

$$D(\lambda) = D \cdot F(\lambda)$$

or in the second case:

$$D(\lambda) = D'(\lambda) \cdot F'(\lambda). \tag{24}$$

This is obtained for photometers with viscor filters.

In this way, the direct measurements of T is:

$$T = \int S(\lambda)D(\lambda)d\lambda = \int S(\lambda)D \cdot F(\lambda)d\lambda = \int S(\lambda)D'(\lambda) \cdot F'(\lambda)d\lambda \tag{25}$$

### 5.3.3 The Determination of the Specific Spectral Irradiance $T(\lambda)$

For a given source $S(\lambda)$, with $D(\lambda)$ known, $T(\lambda)$ can be determined. A knowledge of $D(\lambda)$ is sufficient to determine $T(\lambda)$ for a given wavelength. The spectral mechanism produces only T and not $T(\lambda)$ as a response.

### 5.3.4 Error in the Measurement of the Total Specific Irradiance T

Some differences may be encountered between the function $D(\lambda)$ and the actual spectral characteristic $DF(\lambda)$ or $D'(\lambda)F'(\lambda)$ of the equivalent sensor constructed.

The error $\Delta T = T - T'$ is given by:

$$\Delta T = \int S(\lambda)[D(\lambda) - D'(\lambda)F'(\lambda)]\,d\lambda$$

or

$$\Delta T = \int S(\lambda)[D(\lambda) - D]\,d\lambda \tag{26}$$

if, at the limit, no filter is mounted in front of a uniform spectrally sensitive sensor having the sensitivity D.

### 5.3.5 Approximate Determination of the Specific Irradiance

Taking account of the possibility of a difference occurring between $D(\lambda)$ and $D'(\lambda) \cdot F'(\lambda)$ because of the ageing of $D'(\lambda)$ and/or $F'(\lambda)$ or some other economic reason, it is worthwhile to consider the following ratio:

$$K = \frac{T}{T'} = \frac{\int S(\lambda)D(\lambda)d\lambda}{\int S(\lambda)D'(\lambda)F'(\lambda)d\lambda} \qquad (27)$$

where, as a special case, $D'(\lambda)F'(\lambda)$ can be equal to D.

The total specific irradiance T is then given by:

$$T = K \cdot \int S(\lambda)D'(\lambda) \cdot F'(\lambda)d\lambda. \qquad (28)$$

of course K, given by the equation:

$$\frac{1}{K} = 1 - \frac{\Delta T}{T} \qquad (29)$$

depends not only upon $D(\lambda)$ and $D'(\lambda) \cdot F'(\lambda)$ but also on the spectral irradiance $S(\lambda)$ which is, in general, a function of time.

### 5.3.6 Application of Section 5.3.5

#### 5.3.6.1 Example of the Approximate Determination of the Global Radiation Through Use of a Photometer (Dogniaux, 1974)

In this case, $D(\lambda)$ is the spectral luminous efficiency of the average human eye. T is expressed in klx. *The global radiation*

$$T' = \int S(\lambda)d\lambda \qquad [W\ m^{-2}] \qquad (30)$$

is equal to:

$$\frac{T}{K} = \frac{1}{K}\int S(\lambda)D(\lambda)d\lambda \qquad (31)$$

If T is directly measured with a wide-angle photometer, K is a function of the actual composition of the atmosphere. Figure 5-4 gives K as a function of the elevation angle of the sun, $90 - \Theta$, (where $\Theta$ is the zenith angle) and the turbidity coefficient $\beta$. In this case, the amount of water vapor in the atmosphere, expressed as the thickness of precipitable water (w in cm), must not be considered (see Chapters 3 and 8).

#### 5.3.6.2 Example of the Approximate Determination of the Direct Solar Radiation Through Use of a Photometer (Doginaux, 1974)

As in Section 5.3.6.1, $D(\lambda)$ corresponds to the sensitivity of the average eye; T is in klx, while the direct radiation T' is in W $m^{-2}$. The correction factor K for determining the direct solar radiation (Figure 5-5) is much more sensitive to the sun elevation ($90 - \Theta$), the turbidity coefficient $\beta$, and the water vapor content w, than for determining the global radiation with clear skies. However, if these factors are known, a photometer could be used when the sky is clear.

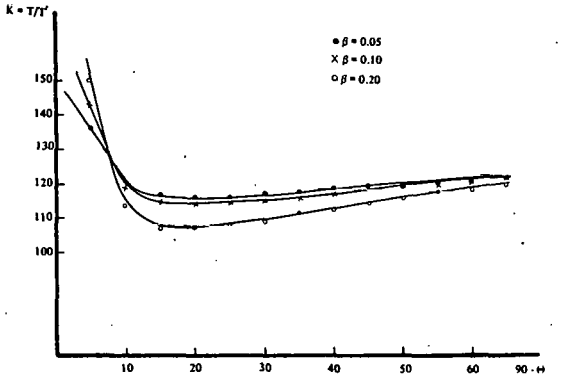


*Figure 5-4 Value of the Factor K for clear sky conditions as a function of the sun elevation, 90 - Θ, (deg) and the turbidity coefficient β for determination of the global radiation. (In the three cases β is quasi-independent of precipitable water amounts between 0.5 and 5 cm.) (Dogniaux, 1974)*

It is apparent that any instrument for measuring the global, diffuse or direct radiation by photometric techniques is worthless if K is not provided for the application intended.

### 5.4 Sample Data

The examples of daylight spectral irradiances shown in Figures 5-6 and 5-7 were published by Kok (1972) from measurements made in Pretoria. They may be used to approximate clear sky values for a given air mass at other locations. Turbidity and total water vapor content which also affect the spectral irradiance have been evaluated (Dogniaux, 1970) or measured (Guzzi et al, 1972).

Figure 5-8 shows the effect of clouds passing in front of the sun at various times of the day. (This is another problem for observations in all-weather conditions.)

With clear-sky conditions, the proportions of direct and diffuse sky spectral irradiance relative to the global spectral irradiance depend on wavelength. This is illustrated in Figure 5-9 for four different elevations of the sun.

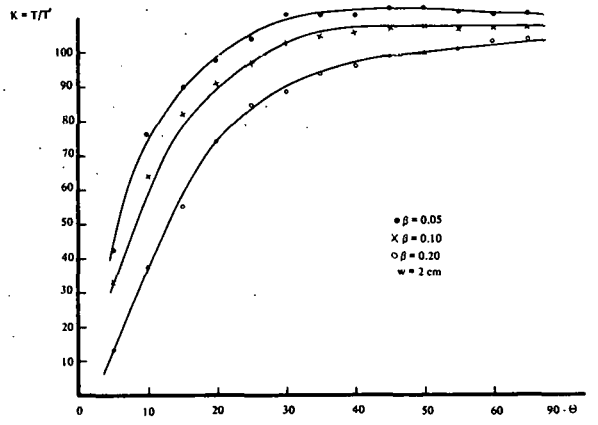


*Figure 5-5 Value of the factor K for clear sky conditions as a function of the sun elevation, 90 - Θ (deg), β and w for determination of the direct solar radiation. (Dogniaux, 1974)*

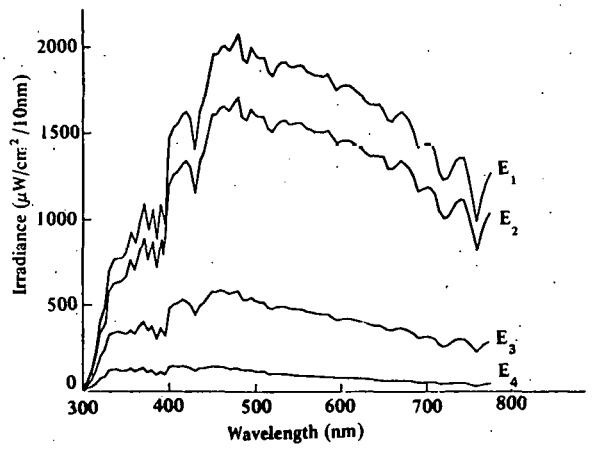


*Figure 5-6 The spectral irradiance distributions for different phases of daylight and different cloud conditions: $E_1$, very hot summer day with a high percentage of reflecting clouds ($m \simeq 0.86$); $E_2$, average summer day ($m \simeq 1$); $E_3$, sky irradiance for cloudy (0.5 cloud cover) summer day ($m \simeq 1$); $E_4$, sky irradiance for clear summer day ($m \simeq 1$). (Kok, 1972)*

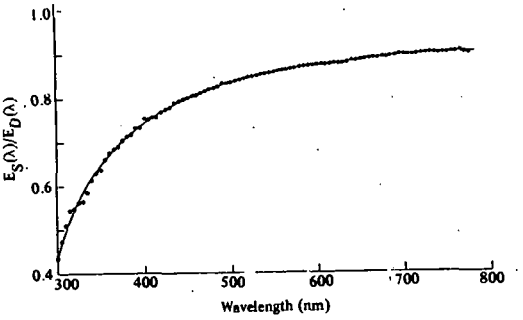


*Figure 5-7 The ratio of direct solar to total daylight irradiance (Kok, 1972).*

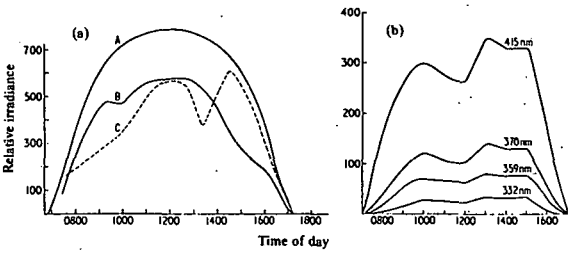


*Figure 5-8 (a) Curves showing the effect of smog on direct solar irradiance; A - theoretical curve for clean, clear skies; B - 25 June 1959. (b) The effect of smog on monochromatic solar irradiances on 22 July 1959 (Kok, 1972).*

## 5.5 Application of Filter Radiometry to Spectral Measurements of Solar Radiation

### 5.5.1 Introduction

Reasonably well-defined bands of solar radiation can often be determined more readily with filters than with a spectrophotometer. In principle, spectral measurements of solar radiation with carefully calibrated filters can be made as easily as pyrheliometric measurements of the total solar intensity. Also, since spectrometric techniques are more appropriate to special laboratory use than to routine field operation, this section will be confined to what has now become known as "filter radiometry" (*IGY*, 1958; *WMO Guide*, 1965).

### 5.5.2 Broad and Narrow Bandpass Optical Filters

Two types of optical filter are employed in meteorological investigations. The first of these is a group of colored glasses manufactured by Schott

(Mainz), while the second are interference filters constructed of multilayers of metals and dielectric materials evaporated onto glass or quartz substrates. Both filter types can be supplied as hemispherical or plane specimens.

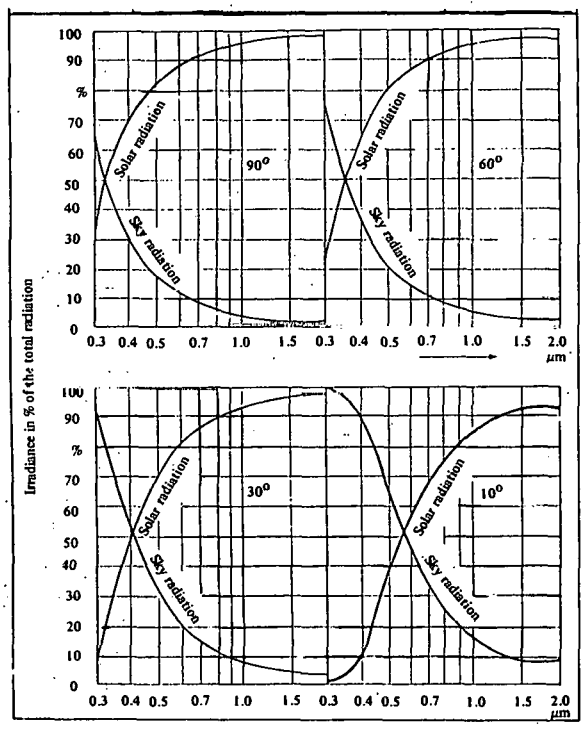


*Figure 5-9 Percentage of solar radiation and sky radiation at different altitudes of the sun (cloudless days).*

### 5.5.2.1 Characteristics of Filters

Each Schott colored glass filter is characterized by three regions with: (1) complete opaqueness to solar radiation; (2) practically uniformly high transmission; (3) intermediate transitional transmission between (1) and (2). The specific filters recommended for international meteorological use are Nos. OG530, RG630 and RG695. The first two have been employed for many years, especially in studies of atmospheric turbidity; the third was introduced during the 1940's. Ideally, these have the following characteristics:

OG530: opaque up to 530 nm,
transparent 530 to 2800 nm;

RG630: opaque up to 630 nm,
transparent 630 to 2800 nm;

RG695: opaque up to 695 nm,
transparent 695 to 2800 nm.

New filter glasses have been added to the Schott series and the whole series has been renumbered. Representative values for the transmittance of Schott filter glasses are given in Table 5-1 (Drummond, 1968).

A series of such filters was examined with a spectrophotometer and their transmission parameters were published (Ångström and Drummond, 1961). Table 5-2 summarizes the variation with temperature of the positions of each center of lower wavelength cutoff, while Table 5-3 shows the variation with glass thickness of the transmittance in the main transmission region. To obtain the amount of solar radiation at wavelengths longer than the lower cutoff, it is, of course, necessary to multiply the amount measured (with the filter in place) by the filter factor in Table 5-1. Each individual filter must, however, be examined since the position of the lower wavelength cutoff may vary from the ideal value by up to ±10 nm so that the filter factor may vary by ±0.005 in general. It is usually desirable to correct the measurements of solar radiation made with an individual filter to values which have been obtained using an ideal filter of the same designation. This can be done by applying the additive corrections given in Table 5-4.

### 5.5.2.2 Design of Filters

Interference filters are designed to isolate relatively small wavelength intervals, generally about 50 nm in the ultraviolet, 100 nm in the visible, and several hundred nm in the near infrared. Apart from blocking energy outside of the main band, possibly the most important properties that a filter should have are a minimum variation in transmittance across the main band and steep cutoff slopes at each edge of the band. Unwanted secondary transmission (occurring elsewhere than in the main band) throughout the solar spectral range of 250-3000 nm should be supressed to levels around optical density 4 (i.e., equivalent to a filter transmittance of 0.0001). Typical transmission curves of narrow bandpass filters are given in Figure 5-10.

Table 5-1

Representative Values for the Transmission of Schott Filter Glass
(2.0 mm thickness, +25°C)

| λ NEW / NM OLD | WG295 / WG7 | GG395 / GG22 | GG400 / ----- | GG495 / GG14 | OG530 / OG1 | OG570 / OG2 | RG610 / RG1 | RG630 / RG2 | RG695 / RG8 | RG715 / RG10 | RG805* / ----- |
|---|---|---|---|---|---|---|---|---|---|---|---|
| 270 | 0.22 | 0.00 | 0.00 | 0.00 | 0.00 | 0.00 | 0.00 | 0.00 | 0.00 | 0.00 | 0.00 |
| 80 | .41 | | | | | | | | | | |
| 90 | .60 | | | | | | | | | | |
| 300 | .74 | | | | | | | | | | |
| 20 | .83 | | | | | | | | | | |
| 40 | .90 | .00 | | | | | | | | | |
| 60 | .91 | .01 | .00 | | | | | | | | |
| 80 | .91 | .31 | .01 | | | | | | | | |
| 400 | .91 | .68 | .52 | | | | | | | | |
| 20 | .91 | .82 | .78 | | | | | | | | |
| 40 | .91 | .87 | .83 | .00 | | | | | | | |
| 60 | .92 | .88 | .87 | .01 | | | | | | | |
| 80 | .92 | .88 | .89 | .27 | | | | | | | |
| 500 | .92 | .89 | .90 | .80 | .00 | | | | | | |
| 20 | .92 | .90 | .90 | .88 | .05 | | | | | | |
| 40 | .92 | .90 | .90 | .90 | .76 | .00 | | | | | |
| 60 | .92 | .90 | .90 | .90 | .88 | .38 | | | | | |
| 80 | .92 | .90 | .90 | .91 | .90 | .83 | .00 | | | | |
| 600 | .92 | .90 | .90 | .91 | .91 | .89 | .33 | .00 | | | |
| 20 | .92 | .90 | .90 | .91 | .91 | .91 | .83 | .26 | | | |
| 40 | .92 | .90 | .90 | .91 | .91 | .91 | .89 | .85 | | | |
| 60 | .92 | .90 | .91 | .91 | .91 | .91 | .90 | .91 | .00 | .00 | |
| 80 | .92 | .90 | .91 | .91 | .91 | .91 | .91 | .91 | .27 | .01 | |
| 700 | .92 | .90 | .91 | .91 | .91 | .91 | .91 | .91 | .84 | .25 | .00 |
| 720 | .92 | .90 | .91 | .91 | .91 | .91 | .91 | .91 | .91 | .74 | .00 |
| 40 | .92 | .90 | .91 | .91 | .91 | .91 | .91 | .92 | .92 | .89 | .00 |
| 60 | .92 | .90 | .91 | .91 | .92 | .91 | .91 | .92 | .92 | .91 | .02 |
| 80 | .92 | .90 | .91 | .91 | .92 | .91 | .91 | .92 | .92 | .92 | .09 |
| 800 | .92 | .90 | .91 | .91 | .92 | .91 | .91 | .92 | .92 | .92 | .34 |
| 20 | .92 | .90 | .91 | .91 | .92 | .91 | .91 | .92 | .92 | .92 | .68 |
| 40 | .92 | .90 | .91 | .91 | .92 | .91 | .91 | .92 | .92 | .92 | .84 |
| 60 | .92 | .90 | .91 | .91 | .92 | .91 | .91 | .92 | .92 | .92 | .88 |
| 80 | .92 | .90 | .91 | .91 | .92 | .91 | .91 | .92 | .92 | .92 | .89 |
| 900 | .92 | .90 | .91 | .91 | .92 | .91 | .91 | .92 | .92 | .92 | .89 |
| 1000 | .92 | .90 | .91 | .91 | .92 | .91 | .91 | .92 | .92 | .92 | .90 |
| 1200 | .92 | .90 | .91 | .91 | .92 | .91 | .91 | .92 | .92 | .92 | .90 |
| 1500 | .92 | .90 | .91 | .91 | .92 | .91 | .91 | .92 | .92 | .92 | .90 |
| 2000 | .91 | .89 | .90 | .90 | .90 | .90 | .91 | .91 | .91 | .91 | .88 |
| 2500 | 0.85 | 0.86 | 0.85 | 0.85 | 0.87 | 0.86 | 0.87 | 0.87 | 0.87 | 0.87 | 0.82 |
| CENTER OF CUTOFF (NM) | 281 | 385 | 397 | 485 | 529 | 562 | 603 | 623 | 686 | 707 | 807 |
| FILTER FACTOR | 1.09 | 1.11 | 1.105 | 1.10 | 1.095 | 1.095 | 1.105 | 1.095 | 1.09 | 1.09 | 1.11 |

*RG805 STANDARD THICKNESS IS 4.0 MM.

N.B. VARIATIONS FROM THESE VALUES OF TRANSMITTANCE AND OF CENTER OF CUTOFF CAN OCCUR WITHIN THE GLASS MELT AS FOLLOWS: UP TO +0.01 - +2 NM, RESPECTIVELY.

Table 5-2

Variation in the Position of the Center of Low Cutoff (in nm) With Temperature and Thickness

| T(°C) | 1.0MM | | | 2.0MM | | | 3.0MM | | |
|---|---|---|---|---|---|---|---|---|---|
| | OG530 | RG630 | RG695 | OG530 | RG630 | RG695 | OG530 | RG630 | RG695 |
| -20 | 522.0 | 616.5 | 682.5 | 527.0 | 621.0 | 688.5 | 530.0 | 624.0 | 692.5 |
| -10 | 523.5 | 618.0 | 684.0 | 528.5 | 622.5 | 690.5 | 531.5 | 625.5 | 694.5 |
| 0 | 524.5 | 619.5 | 686.0 | 529.5 | 624.0 | 692.0 | 532.5 | 627.0 | 696.0 |
| +10 | 526.0 | 621.0 | 688.0 | 531.0 | 625.5 | 694.0 | 533.5 | 628.5 | 698.0 |
| +20 | 527.0 | 622.5 | 689.5 | 532.0 | 627.0 | 695.5 | 535.0 | 630.0 | 699.6 |
| +30 | 528.0 | 623.5 | 691.0 | 533.0 | 628.0 | 697.0 | 536.0 | 631.5 | 701.0 |
| +40 | 529.5 | 625.0 | 693.0 | 534.0 | 629.5 | 699.0 | 537.5 | 632.5 | 703.0 |

Table 5-3

Variation of Transmittance With Glass Thickness in the Main Region

| THICKNESS | 1.0 MM | 2.0 MM | 3.0 MM |
|---|---|---|---|
| TRANSMITTANCE ($\tau$) | 0.912 | 0.909 | 0.907 |
| FILTER FACTOR (FF) | 1.096 | 1.100 | 1.103 |

Table 5-4

Values of the Additive Correction in W $m^{-2}$ Corresponding to a Wavelength Shift of +10 in the Lower Wavelength Cutoff for Specified Air Masses and Turbidity Coefficients

| | OG530 | | | | RG630 | | | | RG695 | | | |
|---|---|---|---|---|---|---|---|---|---|---|---|---|
| | AIR MASS | | | | AIR MASS | | | | AIR MASS | | | |
| TURBIDITY | 1 | 2 | 3 | 4 | 1 | 2 | 3 | 4 | 1 | 2 | 3 | 4 |
| 0.00 | 18.2 | 16.1 | 14.0 | 12.6 | 16.8 | 15.4 | 14.7 | 14.0 | 14.0 | 13.3 | 13.3 | 12.6 |
| 0.05 | 16.1 | 12.6 | 9.8 | 7.7 | 15.4 | 13.3 | 11.2 | 9.8 | 13.3 | 11.9 | 10.5 | 9.8 |
| 0.10 | 14.0 | 9.8 | 7.0 | 4.9 | 14.0 | 10.5 | 8.4 | 6.3 | 11.9 | 9.8 | 8.4 | 7.0 |
| 0.20 | 11.2 | 6.3 | 3.5 | 2.1 | 11.9 | 7.7 | 4.2 | 2.8 | 10.5 | 7.0 | 4.9 | 3.5 |

### 5.5.2.3 Calibration of Filters

Calibration involves spectrophotometric examination of each filter to obtain its curve of transmittance versus wavelength, in the form of either Figure 5-10 (narrow bandpass filters) or Figure 5-11 (broad bandpass filters). The temperature of each filter should be noted during the examination. To attain the highest accuracy in broad filter measurements, where the ambient temperature will be considerably

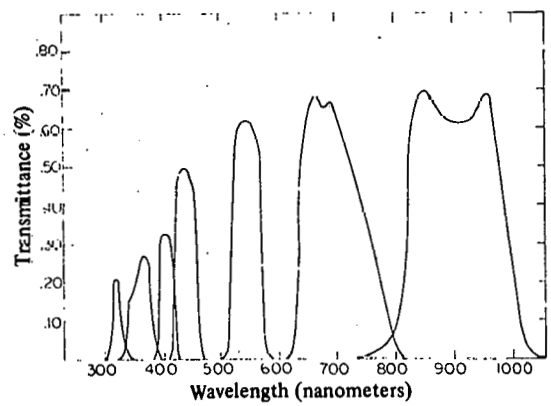


*Figure 5-10 Typical transmission curves of narrow bandpass filters (Drummond et al, 1965).*

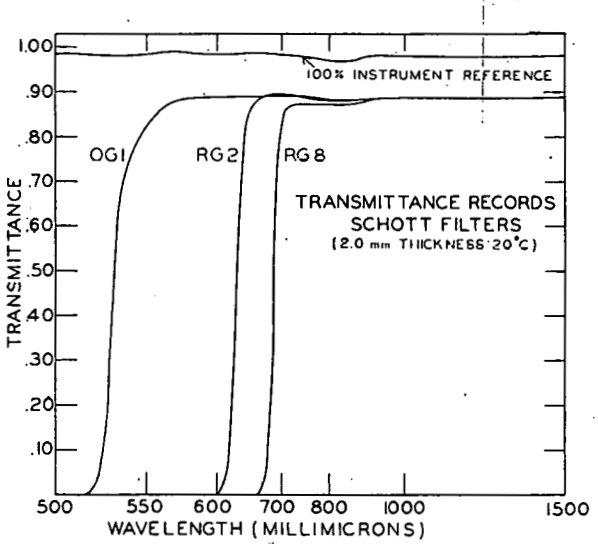


*Figure 5-11 Representative transmittance curves for Schott OG530, and RG695 glass filters (Ångström and Drummond, 1961).*

different from that during filter calibration, a correction of the measured lower cutoff should be made. Temperature has little effect upon the higher filter

cutoff, since the solar irradiance near 2800 nm is extremely low. Temperature may usually be disregarded in narrow band filters (interference filters), since its effect on the shape of the filter envelope is usually negligible over the range of terrestrial temperatures.

The transmission properties of a broad band glass filter are not appreciably influenced by tilting it 10-20° away from the normal to the sun's rays; however, transmittance of a narrow band interference filter has marked wavelength dependence. Although the transmission is usually determined by examining flat specimens, it should also be made through the crown of the hemisphere.

#### 5.5.2.4 Derivation of Filter Factors and Their Application

The basic concept of the filter factor as used here is the ratio of the irradiance within a certain spectral band at the entrance aperture of a filter detector, to the irradiance at the receiving element of the instrument.

As indicated above, broad bandpass filters are characterized by a wavelength termed the center of lower cutoff beyond which the filter transmission is essentially constant over the remainder of the solar spectrum. The filter factor required to evaluate such measurements is therefore, the reciprocal of the filter band transmittance. Typical values are given in Table 5-1 for hemispherical and plane glass specimens. Application of the filter factor is an acceptable first approximation independent of the shape of the solar spectral irradiance and entails a straightforward multiplication of the filter measurements by the appropriate factor.

Treatment of the narrow bandpass filter is more complex, e.g., the filter factor generally varies with the source, although over the range of solar elevation from 90-15° (i.e., sea level air masses 1 to 4) these changes are small for natural exposure conditions. The method of deriving appropriate filter factors first requires consideration of that portion of the source curve which corresponds to the wavelength interval defined by the filter's zero transmittance values (actually $\tau = 0.01$ may be used in practice). The source curve used may be the typical solar spectral irradiance for standard air masses 1 to 4. Then, as dictated by the forms of both the source and the filter calibration curves, and by the filter bandwidth, a number of discrete normalized values $S(\lambda)$ are read from the source curve. Similarly, values of filter transmittance $\tau(\lambda)$ at corresponding wavelengths are tabulated.

The requisite filter factor is given by the ratio of the integral of the source tabulations to the integral of the source-transmittance product tabulation. Mathematically the filter factor is given by:

$$FF = \frac{\int S(\lambda)d\lambda}{\int S(\lambda) \cdot \tau(\lambda)d\lambda}$$

where $S(\lambda)$ is the source of function and $S(\lambda) \cdot \tau(\lambda)$ is the source-filter product transmittance function. In practice, the computations are usually performed using the trapezoidal rule for numerical integration. Typical filter factors for narrow bandpass filters are given in Table 5-5.

Table 5-5

Typical Factors for Parallel Plane, Narrow Bandpass Filters (The Eppley Laboratory)

| No. | Filter Limits (nm) | Filter Factor |
|---|---|---|
| 1 | 305 - 425 | 5.32 |
| 2 | 405 - 550 | 3.18 |
| 3 | 475 - 700 | 2.86 |
| 4 | 700 - 1100 | 4.15 |
| 5 | 900 - 2150 | 1.64 |
| 6 | 1900 - 3000 | 2.11 |

Note that $FF \equiv K$ when $D(\lambda) \equiv 1$ and $D'(\lambda) \cdot F'(\lambda) \equiv \tau(\lambda)$ in Eq. (29) in Section 5.3.5.

### 5.5.3 Pyrheliometric and Pyranometric Measurements

Plane parallel filters are almost always placed around a filter wheel which can be rotated in front of the pyrheliometer aperture. The pyrheliometer

is usually covered by a quartz window but air is allowed to flow freely between the window and the filter. To eliminate the effect caused by multiple reflections between the filter and the window, the filter factor should be reduced approximately one percent.

The first difference between pyrheliometer and pyranometer useage is that in the former instance, the filter is placed over the quartz window of the instrument, while in the latter, the outer hemisphere is replaced by a hemispheric filter. Thus, the measured pyrheliometer signals must be multiplied by the derived filter factor (and corrected as in Section 3.1), while the pyranometer signals must be multiplied by $FF/\tau$, where $\tau$ is the integrated transmittance of the replaced quartz or glass hemisphere.

In contrast with the freely exposed filter placed in front of the aperture of a pyrheliometer, the filter hemisphere of a pyranometer is part of a closed system so that heating effects can result. Since Schott glass filters isolate energy mainly through absorption of unwanted radiation, infrared emission effects by the outer hemisphere will influence the thermopile detector because the inner hemisphere of the pyranometer is warmed (Drummond and Roche, 1965). The recommended multiplicative correction factors are given in Table 5-6. The narrow bandpass hemispherical filters isolate energy mainly through reflection and not absorption, so that the effect, if any, is negligible.

Table 5-6

Corrective Factors to Compensate for Heating Effects of Broad Bandpass Filter Hemispheres

| Filter Hemisphere | OG530 | RG630 | RG695 |
|---|---|---|---|
| Eppley Precision Pyranometer | 0.99 | 0.985 | 0.975 |

When measurements of solar radiation with filters are published, the individual values of the centers of lower cutoff (for Schott filters) or the filter limits (upper and lower wavelengths for interference filters) should be stated. The individual filter factors and any correction factors employed should also be given.

The transmission properties of filters exposed to the atmosphere may change with time. It is therefore important that frequent spectrophotometric examination of filters be made.

### 5.6 Conclusion

Although measurements and evaluations of the spectral irradiances of natural sources have been made for specific conditions, routine systematic observations have not yet been started among radiation climatologists. Wide-spread and continuous efforts would be necessary to make the observations reliable under all weather conditions and to ensure that they are continuous in order to establish a data base from which climatological information may be obtained. Spectral irradiance calibrations are not easy to perform. It is very important to keep in mind the difficulties and need for attaining the objectives.

### References


Ångström, A. K. and Drummond, A. J. 1961. "Basic Concepts Concerning Cutoff Glass Filters Used in Radiation Measurements." *Journal of Meteorology*. No. 18, pp. 360-367.

DIN 5031. 1978. "Optical Radiation Physics and Illumination Engineering, Quantities and Symbols of Photobiologically Effective Radiation." DIN 5031. *Teil.* 10 September 1978.

Dodillet, H. J. 1961. "Der Maximalwert des Phytophotometrischen Strahlungsaquivalentes." *Lichttechnik XIII.* No. 11, pp. 556-558.

Dogniaux, R. 1954. "Activite Erythemale du Rayonnement Solaire en Belgique." *Proceedings 1st International Photobiological Congress, Amsterdam.* pp. 286-292.

Dogniaux, R. 1970. "Variations Qualitatives et Quantitatives des Composantes du Rayonnement Solaire sur une Surface Horizontal par Ciel Serein en Fonction du Trouble Atmospherique." *Inst. Royal Meteorologique de Belgique.* Pub. Series B, No. 62, 22 pp.

Dogniaux, R. 1974. "Representations Analytiques des Composantes du Rayonnement Lumineux Solaire; Conditions de Ciel Serein." *Inst. Royal Meteorologique de Belgique.* Publication Serie A, No. 83, 24 pp.

Dogniaux, R. and Nisen, A. 1975. "Traite de l'eclairage Naturel des Serres et Abris Pour Vegetaux." *Institut Royal Meteorologique de Belgique.*

Drummond, A. J. and Roche, J. J. 1965. "Corrections to be Applied to Measurements Made with Eppley (and other) Spectral Radiometers When Used with Schott Colored Glasses." *Journal of Applied Meteorology.* No. 7, pp. 741-744.

Drummond, A. J., Greer, H. W. and Roche, J. J. 1965. "The Measurement of the Components of Solar Short-Wave and Terrestrial Long-Wave Radiation." *Solar Energy.* No. 9, pp. 127-135.

Drummond, A. J. 1968. "Solar Radiation Instrumentation and Measurement Methods." The Eppley Laboratory, Newport, RI, U. S. A. p. 165.

Gulbrandsen, A. 1978. "On the Use of Pyranometers in the Study of Spectral Solar Radiation and Atmospheric Aerosols." *Journal of Applied Meteorology.* Vol. 17, pp. 899-904.

Guzzi, R., Tomasi, C. and Vittori, O. 1972. "Evidence of Particulate Extinction in the Near Infrared Spectrum of the Sun." *Journal of Atmospheric Science.* Vol. 29, No. 3, pp. 517-523.

*I. G. Y. Instruction Manual, Part VI.* 1958. "Radiation Instruments and Measurements." Pergamon Press.

Kok, C. J. 1972. "Spectral Irradiance of Daylight in Pretoria." *J. Physics D: Appl. Phys.* Vol. 5, pp. 1513-1520.

Lempicki, A., Samelson, H. and Brown, A. 1961. "Slit-Width Error in the Measurement of Absorption Constants." *Journal of the Optical Society of America.* Vol. 51, No. 1.

Vittori, O., Tomasi, C. and Guzzi, R. 1974. "Dessens's Droplets in Near and Middle Infrared Spectrum of the Sun." *Journal of Atmospheric Science.* Vol. 31, No. 1, pp. 261-270.

World Meteorological Organization. 1965. *W. M. O. Guide to Meteorological Instruments and Observing Practices.* "Radiation and Sunshine.", Chapter IX. Geneva, Switzerland.

Wyatt, Clair L. 1978. *Radiometric Calibration: Theory and Methods.* Academic Press.

**Bibliography**

Bringman, M. and Rodskjer, N. "A Small Thermoelectric Pyranometer for Measurement in Field Crops." *Archiv. fur Meteorologie.* Vol. 16, pp. 418-433.

Condit, H. R. and Grum. F. 1964. "Spectral Energy Distribution of Daylight." *Journal of the Optical Society of America.* Vol. 54, pp. 937-944.

Crommelynck, D. 1977. "Calibration of Radiation Instruments for the Measurement of the Radiant Flux on an Arbitrary Source." *Applied Optics.* Vol. 16, pp. 302-305.

Dogniaux, R. 1968. "Distributions Spectrales Energetique et Lumineuse de la Lumiere Naturelle Chromaticite et Luminance." *Lux.* No. 49, 15 pp.

EG & G Electro-optics Division. 1975. *Silicon Photodiode Application Notes, Application Notes D 3000C-1.* U. S. A.

Henderson, S. T. and Hodgkiss, D. 1963. "The Spectral Energy Distribution of Daylight." *British Journal of Applied Physics.* Vol. 14.

Hickey, J. R. "Correlation of Monochromator and Filter Radiometry Determinations of the Spectral Distribution in Large Solar Simulators." *Proceedings of the Institute of Environmental Sciences and American Society of Testing and Materials International Symposium on Solar Radiation.* pp. 95-105.

Lerfald, G. M. and Derr, V. E. 1977. "Final Report on Phase I of the Solar Radiation Atmospheric Transmission Research." *NOAA Technical Memorandum ERL/WPL-18.*

Moon, P. and Spencer, J. 1945. *Journal of the Optical Society of America.* No. 45, pp. 399-427.

Rodskjer, N. 1971. "A Pyranometer with Dome of RG8 for Use in Plant Communities." *Archives fur Meteorologie.* Vol. 19, pp. 307-320.

Sawyer, R. A. 1963. *Experimental Spectroscopy.* New York: Dover Publishing, Inc.

Stair, R. and Johnstone, R. G. 1953. "Ultraviolet Spectral Radiant Energy Reflected from the Moon." *J. Res.* NBS 51, pp. 81-84.

Stair, R. and Johnstone, R. G. 1956. "Preliminary Spectroradiometric Measurements of the Solar Constant." *J. Res.* NBS 57, pp. 205-211.

Taylor, A. H. and Kerr, G. P. 1941. "The Distribution of Energy in the Visible Spectrum of Daylight." *Journal of the Optical Society of America.* Vol. 31, pp. 3-8.

Terrien, J. 1977. "Sur Les Grandeurs Comportant un Facteur Biologique Leurs Definitions et Leurs Unites." *Lux.* No. 94.

CHAPTER 6

# THE MEASUREMENT OF INFRARED RADIATION

M. R. Martin
R. D. Anson
Lawrence Berkeley Laboratory
University of California
Berkeley, California 94720
The United States of America

## 6.1 Introduction

Despite the underlying unity of all electromagnetic wave propagation phenomena, the frequency spectrum is naturally subdivided into a number of reasonably distinct regions (i.e., radio waves, microwaves, infrared, visible, ultraviolet, x-ray, etc.). The reasons behind this subdivision of a theoretically continuous spectrum are not merely historical in nature, but are consequences of the quantum structure of matter itself, and the associated physical processes.

Every piece of matter exchanges energy radiatively with its environment, but the characteristics of the radiation exchanged (both emitted and absorbed) depend on the kind and state of the matter. Radiation from *isolated atoms* occurs in a set of lines with discrete wavelengths and usually falls within the visible and ultraviolet regions of the spectrum. The radiation from *molecules* is more complex, since the atoms making up the molecule can vibrate while the entire molecule can rotate. The wavelengths associated with those molecular motions are frequently within the infrared region. Since vibrations and rotations can be induced by collisions due to thermal agitation, infrared radiation is often thought of as "heat" radiation. A *solid body* emits and absorbs radiation over a continuum of wavelengths. Its surface emissivity varies with wavelength as a function of its material composition and temperature.

If the incident radiative flux is equal to the emitted flux inside a hollow cavity with walls maintained at a constant temperature, the spectral distribution depends uniquely on the temperature and is independent of the material from which the cavity is constructed. Such a cavity approximates what is referred to as an ideal "blackbody". Since many real surfaces have radiative characteristics which are very similar to those of a blackbody, this concept represents a useful idealization. The spectral distributions of radiation emitted from a blackbody at several different temperatures are shown in Figure 6-1.

Infrared radiation emitted from the base of a cloud or the surface of the earth reasonably approximates blackbody radiation provided the radiating surface has a uniform temperature (typically in the range of 240-310 K). Such radiation is often referred to as "terrestrial radiation" to distinguish it from the "solar radiation" produced in the 6000 K temperature region at the surface of the sun.

### 6.1.1 Detection of Infrared Radiation

Two general categories of detectors are used to convert infrared radiation into a measurable signal (electrical current, voltage or pressure), namely, thermal detectors and photon detectors.

1. Thermal Detectors: thermocouple
   thermopile
   thermistor
   pyroelectric
   Golay cell

2. Photon Detector: semiconductor devices using, e.g., GaAs, InAs, Si, InSb, Pb;
photochemical reactions (photographic plate for near-infrared detection).

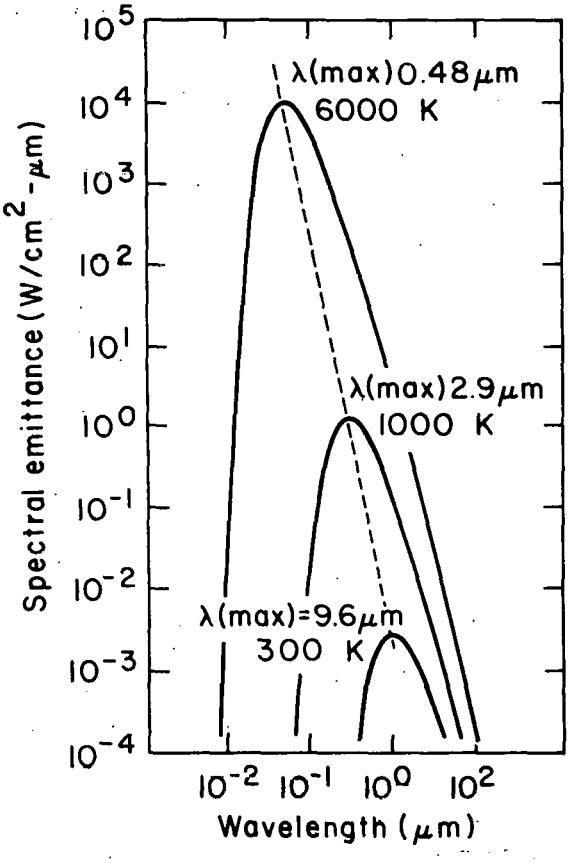


*Figure 6-1 Spectral distributions emitted by a blackbody radiator at various temperatures*

Thermal detectors operate on the principle that a particular physical property (e.g., resistivity, pressure of certain constituent materials varies with temperature. Such detectors must be designed so that their temperature is affected primarily by the balance of the emitted and absorbed infrared radiation fields rather than by convection and conduction processes.

Photon detectors are made of semiconductor materials capable of absorbing infrared radiation and producing electron-hole pairs. Depending on the material used, either a pn-junction (interface) voltage is generated or a change in conductivity is produced which is a function of the number of incident photons. In some cases the charges in each electron-hole pair are separated by a magnetic field (photoelectromagnetic detectors) or electrons are emitted from the surface of the material and collected at an anode, thereby giving rise to an electric current. Well-designed photon detectors are considerably more sensitive than thermal detectors over a relatively limited spectral region, but require cooling to low temperatures (typically to the temperature of liquid nitrogen) to achieve an acceptable signal-to-noise ratio. Cooled detectors are commonly used in sensitive laboratory, satellite, and balloon experiments, but are often unsuitable for field use. Photochemical detectors (photographic plates) are mentioned for completeness, but their use is restricted to the shorter wavelengths of the "near infrared".

Figure 6-2 shows the detectivity[1] (D*) of a number of commonly available detector materials. The spectral response of all thermal detectors is quite flat over a very broad wavelength region as compared with the more sensitive photon detectors. Detectors made from these materials are readily available from many manufacturers, and new materials are constantly being investigated. Additional information on infrared detectors may be found in Drummond (1970), Gillham (1970) and Wolfe (1965).

### 6.1.2 Infrared Optics

Although the design of infrared optical systems may appear to be quite unlike the design of visible optical systems, their similarities and differences are slight and can generally be understood by considering the following three factors:

1) Since infrared radiation follows the same physical laws as visible radiation the same

[1] "Detectivity" is a standard measure of the maximum possible sensitivity as limited by the inherent detector noise. Specifically, $D^* = \sqrt{A\Delta f}/NEP$, where A is the detector area, $\Delta f$ is the electrical bandwidth and NEP is the spectral Noise Equivalent Power (i.e., monochromatic incident power required to yield a signal-to-noise ratio of unity).

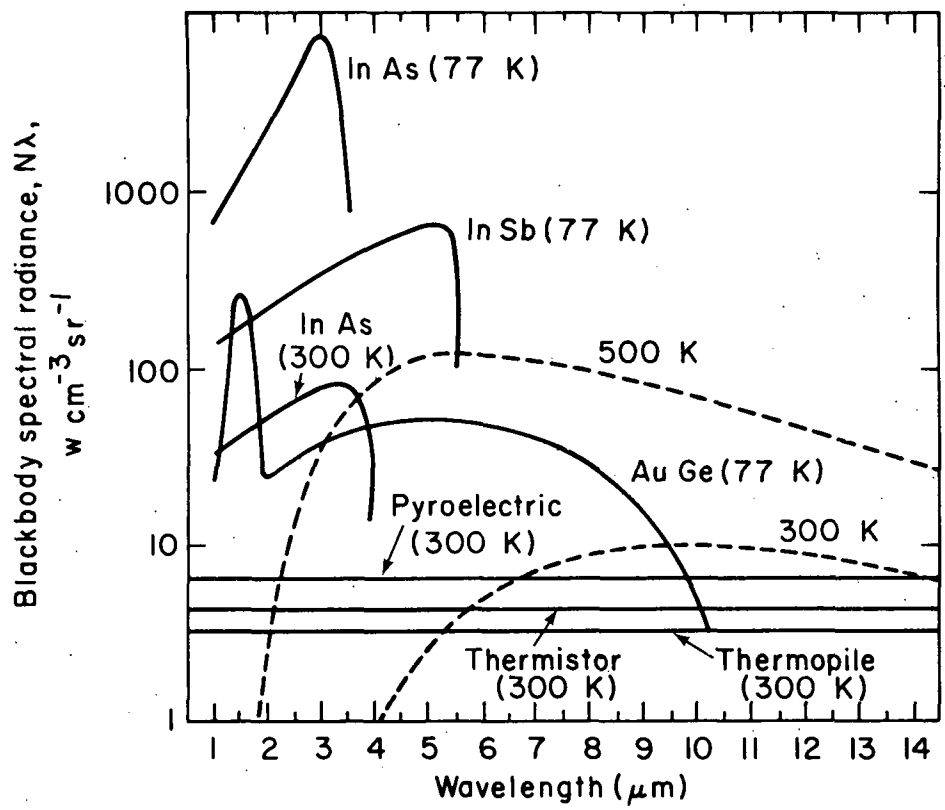


*Figure 6-2 Detectivity (D*) of various infrared photon and thermal detectors (solid lines). Blackbody spectral radiance curve is shown (dashed lines) for reference purposes.*

*types* of instrument components can be used (e.g., lenses, mirrors, diffraction gratings, prisms, and filters) in applications involving both visible and infrared devices.

2) Properties of optical materials used for the visible region can differ markedly from those for the infrared region. Glass that is transparent to visible radiation is opaque to the infrared. Germanium, which is opaque, with a metallic appearance in visible light, is partially transparent over a broad wavelength region in the infrared. Polyethylene film is largely transparent throughout both regions. Obviously, many of the materials used to make infrared optical components have very different properties from those used to build conventional visible optical instruments.

3) Since infrared radiation is emitted from bodies at normal ambient temperatures, all the components of an infrared optical system emit such radiation. Thus it is a significant source of noise in an infrared system. (Imagine an optical telescope in which the lenses, mirrors and supporting structure glow brightly!) Techniques have been developed so that reliable infrared measurements can be made despite this drawback, but they have no exact visible optical analogue.

Infrared transmittance values for several materials frequently used in the manufacture of infrared lenses, windows and base plates for filters are shown as a function of wavelength in Figure 6-3.

Some inorganic salts (e.g., NaCl, KBr) have high transmission values in the infrared but are water soluble, which limits their application to instruments sealed from outside moisture. A polished metal surface is an excellent reflector of infrared radiation: therefore, any type of front surface mirror can be

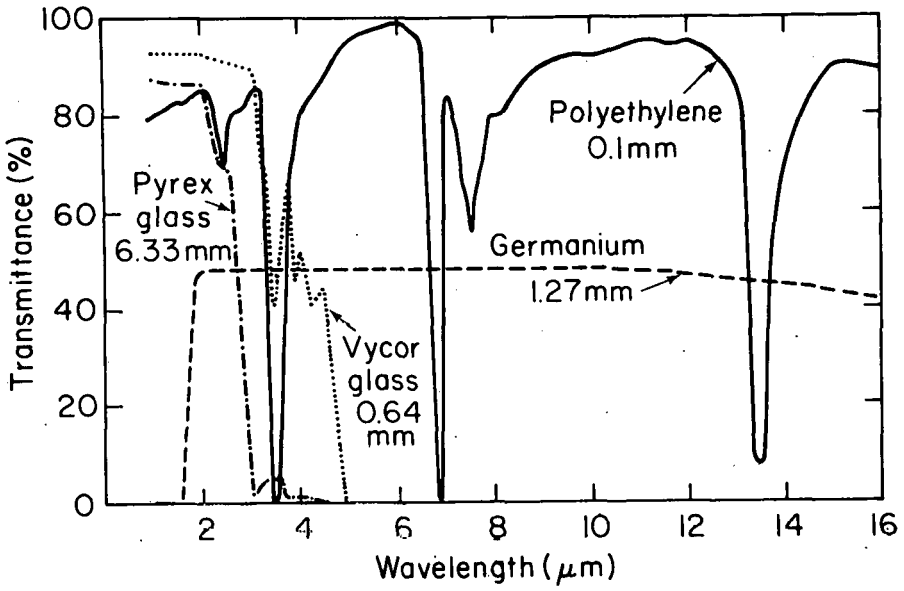


*Figure 6-3 Spectral infrared transmittances through various thicknesses of common materials used in optical systems*

designed similarly for both infrared and visible optical systems. Coulson (1975) and Wolfe (1965) give more details about infrared optics.

### 6.1.3 Characteristics of Atmospheric Infrared Radiation

Except for measurements made in the laboratory, atmospheric infrared radiation is encountered either as a noisy background nuisance or as a signal being investigated. The sky as viewed by hypothetical infrared-sensitive eyes would have a spectacularly different appearance from the visible sky. The bases of ominous thunderhead clouds or stratus would have a bright glow, while high cirrus clouds would have a dull gray color. Instead of being uniformly transparent, the "clean" air would absorb and emit radiation so strongly that at some wavelengths an object a few centimeters away from the observer would be obscured. At other wavelengths the entire atmosphere would be almost completely transparent.

Because the atmosphere is primarily composed of gaseous substances it absorbs and emits infrared radiation in spectral bands characteristic of the constituent molecules. As shown in Table 6-1, virtually all infrared emission from the atmosphere is due to water vapor, carbon dioxide, and, to a lesser extent, ozone. Nitrogen and oxygen gases are transparent throughout this region. Modern high resolution spectroscopic instruments can, of course, detect numerous trace-gas constituents, but the major features of the atmospheric infrared spectrum are due to the above three gases.

Table 6-1

Gaseous Atmospheric Constituents Showing the Strongest Infrared Radiation Bands for Each

| Atmospheric Constituent | Abundance | Wavelength (μm) |
|---|---|---|
| Nitrogen | 78% | — |
| Oxygen | 21% | — |
| Carbon Dioxide | 0.033% | 2.7 |
| | | 4.3 |
| | | 11.4-20 |
| Ozone | Variable | 9.6 |
| Water Vapor | Variable | 2.7 |
| | | 6.3 |
| Trace Gases | ≲0.5% | — |

Infrared radiation has many important uses, e.g., for satellite sensors, photography, and studies of night visibility. Its full potential for heating and cooling applications apparently has not been realized. The scientist and the engineer will need to combine their experiences to optimize the effects of infrared radiation for heating and cooling. For this reason an extensive scientific description of the characteristics of atmospheric infrared radiation is included. In desert areas infrared re-radiation from the ground to the night sky results in surface cooling which is quite noticeable although the process of emission may not be well understood. The information below may aid in understanding the phenomenon and lead to additional applications for these regions.

Figure 6-4 shows a typical spectral distribution of the atmospheric radiation received at ground level under clear sky conditions. The region of low atmospheric radiance between approximately 8 and 12 mm is known as the atmospheric infrared "window", since low emissivity gives rise to high transmissivity. Much of the radiant energy from the earth's surface passes into outer space within this spectral region.

The spectral details of this window change as the water vapor content, aerosol concentration, condensed water droplet abundance, and ozone layer thickness vary. If low clouds obscure the sky the window vanishes so that the observed incident infrared sky radiation approximates the blackbody distribution indicated by the dashed lines in Figure 6-4.

References to the "effective sky temperature" can sometimes be misleading since the sky is made up of regions having a variety of temperatures between approximately 240 K and 310 K. Furthermore, in a relatively transparent region of the spectrum the "temperature" of the atmosphere is an average of the temperatures for layers of air extending from the ground up to its highest and (coldest) levels, while in an opaque region the relevant "temperature" is that measured close to the instrument. An effective sky temperature may be defined as the temperature attained by a blackbody in radiative equilibrium with the sky. While this may be a useful definition for some purposes, it should be emphasized that the spectral distribution of radiation received from the sky does not closely resemble the distribution for a blackbody radiation except under heavy overcast conditions. Further information on the characteristics of atmospheric infrared are given by Allan (1971), Brunt (1932), Coulson (1975), Kondrateyev (1965), Kuhn (1970), Sellers (1965), Stringer (1972), Suomi (1958), Swinbank (1963) and Wolfe (1965).

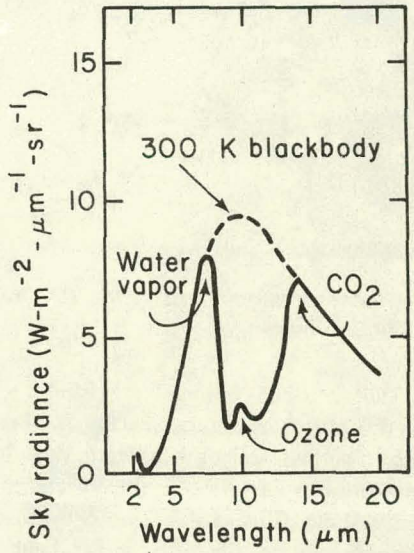


*Figure 6-4 Infrared sky radiance as a function of wavelength. This curve varies with atmospheric temperatures and gaseous constituents*

## 6.2 Infrared Radiometers

### 6.2.1 General Characteristics

Infrared radiometers are of two general types: instruments that measure (1) spectral intensity values, and (2) the total radiation received from wavelength regions. Many measurements of meteorological interest (e.g., agricultural and hydrological heat-balance applications) require only a determination of the net radiative flux so that the more elaborate and expensive spectral instruments are not needed.

A radiometer which measures the total (visible plus infrared) radiation incident on it is known as a pyrradiometer, while one which measures only the infrared radiation is called a pyrgeometer. Both measure the radiation received on their sensing sur-

faces from the entire hemisphere. A *net* pyrradiometer measures the net radiative energy flowing through the sensors from one hemisphere (upper or lower) to the other. Both pyrradiometers and net pyrradiometers are in common use, and are commonly quite similar in construction, e.g., a CSIRO net pyrradiometer can be modified to operate as a pyrradiometer (Figure 6-5).

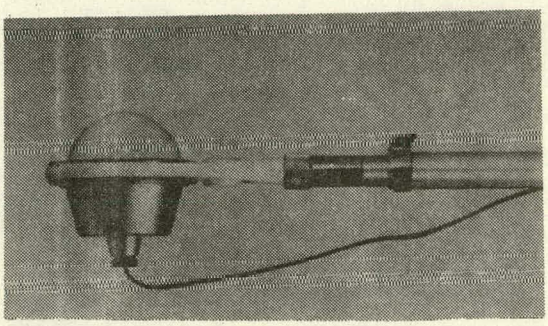

*Figure 6-5 A pyrradiometer constructed from a modified CSIRO pyrradiometer.*

Non-spectral radiometers ideally register the temperature of the sensor as determined by the balance between the absorbed and emitted radiative fluxes. This temperature can also be affected by conductive and convective heat flow paths from the sensor to the environment. While the conductive heat flow can be maintained at a negligible level by careful mechanical design, the convective heat flow presents a more difficult problem. In practice, radiometers are either calibrated for different wind velocities, or the convective losses must be controlled within calculable limits or suppressed.

Convection control may be achieved by forcing a steady stream of air to flow over the sensor receiving surfaces. A limited or total suppression of the convective losses may be obtained by enclosing the sensor inside a transparent shield. Cover sheets or hemispherical domes for pyrradiometers are generally made of a thin polyethylene material, whereas domes for pyrgeometers are made of a material similar to silicon or germanium. The latter are transparent over a wide range of infrared wavelengths but are opaque to visible radiation. Characteristics of the most important non-spectral radiometers are discussed in Section 6.2.2.

Two important sources of instrumental error are common to all types of pyrradiometers and pyrgeometers: variations of the spectral sensitivity of the sensor coating, and deviations of the sensor absorption characteristics form an ideal cosine law (Lambertian surface). The black paints used for coating sensor surfaces do not have the same absorption properties in the infrared region so that an undesirable degree of spectral selectivity may be introduced into the radiation measurements. The black paints used in pyrradiometers also absorb solar radiation. Therefore, some manufacturers paint 5-10% of the sensor surface white to compensate for this absorption by reflecting part of the visible radiation while keeping the infrared absorption almost constant.

The cosine error also partially results from the characteristics of the black coating. An ideal black Lambertian surface absorbs the incident radiation in proportion to the cosine of the angle of incidence at the surface. Real painted surfaces do not absorb according to a perfect cosine law, so that this deviation must be considered to interpret experimental results. Further deviations from the cosine law may be caused by the protective dome or sheets of transparent material used to suppress convection from the sensor plates.

### 6.2.2 Pyrradiometers and Pyrgeometers

Several techniques have been developed for measuring total visible and infrared radiation, but only a few are used on commercially available pyrradiometers. The reader is referred to the literature listed at the end of this section for details about instruments of current and historical interest.

Basically, all modern pyrradiometers and pyrgeometers use the thermopile as the sensing element. The voltage output of the thermopile is a function of its temperature, which in turn, depends on the radiative, convective, and conductive heat balance at its surface. Commercially available instruments are discussed in the next three sections according to the way that the problem of convective heat transfer between the sensor element and ambient air is handled. Tables 6-2a and 6-2b list the radiometer characteristics obtained from a variety of sources, most of which are ultimately traceable to the instrument literature of each manufacturer.

## Table 6-2a

## A Summary of Net Pyrradiometer Characteristics

| INFRARED INSTRUMENT | DETECTOR | SENSOR SURFACE | METHOD OF CONVECTION SUPPRESSION | RESPONSE ($\mu V/W\ m^{-2}$) | LINEARITY OF RESPONSE (%) | ERRORS DUE TO TEMPERATURE SENSITIVITY | DEVIATION FROM COSINE RESPONSE | IMPEDANCE (ohms) | RESPONSE TIME (SECS) 63% | RESPONSE TIME (SECS) 95% | REFERENCE | REMARKS |
|---|---|---|---|---|---|---|---|---|---|---|---|---|
| PYRGEOMETER | | | | | | | | | | | | |
| "Precision Infrared Radiometer" (EPPLEY) | 60 Junction Thermopile Copper-Constantan | Parson's Optical Black Lacquer | Silicon Dome w/interference filter | 5 | ±1 | ±0.5% -20 to +40°C | ±5% @ 80° | 700 | 1 | ---- | a, b, e | Prior to 1977 the dome was constructed of KRS-5. Some early models used a different thermopile. Spectral range 4-50 μm. Silica gel desiccant. |
| NET PYRRADIOMETERS (Ventilated Instruments) | | | | | | | | | | | | |
| "Net Pyrradiometer" (KEW OBSERVATORY) | 120 Junction Copper-Constantan Thermopile | Aluminum Plates w/optical black paint | Ventilating Blower | ---- | ---- | ------ | "Satisfactory" | ------ | ---- | ---- | b | Moderate sensitivity to wind speed and direction; calibration stable to within ±5% over a six month period. |
| "Net Radiometer" (SUOMI, FRANSILLA, AND ISLITZER) | 240 Junction Thermopile Copper-Constantan | *Fuller's Velvet-Black* on Thermopile Wires | Ventilating Blower 20-25 $mS^{-1}$ | 2 | ±2 | ------ | ±1% | ------ | ---- | ≲5 | b | Adjustable wind vane & electric heater; 6% of sensor is coated with white paint. |
| "Net Pyrradiometer" Gier & Dunkle (TELEDYNE GEOTECH) | 800 Junction Thermopile Silver-Constantan | 3M Nextel C101-10 | Ventilating Blower | 2.2 | ±1 | ±1% | ±7% @ 80° (10μm) ±27% @ 80° (20μm) | 440 | 10 | ---- | a, b, e | Angular and wavelength dependence of sensitivity is due to lacquer. Spectral range .3-100μm. Model TCN-188-01. |
| NET PYRRADIOMETERS (Shielded Instruments) | | | | | | | | | | | | |
| "Pyrradiometer" of the Physicometeorological Observatory, Davos, Switzerland (DR. C. FROHLICH) | 60 Thermoelement Moll Thermopile Copper Constantan | Blackened | 0.05 mm Polyethelene *Dome (Lupolen)* | 10 | ---- | 0.1%/°C | ±3% @ 80°C | 170 | 2 | ---- | b | Model TD 25-60C. |
| "Net Radiometer" (HY-CAL ENGINEERING) | Thermopile | Fused Graphite | Dome | 3.7 | 0 | 0% -50 to +250°F | ±2% down to 70° | 2500 | ---- | ---- | d | Correction curve available for temperatures from -50 to -320°F Model P-8400-L. Spectral range (μm) >.25. |
| "Universal Radiation Meter" Georgi (KAHL) | 14 Thermoelement Moll Thermopile Manganin-Constantan | Blackened | Polyethylene Dome | 12 | ---- | ------ | ------ | 7 | ---- | ---- | b | Designed for many types of radiation measurements. Interchangeable covers of glass & polyethylene. |
| "Net Pyrradiometer" Schulze (DR. BRUNO LANGE) | Semiconductor Thermopile | Black Paint with White Center | Polyethylene Domes/ Ventilators Blow into Cavity through Radiation Shields | 94 | ---- | +4% @ -10°C -13% @ +40°C | ------ | 3 | ---- | ≲150 | b | Earlier models had a silver-constantan thermopile. Center portion of sensor is coated with white paint. |

REFERENCES:
a – Latimer (1971)
b – Coulson (1975)
c – Sellers (1965)
d – Carter et al (1977)
e – Manufacturer's Literature

## Table 6-2b

## A Summary of Net Pyrradiometer Characteristics

| INFRARED INSTRUMENT | DETECTOR | SENSOR SURFACE | METHOD OF CONVECTION SUPPRESSION | RESPONSE ($\mu V/W\ m^{-2}$) | LINEARITY OF RESPONSE (%) | ERRORS DUE TO TEMPERATURE SENSITIVITY | DEVIATION FROM COSINE RESPONSE | IMPEDANCE (ohms) | RESPONSE TIME (SECS) 63% | 95% | REFERENCE | REMARKS |
|---|---|---|---|---|---|---|---|---|---|---|---|---|
| NET PYRRADIOMETERS *(Shielded Instruments cont.)* | | | | | | | | | | | | |
| "Net Pyrradiometer" CSIRO/Funk (MIDDLETON) | 250 Junction Thermopile Copper-Constantan | Parson's Optical Black on Aluminum | 0.05 mm Polyethylene Domes | 43 | ±1 | ----- | ±1.5% @ 75° | 80 | 10 | <90 | b, d, e | Domes inflated with nitrogen; heating ring to reduce condensation; 5% of sensor is coated w/white paint. Silica gel desiccant. Spectral range 3-40μm. Model CNI. |
| "Radiometer" (MOLECTRON) | Pyroelectric | Absorbing Black | ----- | Direct Reading | 2%/50W; 5%/200mW | 0.2%/°C | ----- | ----- | --- | --- | d | Model PR200. Spectral range .3-40μm. Sensor artifically aged & protected against corrosion & oxidation. |
| "Pyrradiometer" (PHILIPP SCHENK) | 32 Junction Thermopile Copper-Constantan | Black | Lupolene Domes | 13 | 100% | ±1%/°C | ±1-3% @ 80° | 5 | --- | 20 | d | Desiccant blue gel container. Spectral range 0.3-50μm. Model 8110. |
| "Net Pyrradiometer" (SIEMEN ERSKING) | Thermopile | Eppley Parson Black | Domes | 13 | ±2% | -0.07%/°C | ----- | 50 | --- | 60 | d | Dry air desiccant. Spectral range 0.4-100μm |
| "Pyrgeometer" Model 4064 (SPECTRAN) | Self-generating Thermopile | 3M Nextel No. 101-C10 | Domes | 7 | 0.1 | .03%/°C | ----- | 500 | --- | 1 | d | Spectral range .20-20μm. Desiccant dry nitrogen. Model 4064. |
| "Economical Net Pyrradiometer" (SUOMI-KUHN) | 2 Bead Thermistors | Blackened Aluminum Foil | Double Layer of Polyethylene Film | ----- | ----- | ----- | -10% @ 25° -37% @ 85° | ----- | 25 | --- | b | Frequently used in radiosonde measurements. |
| "Linear Net Radiometer" (SWISSTECO) | Thermopile Copper-Constantan | Optical Black | Dome | 140 | ±1 | ±0.01%/°C | -6% | 380 | --- | <25 | d | Spectral range .3-60μm. Desiccant air flush. |
| "Net Pyrradiometer" (C. W. THORNTHWAITE) | Thermopile | Mautz 9300S Black | 0.05 mm Polyethylene Domes | 20 | ±2 | "NIL" | <2% | 35 | --- | --- | b, e | Domes inflated with dry air or nitrogen. Model 605. Spectral range .3-60μm. |
| "Net Radiometer" Fritschen (SCIENCE ASSOCIATES, WEATHERMEASURE) | 22 Junction Thermopile Maganin-Constantan | Blackened; 10% Area in White Paint | 0.15 mm Polyethylene Domes | 5 | ±1 | 0.23%/°C if compensated, 0.07%/°C | ±5% @ 80° | 38 | 2 | 35 | a, b | Domes inflated with dry air. 10% of sensor is coated with white paint. Spectral range 0.3-60μm. Model 621/Model R421. |
| "Net Pyrradiometer" (YANISHEVSKY) | 600 Junction Thermopile Silver-Constantan | Blackened Copper | None (Wind Monitored During Measurement) | 11 | ----- | ----- | ----- | 40 | --- | 12 | b | Correction factor for the wind is 25% @ 12 m/sec. |

REFERENCES:
a – Latimer (1971)
b – Coulson (1975)
c – Sellers (1965)
d – Carter et al (1977)
e – Manufacturer's Literature

These sources should be used with caution since they may inadvertently contain errors and/or omissions, and usually do not reflect actual operating experience.

### 6.2.3 Calibrated Instruments

This is the simplest type of pyrradiometer since no provision is made to inhibit convective heat transfer. Such instruments are individually calibrated by measuring the radiation levels at various wind speeds. The output is still suspect, since convection currents depend on the sensor temperature and orientation, as well as the ambient temperature, and wind speed. A typical instrument is the Yanishevsky net pyrradiometer (see Coulson, 1975) which is widely used in the Soviet Union.

### 6.2.4 Ventilated Instruments

Convective heat transfer to and from the sensing plate is controlled by forcing a steady stream of air to flow over the sensor. As long as the ambient wind does not cause this forced flow to change significantly, the thermal boundary layer at the sensor surface will remain steady allowing the instrument to be calibrated with consistent results. Typical instruments are those designed by Gier and Dunkle (manufactured by Teledyne Geotech, Figure 6-6), and Suomi et al (Coulson, 1975; Sellers, 1965) and the net pyrradiometer of the Kew Observatory (Coulson, 1975). Such instruments are less accurate in a cross-wind than they are in a wind parallel to the ventilating air flow. Performance characteristics for one design—Suomi et al (Coulson, 1975)—indicate that a wind speed of 12 m $s^{-1}$ produces no change in the observed reading when the wind blows in the same direction as the ventilating flow, but a +0.3% change, if the wind blows in the opposite direction while a cross-wind of the same speed yields a +2% change if the wind blows at right angles.

### 6.2.5 Shielded Instruments

Shielded pyrradiometers are equipped with a dome or cover sheet that is largely transparent throughout the wavelength region of interest. All pyrgeometers have such domes, since it is necessary to block the visible radiation while transmitting the infrared (Figure 6-7). If polyethylene is selected as the mate-

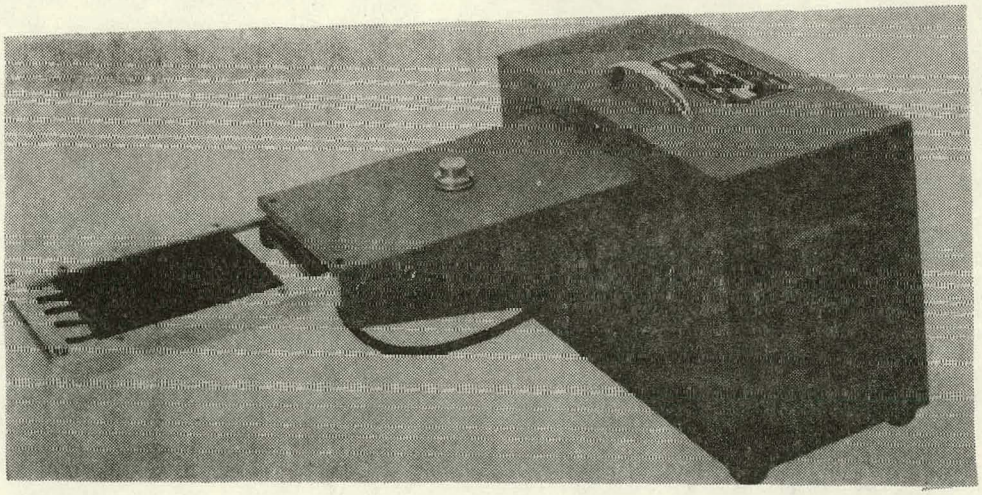

*Figure 6-6 An unshielded net pyrradiometer of the Gier and Dunkle design. Manufactured by Teledyne Geotech.*

erial for a pyrradiometer dome, it should be as thin as possible (typically 0.05 mm or less) since it absorbs radiation in certain infrared bands, but is generally transparent elsewhere. The dome is usually inflated with low pressure dry air or nitrogen which also suppresses condensation inside it. The CSIRO, Thornthwaite, Fritschen and Schulze net pyrradiometers are examples in common use (Figures 6-8, 6-9, 6-10, 6-11a and 6-11b).

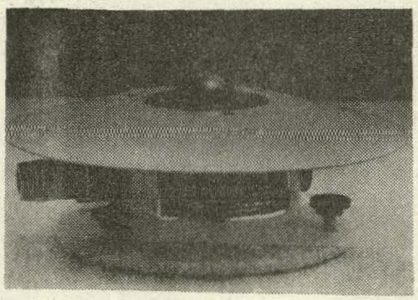

*Figure 6-7 The Eppley model PIR (precision infrared radiometer), a pyrgeometer that measures only infrared radiation.*

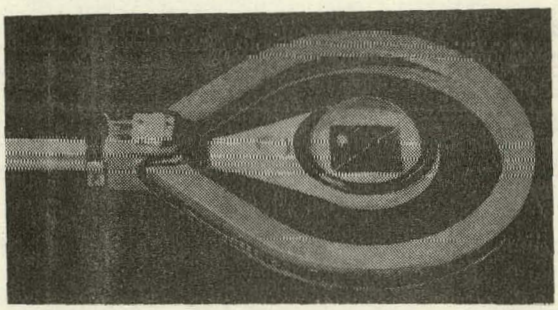

*Figure 6-8 A CSIRO net pyrradiometer equipped with an optional heating ring to prevent condensation.*

A desiccant is sometimes inserted to prevent condensation (e.g., Eppley model PIR pyrgeometer) if the gas pressure is not required to maintain the shape of the dome. The Suomi-Kuhn "economical" net pyrradiometer (Sellers, 1965) uses a flat stretched double polyethlene film instead of a dome to suppress the convective heat transfer. However, the flat geometry of the polyethylene window is largely responsible for the poor cosine response of the instrument.

Many references discuss different types of pyrradiometers and pyrgeometers: Carter et al (1976, 1977), Coulson (1975), CSAGI (1958), Fretschan (1963), Idso (1970), Latimer (1971), Suomi and Kuhn (1958), Swan et al (1961), Tanner et al (1960), and WMO (1971).

### 6.2.6 Spectral Radiometers

This section is intended only as a brief introduction to the basic characteristics of three types of spectral instruments used for spectral infrared measurements: prism, diffraction grating, and interference filter. A short bibliography is appended to aid the reader who requires more detailed information. Many spectral radiometers are designed and built to suitable specific purposes; general purpose spectrometers are available from some manufacturers. More information may be found in: Coulson (1975), CSAGI (1958), Gillham (1970), Idso (1971), Latimer (1971), Sellers (1965), Stringer (1972), Tanner (1963) and WMO (1971).

Several types of spectral radiometers are used for remote sensing of temperature for measuring optical properties of materials, for constructing satellite infrared-sensing devices, for detecting gaseous atmospheric constituents, and for numerous other applications.

Thermal detectors (thermocouples, thermistors, pyroelectric) are also used except for those applications requiring cooled solid state detectors to obtain precise measurements of low infrared intensity. By combining an optical chopper and phase locked amplifier with a reference blackbody cavity the signal-to-noise ratio is substantially increased so that an absolute measuring instrument results. This is a characteristic feature of many spectral instruments.

Blazed reflection diffraction gratings are normally used instead of transmission gratings for infrared instruments. Compared to a single reflection from a metal surface, the transmission of radiation through two surfaces of a transparent material results in both decreased intensity and spectral distortion of the radiation. Specific examples of grating spectrometers used for atmospheric measurements may be found in Harrison (1973) and Williams et al (1970).

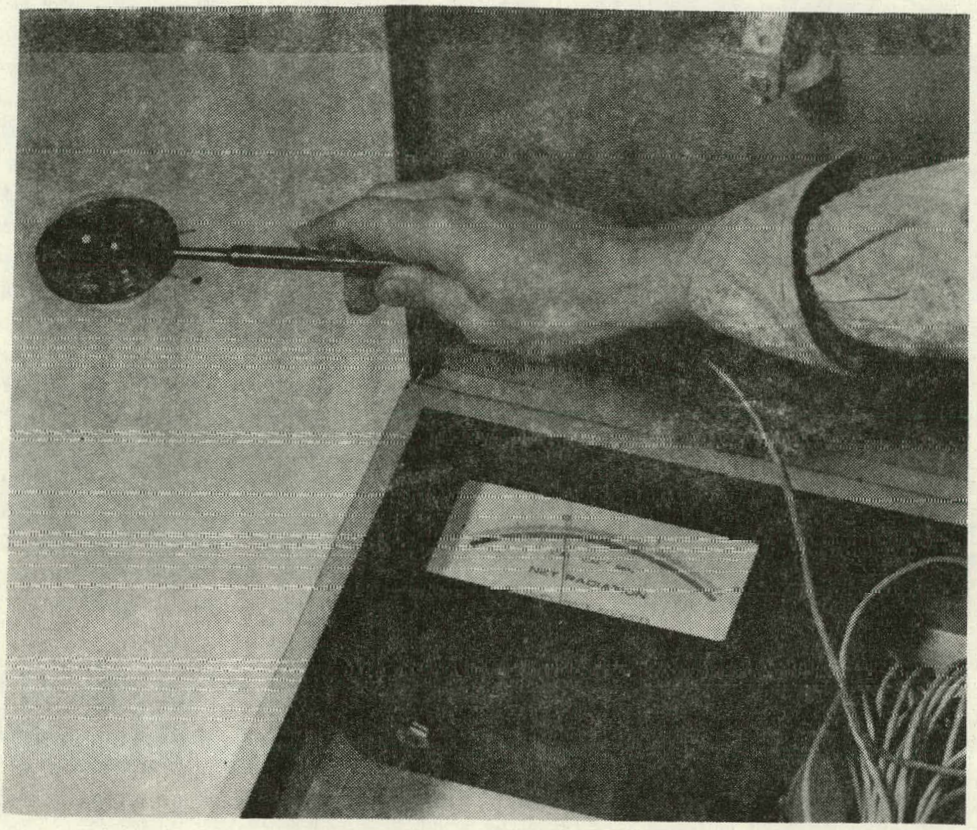

*Figure 6-9 A miniature net pyrradiometer manufactured by Thornthwaite and Associates*

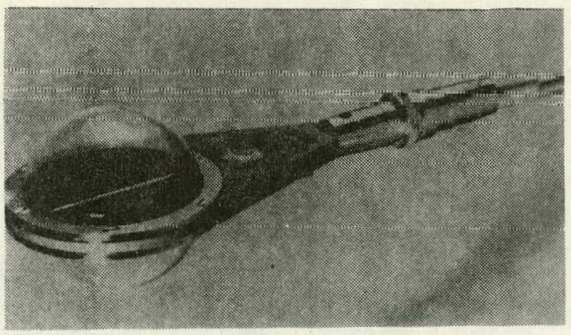

*Figure 6-10 A Fritschen type net pyrradiometer*

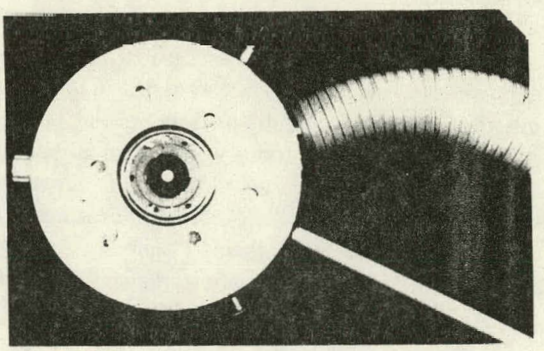

*Figure 6-11a A shielded net pyrradiometer of the Schulze type*

Prism spectrometers have long been used for medium resolution applications (Kondrateyev et al (1965; Oetjen et al, 1960; Sloan et al, 1955). Examples of common materials used to make infrared prisms

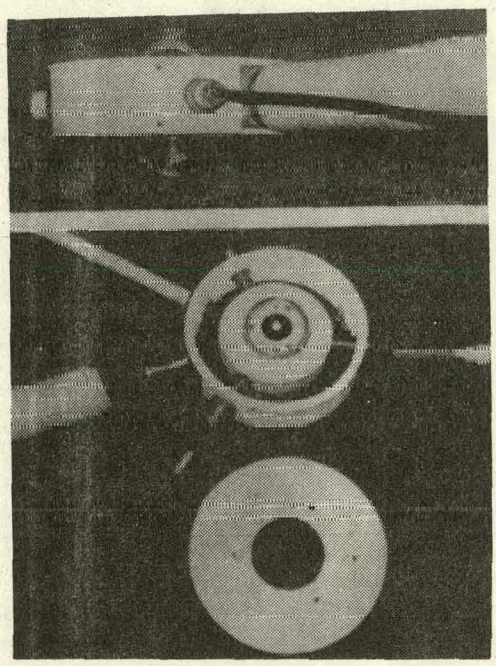

*Figure 6-11b A shielded net pyrradiometer of the Schulze type*

are sodium cloride, potassium chloride and KRS-5 (thallium bromide-iodide). The choice of material for a given application depends on its mechanical and chemical properties, e.g., the water solubility, indices of refraction and dispersion. Wolfe (1965) has useful tables of the appropriate properties of suitable materials.

Spectral infrared radiometers using interference filters are very common and are available in numerous configurations from manufacturers. Special purpose radiometers can continuously monitor a specific wavelength band, and the addition of a rotating filter wheel enables it to make measurements over a number of such bands (typically 4 or 8). Pass bands of interference filters range from "windows" approximately 1% wide (e.g., a bandwidth of 0.1 mm centered about a wavelength of 10 mm) to open-ended high pass or low pass filters. Several manufacturers offer a selection of stock filters and can produce custom filters on request.

An interference filter consists of a number of optical coatings deposited on a substrate; its transmission characteristics depend on the path length of the radiation through each layer. Such filters are designed to operate such that the radiation falls normal to surface; the filter transmission changes when the radiation is incident at other angles. Thus, these filters are primarily limited to use in collimating instruments, but can also be incorporated in hemispherical domes, but only with some difficulty. Another technical problem is encountered in fabricating interference filters on curved surfaces. An interesting new development for certain applications is the continuously variable filter. Interference coatings of gradually varying thicknesses are deposited on a circular substrate so that the pass band changes continuously as the filter wheel is rotated. An instrument equipped with such a filter can scan a portion of the spectrum and yield results comparable to those of a low-resolution diffraction grating or prism spectrometer while using a much simpler optical system. Robert (1976) in France has constructed such a system for monitoring atmospheric infrared radiation.

The selection of one of these types of spectral instruments depends on the wavelength band to be measured, the spectral resolution desired, the source intensity, the environmental operating conditions, and the requirements for unattended operation.

**References**


Allen, J. R. 1971. "Measurements of Cloud Emissivity in the 8-13 $\mu$ Waveband." *Journal of Applied Meteorology*. 10:260-265.

Brunt, D. 1932. "Notes on Radiation in the Atmosphere." *Quarterly Journal of the Royal Meteorological Society*. 58:389-420.

Carter, E. A., Greenbaum, S. A. and Patel, A. M. 1976. *Listing of Solar Radiation Measuring Equipment and Glossary*. ERDA/NASA/31295/76-3. The University of Alabama in Huntsville.

Carter, E. A., Breithaupt, W. G., Dahagam, C. S. and Patel, A. M. 1977. *Catalog of Solar Radiation Measuring Equipment*. ERDA, Division of Solar Energy. Contract No. EG-77-S-05-5362. Report No. ORO/5362-1.

Coulson, K. L. 1975. *Solar and Terrestrial Radiation: Methods and Measurements.* New York: Academic Press.

CSAGI. 1958. "Radiation Instruments and Measurements." *Annals of the International Geophysical Year.* 5:371-466.

Drummond, A. J., ed. 1970. "Precision Radiometry." *Advances in Geophysics.* Vol. 14. New York and London: Academic Press.

Fritschen, L. J. 1963. "Construction and Evaluation of a Miniature Net Radiometer." *Journal of Applied Meteorology.* 2:165-172.

Gillham, E. J. 1970. "Radiometry From the Viewpoint of the Detector." *Advances in Geophysics.* Vol. 14, A. J. Drummond, ed. New York and London: Academic Press.

Harrison, A. W. 1973. "Atmospheric Thermal Emission 2.5-4.2 $\mu$." *Boundary-Layer Meteorology.* 5:365-372.

Idso, S. B. 1970. "The Relative Sensitivities of Polyethylene Shielded Net Radiometers for Short and Long Wave Radiation." *Review of Scientific Instruments.* 41:939-943.

Idso, S. B. 1971. "A Simple Technique for the Calibration of Long Wave Radiation Probes." *Agricultural Meteorology.* 8:235-243.

Kondrateyev, K. Ya., Badinov, I. Ya., Ashchulov, S. V. and Andreev, S. D. 1965. "Equipment for the Study of Infrared Absorption and Heat Radiation Spectra of the Atmosphere." *Bulletin, Acad. Sci., U. S. S. R., Atmospheric and Oceanic Physics.* 1:175, (trans. from the Russian).

Kondrateyev, K. Ya. 1965. *Radiative Heat Exchange in the Atmosphere.* Oxford: Pergamon Press.

Kuhn, P. M. 1970. "Applications of Thermal Radiation Measurements in Atmospheric Science." *Advances in Geophysics.* A. J. Drummond, ed. No. 14. New York and London: Academic Press.

Latimer, J. R. 1972. "Radiation Measurements." *International Field Year for the Great Lakes, Technical Manual Series No. 2.* The Secretariat Canadian National Committee for the International Hydrological Decade. Information Canada, Ottowa, Canada.

Oetjen, R. A., Bell, E. E., Young, J. and Eisner, L. 1960. "Spectral Radiance of Sky and Terrain at Wavelengths Between 1 and 20 Microns, Part 1: Instrumentation." *Journal of the Optical Society of America.* 50:1308-1313.

Robert, C. 1976 or 1977. *Contribution a l'Etude de Rayonnment Infrarouge de l'Atmosphere.* Ph. D. Thesis, University of Paris.

Sellers, W. D. 1965. *Physical Climatology.* Chicago and London: University of Chicago Press.

Sloan, R., Shaw, J. H. and Williams, D. 1955. "Infrared Emission Spectrum of the Atmosphere." *Journal of the Optical Society of America.* 45:455-460.

Stringer, E. T. 1972. *Techniques of Climatology.* San Francisco: W. H. Freeman and Company.

Suomi, V. E., Staley, D. O. and Kuhn, P. M. 1958. "A Direct Measurement of Infrared Radiation Divergence to 160 mb." *Quarterly Journal of the Royal Meteorological Society.* 84:472-74.

Suomi, V. E. and Kuhn, P. M. 1958. "An Economical Net Radiometer." *Tellus.* 10:160-163.

Swan, J. B., Federer, C. A. and Tanner, C. B. 1961. "Economical Radiometer Performance, Construction and Theory." *Soils Bulletin* No. 4. University of Wisconsin, Madison.

Swinbank. W. C. 1963. "Long Wave Radiation from Clear Skies." *Quarterly Journal of the Royal Meteorological Society.* 89:339-348.

Tanner, C. B., Businger, J. A. and Kuhn, P. M. 1960. "The Economical Net Radiometer." *Journal of Geophysical Research.* 65:3657-3667.

Tanner, C. B. 1963. "Basic Instrumentation and Measurements for Plant Environment and Micrometeorology." *Soils Bulletin.* No. 6, University of Wisconsin, Madison.

Williams W. J., Murcray, F. H., Murcray, D. G. and Kyle, T. G. 1970. *Flow of Radiation in the Earth's Atmosphere.* A report prepared at Denver University, Colorado, National Technical Information Service, 5285 Port Royal Road, Springfield, VA 22161.

Wolfe, W. L., ed. 1965. *Handbook of Military Infrared Technology.* Office of Naval Research, U. S. Government Printing Office, Washington, DC.

World Meteorological Organization. 1971. *Guide to Meteorological Instruments and Observing Practices.* 4th Edition, WMO/No. 8, TP 3, Geneva, Switzerland.

CHAPTER 7

# THE MEASUREMENT OF CIRCUMSOLAR RADIATION

A. J. Hunt, D. F. Grether and M. Wahlig
Lawrence Berkeley Laboratory
University of California
Berkeley, California 94720
The United States of America

## 7.1 Introduction and Background

Circumsolar radiation refers to the light that has its apparent origin in the region of the sky around the sun. The term *solar aureole* is often used to describe easily observable or characteristic occurrences of circumsolar radiation. The phenomenon can easily be observed by using a finger or nearby object to block the direct sunlight from entering the eye and examining the light that streams around the occulting object. The intensity can drop off rapidly or slowly as a function of distance from the sun, vary considerably in color, or form colored rings around the sun.

Circumsolar radiation is caused by the scattering of light by small particles in the earth's atmosphere. The aerosol particles may be composed of ice crystals or water droplets in thin clouds. They may be dust or sea salt particles, smoke or fumes, photochemical pollutants, sulfuric acid droplets, solid particles with a water mantle, flocks formed of a loose aggregate of smaller particles, or any of a large variety of solid, liquid or heterogeneous materials that are small enough to be airborne.

The amount and character of circumsolar radiation vary widely with geographic location, climate, season, time of day and observing wavelength. Some of the more striking cases can be observed in the presence of high, thin cirrus clouds.

Some of the general characteristics of circumsolar radiation can be inferred from calculations of scattering. The diffraction from a sphere may be rigorously calculated if its size, complex index of refraction, and the wavelength of incident light are known (Mie, 1908; see, e.g., van de Hulst, 1957). If the sphere is large compared to the wavelength of light, the scattered light intensity will peak in the forward direction. If the sphere is small or comparable in size to the wavelength of light, the scattering will be more isotropically distributed in angle. For a single non-absorbing sphere the character of the angular distribution may be quite complex. However, if the calculation is performed for a size distribution of spheres and the resulting intensities added, or if the sphere is absorbing, the individual lobes of the scattering pattern disappear. Nevertheless, the same general trends with size are followed. These calculations may be applied to particles in the earth's atmosphere, but caution must be exercised. The assumption that there is just one type of uniform spherical particle with known size distribution clearly breaks down if the variety and complexity of the particles in the atmosphere are considered.

A number of workers have calculated theoretical circumsolar profiles based on Mie or Rayleigh scattering (Deirmendjian, 1957, 1959, 1970; van de Hulst, 1957; Eiden, 1968; Green et al, 1971; Grassl, 1971; Deepak, 1973). These calculations predict aureole profiles for spherical, homogeneous particles by assuming various size distributions and indices of refraction. In clear atmospheres the scattering is dominated by the gaseous component (Rayleigh scattering) and there is good agreement between the model and experimental data. When a substantial aerosol component is included the agreement varies.

Because the aerosol composition of the atmosphere is highly variable, these models are more useful for understanding general behavior than for predicting actual values.

Atmospheric aerosols have many effects on the incoming and outgoing radiation in the earth's troposphere and stratosphere. They can affect the overall heat balance of the earth, produce marked local changes in climate and affect the angular distribution of downcoming solar radiation. Accordingly, measurements of the circumsolar component of sunlight have been performed for various purposes. Early interest in circumsolar data grew from the desire to determine the errors in the measurement of the direct beam radiation from the sun and its effects on the pyrheliometric scale (see, e.g., Ångström and Rodhe, 1966, Ångström, 1974 a and b). In recent years the advent of high speed computers made it possible to use the Mie calculation in conjunction with circumsolar measurements as a sensitive probe of aerosol scattering properties. Most recently, with the upsurge of solar energy collection, interest has increased in determining the effect of circumsolar radiation on the properties of focusing collectors. This interest arises because of the overestimate of direct beam solar radiation produced by pyrheliometer measurements and the dependence of the performance of a focusing collector on the details of the distribution of light near the solar disc.

In aerosol studies, measurements over larger angles from the sun were generally made, while in pyroheliometric and solar collection investigations, measurement on the near forward scattering profile were required. The differences in angular ranges used generally lead to different instrumental techniques. In the next section, general measurements of circumsolar radiation are discussed. The final section describes specific instrumental techniques and their areas of application.

## 7.2 Measurement Considerations

### 7.2.1 Angular Range

Determination of the desired angular range (minimum and maximum angles from the center of the sun) is one of the first considerations of the measurement of circumsolar radiation. If the sun's disc is included in the measurement, the attendant problems of detecting a wide range of light intensities and reducing the instrumental scattered light require great care and consideration. The difficulty arises from the extreme contrast between the brightness of the solar disc and the surrounding sky. On a clear day the difference in brightness between the center of the sun and the sky 3° away can easily exceed 5 orders of magnitude. Under identical conditions the intensity of the sky at the edge of the solar disc can drop three to four orders of magnitude within 0.1°.

The use intended for the data will determine the maximum measurement angle. For solar energy resource evaluations pertinent to focusing collectors the maximum angle will be small, probably less than 5°. For measurements to be used for aerosol modeling calculations the maximum angle would be larger, in the range of 10°-40°, depending on the needs and interests of the modeler; may also be satisfactory to exclude entirely the light from the solar disc.

### 7.2.2 Angular Resolution

The angular resolution required for a measurement depends on the rate of change of sky intensity with angle. It is clear that in the vicinity of the sun the angular resolution must be much better than in some area of the sky where the intensity is changing slowly. If the angular range is chosen to exclude the sun, this resolution requirement is usually not acute. If the intensity profile at the solar disc is desired, the aperture size must be chosen small enough to obtain the desired detail. The requirement of a small aperture conflicts with obtaining a good signal-to-noise ratio at larger angles. In determining the effective angular resolution, the internal instrumental scattering and diffraction effects must be folded in with the purely mechanical contributions to measurement resolution.

### 7.2.3 Angular Direction

For measurements that are not made in annuli about the sun but rather along radii, the orientation of each radius is an additional factor that must be evaluated in the instrumental design. The major directions for scanning would be at constant values of almucantor, solar vertical, solar declination, or right ascension. In solar resource measurements confined to small angles this distinction is not very

important except for angles very near the horizon. For use in aerosol modeling, an almucantor or solar vertical scan is preferred because of the symmetry of the scan with respect to the variation in air mass.

### 7.2.4 Spectral Dependence

The circumsolar intensity profile changes in magnitude and character as a function of wavelength. Both the central values and the widths of the wavelength pass bands selected would depend on the data application. In measurements of solar resources, the spectral characteristics of the receiver are important. If the receiver has the characteristics of a black body, then measurements integrating over a broad spectral range are desirable. If the receiver has a strong spectral dependence (e.g., photocells or selective coatings) more spectral selectivity may be necessary. For purposes of aerosol modeling one or more band pass filters enhance the resolution of the technique. A narrow band pass is rarely required, since aerosol properties usually change slowly with wavelength.

### 7.2.5 Other Considerations

One of the most important, and often overlooked, aspects of circumsolar radiation is its change with time. This can be very rapid when the projection of a cloud edge crosses the detector, or can be nearly constant for hours. Thus, there are no easy guidelines to follow for timing or scheduling measurements.

Another factor to be considered in the instrument design for circumsolar measurement is the accuracy needed to track the sun. A simple clock-driven equatorial mount will lead to errors arising from the change in the sun's declination during the day. If high resolution scans through the solar disc are desired, the tracking accuracy will usually require that the clock drive be supplemented with an active guidance system.

Various supplemental solar and meteorological measurements can be useful in interpreting the data. If absolute radiometric data from the sky are not an integral part of the circumsolar measurements, it is usually necessary to have simultaneous pyrheliometer measurements for calibration purposes.

## 7.3 Instrumental Techniques for Measuring Circumsolar Radiation

### 7.3.1 Visual

Circumsolar radiation can be observed visually if some method is provided to shield the eye from the extreme brightness of the solar disc. As previously mentioned, a finger at arm's length or a nearby pole or chimney may be used. This rather crude technique provides both for monitoring the variation, and for alerting the observer to any unusual or interesting variations in the circumsolar radiation.

Newton observed the solar aureole (he used the term *corona*) by studying the reflection of the sun in still water. A number of other visual techniques can be used to study the solar aureole and much insight into atmospheric optics can be gained by such observations. (Minneart, 1954). More recently, a visual classification scheme was proposed using an occulting object and a neutral density step wedge (Volz, unpublished). Another way of viewing the phenomenon with the naked eye is to observe the circumlunar radiation at night. The much lower brightness of the moon makes the observation more comfortable; and the measurement can still supply valuable information about atmospheric scattering processes.

### 7.3.2 Photographic

A similar but less subjective measurement technique is to make a permanent recording of the appearance of the sky by using photographic film. This method has several attractive features: the record is simple and inexpensive to make; spectral information can be obtained with color film or filters; and sky conditions can be recorded. Two main approaches to measurement utilize: (1) a film with a photographic latitude wide enough to allow simultaneous photographs of both the solar and circumsolar components in conjunction with special processing techniques (Robertson and Banker, 1974); (2) a circular occulting disc consisting of a neutral density filter to reduce the intensity of the sun and the low-angle circumsolar light (Green et al, 1971; Ward et al, 1973). The wide-latitude film technique can have over six orders of magnitude of dynamic exposure range (although published data indicates a maximum exposure

variation of only about 20,000). The field of view is dependent on the optics of the camera.

The angular resolution of the method is dependent on the scattering, diffraction, chromatic aberration, and multiple solar images produced by the lens. If an occulting disc is not used it is very difficult to reduce the internal scattering in the camera to a level low enough to make use of the dynamic range of the film. The spectral range is limited by the response of the film and the transmission characteristics of the camera optics.

The relative ease of recording the data is strongly offset by the data-measuring process. For some measurements the film can be developed, examined, placed in a microdensiometer and scanned. However, for monitoring purposes, the data-measuring process would probably have to be automated, the film processing steps carefully monitored and ancillary time, horizon, and absolute radiation reference, calibration or fiducial information input onto the film. In measuring the film, the brightness of most of the sky is usually ignored by scanning radially in the solar vertical or almucantor plane. For these reasons, the technique is probably most applicable for measuring occasional unusual aureole occurrences, for comparison checking during other measurements (e.g., pyrheliometer intercomparison), for determining the scattering profiles of recurring sky conditions, or for general surveying of the sky when qualitative rather than quantitative measurements are needed.

### 7.3.3 Scanning Aperture Instruments

The most widely used class of instruments for measuring circumsolar radiation utilizes a photodetector or thermopile as the detector element; the instrument geometry restricts the field of view.

There are several scanning instrument designs that vary in aperture geometry and in the method of scanning. The detector can be exposed to the sky through a small circular opening or a straight slit. The circular area can be scanned along various radii from the center of the sun or raster-style over much of the heavens.

A scanning sun photometer developed for aerosol studies involving the solar aureole was reported by Eiden (1968). The sky was scanned in right ascension from 1° to 15° from the sun using an acceptance angle of 0.5°. An open-tube design with multiple baffling reduced the internal scattering and diffraction. The photomultiplier tubes used as detectors were calibrated with a standard radiation source after each set of runs. The instrument had an auxiliary photometer to measure turbidity and provide a signal for an active guidance system. The sky was scanned in five narrow wavelength bands from 0.448 to 0.847 $\mu$m. One scan required 10 min and the data were recorded on chart paper.

Three series of measurements were performed, two at high altitude stations to determine background scattering for clear continental and maritime atmospheres and one in an industrial area to study highly turbid conditions. One result of the work was the discovery that large particles (radius $\geq$ 150 $\mu$m) played a more significant role in atmospheric scattering than had earlier been suspected, leading to a strong enhancement of the very near forward-scattered radiation.

A circumsolar telescope, designed primarily to determine the effect of circumsolar radiation on highly concentrating solar collectors, was described by Grether and co-workers (1975 a and b; 1976 a and b). The instrument was built as a reflecting telescope that forms an image of the sun and adjacent sky on an aperture plate set off to the side of the incoming light. The telescope scans in constant declination across the solar disc from −3° to +3° (relative to the center of the sun). The aperture diameter is 1.5 ft (0.47 m) when the instrument points to within 0.5° of the sun's center, becoming 5.0 ft (1.52 m) from 0.5° to 3°. An active solar guider keeps the tracking platform pointed accurately at the center of the sun. A fused silica window protects the mirror from the environment. A combination of baffling, light trapping, and vignetting reduces the scattered and diffracted light to a low level. A pyroelectric crystal is used as the detector element. Because of the instrument's wide dynamic range, it can make accurate measurements both of the intensity of the solar disc and the circumsolar region even on very clear days.

The telescope measures profiles using eight broad band filters and an open aperture. Simultaneous measurements are made through identical filters by an Active Cavity Radiometer (a pyrheliometer) to

provide absolute intensity calibration and broad band turbidity data. Each scan takes one min and the total sequence, 10 min. The scan information is digitized every 1.5′ of arc (every 0.25″) and written on magnetic tape. These telescopes are different from most circumsolar instruments since they can operate unattended. Measurements begin automatically before dawn and continue until after sunset every day.

A total of four telescopes were built and operated at various sites across the United States to provide measurements of circumsolar radiation at locations of interest to the U. S. Solar Energy Program.

An instrument to study aerosol scattering, designed to be carried in an airplane was reported by Twitty et al (1976). The photometer was rotated continuously around a vertical axis, sweeping a slit-shaped aperture in a complete almucantor scan; however, the published data only extend ±40° from the sun. The field of view of the detector was determined by a slit in the vertical direction having dimensions of 0.6° by 5.0°. A lens and sunshade prevented direct solar radiation from illuminating the lens at angles greater than 1.5° from the sun. Since the instrument was airborne it was not possible to accurately align the center of the slit with the sun. To overcome this problem, an auxiliary detector determined the actual zenith angle of the sun, so that a correction factor could be applied to obtain the true angular radiance function. The measurements were made with a PIN photodiode and a filter centered at a wavelength of 0.54 μm. Scans were made at 30-s intervals. The output signals passed into an analog-to-digital converter and a serial tape recorder.

The photometer was calibrated by matching the output at angles greater than 40° with the diffuse radiance calculated from Rayleigh theory. Auxiliary data on the aerosols were provided by a broad band nephelometer and a ground-based lidar system. A series of measurements was made at various altitudes over Lake Superior in May of 1973. The consistency of the lidar and scanning photometer data lead the authors to suggest that the aureole measurements may be used to calibrate the lidar back-scatter returns.

A scanning photometer designed to measure the intensity of light from any part of the sky was described by Kleckner and co-workers (1975). The basic optics of the system consist of two mirrors in an alt-azimuth drive arrangement capable of viewing any part of the sky. The 2°-field of view of the optics is swept in a series of ascending almucantor scans around the sky or swept in the solar vertical plane. The operation of the instrument is automatically controlled by a minicomputer. Any of seven broadband filters having cut-offs from 0.368 to 1.065 μm may be selected.

The instrument utilizes a silicon PIN photodetector. The position of the sun is calculated by using an internal clock. The scheduling of the measurements is selectable, but the basic program controls sweeps of the entire sky every 30 min and performs zenith and solar almucantor scans more often. The data are recorded on magnetic cassette tapes. At least six instruments are scheduled to be built and deployed in the western and northern United States.

Platt (1976) described a solar aureole radiometer, which had a sun shade supported by rods, two apertures and a lens. The instrument is pointed in a fixed direction and the sun allowed to transit the field of view of about 1.4°, the extent of the usable angular scan is dependent on the stability of sky conditions. A Barnes thermister serves as the detector. Neutral density filters are inserted to decrease the intensity whenever the photometer is pointed at or near the sun. Pairs of cut-on and cut-off filters determine the spectral response of the photometer. A chart recorder is used to retain the data.

A solar aureole photometer utilizing a slit geometry for ground-based measurements was described by Lerfald (1977). Basically, the instrument views a slit of the sky that scans the sun from −8° to +8°. The slit size and shape are varied with radial distance from the center of the sun by a combination of a rotating radial slit and a linear detector. The width of the slit varies from 0.1° at the center to 0.5° at 8° away. The height of the slit also varies with radial distance. The scan can be made in either the almucantor or solar vertical. The instrument is attached to an equatorial mount and the pointing is checked hourly. The measurements are made using three wide-band filters in the visible region as well as no filters. The silicon detector determines the wavelength response in the no-filter mode. A complete scan can be made in either 10 or 100 s. The data are converted to digital form, and written on magnetic tape. The

instrument has been used for field measurements along with a wide variety of lidar, solar, meteorological, particulate and background measurements.

### 7.3.4 Non-scanning Instruments

Some of the earliest measurements of circumsolar radiation were performed using an instrument developed by C. G. Abbot and L. B. Aldrich as part of the Smithsonian Astrophysical Observatory's program to measure solar radiation. A description of the data measurements and their analysis was given by Ångström (1974 a and b). The instrument consisted of a shaded pyranometer that measured the brightness of the sky in a band 10° wide, concentric with the sun. The middle of the band was 8°30′ from the solar limb. The instrument relied on an absolute calibration and had no filters. Measurements were made over many years from two high altitude mountain stations, and were used to study long-term changes in the scattering properties of the atmosphere.

More recently, Jeys and Vant-Hull (1976) described an instrument to determine the amount of circumsolar radiation within annular regions around the center of the sun. Measurement was made by attaching three brass collimating tubes to an Eppley Normal Incident Pyrheliometer. The tubes were of different lengths to give full angle fields of view of 4.04°, 2.86° and 2.02°. The instrument was centered on the sun and a turret containing tubes was rotated and readings taken for each setting, using no filters and a thermopile detector. A complete set of measurements required about 10 min and was recorded on a chart.

Another approach for determining aureole brightness was described by Shaw and Deehr (1975) who utilized a photoelectric coronameter with 2 PIN silicon photodetectors. The instrument compares the brightness of the sky at points 2° and 6.5° from the solar limb. The instrument whose design is similar to that of a coronagraph, has occulting discs and several stops to reduce scattered and diffracted light. It can be operated with interference filters.

There is only one instrument commercially available, the variable field-of-view pyrheliometer built by The Eppley Laboratory, Inc.* It incorporates a thermopile detector. A single lens with a variable diaphragm is situated at the focal plane. A series of baffles limits the field of view to a maximum of 6°. The aperture can be reduced to a minimum of 40′ of arc. Because the device is rotated on an equatorial mount the tracking must be checked frequently. There is no provision for filters.

### 7.3.5 Other Measurements

This review has included a brief summary of the types of instrument that have been built to measure circumsolar radiation and does not pretend to be an exhaustive treatment. Some aureole measurements reported in the Russian literature have not been given because descriptions of the instruments were not available. However, there appears to have been a long history of interest in the aureole starting with Fesenkov in the 1930's, continuing up to recent times (see, e.g., Pavlov, 1965; Gorchakov and Isakov, 1974). The photographic technique has probably had more widespread use than indicated by the few samples of measurement reported here.

### References


Ångström, A. and Rodhe, B. 1966. "Pyrheliometric Measurements with Special Regard to the Circumsolar Sky Radiation." *Tellus.* 18:25-33.

Ångström, A. 1974a. "Circumsolar Sky Radiation and Turbidity of the Atmosphere." *Applied Optics.* 13:474-477.

Ångström, A. 1974b. "Circumsolar Radiation as a Measure of the Turbidity of the Atmosphere, Part 2." *Applied Optics.* 13:1477-80.

Deepak, A. 1973. "Double Scattering Corrections for the Theory of the Sun's Aureole." *NASA Technical Memorandum, NASA TM X-64800.* 20 pp. Marshall Space Flight Center, Huntsville, AL. U. S. A.


*Manufactured on request by The Eppley Laboratory, Inc., 12 Sheffield Ave., Newport, RI, 02840, U.S.A.

Deirmendjian, D. 1957. "Theory of the Solar Aureole, Part 1, Scattering and Radiative Transfer." *Annales de Geophysique.* 13:286-306.

Deirmendjian, D. 1959. "Theory of the Solar Aureole, Part 2." *Annales de Geophysique.* 15:218-249.

Deirmendjian, D. 1970. "Use of Scattering Techniques in Cloud Microphysics Research I. The Aureole Method." *Rand Technical Report R-590-PR.*

Eiden, R. 1968. "Calculations and Measurements of the Spectral Radiance of the Solar Aureole." *Tellus.* 20:380-398.

Gorchakov, G. I. and Isakov, A. A. 1974. "The Aureole Scattering Functions of Haze." Izb. *Atmospheric and Oceanic Physics.* 10:504-511.

Grassl, H. 1971. (Letters to the Editor), "Calculated Circumsolar Radiation as a Function of Aerosol Type, Field of View, Wavelength and Optical Depth." *Applied Optics.* 10:2542-43.

Green, A. E. S., Deepak, A. and Lipofsky, B. J. 1971. "Interpretation of the Sun's Aureole Based on Atmospheric Aerosol Models." *Applied Optics.* 10:1263-79.

Grether, D. F., Nelson, J. and Wahlig, M. 1975a. "Measurements of Circumsolar Radiation." *Proceedings of Symposium of Optics in Solar Energy Utilization, 19th Annual Technical Symposium of The Society of Photo-Optical Instrumentation Engineers, San Diego, CA., August 18-22, 1975.*

Grether, D. F., Nelson, J. and Wahlig, M. 1975b. *Lawrence Berkeley Laboratory Technical Report, UCID 3705 or NSF/RANN/SE/AG-536-PR/74/4.*

Grether, D. F., Hunt, A. J. and Wahlig, M. 1976a. "Results From Circumsolar Radiation Measurements." *Proceedings of the International Solar Energy Society Meeting, Winnepeg, Canada, August 16-20, 1976.*

Grether, D. F., Hunt, A. J. and Wahlig, M. 1976b. *Proceedings of the OAS/NASA Topical Meeting on Atmospheric Aerosols, Their Optical Properties and Effects. Williamsburg, VA., December 13-15, 1976.*

Hickey, J. R. and Karoli, A. R. 1977. *Proceedings of the 1977 Annual Meeting of the American Society of the International Solar Energy Society, Orlando, Fl. June 6-10, 1977.*

Jeys, T. H. and Vant-Hull, L. L. 1976. "The Contribution of the Solar Aureole to the Measurement of Pyrheliometers." *Solar Energy.* 18:343-348.

Kleckner, E. W., Smith, L. L. and Hoch, R. J. 1975. *Proceedings of the Symposium on Optics in Solar Energy Utilization, 19th Annual Technical Symposium of the Society of Photo-Optical Instrumentation Engineers, San Diego, CA., August 18-22, 1975.*

Lerfald, G. M. 1977. "A Solar Aureole Photometer For Use in Measuring Size Distributions of Particles in the Atmosphere." *NOAA-Boulder Technical Memorandum.*

Mie, G. 1908. "Beitrage tur Optik Truben Medien, Speciell Killordaler Metallosungen." *Ann. Physik.* 25:377-445.

Minnaert, M. 1954. *The Nature of Light and Color in the Open Air.* New York: Dover Publications

Pavlov, V. E. 1965. "Empirical Formula for the Atmospheric Scattering Indicatrix Which Takes into Account the Circumsolar Aureole." *Soviet Astronomy - AJ.* Vol. 9, No. 2, p. 340.

Platt, C. M. R. 1976. "Solar Aureole Radiometer for Atmospheric Aerosol Studies." *Journal of Applied Meteorology.* 15:1323-27.

Robertson, C. E. And Banker, J. H. 1974. "Photographic Technique to Determine the Apparent Energy Distribution of the Solar Aureole." *Sandia Laboratories, Albuquerque, NM. Report SLA-74-0090, Contract AT(29-1)-789.*

Shaw, G. E. and Deehr, C. S. 1975. (Notes and correspondence) "A Photoelectric Coronameter for Atmospheric Turbidity Studies." *Journal of Applied Meteorology*. 14:1203-05.

Twitty, J. T., Parent, R. J., Weinman, J. A. and Eloranta, E. W. 1976. "Aerosol Size Distributions: Remote Determination from Air-Borne Measurements of the Solar Aureole." *Applied Optics*. 15:980-89.

van de Hulst, H. C. 1957. *Light Scattering by Small Particles*. New York: John Wiley & Sons, 470 p.

Ward, G., Cushing, K. M., McPeters, R. D. and Green, A. E. S. 1973. "Atmospheric Aerosol Index of Refraction and Size-Altitude Distribution From Bistatic Laser Scattering and Solar Aureole Measurements." *Applied Optics*. 12:2585-92.

CHAPTER 8

# SOME EMPIRICAL PROPERTIES OF SOLAR RADIATION AND RELATED PARAMETERS

**Peter Valko**
**Swiss Meteorological Institute**
**Krahbuhlstrasse 58**
**CH-8044 Zurich**
**Switzerland**

## 8.1 Introduction

As shown in the preceding chapters, incoming solar radiation outside the atmosphere varies with time of year, time of day and with geographic latitude. Due to interactions with the atmosphere and the earth's surface, non-periodic temporal changes, as well as non-zonal spatial variations are superimposed on the primary patterns. Besides direct solar radiation, scattered and reflected components are also effective. Intensity, direction and spectral composition of all components vary strongly both with time and from site to site.

Radiation data, applicable as standards in solar energy engineering, are valid for mean conditions over a limited area. Such data are gained either by using many years of records or by model computations. The variability of the radiation fluxes from the standard conditions is also important. The objectives of the present chapter are to describe the variations underlying the standard values.

Four main properties and their limiting effects on radiation standards will be discussed here in more detail:

*temporal* variability -
: mean values have decreasing significance with decreasing time intervals;

*spatial* variability -
: data from stations nearby or data interpolated between stations is necessary in many cases;

*angular* variability -
: radiation falling on inclined surfaces facing in different directions has, in general, to be computed under simplified assumptions;

*combined frequency distributions* of radiation with other parameters, e.g., temperature and wind velocity, may yield rather different results than combined single-parameter distributions.

The significance of these aspects will be demonstrated by a set of empirical results concerning shortwave solar radiation and related meteorological parameters. The subdivisions are more suitable to the kind of data, than to the single properties listed above. Predominately Swiss data have been used for reasons of accessibility to the author, but the purpose is to show the types of graphs rather than the numerical values themselves. Nevertheless, for comparable climates some generalization may be indicated.

Definitions and explanations of the physical quantities are given in the preceding chapters, particularly Chapter 3.

## 8.2 Turbidity and Precipitable Water

Even a cloud-free atmosphere may attenuate radiation fluxes considerably. Extinction and absorption of radiation by haze, dust particles and water vapor are mainly responsible for the attenuation.

Therefore the range of intensity variations under clear sky conditions depends first on variations of air turbidity and precipitable water, w.

Figures 8-1 to 8-3 use Schüepp's (1949) turbidity coefficient B as computed from pyrheliometer measurements of direct solar radiation. Data for Figure 8-1 for the United States stations have been taken from Figures 2 and 10 of Appendix II to this handbook; the curves for Stanleyville and Leopoldville were drawn using measurements of de Coster and Schüepp (1956) and Schüepp (1954, 1955). As may be seen, not only the range of the monthly means but also the rate of the seasonal changes is different for each climate. The influence of altitude above sea level is demonstrated in Figure 8-2, while the variability within and between single calendar months is shown in Figure 8-3. Both figures (Valko, 1970a, 1971) were prepared by using daily mean values of B. The measurements in Figure 8-2 cover a period of 2-3 years for each station. As shown first by Volz (1963) turbidity tends to follow a logarithmic-normal distribution (B is measured on a log-scale). Conducting an $\chi^2$ test on the Locarno-Monti data should also show this relationship.

The extent to which direct solar radiation at normal incidence, I, is affected by changes of B and w is demonstrated in Figure 8-4. The curves drawn for the absolute air masses m = 1, 2 and 5 show that direct ray intensity depends much more on turbidity than on precipitable water. A very clean and dry atmosphere, characterized by B = 0.05 and w = 0.5 cm was chosen for reference (see Valko, 1970a, 1971). When computing the functions $I = f_1(B)$, w = 0.5 was kept constant while correspondingly B = 0.05 = constant for $I = f_2(w)$.

As discussed below, the intensity and angular distribution of diffuse radiation are also rather sensitive to changes in turbidity.

## 8.3 Duration of Sunshine

### 8.3.1 Sunshine and Cloudiness

Clouds have the greatest effect on radiation fluxes. If they shade the sun, the direct intensity vanishes to zero, while the sky radiation $G_d$ does not change with increasing cloud amount N until about N = 3-4 (expressed at tenths of the sky covered). It continues to increase to a maximum at about N = 8-9 and then decreases as the cloud covers more and more of the sky. In Figure 8-5 only low and middle clouds are considered. It is worth noting that, comparing *relative*

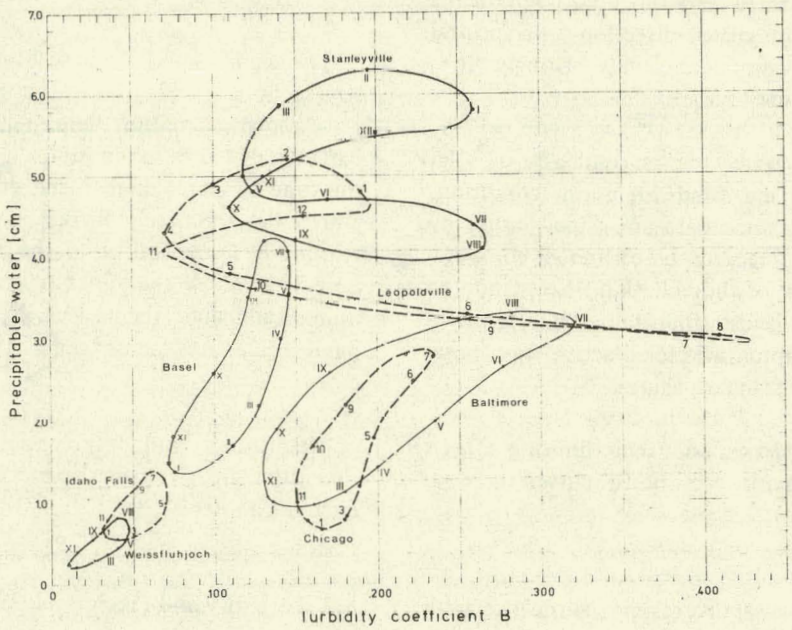


*Figure 8-1 Monthly mean values of the turbidity coefficient and precipitable water at various places, representing different climatic regions.*

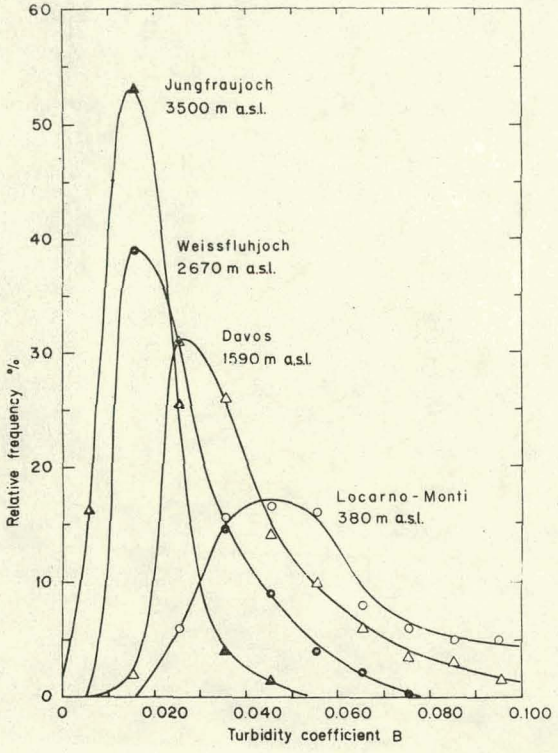


*Figure 8-2 Frequency distributions of turbidity coefficient for stations at different altitudes a. m.s.l. in the Swiss Alps.*

effects, high turbidity may increase sky radiation more than cloud amount alone does, especially for large solar elevation angles. In the figure about 900 instantaneous intensity values are involved, measured simultaneously at Locarno-Monti and selected from a 5-year period (Valko, 1966).

Records of sunshine are generally a good measure of the effect of clouds. Thin cirrus, however, or small cloud amounts may be present without interrupting the direct rays of the sun at all. For a great number of places sunshine duration is the most commonly available information on solar radiation. Records cover generally a time period of several years; at some stations measurements extend back to the last century. Sunshine data are therefore most useful for statistical treatment. Since the threshold sensitivity for direct sun radiation at normal incidence is about 200 W $m^{-2}$ for most devices in use (see Chapter 9), sunshine data gives information only on the time when $I \geq 200$ W $m^{-2}$.

### 8.3.2 Frequency Distributions

Information on solar availability is important on an hourly and daily time scale as well as over periods of several days. As is apparent from Figure 8-6 the variability of sunshine totals increases with decreasing integration time. For hourly and 1-day totals the curves show the typical U-shape. To demonstrate this, December and July were chosen as the months having the greatest difference between the frequencies of the boundary values, 0 and 100% relative sunshine. For periods of consecutive days, the distributions approach the normal distribution as the length of period increases.

Figure 8-7 illustrates cumulative frequency curves (1 - 99%) on a continuous time scale for Neuchâtel, January (Valko, 1973b). Such graphs may be used to answer energy storage questions such as: what is the probability, that through periods of n consecutive days the total sunshine amounts to less than t hours? The corresponding frequency curves also indicate clearly how many times more sunshine may be expected in winter months at mountain summits than at lowland sites. Table 8-1 gives such a comparison for St. Gallen (1931-1970) and Säntis (1901-1970).

Table 8-1

Sunshine Hours Accumulated on Consecutive January Days, Expected with 1, 50 and 99% Probabilities at Stations with Different Altitudes

| Station | Cum. Prob. (%) | Total Hours of Sunshine on 5 | 15 | 31 (days) |
|---|---|---|---|---|
| St. Gallen | 1 | 22 | 42 | 84 |
| 664 m a.s.l. | 50 | 5 | 19 | 35 |
| | 99 | 0.05 | 2 | 6 |
| Säntis | 1 | 45 | 116 | 208 |
| 2500 m a. s. l. | 50 | 16 | 51 | 105 |
| | 99 | 0.2 | 10 | 44 |

Such comparisons may indicate, for instance, whether flat plate collectors or concentrators should be installed.

The information value of sunshine data is of course limited. Even in the last example of possible decisions it is also necessary to know the share of diffuse radiation in the global energy input. Figure 8-8 presents the frequency distribution of this pro-

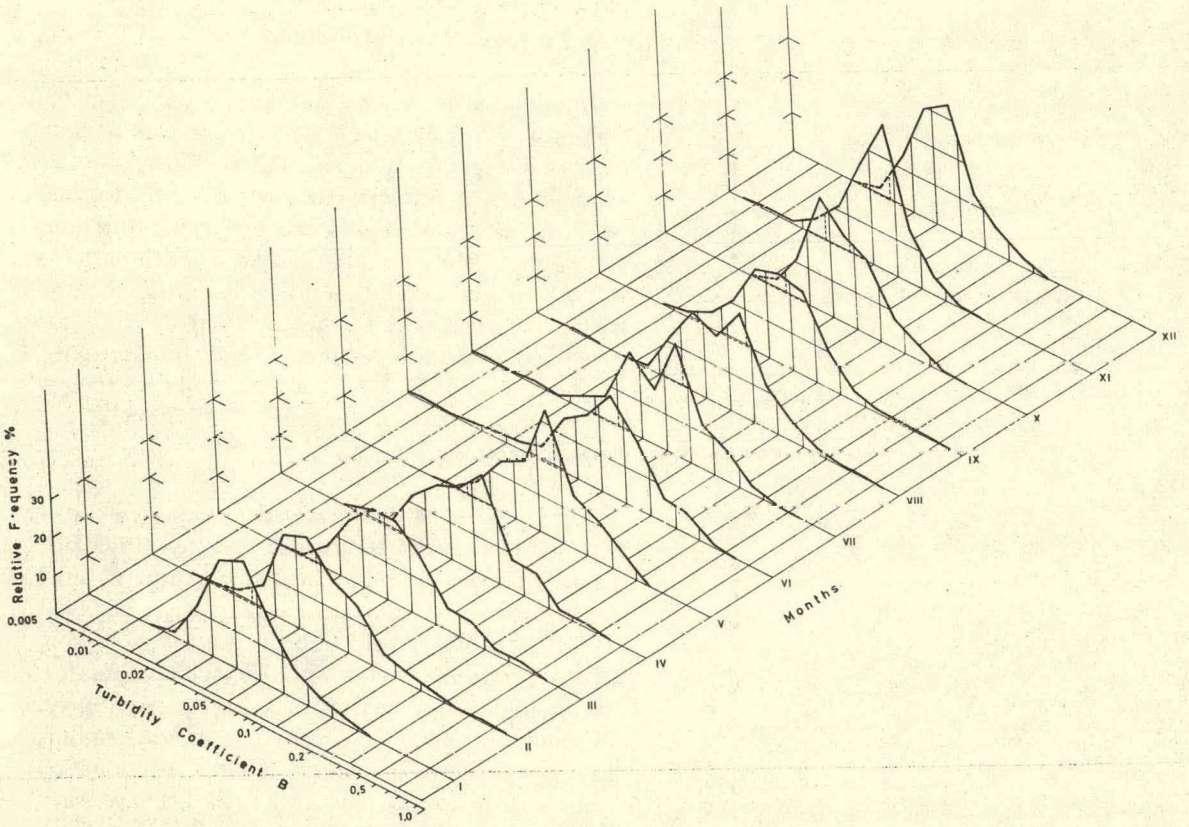


*Figure 8-3 Frequency distributions of the turbidity coefficient for each calendar month; a long-term record (1935-1969) at Locarno-Monti (southern Switzerland) was used.*

portion (for hourly values $\geq 23$ W m$^{-2}$) of horizontal surface irradiance as measured at Locarno-Monti during 1958-1971.

### 8.3.3 Spatial Variability

Precisely for the site of interest, the necessary data is, in general, not available. The error caused by adapting data from the nearest station, or by interpolating data between neighboring stations, is of practical significance for solar energy applications. Special care must be taken in regions with non-homogeneous climates.

A network of sufficient density with sufficiently long radiation records hardly exists. However, sunshine data for many countries fulfill these criteria and might suitably replace radiation data in spatial correlation studies. Since a real representativeness depends also on integration time, both aspects have to be considered jointly.

Figures 8-9 to 8-12 give some preliminary results of this kind, while Figure 8-13 summarizes the relationships found for hourly, daily, monthly, and yearly totals. Figure 8-13 is valid for the climatologically homogeneous region of central Switzerland north of the Alps. For the sake of comparison Figure 8-11 also shows the section of the regression line for 150-300 km obtained by Suckling and Hay (1976) for daily totals of *global radiation*. This study is based on a five-year period of data measured at 8 stations in western Canada having a maximum separation distance of 1180 km. As may be seen from Figures 8-11 and 8-13, the correlation coefficients for daily global radiation in western Canada are higher than those for daily sunshine hours in central Switzerland. According to Figure 8-13 for July daily sunshine correlations R = 0.7 at about 270 km while the Canadian study shows this value for a station separation distance of 950 km, in spite of the mountainous topography. One possible reason for this might be that the *in situ* variability of daily sunshine is greater

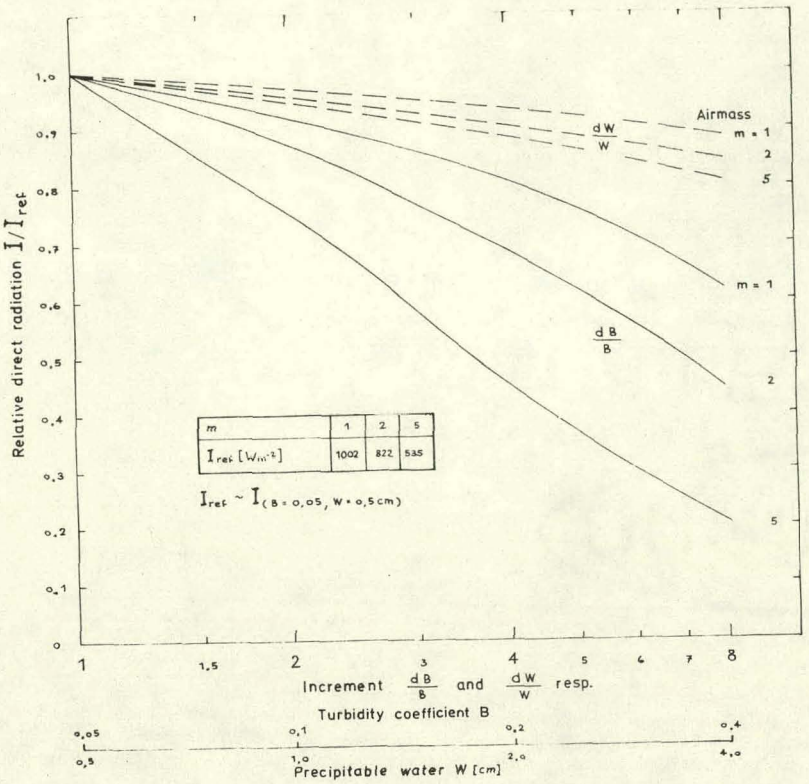


*Figure 8-4 Direct solar flux at normal incidence versus turbidity coefficient and precipitable water for air masses 1, 2 and 5.*

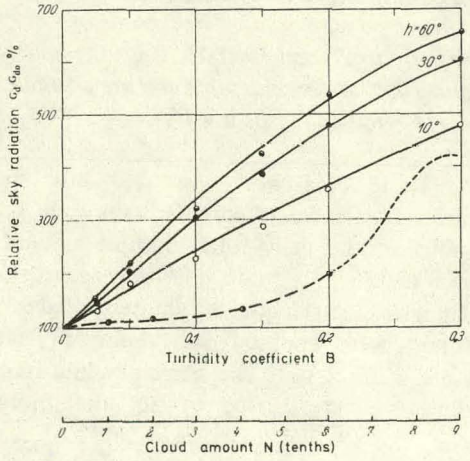


*Figure 8-5 Relative increase of sky radiation with turbidity coefficient for different solar heights and cloud amounts (dashed curve is related to the cloud amount scale below).*

than that of global radiation. By plotting the variation coefficient (standard deviation normalized to the corresponding mean) against integration time in Figure 8-14 illustrates this property is shown to be different for different stations and months. As a first check, variation coefficients of daily global radiation for Kloten and Davos, computed for the whole year, were also entered on this figure. These are much lower indeed, as one would expect, when compared with the corresponding sunshine variation coefficients; the yearly mean should have a value somewhere between the July and December extremes.

## 8.4 Short Period Fluctuations

Depending on the response time of the solar energy collecting system short-term fluctuations of the radiation input may influence its operation differently. By using appropriate instantaneous

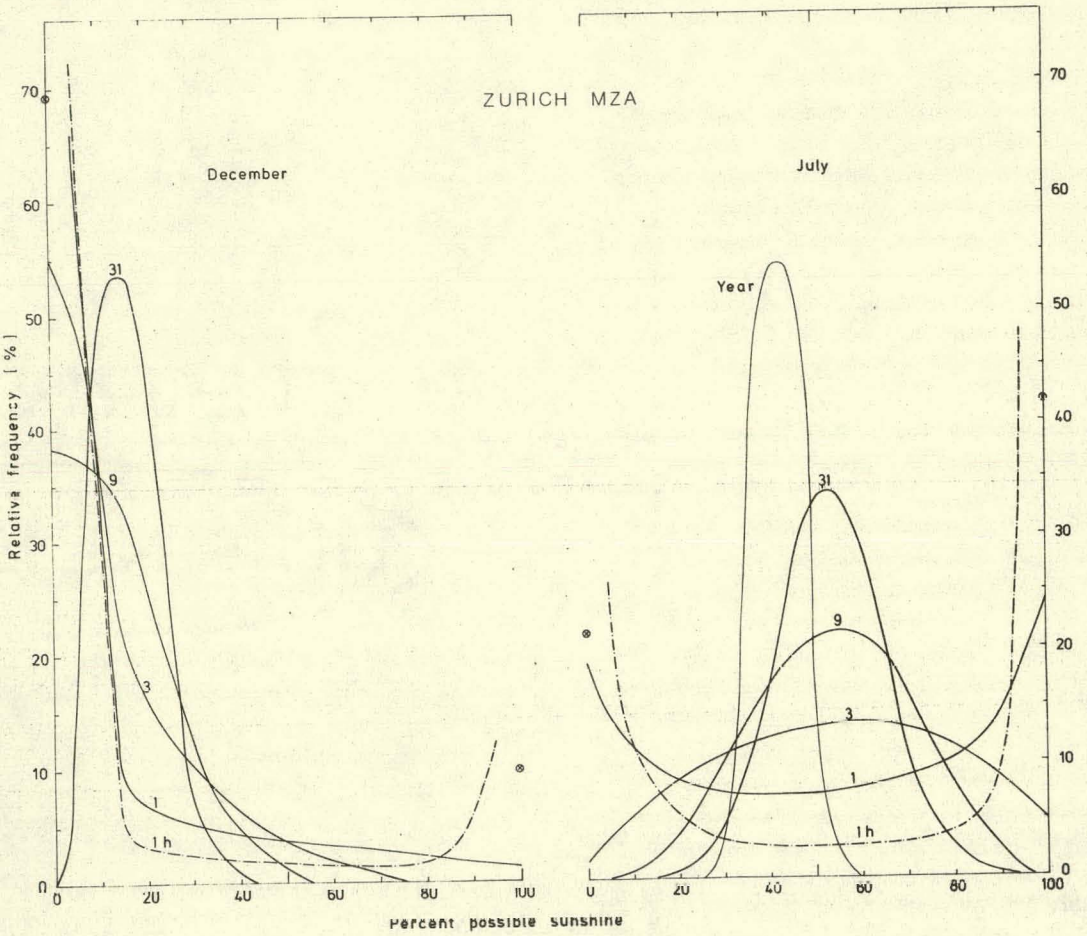


*Figure 8-6 Frequency distributions of sunshine duration; totals are computed over different integration time periods. Each distribution is normalized to its own maximum possible value. The records of Zurich Meteorological Institute cover the periods 1901-1970 for the daily totals and 1931-1970 for the hourly values. The relative contributions of the boundary values 0 and 100% are considerable and are characteristic for winter (December) and summer (July) cloudiness, respectively.*

records, the time structure of the direct beam interruptions, viz., the fluctuation of the radiation fluxes, may be analyzed statistically.

### 8.4.1 Periods With and Without Sunshine

For this purpose 65 years of sunshine records from three stations (Locarno-Monti, 1938-1973; Zurich-Kloten, 1960-1974; Zurich-Meteor. Institute, 1960-1974) were submitted to a minute-by-minute evaluation procedure: for every minute between sunrise and sunset the information "yes" or "no" (sunshine) was made available for computer input. These data were separated into months; within each calendar month the days were grouped according to the daily total sunshine amount: $\leq 1$ hour, 1-2, 2-4, . . ., 14-16 h. Within each day-group the number and length of uninterrupted intervals with sun were counted and the complementary intervals without sun. The corresponding frequency distributions were related to the total number of periods, and also expressed as number of cases per day. The number of days with and without sun as well as the proportion of days with sun falling in the individual groups has, of course, been considered. Care was taken, that between sunrise and the time

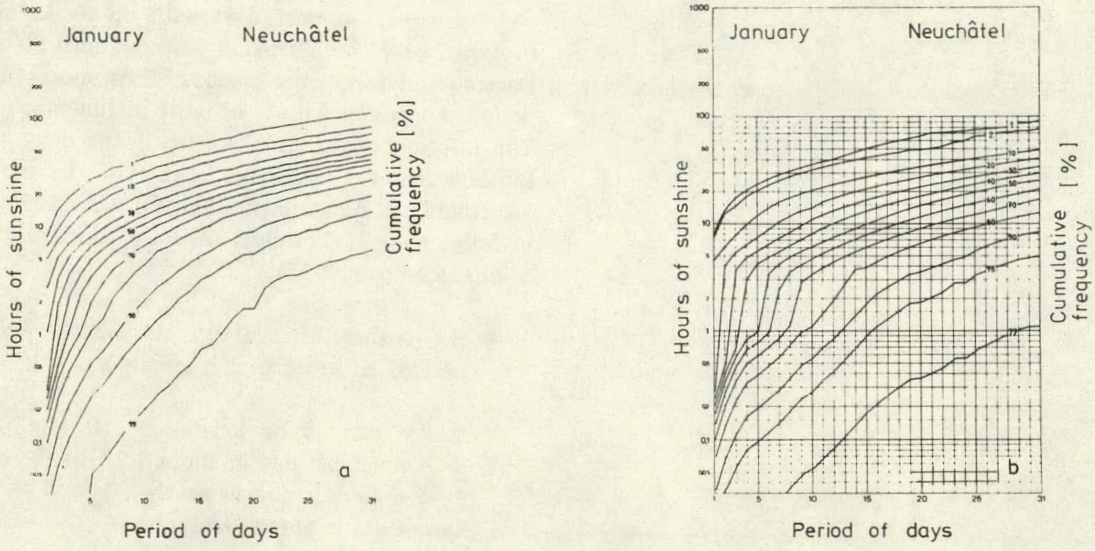


*Figure 8-7 Cumulative frequency distribution of sunshine hours accumulated over periods of $n \leq 31$ consecutive days in January for Neuchâtel. The entire 40-year (1931-1970) period of record was used: a) to its full extent. Example: There is a chance of about 5% of receiving 25 h of sunshine during a 10-day period, but it is almost certain (99% frequency curve) that at least 10 min of sunshine would be received. b) restricted to days with at least one uninterrupted period of sunshine lasting at least 2 h.*

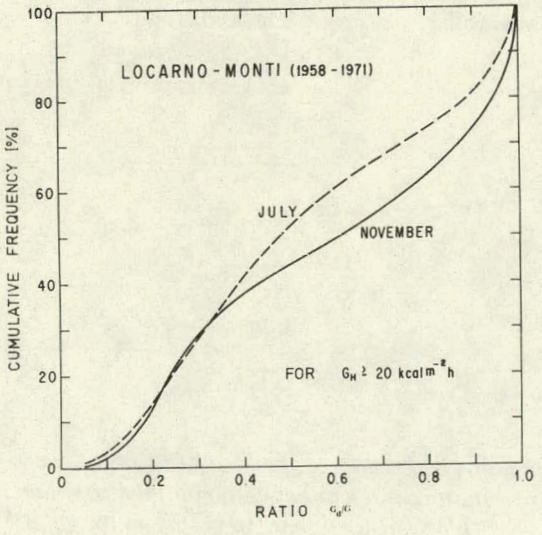


*Figure 8-8 Cumulative frequency distribution of the ratio: sky radiation/global radiation for Locarno-Monti. July and November curves show the greatest deviation from each other.*

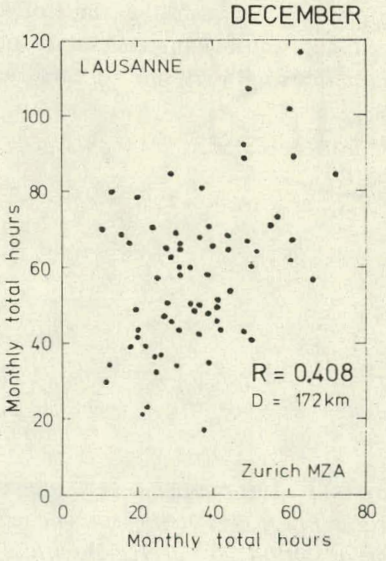


*Figure 8-9 December totals of sunshine hours recorded at Lausanne and Zurich, separated by 172 km, are only weakly correlated (corr. coeff. R = 0.408). Period of record used: 1901-1970.*

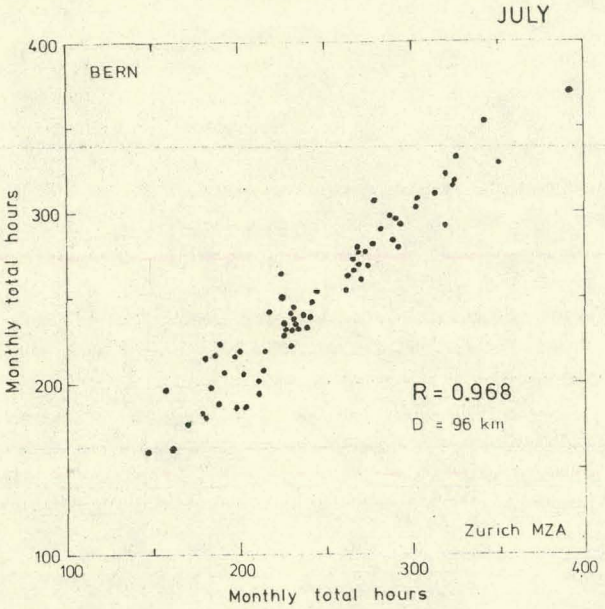


*Figure 8-10 Compared with Figure 8-9 the correlation coefficient for July is much higher. This improvement may be attributed much more to stable weather conditions than to the shorter distance between the two stations.*

of the first trace burned on the recording strip (and corresponding between the time of the last trace burned and sunset) intervals were not categorized as "periods without sun" if these were not caused by clouds (the threshold sensitivity of the strips was investigated recently by Baumgartner, 1978).

In this way summer days with up to 43 interruptions were found. At Locarno-Monti 50% of December days each contained 2 or more sunny periods compared with 7 or more in June and July. The information is more precise if the daily total sunshine amount and the lengths of the periods are combined. As an illustration, for Locarno-Monti, in July, with 10-12 hours of daily sunshine there results (see Figure 8-15):

- the chance, that a day contains *at least* 2 periods of *at least* 2 h length is about 3.2%;
- sunny periods of lengths $\geq$ 10 min occur $\geq$ 8 times per day in about 1.2% of the cases; $\geq$ 4 times per day in nearly 5%; and at least once a day in about 48%;
- only 1-2% of the days contain 12 h of uninterrupted sunshine (curve 1).

It should also be noted, that July days with 1-2 h of sunshine make up 2.8% of all days with sun and the proportion with 10-12 h is 19.1%; furthermore, during all 36 years no July occurred with less than 28 days having at least 1-min of sun, while in 18 years all 31 days were "days with sun".

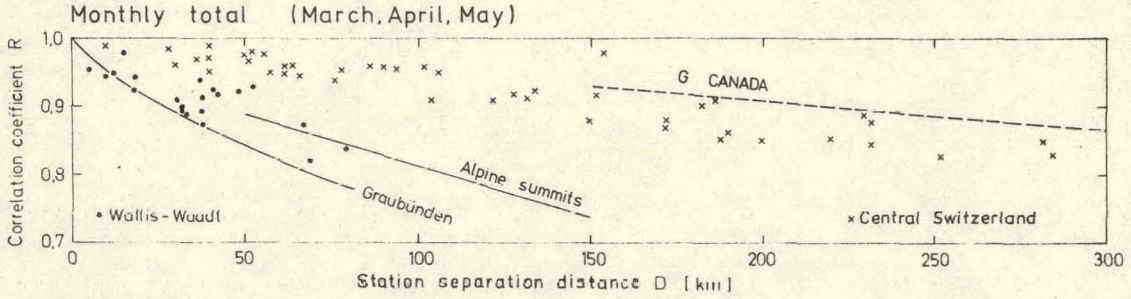


*Figure 8-11 This figure has been prepared by using all individual results of the kind of Figures 8-9 and 8-10, but only considering spring conditions. The correlation coefficient between monthly sunshine totals of station pairs decreases with separation distance. This decrease is more pronounced for alpine topography (stations in the valleys or on slopes) than for the lowland planes. Also mountain summits (2500 - 3500 m a.s.l.) show more spatial consistency of sunshine than the valleys.*
*Legend: × = central Switzerland (lowland); • = the southwestern Swiss Alps.*
*For "Graubünden" (southeastern Swiss Alps) and the summit stations only the regression curves were drawn, the entries themselves being omitted for the sake of clarity. The dashed line also shows part of the regression line found in Canadian global radiation data.*

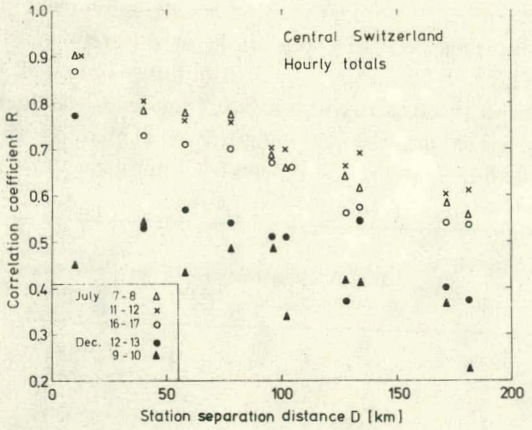


*Figure 8-12 The correlation between hourly sunshine values of station-pairs is markedly worse than that between monthly totals (in Figure 8-11 only the entries for central Switzerland should be considered for this comparison). The influence of the season and time of day on the relationship R = f(D) can be explained by the associated meteorological factors.*

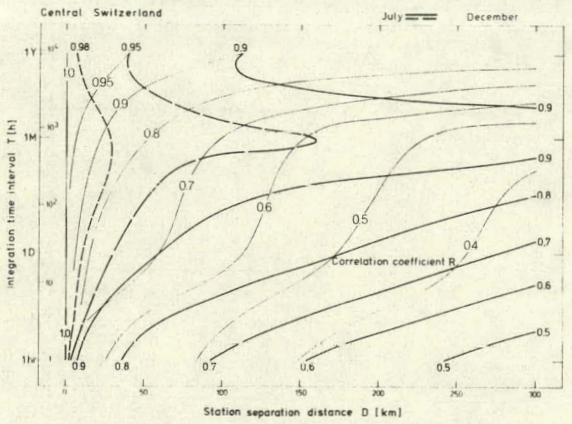


*Figure 8-13 Dependence of the correlation coefficient between sunshine totals of station-pairs on station separation distance and integration time for July (thick curves) and December (thin curves) for central Switzerland. The hourly values were entered taking into account the mean regression lines in Figure 8-12. July coefficients are always higher than the December values, and even higher than that for the totals over the whole year because of the effect of months with greater cloud variability. The curves above the 1-month ordinate gradually approach each other as the corresponding time sectors of the year become larger. For D = O, R ≡ 1 for any integration time.*

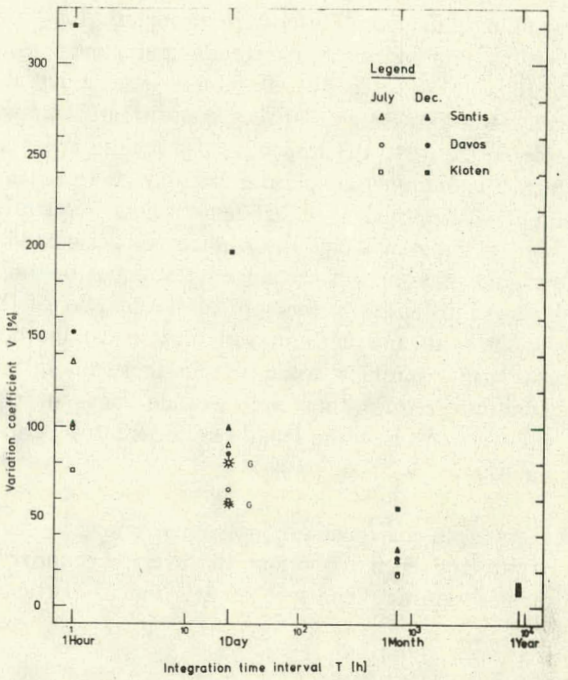


*Figure 8-14 Relationship between the coefficient of variation of sunshine hours and the integration time, found using many years of July and December records at three stations (2500, 1580 and 430 m a.s.l.). The corresponding 1-day coefficients of variation of global radiation computed over all months for Zurich-Kloten and Davos amount to 75% and 58%, respectively.*

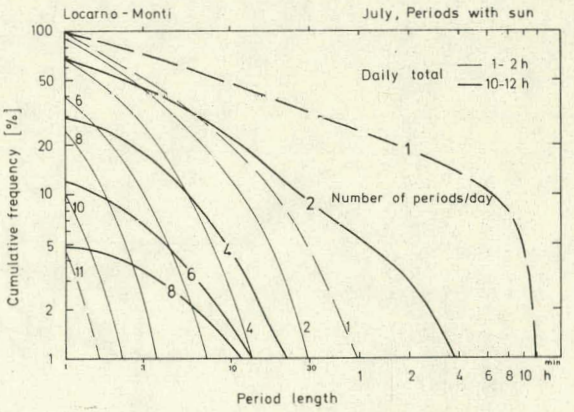


*Figure 8-15 Cumulative frequency distribution of the number of sunny periods per day for July, Locarno-Monti. Thin curves were drawn for days having 1-2 h of daily sunshine; and thick curves, for 10-12 h of daily sunshine.*

In a similar manner Figures 8-16 a-d present in pairs the frequency distributions of periods with and without sun for Zurich-Meteorological Institute. Groups representing very cloudy and almost clear days were selected for December and July; the daily sunshine totals between months are comparable if related to the respective day lengths. With an increasing number of periods per day, the available time is composed of equal lengths less frequently. For an individual day the number of periods with sun and without sun are, of course, equal or differ by ±1. Furthermore, the sum of the lengths of the periods with and without sun must equal the possible daily sunshine total. Within these limitations there can remain, however, a wide range of possibilities as to how the lengths of consecutive periods may vary.

As a further example, one can show for each month and each day-group the average number of periods per day and probability that a particular period length may occur once or more during that day. Three graphs containing this information are presented to compare the effect of daily total sunshine (Figure 8-17), conditions at different stations (Figure 8-18) and the distributions obtained for periods with and without sun (Figure 8-19). Figure 8-17 contains the following groups of periods covering all lengths and their mean total numbers:

| Group No. | Daily Total Sunshine S (h) | Number of Periods Per Day | Proportion of All October Days With Sun (%) |
|---|---|---|---|
| 1 | $S \leq 1$ | 4.2 | 8.5 |
| 2 | $1 < S \leq 2$ | 5.5 | 5.8 |
| 3 | $2 < S \leq 4$ | 8.6 | 10.8 |
| 4 | $4 < S \leq 6$ | 10.2 | 13.9 |
| 5 | $6 < S \leq 8$ | 6.3 | 15.8 |
| 6 | $8 < S \leq 10$ | 2.5 | 41.9 |
| 7 | $S > 10$ | 0.6 | 3.3 |
| | | | 100.0 |

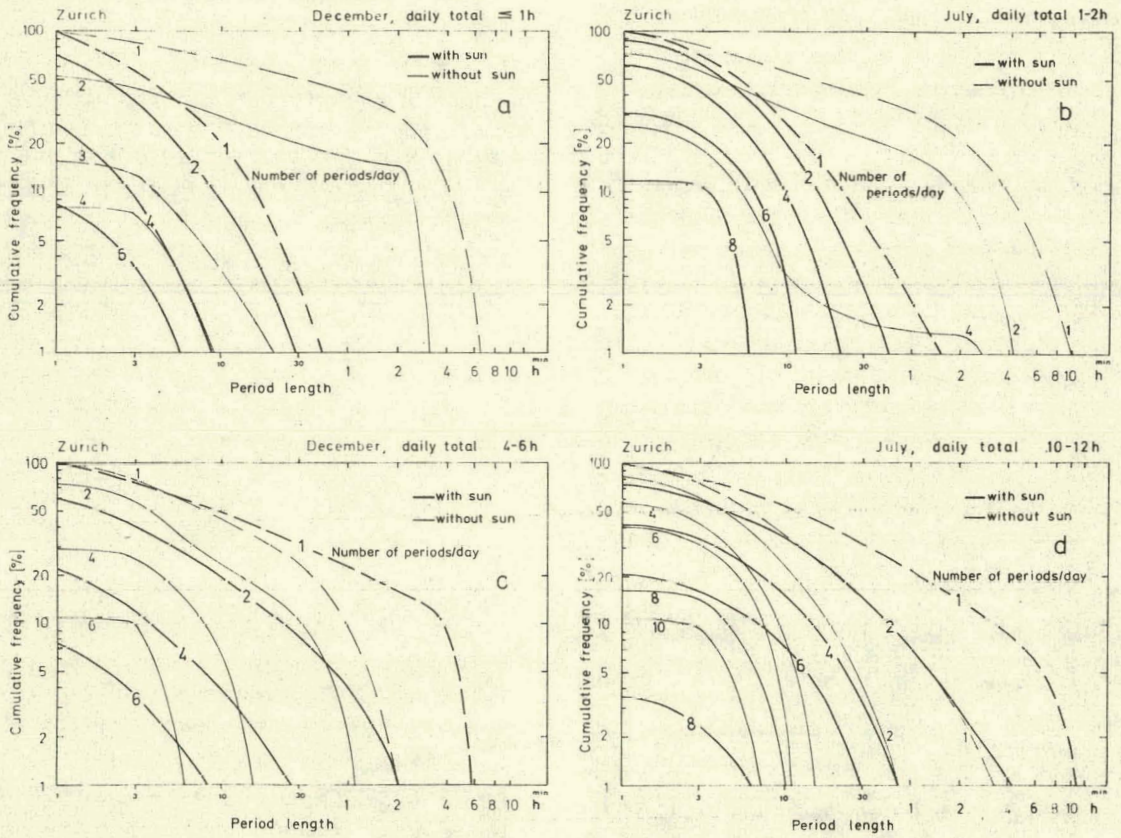


*Figure 8-16 a-d Same as Figure 8-15, except for Zurich-Meteorological Institute for periods with (thick curves) and without (thin curves) sun, considering rather cloudy and more or less clear days as well.*

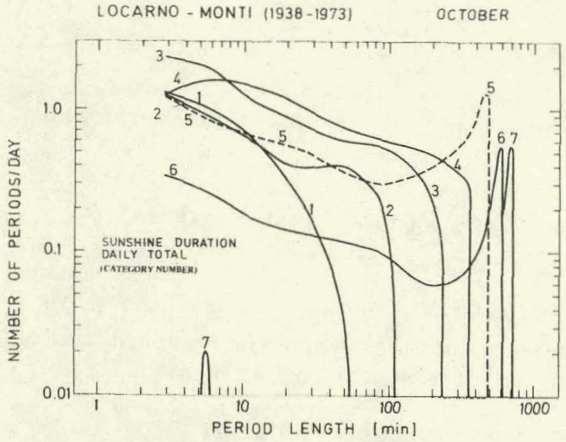


*Figure 8-17 Expected number of periods of any particular length occurring at Locarno-Monti on October days with different daily total sunshine amounts.*

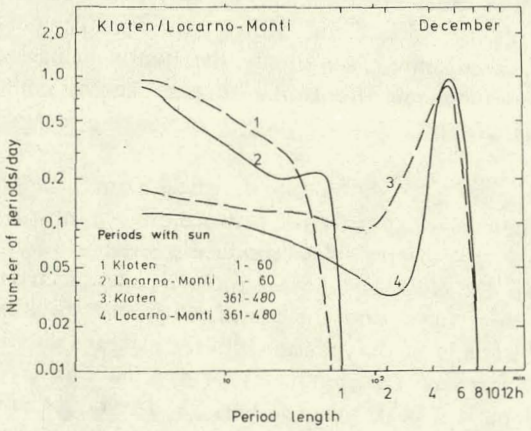


*Figure 8-18 Same as Figure 8-17, except for cloudy and clear December days as compared at two sites.*

As Figure 8-17 shows, the more sunshine available, the more periods may occur; this is valid up to about 5 h of daily sunshine. For more than 5 h the maxima shift more and more towards the longer periods; on very clear days (curve 7) direct solar beam interruptions are very seldom and may last a few minutes at the most. Figure 8-18 demonstrates, that under the same conditions, the tendency towards longer uninterrupted sunny periods is more pronounced for Locarno-Monti than for Zurich-Kloten.

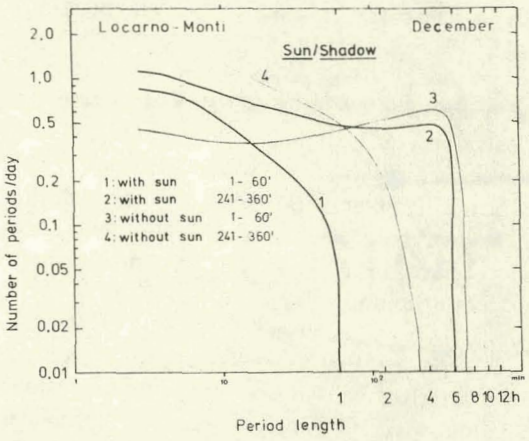


*Figure 8-19 Same as Figure 8-17, except for December, comparing in pairs the complementary frequency distributions for periods with and without sunshine.*

For all curves $S = \int_i n_i L_i dL$

and for Figure 8-19, $S^* \sim S = \int_j n_j L_j dL$

where $n_i$ denotes the number of periods with sun of length $L_i$; $n_j$ denotes the number of periods without sun of length $L_j$; S is the actual and S* the possible hours of sunshine per day.

For all three diagrams curves were constructed by subdividing the L scale according to the powers of 2 (2-4- . . . -1024 min) to obtain classes of constant logarithmic width log dL = 0.3010. Further results have been published in Valko (1976) and extensive tabulations in Valko (1979).

### 8.4.2 Statistical Power Spectra of Radiation Fluxes

Records of wind velocity versus time during storms show a large number of fluctuations at various frequencies. Statistical spectral analysis of such records helped to discover characteristic laws about the form of the spectral density function over different frequency ranges. In this connection studies of Van der Hoven (1957) and Davenport (1961) should be mentioned. The similarity between wind and radiation records for a day with rapidly changing cloudiness is in some respects only apparent.

As already demonstrated by Meinel and Meinel (1976), statistical power spectra of direct radiation for a clear and a cloudy day are markedly different.

*Power* and *Spectra* as used in this section are statistical terms and should not be confused with the power and spectrum of solar radiation. If the reader is not familiar with the significance of this statistical analysis, delay of this section until the references have been reviewed will not distract from other portions of this book.

It was expected, that using several years of record, some characteristic behavior of intensity fluctuations might be detected. For such experiments horizontal surface global and diffuse radiation (G, $G_d$) records from Zurich-Kloten (1963-1972) and Davos (1958-1970) as well as vertical surface (facing east, south, west and north) global radiation records from Locarno-Monti (1961-1971) were at our disposal. The whole material was stored as 5-min-integration-step-values. In this way statistical spectra could be computed using a great number of single daily records for each calendar month, within the frequency range of 6 cycles per h and the daily wave.*

For the computations the Sande-Tukey radix-2 Fast Fourier Transform as described by Bloomfield (1976) was used. This gives statistical spectral estimates for frequencies from $1.3 \cdot 10^{-5}$ to $1.7 \cdot 10^{-3}$ Hz in steps of $1.3 \cdot 10^{-5}$ Hz (period range 10 min to 20 h), altogether n = 128 terms. With the Fourier coefficients

$$A_j = \frac{2}{n}\sum_{t=0}^{n-1} x_t \cos\omega_j t$$

and

$$B_j = \frac{2}{n}\sum_{t=0}^{n-1} x_t \sin\omega_j t$$

the input sequence (5-min values) can be represented as

$$x_t = A_0 + \sum_{0<j<n/2} (A_j \cos\omega_j t + B_j \sin\omega_j t) + (-1)^t A_{n/2}$$

$t = 0, \ldots, n-1$

and the statistical power spectrum can be calculated from each of the Fourier coefficients as

$$P(\omega_j) = (A_j^2 + B_j^2).$$

The procedure was applied to the 5-min sequences of each single day both for $G_d$ and the difference $I_H = G - G_d$. At this stage of the investigations horizontal direct beam intensity $I_H$ was not converted to surfaces at other orientations. For the vertical surface records the global and diffuse components could not be separated, since only the hourly values of the simultaneous horizontal surface records could be used.

Figure 8-20 shows the statistical power spectra of individual days together with the original records—cloudy and overcast days produce a variable spectra, while the clear days have a more regular spectrum. All three days show the characteristic daily peak on the left end of the spectra, with the highest value for the clear day. The cloudy day seems to have different pronounced peaks near periods 23, 14 and 11 min, but no significant peak can be detected if a greater number of individual day spectra are combined to form an average curve (Figure 8-21). This was obtained by averaging the powers for individual days at discrete Fourier frequencies.

Considering the large variety of clouds driven by different wind velocities at different heights, the formation of clouds in a certain part of the sky, their dissolution in another, it is not surprising that using pyranometer records results in no significant spectral peaks. Nevertheless it is useful to quantify the incoming total energy fluctuations. One possible way of doing this is shown in the

*The figures presented in this section are the first results of a study currently being done together with M. A. Korab, Institute for Information Science, Technical University, Zurich. The ultimate object of the study is to examine the dynamic behavior of radiation fluxes over as broad a frequency range as possible.

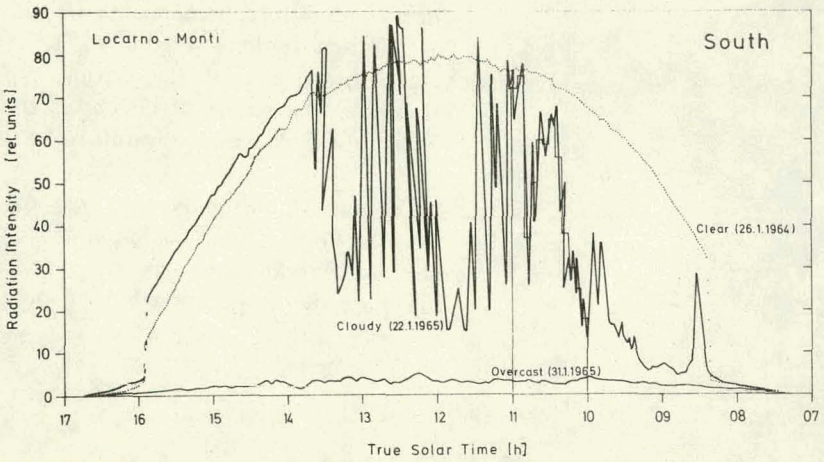


*Figure 8-20 Global radiation recorded on a south-facing vertical surface at Locarno-Monti during three individual January days. 8-20-a, above, is original daily records with the 5-min step approximation between 10-11 h for the cloudy day.*

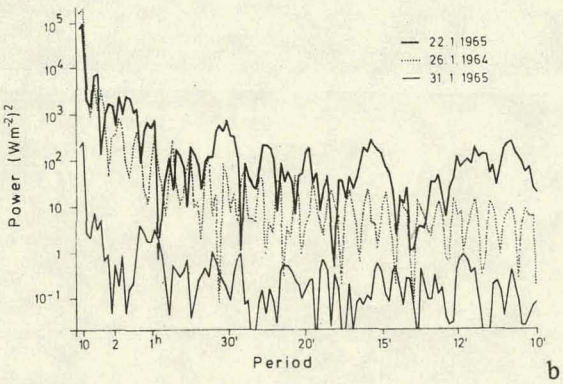


*8-20-b Statistical power spectra*

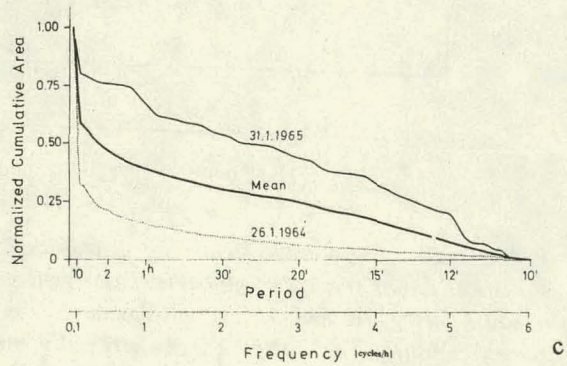


*8-20-c Normalized cumulative area for the clear-day (lower curve) and the overcast day (upper curve) together with the mean over 280 January days.*

lowest graph of Figure 8-20. The ordinate at each frequency gives the relative contribution to the total variation of frequencies above that selected, within the range of Fourier frequencies. The curves were prepared by summing up the products of power times frequency and plotting them against frequency. The areas under these curves were normalized with respect to the total area

$$\frac{\sum_{j}^{128} \omega_j P(\omega_j)\Delta\omega}{\sum_{j=1}^{128} \omega_j P(\omega_j)\Delta\omega}$$

Figures 8-22 and 8-23 illustrate the ranges of possible fluctuation and their corresponding possible relative spectral contributions to the total spectrum. Spectra at the 1, 10, 50, 90 and 99% frequency levels are presented using all available January days for Locarno and Davos, the latter being valid for the direct radiation $G - G_d$. Both diagrams also contain the mean statistical spectra; as may be seen, the distributions are both negatively skewed. The daily peak is well pronounced even for days with thick overcast skies.

Figure 8-24 compares mean statistical power spectra of global radiation for different facing vertical surfaces. If the more or less similar slopes of the east-

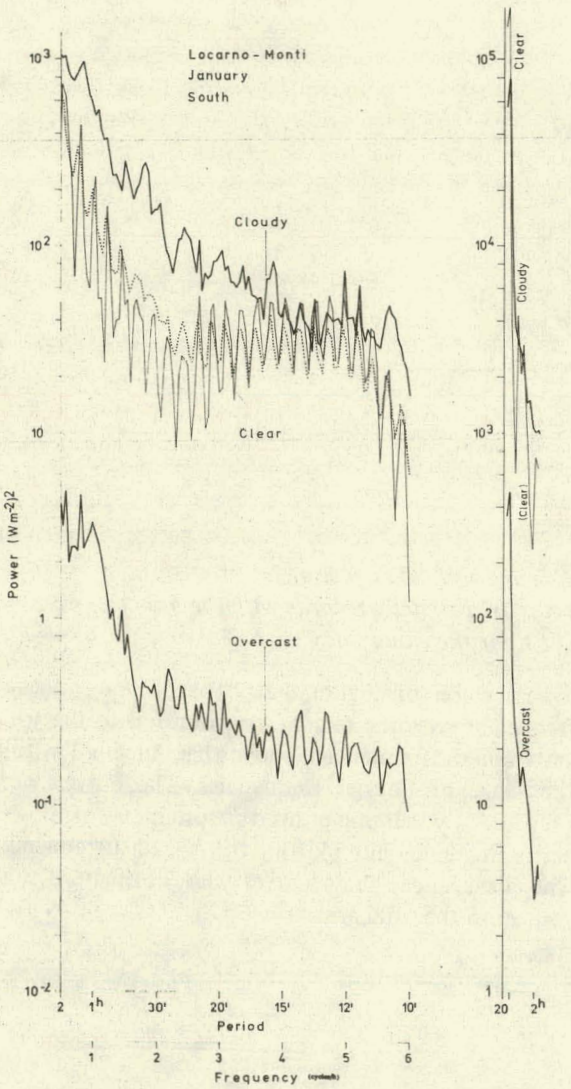


*Figure 8-21 Statistical power spectra of global radiation falling on a south-facing vertical surface on January days at Locarno-Monti.*
*upper curve: average over 22 cloudy days*
*dotted curve: average over all 280 January days*
*thin curve: average over 30 clear days*
*lowest curve: average over 22 overcast days*
*On the right-hand side the 2 to 20 h period range is separately drawn. The ordinate on the right is shifted 2 decades relative to that on the left and is enlarged 5:1 compared with Figure 8-20.*

and west-surface curves had occurred for the summer months, one could conclude that this is due to enhanced cloud activity in the afternoon. However, this could not be confirmed.

The last group of diagrams compare horizontal surface spectra for months (Figure 8-25), for the direct and diffuse components (Figure 8-26) and for different stations (Figure 8-27). As in the previous figures, besides the obvious differences in magnitude, the slopes of all curves show a similar characteristic decrease towards higher frequencies.

The results exemplify the type of information which could be used as input for modeling the dynamic behavior of a solar energy collector system. This type of computation can be done reasonably

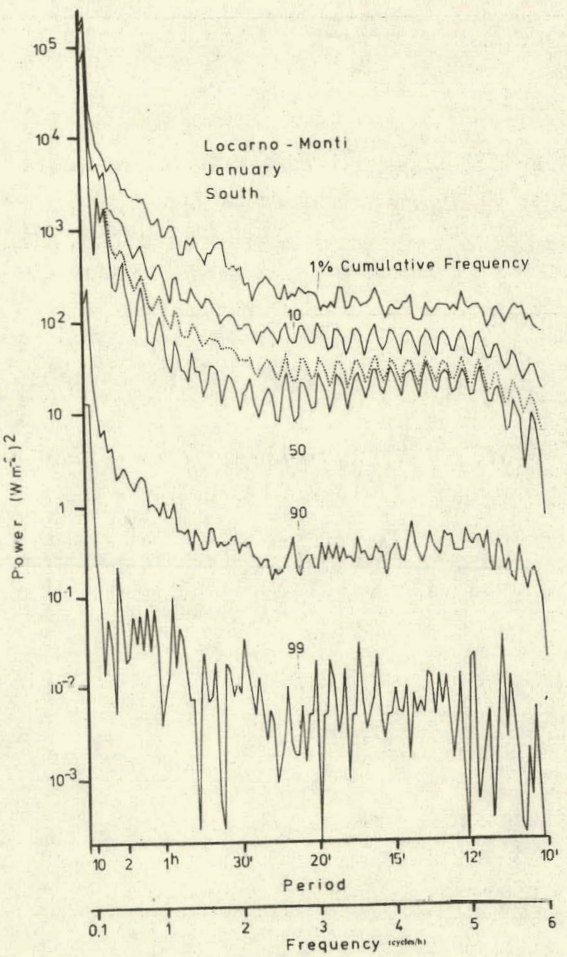


*Figure 8-22 Cumulative frequency distribution of statistical power spectra of global radiation falling on a south-facing vertical surface on January days at Locarno-Monti. The dotted curve marks the mean statistical spectrum. The ordinate is enlarged 2:1 compared with Figure 8-20.*

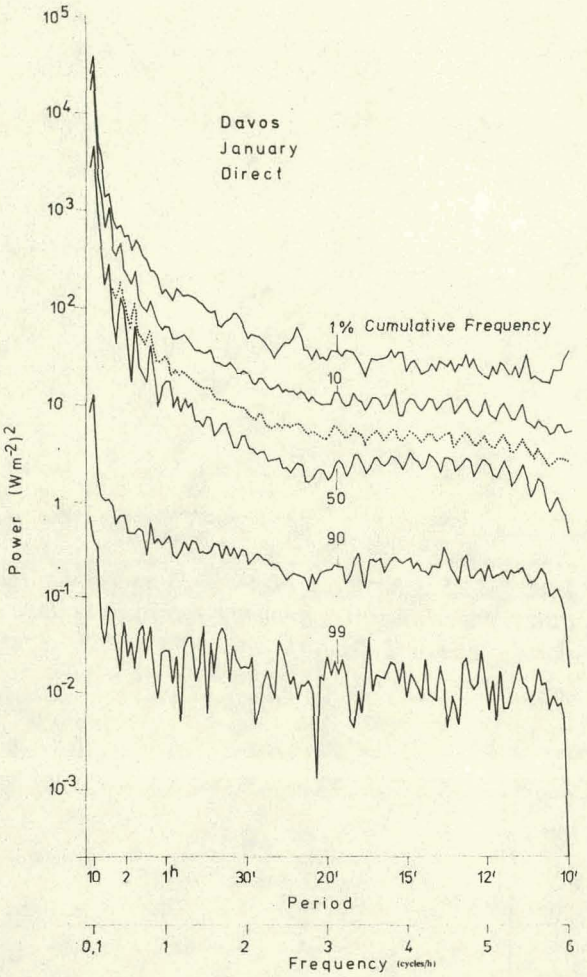


*Figure 8-23 Same as Figure 8-22 except for direct radiation recorded on a horizontal surface during 390 January days at Davos.*

only when a suitable system is chosen. To achieve meaningful and realistic results, such numerical experiments can only be made in collaboration with solar technologists.

## 8.5 Angular Distribution of Diffuse Radiation

The physical background to this problem and its significance for solar energy applications, as well as computation methods using simplified models have been outlined in Chapters 3 and 4, Sections 3.5.2, 3.6 and 4.5. As may be seen from these discussions, direct solar irradiance of a surface having arbitrary exposure may be calculated by simple trigonometry, whereas the diffuse fluxes must be computed by more difficult means. The angular distributions of the sky and the ground-reflected components should be known; both of these depend on a number of astronomical, atmospheric and site-specific parameters.

### 8.5.1 Existing Measured Data

Measurements of the radiance distribution as well as integrated radiance data from tilted surface pyranometers (Eq. (9) in Section 3.5.2) show that compu-

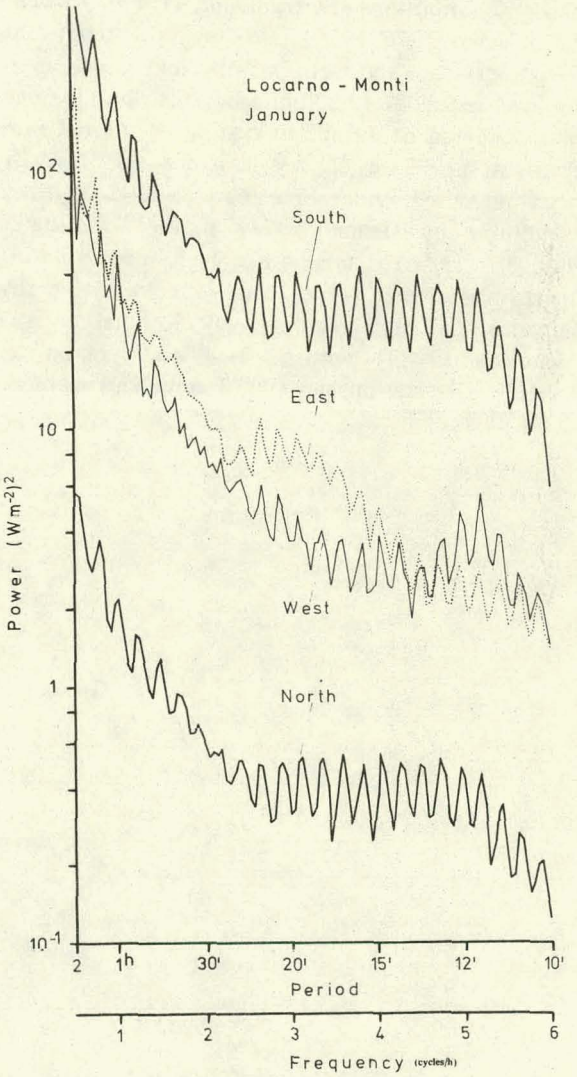


*Figure 8-24 Average statistical power spectra of global radiation falling onto differently orientated vertical surfaces on January days at Locarno-Monti. Each curve involves 280 individual days of record.*

tational models do not give satisfactory results. Moreover, such measurements are sparse and the parameters influencing them (i.e., turbidity, ground albedo, cloud characteristics) are often not measured simultaneously. Therefore an urgent need exists to establish a suitable data base, and to derive computational rules having general validity and applicability by detecting empirical relationships.

#### 8.5.1.1 Radiance Measurements

Since the early measurements of spectral sky luminance by Dorno (1919) several measured luminance distributions (Krochmann, 1973; Liebelt, 1978; Valko, 1976, 1979) have shown that significant deviations from the isotropic case may occur, even for overcast skies (the luminance distribution may be considered as an approximation to the radiance distribution). Spectral sky radiance has recently been measured under both clear and cloudy sky conditions by Dehne (1974) at the wavelengths 409, 561 and 620 nm with a high speed rotating spectrophotometer. The total spectrum of sky radiance has been measured by Kondratyev and Manolova (1959) with a modified pyranometer of 10° full view angle (0.0239 steradian) scanning

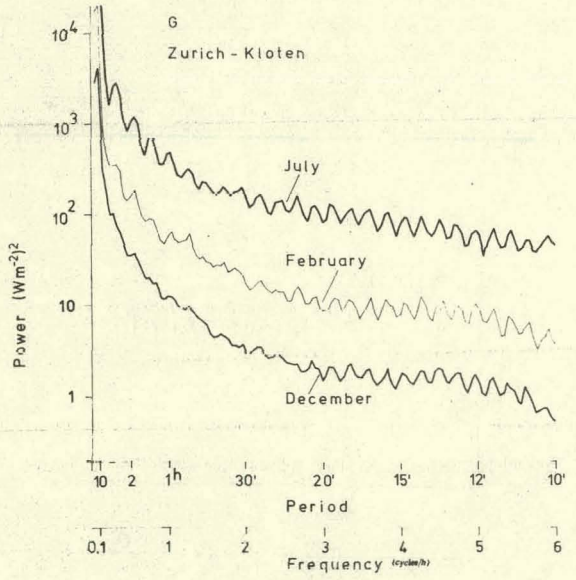


*Figure 8-25 Same as Figure 8-24 except global radiation recorded on a horizontal surface at Zurich-Kloten during December (273 days), February (232 days) and July (300 days).*

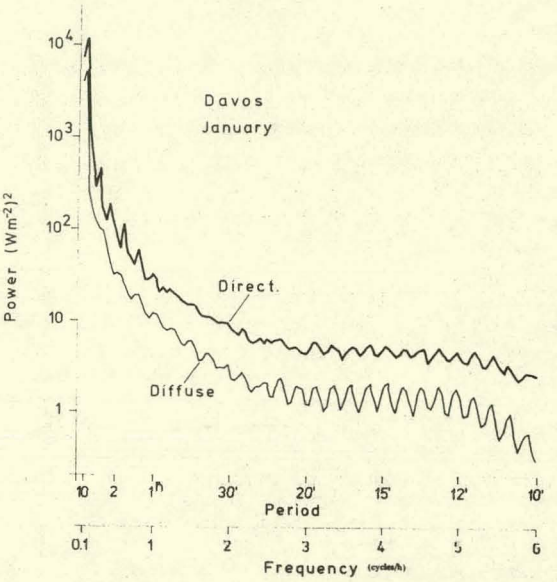


*Figure 8-26 Same as Figure 8-25 except for the direct and diffuse components recorded at Davos during January (390 days).*

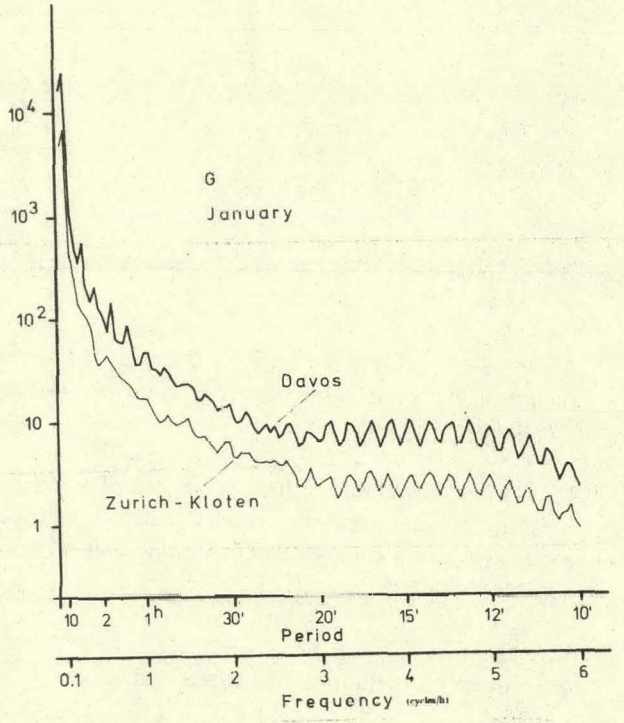


*Figure 8-27 Same as Figure 8-25 except for January; the Davos curve involves 390 days of record, compared to 249 for Zurich-Kloten.*

the sky in 37 directions. To make similar measurements Steven (1977) as well as McArthur and Hay (1978) used a Linke-Feussner actinometer with about the same view angle (10°12′): Steven measured at 34 points of the sky in 40 min; McArthur and Hay at 21 points in 14 min. Earlier experiments with an automatic sky scanning radiometer using a Moll-type thermopile (also having 10°12′ full aperture) have been made by Van Deventer and Joubert (1966) who scanned the sky at 120 points over a 30-min period. All these results illustrate the dependence of the distribution patterns on different atmospheric conditions, but are not (as yet) numerous enough to allow generalizations to be made.

Densitometric evaluations of all-sky (fish-eye) photographs, as demonstrated by McArthur and Hay (1978, 1979), may be a promising technique. However, many problems concerning film quality and film development remain to be solved before the results can be calibrated and compared with each other.

Measurements of the angular distribution of the reflected fluxes are not as numerous as those of sky radiance. Kondratyev and Manolova (1959) carried out such measurements with the modified pyranometer mentioned above. By computing the diffuse irradiance of tilted surfaces, once by using the measured distributions and once by assuming isotropic reflection, they achieved good agreement in all cases except for steep surfaces. Considering the great variability of ground types, the possibilities for making generalizations are limited.

#### 8.5.1.2 Measurements of Irradiation of Vertical and Inclined Surfaces

Besides solar energy utilization, pyranometer data for inclined and vertical surfaces are required for conventional heating and air conditioning of buildings and for daylight design. Global irradiation measurements were made and analyzed in a more general climatological manner during previous years by Ambrosetti and Thams (1953), Shulze (1954), Gräfe (1956), Funk (1965) and Schramm and Thams (1967a, b); a survey of the results of Russian authors is given by Kondratyev (1969) Chapter 8-4 and Kondratyev and Fedorova (1977). Analyses of the dependence of instantaneous (irradiance) values on angular parameters and (in part) on turbidity were made by Parmelee (1954), Volz (1958), Threlkeld (1963), Heywood (1966) and Van Deventer and Dold (1966). The results of Kondratyev and Manolova (1959) are also reported by Kondratyev (1969) and Kondratyev and Fedorova (1977). Among these, studies of the diffuse irradiance alone were made by Parmlee for vertical surfaces under clear sky conditions; the dependence on atmospheric turbidity in particular was investigated. Although Kondratyev and Manolova, Threlkeld, and Van Deventer and Dold did not analyze the influence of turbidity, they could separate the sky and the ground-reflected components of the total diffuse flux and analyze their dependence on solar height and surface exposure.

The results indicate that further efforts would be required to parameterize and generalize the data on a broad basis. Therefore it is worth noting that at several stations recording horizontal global and diffuse radiation or direct radiation at normal incidence, measurements with pyranometers with tilted exposures have also been made, especially in recent years. Though not complete, Tables 8-2a and 8-2b summarize these activities.

The survey above is based on reports of Josefsson (1978), Dogniaux (1978), Hay (1978b), Collingbourne (1975) and an Austrian Solar and Space Agency study group (1977). If not stated otherwise, the measured parameter is global radiation. Pyranometer orientation has been noted by letters, with the figures denoting the inclination angle to the horizontal. Where no further specifications were available, the instrument exposures were subscripted with "v" (vertical) or "i" (inclined).

### 8.5.2 Parameterization of Vertical Surface Irradiance for Clear Skies

Table 8-2a shows that Locarno-Monti has a suitable data base for a more detailed investigation. At this site, among other radiation quantities, the direct irradiance at normal incidence was measured using a pyrheliometer with broad-band Schott filters. Measurements were taken at hourly intervals on clear days; otherwise whenever the sun's disc was free of clouds. For the analysis, 1700 sets of simultaneous clear sky global irradiances $G_v$, associated with the time of the pyrheliometer readings, were selected

## Table 8-2a

## Survey on Available Records Measured with Pyranometers Having Vertical and Inclined Positions at Stations Currently Operating or Which Have Operated Recently

| Country | Station | Instrument Exposure | Period of Record |
|---|---|---|---|
| **Austria** | Sonnblick | S60 | |
| | Innsbruck | S30, S60 | 11.75 - 04.76 |
| **Belgium** | Mons | | |
| **Canada** | Toronto | S30, S60, S90 | 10.76 - |
| | Vancouver | S30, S60, S90 | 01.77 - |
| **Denmark** | Karup | V, incl. | 06.78 - |
| | Lyngby | V | 05.77 - 08.78 |
| **France** | Trappes | N90 | 01.75 - 02.75 |
| | | S50 | 01.73 - 12.73 |
| | | SE50 | 15.03.74 - 09.74 |
| | Carpentras | S90 | 11.07.74 - 07.75 |
| | | S44 | 01.73 - 12.73 |
| | | SW44 | 04.74 - 05.74 |
| | | E90, S90, W90, N90, (S90, N90)* | |
| | | S45, S90 (diff.) | 12.78 - |
| | Odeillo | S90 | 04.71 - 06.75 |
| | | S90 (diff.) | 05.75 - 06.78 |
| | | S42 | 05.75 - 12.78 |
| **F. R. Germany** | Hamburg | E90, S90, W90, N90, S45 | 01.52 - 12.54 |
| | Aachen | S48 | 9.75 - 12.78 |
| | Jülich | S30, S60, S90 | 01.09.78 - |
| | Darmstadt | S20, S40, S60 | 01.11.79 - |
| | Holzkirchen | E90, S90, W90, N90 | 01.73 - 12.74 |
| **Ireland** | Valentia | S90 | 03.76 - |
| **Sweden** | Norrköping | S60 (global) + S60 (diff.) | 07.78 - |
| **Switzerland** | Locarno-Monti | E90, S90, W90, N90 | 05.61 - 11.71 |
| | | S30, S60 | 08.60 - 10.62 |
| | | E30, W30 | 10.62 - 12.66 |
| | Geneva | S45, E90, S90, W90, N90 | 06.79 - |
| **United Kingdom** | Easthampstead | E90, S90, W90, N90 incl. | 01.67 - |
| | Bracknell | E90, S90, W90, N90 (screened from ground refl. rad.) | 66 - 73 |
| | Cardiff | N45,90; NE45,90; E45,90; SE45,90; S45,90; SW45,90; W45,90; NW45,90 | 05.78 - |

*Two pyranometers, facing South and North respectively, are screened from the sky, this measuring the ground reflected radiation separately.

## Table 8-2b

## Survey on Available Records Measured with Pyranometers Having Vertical and Inclined Positions at Stations Currently Operating or Which Have Operated Recently - U. S. A. Stations Only

| Country | Station | Instrument Exposure | Period of Record |
|---|---|---|---|
| United States of America | Alabama | | |
| | Huntsville (UAH) | S35 | 06.79 - |
| | Alaska | | |
| | Barrow (Smithsonian Radiation Laboratory) | Various angles | 68 - |
| | Fairbanks (U. of AK) | S65, S90 | 12.77 - |
| | Arizona | | |
| | Mesa (GM Proving Grounds) | S45 | 66 - |
| | Phoenix (Desert Sunshine Exposure) | S45 | 69 - |
| | Tempe (AZ State U.) | S45 | 01.77 - |
| | Yuma (Yuma Proving Ground, USA) | S45 | 75 - |
| | Delaware | | |
| | Newark (U. of DE) | S45 | 01.74 - |
| | Mississippi | | |
| | Canton (Lockheed) | Not Indicated | 03.78 - |
| | New Mexico | | |
| | Los Alamos (Solar Energy Group) | | 74 - |
| | Oregon | | |
| | Banks (PGE) | | 01.76 - |
| | Eugene | | 04.74 - |
| | (U. of OR) | | 02.77 - |
| | Gladstone (PGE) | | 02.76 - |
| | Portland (PPL) | | 76 - |
| | Salem (PGE) | | 11.77 - |
| | Tigard (PPL) | | 75 - |
| | Texas | | |
| | College Station (TX A&M U.) | | 03.01.73 - 12.07.73 |
| | San Antonio (Trinity U.) | | 04.78 - |
| | Wisconsin | | |
| | Madison (U. of WI.) | | 03.77 - |
| Meteorological Research & Traning Sites in the U. S. A. | | | |
| | Alaska | | |
| | Fairbanks (U. of AK) | Various angles | 01.79 - |
| | California | | |
| | Davis | Various angles | 01.79 - |
| | Georgia | | |
| | Atlanta | Various angles | 01.79 - |
| | Hawaii | | |
| | Manoa | Various angles | 01.79 - |
| | Michigan | | |
| | Ann Arbor | Various angles | 01.79 - |
| | New York | | |
| | Albany | Various angles | 01.79 - |
| | Oregon | | |
| | Corvalis | Various angles | 01.79 - |
| | Texas | | |
| | San Antonio | Various angles | 01.79 - |

from the period 1961-1966. By computing $G_{d,v} = G_v - I_v$ for the east-, west-, south- and north-facing vertical surfaces, an empirical solution of the relationship $G_{d,v} = f(h, a, B)$ could be found (Valko, 1967, 1970b, 1970c) (a denotes the angle between the surface-normal and the azimuth of the sun). The absolute values are tabulated in *Meteoplan No. 1* (Valko, 1975) and Figure 8-28 shows the ratio $G_{d,v}/G_d$ for the constant turbidity levels B = 0.050, 0.100 and 0.200. $G_{d,v}$ includes the reflected component. The albedo of the site (concrete roof) is assumed to be 0.2.

---

Editor's Note: In this chapter the following symbols are used extensively:

h - denotes the elevation angle of the sun and is equal to 90 - Θ, the solar zenith angle.

a - denotes the unique angle between the sun (γ) and the azimuth orientation of an inclined or vertical surface (ψ).

It may be seen that

- the distributions are not isotropic, especially for smaller solar elevation angles;
- solar elevation has opposite effects for surfaces facing towards and away from the sun and the azimuth at which the inversion takes place increases with increasing turbidity as shown in points a, b, and c in Figure 8-28.
- for constant solar elevation the slopes of the curves depend on turbidity. For a better interpretation of Figure 8-28, the corresponding absolute values of $G_d$ are summarized in Table 8-3.

From these results (Figure 8-28, Table 8-3) it may be concluded that

- the dependence on solar elevation is most pronounced for clean air (low turbidity), due to the small and almost evenly distributed radiance over the whole sky, as well as the high ground-reflected component;

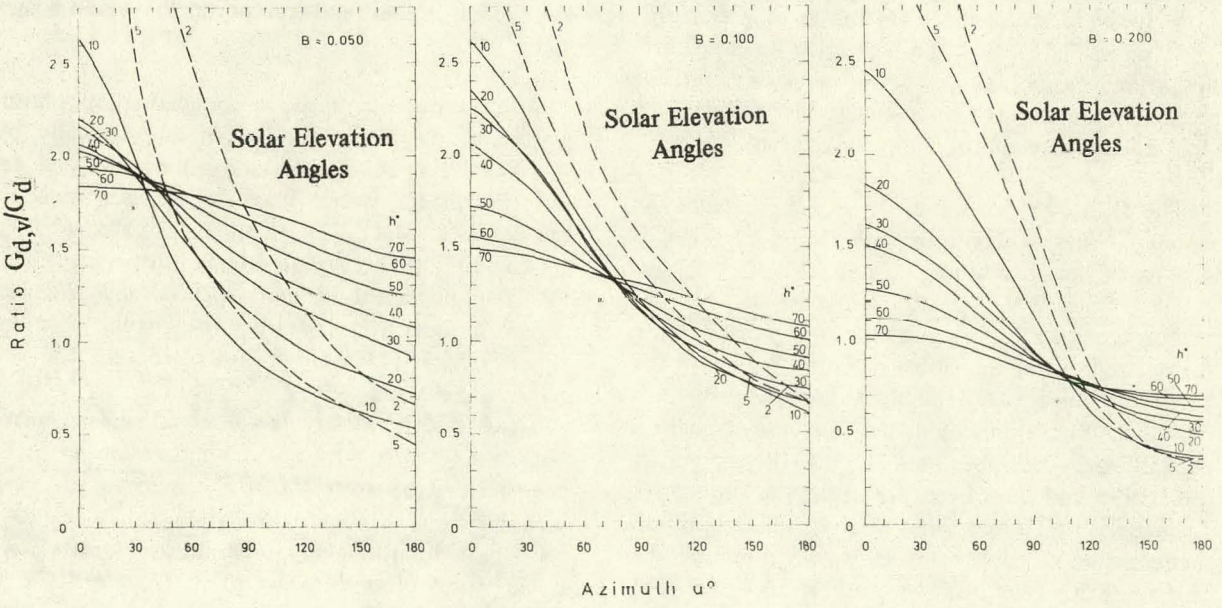


*Figure 8-28 Ratio $G_{d,v}/G_d$ of diffuse irradiance on vertical surfaces to that on a horizontal surface as a function of the angle between the surface-normal and the azimuth of the sun, a, and solar elevation, h, for selected values of the turbidity coefficient B.*

Table 8-3

Variation of the Diffuse Irradiance of a Horizontal Surface With Solar Elevation h ($90^\circ$ - Solar Zenith Angle, $\Theta$) and Atmospheric Turbidity B for Clear Sky Conditions (Valko, 1975). Values are in W $m^{-2}$.

| B \ h | 2 | 5 | 10 | 20 | 30 | 40 | 50 | 60 | 70 |
|---|---|---|---|---|---|---|---|---|---|
| 0.050 | 7 | 21 | 37 | 55 | 65 | 74 | 79 | 84 | 87 |
| 0.100 | 10 | 28 | 48 | 73 | 94 | 109 | 119 | 124 | 128 |
| 0.200 | 22 | 47 | 78 | 120 | 151 | 173 | 191 | 207 | 220 |

- for higher turbidities the circumsolar sky radiates much more than the sky at greater angular distances away from the sun; therefore the dependence on the angle of incidence, i, between the direct beam and the surface normal is markedly strong;

- for the same solar elevation the ratio ($G_{d,v}/G_d$) decreases with increasing turbidity, since the diffuse irradiance of the horizontal surface increases more rapidly with turbidity than that of the vertical surface;

- for very strong haze (in the investigation the values $0.3 \leq B \leq 0.6$ were also involved) differences between reflected and sky diffuse components are suppressed and angular influences are almost completely absent.

The diffuse proportion of the global irradiance for cloudless skies is significant and may be as high as 40% for higher turbidities.

For the sake of comparison, in Figure 8-29 the daily variations of the global radiation falling on the horizontal surface (H) and the four vertical surfaces (N, E, S, W) are presented. The curves are based on all July and December data for the 10-year period 1961-1970 and have been drawn for the cumulative frequencies 1, 10 and 50%, with M being the arithmetic mean in each case. It is worth noting the characteristic features, i.e., differences between summer and winter, between surface orientations, the dependence on time of day at the different frequency levels and the skewness of the distributions (50% and M curves being separated). The 1% curves are drawn for the period from sunrise to sunset, whereas the others are for shorter periods of the day.

These results, which are summarized in *Metroplan No. 1*, have either been used or verified through comparison with other measured data or models by Tonne (1967), Puskas (1973), Page (1975), Kondratyev et al (1978), Steven and Unsworth (1979b), Rodgers et al (1979) as well as by Steven and Unsworth (1979a). They are also confirmed by recent measurements discussed in the following section.

### 8.5.3 Parameterization of Irradiance for an Inclined Surface: The General Case

#### 8.5.3.1 Data Acquisition

As experience has shown, only systematic, precise measurements may lead to a more general solution. For this purpose a mobile system equipped with different radiation measuring devices was developed and put into operation during 1974. The photographs in Figure 8-30 show the main components of the instrumentation, which are controlled by a DEC PDP-8 computer on board a caravan, which houses (and transports) the whole equipment.

The measurements are accompanied by photographs of the sky dome, taken automatically by a fish-eye camera. Results and a more detailed description of the system have already been reported by Bener et al (1973); Heimo and Valko (1977); Valko (1977). The system will be further expanded by instruments for scanning spectral sky radiance, and two units for measuring the angular distribution of reflected radiation from the ground.

Using this mobile unit, several measurement trips were made during different seasons at Swiss sites located up to 1700 m above mean sea level. The durations of these trips varied from a few days to over a month. Many other measurements were made during the summers of 1977 and 1979 at Carpentras, Southern France. Less successful, because of bad weather, was at a location in Hamburg during 1978. Until now several thousand simultaneous sets of direct solar irradiance and inclined

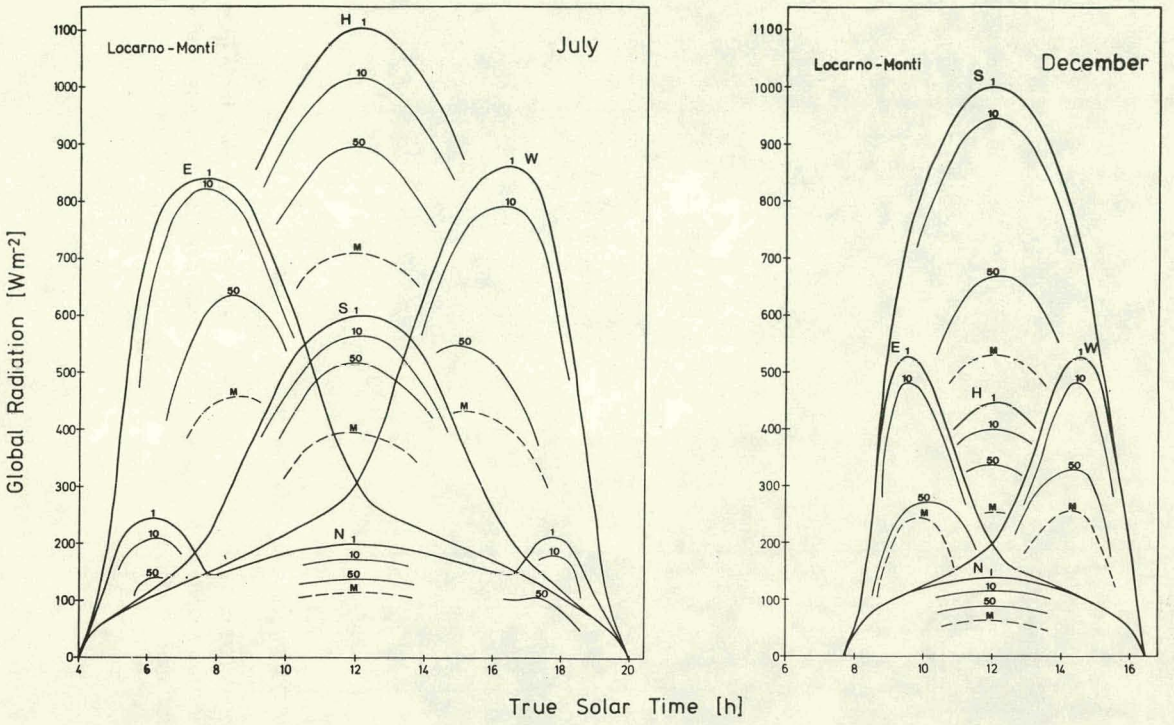


*Figure 8-29 Daily variations of the global radiation falling on vertical and horizontal surfaces during July and December at Locarno-Monti. Curves were drawn for different percentages of the corresponding cumulative frequency distributions.*

surface pyranometer measurements (about half a million individually measured values) have been compiled under various atmospheric and site-specific conditions. Each set of data covers a period of 6 min. In some cases four such data sets, measured one after the other without interruption, were averaged to give one representative value.

### 8.5.3.2 Clear Sky Conditions

Figure 8-31 gives an example for a set of such measurements, composed of four parts. The 77 pyranometer reading and the corresponding 121 measurements made by the four pyroelectric detectors are analyzed in polar diagrams. The contours were drawn by eye in steps of 100 W $m^{-2}$ for the global and 50 W $m^{-2}$ for the diffuse irradiance distributions. The diffuse irradiances (top right) have been computed by subtracting the direct solar component from the corresponding global value. The position of the sun is marked by ☼ at the angular height of 45° and the turbidity coefficient takes the rather high value of 0.280; the direct irradiance at normal incidence is only 537 W $m^{-2}$ over the entire spectrum.

For different surface exposures the global irradiances may differ by a factor of 10, the diffuse irradiances by more than 4, due to the strong anisotropy of sky radiance. Since the circumsolar radiance may drop by $10^{-3}$-$10^{-4}$ at an angular distance of 1-2° from the edge of the solar disc (see Chapter 7), the variations of sky radiance, as measured by instruments having a full view angle of 5°, are only meaningful if the immediate vicinity of the sun is excluded. Sky radiance takes its minimum value at about 90° angular distance away from the sun as demonstrated by the pyroelectric scanning values and the photograph. The latter clearly shows the brightening of the horizon opposite the sun.

For clean air the absolute values as well as the pattern of the diffuse irradiance distribution are rather different, as demonstrated in Figure 8-32. The solar elevation of 47° is comparable with the

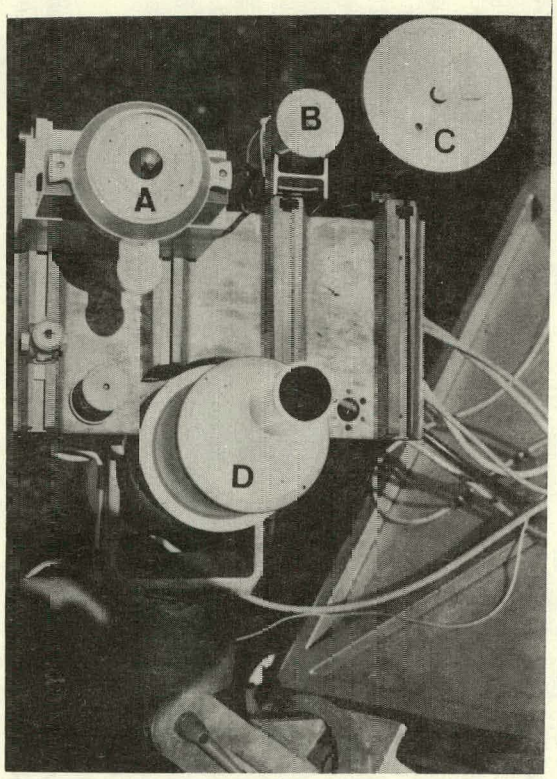


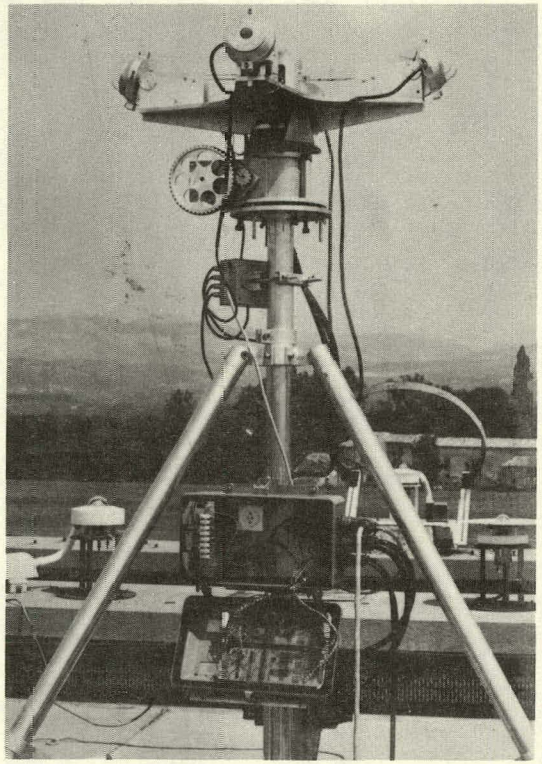

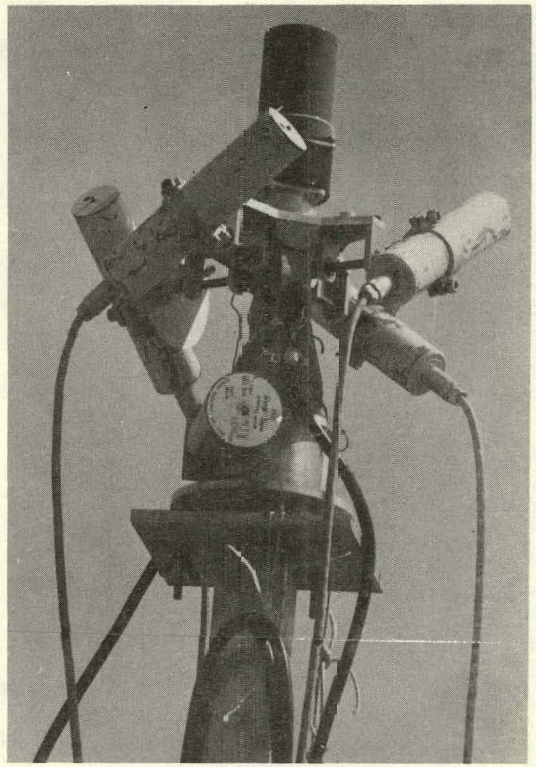

*Figure 8-30 Main components of the mobile system for solar radiation measurements*

*8-30a On the automobile roof four instruments are mounted on an automatic sun-tracker: pyranometer (A), photovoltaic detector (B), absolute radiometer (C) with broad band Schott-Filters GG1, RG2 and RG8 and spectroradiometer (D) measuring at 16 different wavelengths.*

*8-30b Four pyranometers are driven by step motors and measure radiation at 77 different tilt angles and directions in about 6 min.*

*8-30c Four photovoltaic detectors scan the sky (full view angle of 5° ~ 0.00598 sr) at 121 points in about 2 min.*

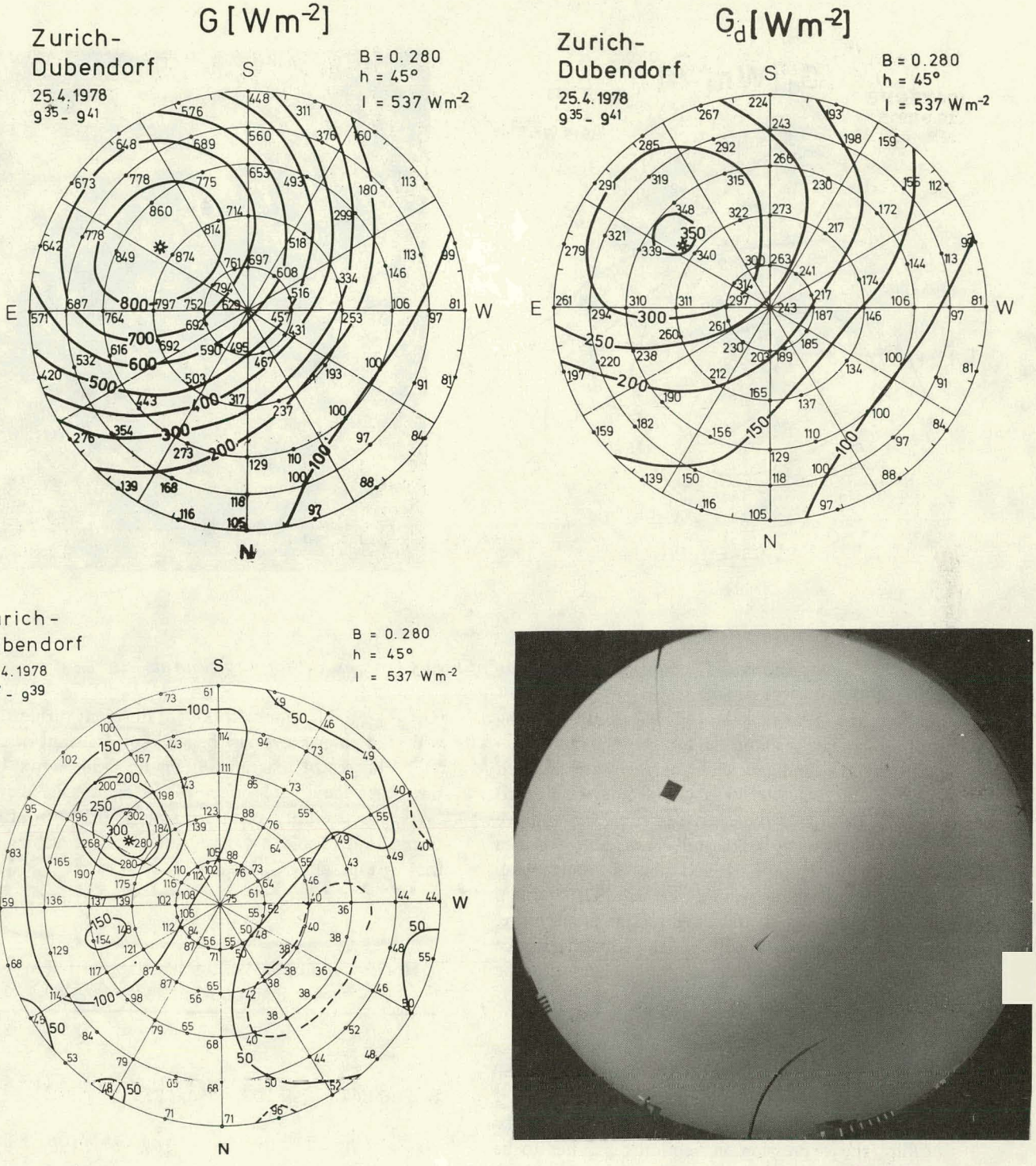


*Figure 8-31 Simultaneous angular distributions of: the global (top left) and diffuse (top right) irradiances for differently orientated and tilted surfaces; the sky radiance in relative units (bottom left); and visualized by the correspoding fish-eye picture (bottom right) – clear sky conditions, strong turbidity.*

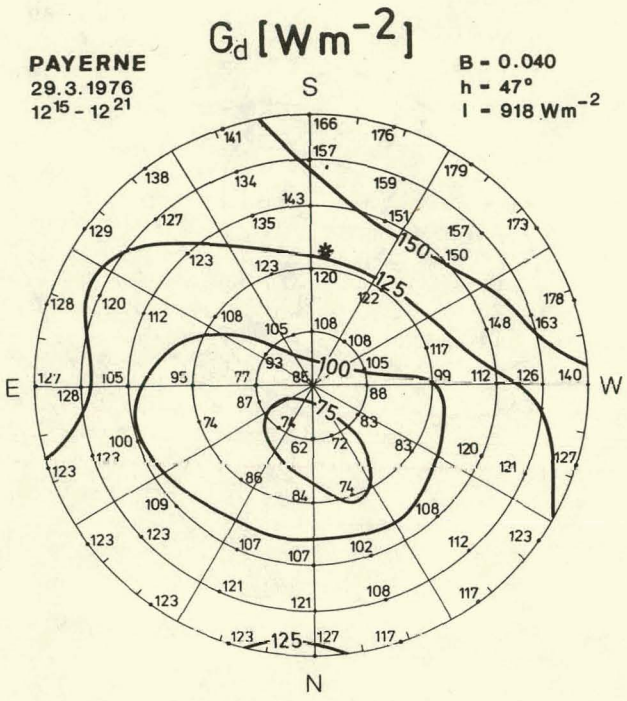


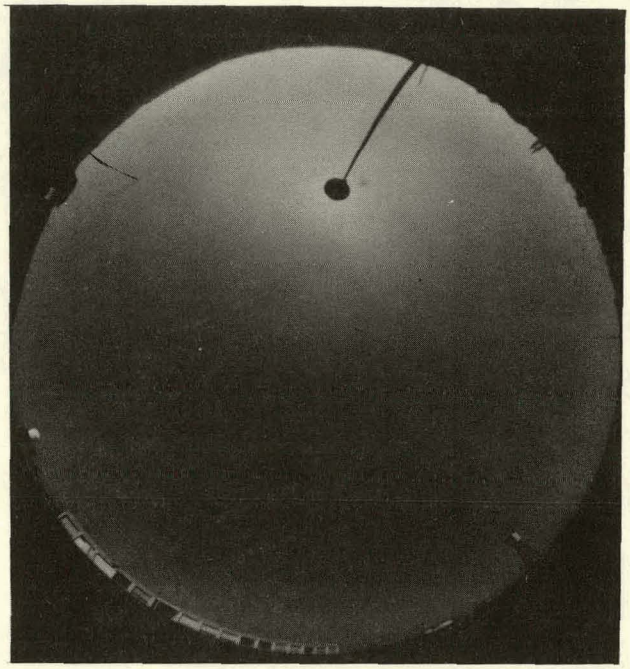

*Figure 8-32 Same as the right half of Figure 8-31, except for very clean air*

value for the former case (45°), turbidities being therefore largely responsible for the marked differences. Payerne and Zurich-Dubendorf are situated at about the same height above sea level (400 m) and both have a fairly open horizon. The fish-eye photograph shows a larger and darker blue sky area than that of Figure 8-31 and only a rather small aureole of brightness around the sun. The horizon opposite the sun is, in this case, clearer than before, due to high ground reflection. The global irradiance for the optimum tilt normal to the sun may be immediately estimated at $I + G_d \simeq 1040$ W m$^{-2}$.

The two examples were selected from numerous cases covering the turbidity range $0.037 \leq B \leq 0.360$ as well as the solar elevation angle interval $5° \leq h \leq 70°$. To summarize the results in a parametric relationship, the expression in Section 8.5.2 has to be expanded by introducing also the tilt angle, s, i.e., for the same site or different sites having the same albedo and height above mean sea level:

$$G_{d,i} = f(h, a, s, B).$$

Plotting again the ratio $G_{d,i}/G_d$, Figure 8-33 presents ($G_{d,i}/G_d$, a, s) - intersections for different turbidities with the solar elevation being kept constant at 35 ±1°. The set of diagrams in Figure 8-34 shows, on the other hand, the effect of different solar elevations, the turbidity coefficient being 0.100 ± 0.010 throughout. Table 8-4 gives the absolute values of the corresponding $G_d$ data.

Table 8-4

Horizontal Surface Diffuse Irradiances in W m$^{-2}$ for Figures 8-33 and 8-34

| | | | | |
|---|---|---|---|---|
| | h = 35° | | | |
| B | 0.047 | 0.100 | 0.185 | 0.270 |
| $G_d$ | 70 | 109 | 162 | 198 |
| | B = 0.100 | | | |
| h | 15 | 35 | 60 | |
| $G_d$ | 62 | 109 | 115 | |

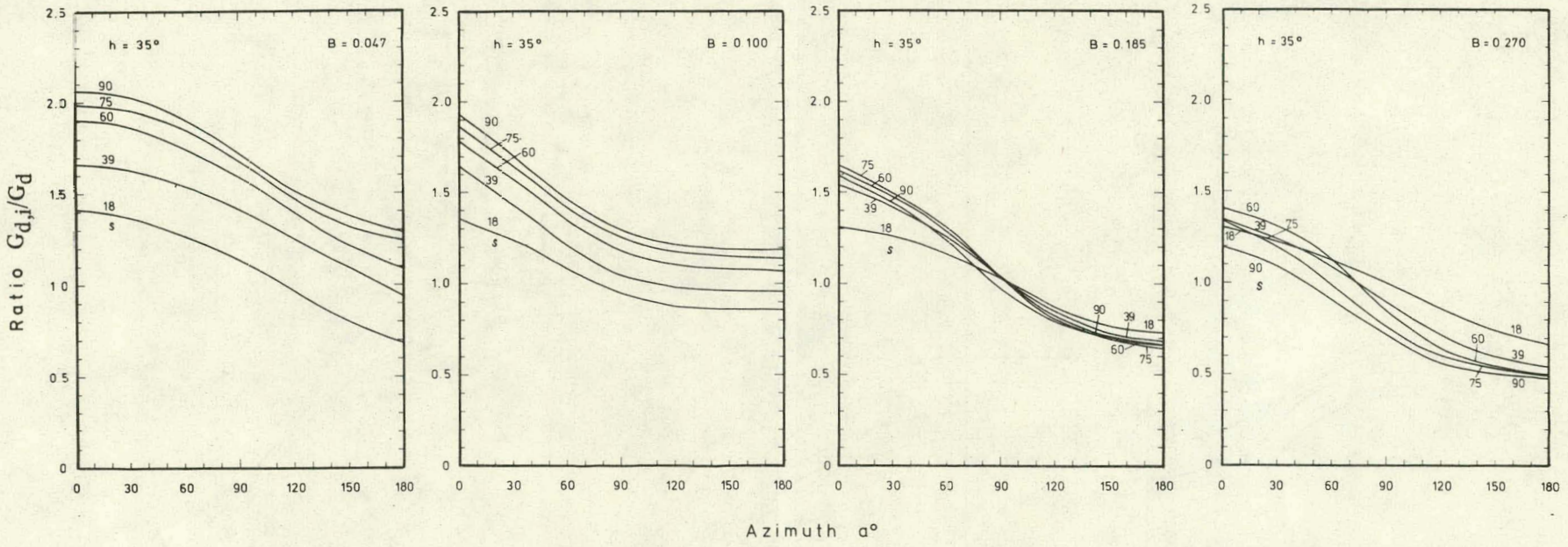


*Figure 8-33 Ratio $G_{d,i}/G_d$ of diffuse irradiance of inclined surfaces to that of the horizontal surface as a function of the angle between the orientation of the inclined surface and the azimuth of the sun, a, inclination angle, s, and turbidity coefficient, B. A constant solar elevation angle (90 - Θ) (35°) was used throughout.*

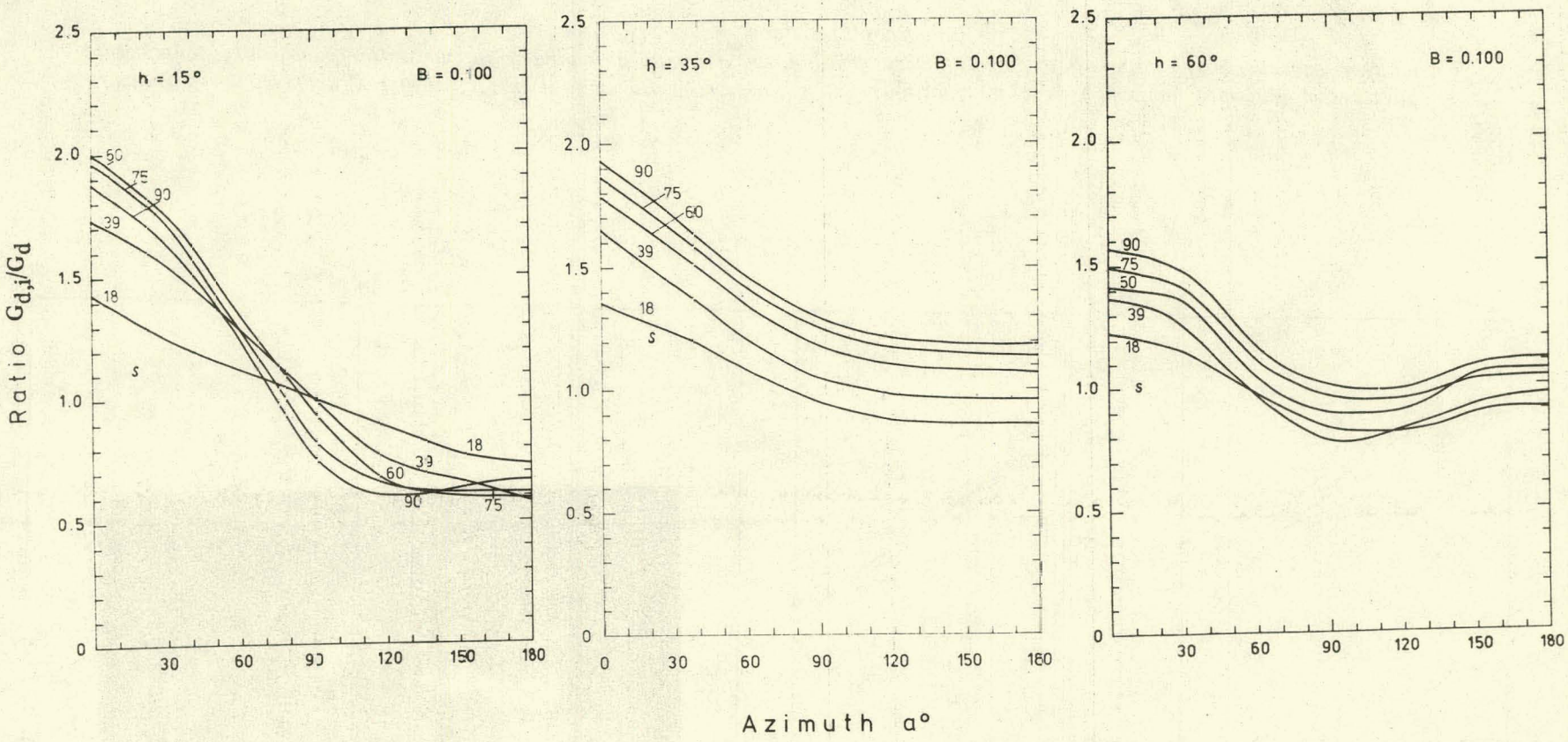


*Figure 8-34 Same as Figure 8-33, except the ratio functions are shown for successively larger solar height angles, the turbidity coefficient being held constant ( B = 0.100) throughout.*

In contrast to Figure 8-28, Figures 8-33 and 8-34 represent only typical examples, i.e., they are not the result of an averaging procedure involving all cases. Only comparable sites (altitude a. m.s.l. $<$ 500 m, open horizon, estimated average albedo $\sim$ 0.15), outside of cities have been chosen. The figures show essentially similar features to those discussed in Section 8.5.2 and may be explained by the causal factors already formulated.

As demonstrated, the deviation from isotropy and the dependence of both the amount and the distribution patterns on turbidity are the essential features of the diffuse irradiance field. By arranging the parameters in a different way, i.e., plotting the ratios $G_{d,i}/G_d$ against the inclination angle of the instrument as abscissa and drawing curves for constant angle from the azimuth of the instrument normal and the azimuth of the sun, good agreement has been found with measurements presented by Kondratyev (1969) (Figures 8-11 and 8-12), valid for an albedo of 0.20, if an appropriate turbidity ($\sim$ 0.150) is chosen. Also the results of Temps and Coulson (1977) given for h = 34° and B = 0.04, as gained by pyranometer measurements in 49 directions, are in good agreement with our data (e.g., first field of Figure 8-33).

### 8.5.3.3 Cloudy Sky Conditions

Figure 8-35 demonstrates in a similar way as Figure 8-31 the corresponding measured results together with the fish-eye photograph except for a sky covered by 3/10 - 4/10 of cumulus clouds. The picture shows that the sky zones around the sun are markedly brightened by a screen of precondensation between the individual cloud formations. The solar disc itself being free of clouds, global irradiance shows a solar-concentrated distribution as before for clear skies. The regularity of the diffuse irradiance patterns is already somewhat disturbed by the radiance distribution of the irregular cloud structure. The radiance pattern, as measured with the 5° scanner, follows fairly well the bright and dark areas as shown in the photograph. It should be mentioned that the visual impression of the horizon and the measured values entered around the outer circle (bottom left) cannot be strictly consistent, since at least the lower half of the instrument's view angle is filled by the surrounding terrain. The diffuse share of the global irradiance for the sun-facing optimum tilt is about 32%; this value is rather high but is less than for the case of high turbidity presented in Figure 8-31 ($\sim$ 40%). For the clean air example of Figure 8-32 the corresponding value amounts to only 12%.

For a systematic survey of the influence of clouds on the diffuse irradiance distributions the multiparametric relationship written in an expanded general form should be solved:

$$G_d = f(h, a, s, B, p, \rho, C_1, C_2, \ldots, C_N)$$

where p denotes the atmospheric pressure required to consider the effect of Rayleigh scattering at different altitudes, $\rho$ denotes the ground albedo and $C_1$ to $C_N$ symbolize an appropriate number of cloud characteristics. These latter may follow the subdivisions of climatological practice, i.e., expressing cloud amount in tenths of the sky covered and distinguishing between the three main cloud types. A solution in terms of these parameters would be advantageous, since these data are available for many sites. The fully equipped mobile system will allow additional parameterization involving the angular distributions of ground reflected radiance and cloud structure, the latter being obtained possibly by densitometric evaluation of the fish-eye photographs.

At the present stage of the project, the effect of cirrus, stratiform and cumulus clouds can be demonstrated by a set of polar diagrams drawn for different cloud amounts. For broken cloudiness the appearance of the sky may change considerably during the measurement of the 77 pyranometer positions. In order to moderate the effects of chance when sampling, 4 separate measurements were averaged at each exposure producing one quasi-simultaneous distribution. This was done by subtracting the direct radiation component from each of the corresponding pyranometer values and then averaging the resultant diffuse irradiances.

Figures 8-36 to 8-38 demonstrate the results for the three types of clouds. At the center of each diagram all 4 values of the horizontal irradiance, obtained simultaneously by all 4 instruments, are entered. These show a few small deviations from each other, but, since only the diffuse components are compared, the agreement can be considered to

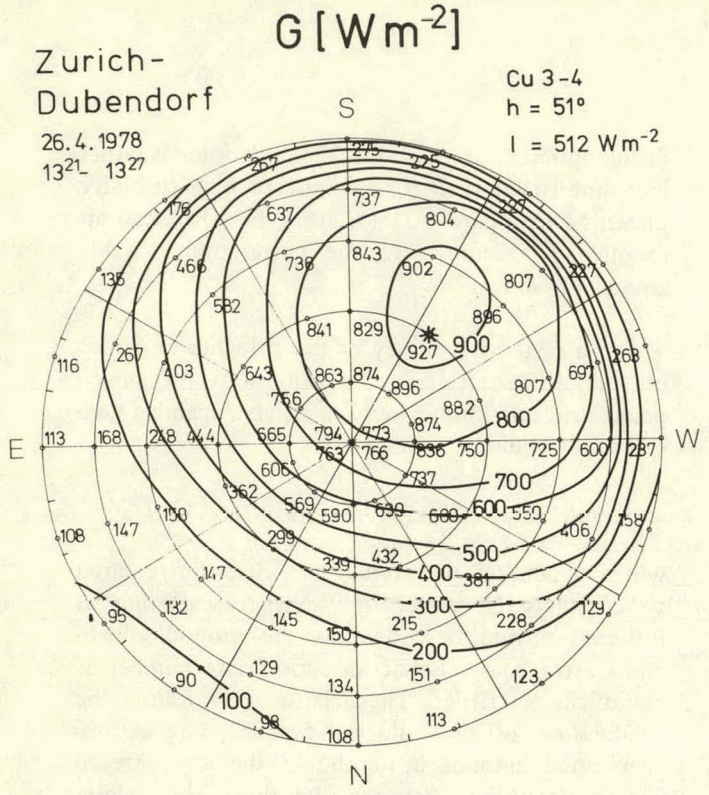


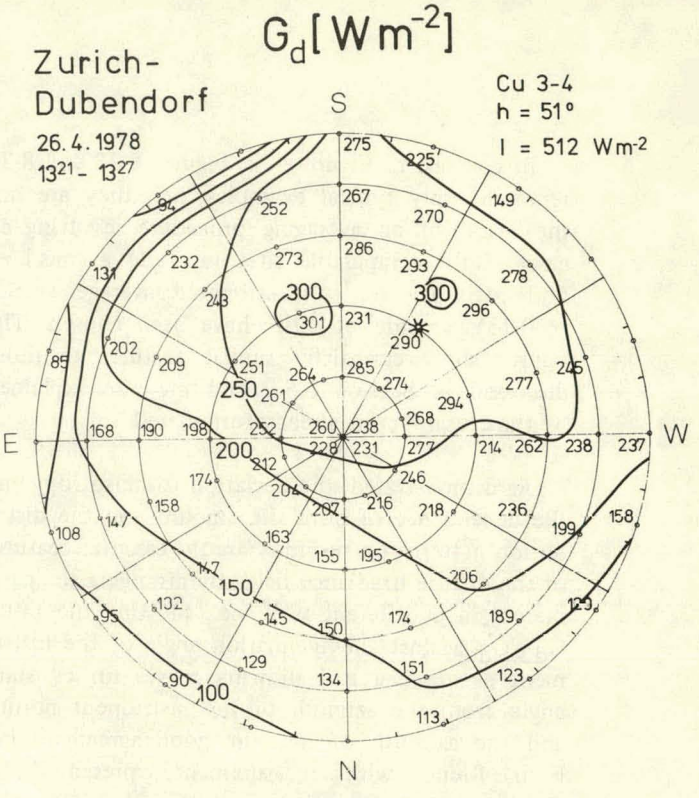


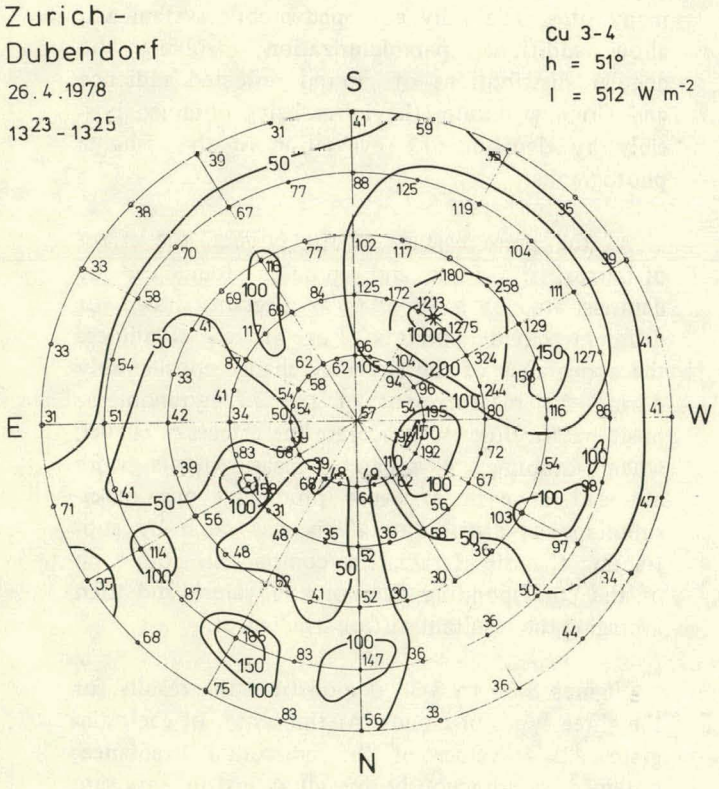


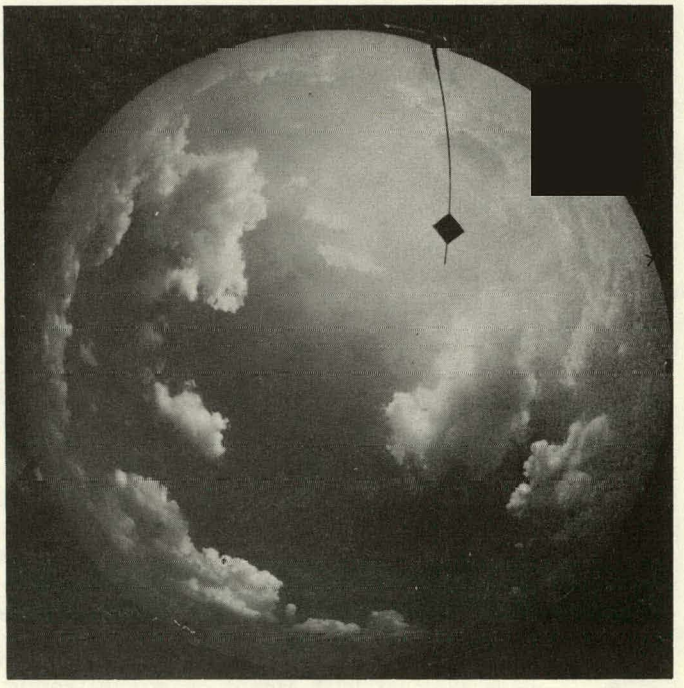

***Figure 8-35*** ***Same as Figure*** *8-31, except for a cloudy sky covered by 3/10 - 4/10 of cumulus cloud and for a solar height of 51°.*

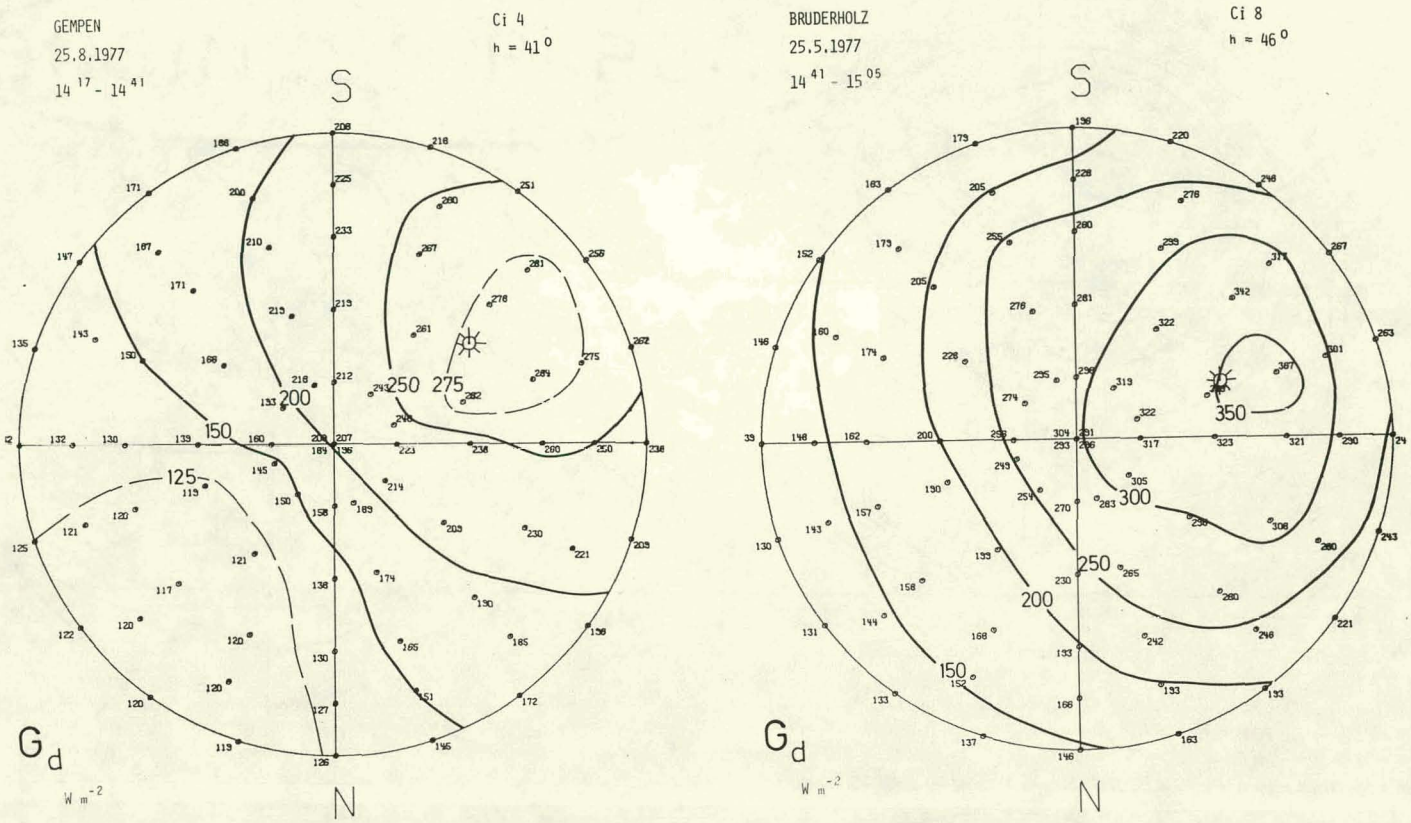


*Figure 8-36 Angular distribution of diffuse irradiance for various amounts of cirrus-type cloud.*

be fairly satisfactory. In selecting the examples, attention was paid that, especially for smaller cloud amounts, cloudiness should dominantly occur in sky zones around and near the sun. The solar height varies from case to case, but the effect of this difference should be secondary when compared with that of cloud amount (entered in the upper right of each diagram and expressed in tenths of sky covered). To illustrate the cloud distribution effects better, polar diagrams containing absolute values have been chosen, however, the figures may, of course, be transformed into ratio function analogs as in Figures 8-33 and 8-34.

Cirrus clouds (Figure 8-36) act similarly to turbidity and produce regular patterns comparable with those in Figure 8-31 (top right); increasing cloud amount corresponds to increasing turbidity, except that the difference in irradiance between surfaces facing the sun and facing away from the sun is smaller in the case of cirrus. Stratiform clouds on the other hand (Figure 8-37), are dense enough to shade the direct solar beam much more than cirrus, the patterns no longer being concentrated near the sun, but shifted towards the zenith. For the fully overcast sky the diagram (bottom left) represents the effect of a stratus layer with fog lying underneath. Here the zenith symmetry is practically perfect. The fish-eye photograph demonstrates the corresponding state of the sky; it shows that even for this overcast case the isotropic assumption is not valid. This result was also found by Garg et al (1974) for overcast skies of altostratus clouds. They measured global irradiances on surfaces tilted by 30°, 45°, 60° and 90° to the horizontal and oriented at 0° and 180° in azimuth with respect to the sun. They also found considerable azumuth anisotropy in contrast to the case shown here; however, this may be more an effect of fog than of the stratus lying above.

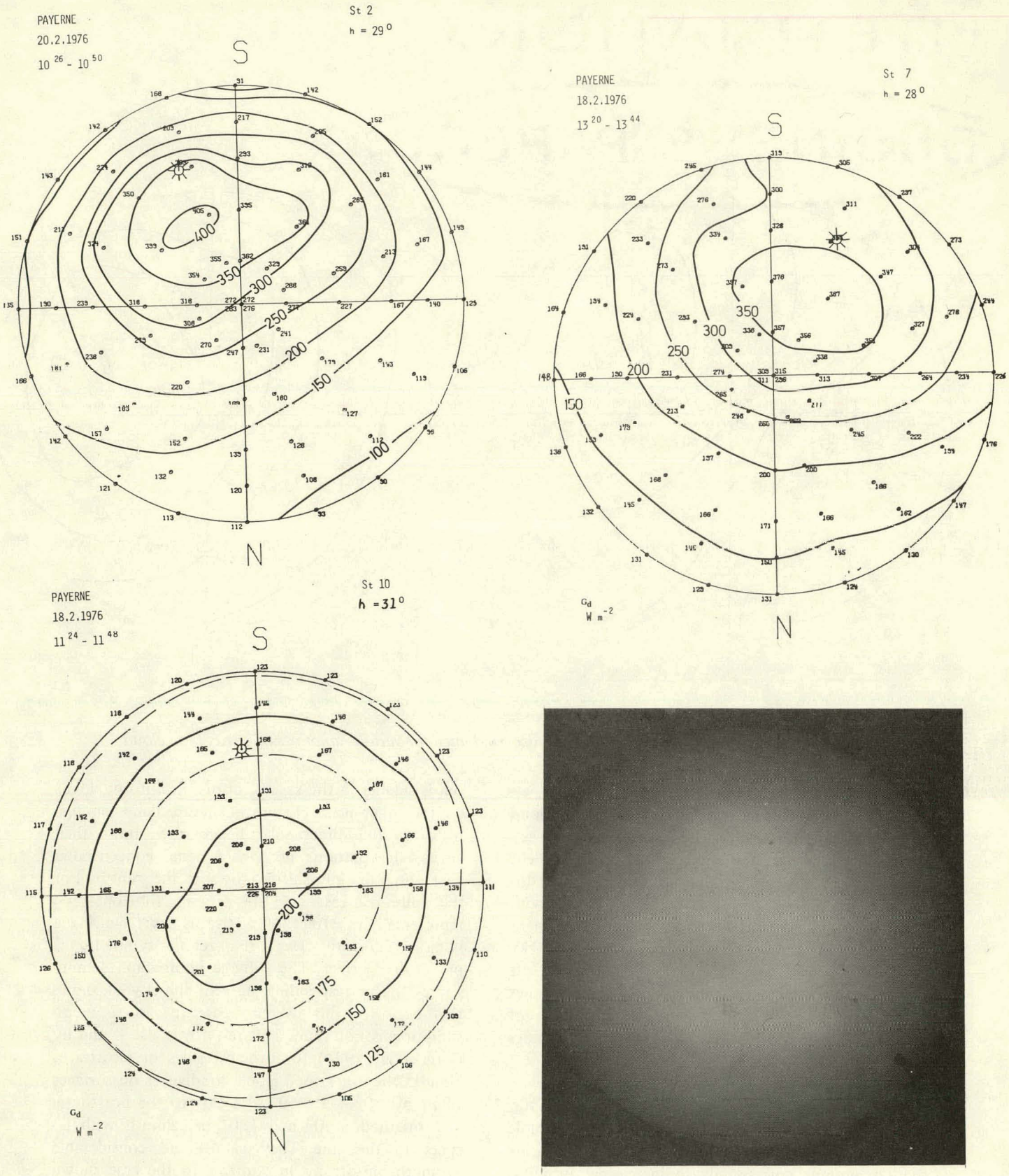


*Figure 8-37 Same as Figure 8-36, except for altostratus cloud, along with the fish-eye photograph for the overcast case (bottom left).*

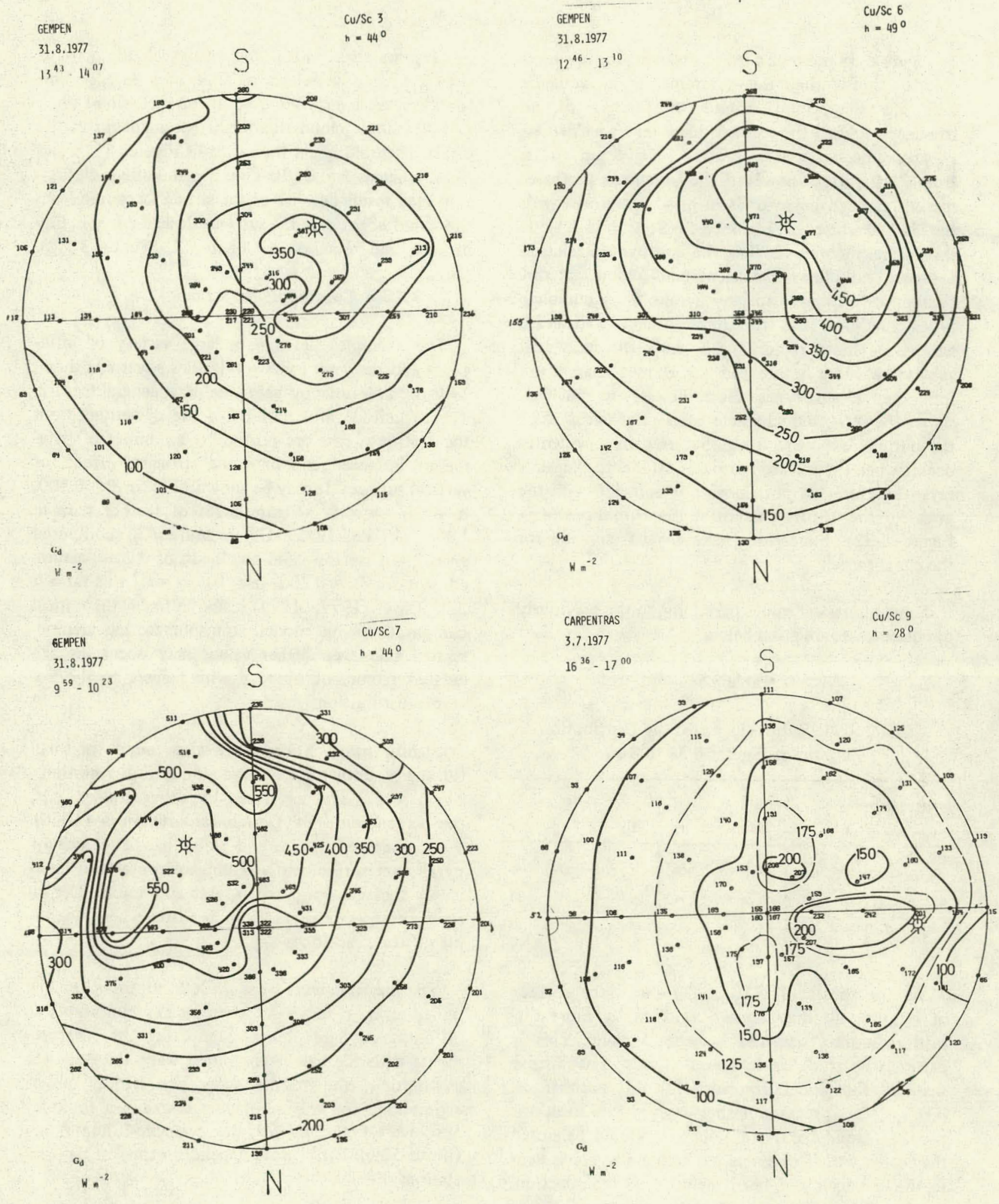


*Figure 8-38 Same as Figures 8-36 and 8-37 for different amounts of low-level cloud.*

Figure 8-38 presents a set of diagrams for low level clouds. Considering the diagrams as a sequence with increasing cloud amount, the increase of the irradiance toward the sun is evident and is particularly pronounced between 6/10 - 7/10 cloud cover; from 7/10 - 9/10, however, the irradiance decreases markedly. Such behavior is in good agreement with the dashed curve of Figure 8-5 (Section 8.3.1). It should be mentioned that the positive correlation between turbidity coefficient and cloud amount (Valko, 1966) may also play a role. Since cumulus-type cloudiness has the most irregular structure and varies most rapidly with time, the individual values are more influenced by chance than those for other cloud types. Nevertheless, the patterns show the essential characteristics. For clear skies the optimal exposure for global irradiance evidently occurs when the surface normal is parallel to the sun's rays; therefore, its peak does not coincide with the peak for the diffuse pattern at low turbidities (e.g., Figure 8-32), but both peaks always coincide for the cloudy cases.

Some numerical values pertaining to the previously discussed cases are given below.

Table 8-5

Characteristic Ratios (in %) for the Distribution Patterns of Figures 8-36 to 8-37

| Cloud Type | Ci | | St | | | Cu/Sc | | | |
|---|---|---|---|---|---|---|---|---|---|
| Cloud Amount | 4 | 8 | 2 | 7 | 10 | 3 | 6 | 7 | 9 |
| $G_{d,max}/G_d$ | 142 | 124 | 147 | 126 | 100 | 172 | 138 | 179 | 149 |
| $G_{d,max}/G_{max}$ | 32 | 69 | 78 | 98 | 99 | 98 | 56 | 56 | 81 |
| $G_d/G$ | 34 | 82 | 84 | 78 | 100 | 73 | 59 | 52 | 75 |

As the values of $G_{d,max}/G_d$ show, the surface of optimal tilt may receive significantly more diffuse radiation than the horizontal plane. This is particularly true for low-level clouds. The diffuse share of the global irradiance for this optimal tilt ($G_{d,max}/G_{max}$) takes rather high values even for partially cloudy skies, although it should be noted that cases with cloudiness excluding sky zones near to the sun have not been included in the selection. $G_{d,max}/G_{max}$ may significantly deviate from the corresponding horizontal ratio $G_d/G$. Furthermore, it appears that with increasing cloud amount $G_{d,max}/G_{max}$ increases to $G_{d,max} = G_{max}$. This function takes a *different* form for each cloud type. For stratiform cloud this might be analogous to the effect of turbidity on the ratios in Figures 8-28 and 8-34, whereas for Cu/Sc cloud, a modified relationship may result because of the strong scattering from the cloud edges near the sun (see dashed curve in Figure 8-5 and remarks in Chapter 3, Section 3.5.2).

### 8.5.3.4 Concluding Remarks

The examples illustrate a large variety of influences and show up some regularities governing them, with the non-isotropy being the most general feature. The magnitude and pattern of the deviations from the isotropic case are related to a number of parameters discussed and have the strongest effect for vertical surfaces. It may be shown, that for B = 0.100, h = 30°, a = 0° (Figure 8-28; of further data in Valko, 1970c, 1975); $G_{d,v}$measured/$G_{d,v}$computed gives 2.4 if isotropy and an albedo of 0.2 are assumed, but for B = 0.200, h = 10°, a = 0° this ratio is 3.9. Dave (1977, 1979) using refined theoretical computations on model atmospheres, has demonstrated that even higher values may occur; he calculated factors of up to 6 with respect to the isotropic distribution.

Significant deviations were also found for small tilt angles, both for clear and cloudy sky conditions. These results are confirmed by other studies, e.g., the experiments of Garnier and Ohmura (1970). They measured diffuse and global irradiance using a pyranometer tilted 20° to the horizontal and alternately facing toward north, east and south. The instrument was shielded from the sun when measuring diffuse irradiance.

The measurements were made in southern Quebec under clear, cloudy and overcast sky conditions at different daylight hours. Comparing the measurements with the values computed using the isotropic assumption, the results show the typical underestimations for the sun-facing slopes (up to 26%) and overestimations for the opposite-facing slopes (up to 56%). Differences depend on time of day and state of the sky.

Further comparisons may be expected when the system of three rotating pyranometers, described by Svendsen (1979), produces irradiance data at 26 measurement positions. Another experiment in Cabauw, Netherlands, using 14 pyranometers exposed in horizontal, inverted, vertical and inclined positions with different orientations, was started by Slob (1979) in April 1979. As the direct solar beam is also measured, useful comparisons with the computed diffuse irradiances should be possible in the near future.

A generalization, using all the available data could be undertaken as a first solution of the expanded relationship in Section 8.5.3.3 (Valko, 1966). The relationship $G_d = f(h, B, N_1, N_2)$ was solved by empirically using data covering 5 years, measured at Locarno-Monti; $N_1$ is the amounts of low-level and stratus clouds combined; $N_2$ that of cirrus alone. The solution was fitted by an analytical expression of the form

$$G_d = c_1 [a_1 \sin^{b_1} h + (a_2 \sin^{b_2} h)(B - c_2)^{b_3}] \cdot [a_4 10^{b_4 N_1} + a_5 N_2 + c_3]$$

where $a_i$, $b_i$, $c_i$ are appropriate constants. It is intended to derive corresponding expressions for the $G_{d,i}/G_d$ - functions, using all available data in a similar manner to that of the examples discussed. It may also be possible to formulate some rules of thumb involving ratios such as those listed in Table 8-5, and eventually $G_{d,min}/G_d$ and suitable angular parameters. Since the scanning devices—both for the sky dome and for the reflected fluxes—will produce much more *simultaneous* data, general results can only be drawn after the data base has been established.

### 8.5.4 Models for Computing Inclined Surface Irradiation

#### 8.5.4.1 Survey on Methods

Because of a lack of data, numerous methods have been developed, especially during the last few years. Some methods are based on exact theoretical model-calculations, but the majority use simplifying assumptions to handle the available horizontal surface irradiation data and other meteorological parameters.

Until the various previously mentioned results are replaced by more general and better solutions, existing methods have to be used. This is not the place to present a detailed comparative analysis of the numerous methods, but a first guide can be given and should help practicians in selecting the one appropriate for their purpose.

In the following synopsis, only those methods which include clear instructions for computing the diffuse component of the total irradiation of inclined surfaces have been considered. These were distinguished according to the time scale of the resulting (output) data, to the sky conditions required for application (arbitrary or clear sky only) and to the radiance distribution assumed (isotropic or anisotropic). Table 8-6 presents results of the survey. The synopsis is an extract based on a report of Bener (1979), who consulted theoretical and empirical studies, as well as the relevant papers compiled and evaluated by May (1978), Perrin de Brichambaut (1978b) and Krochmann (1978).

The original papers were available for all entries in Table 8-6, except those of Kusuda and Ishii (1977) and Basnett (1975), for which entries were based on the May (1978). The goodness of fit versus measured data is illustrated by a few examples below.

#### 8.5.4.2 Testing Selected Methods

The computational methods using measured data obtained from many sources will be extensively tested under international solar radiation data acquisition programs. Already available are the results of Page (1979) who tested his own methods using some of the data sets listed in Table 8-2. For global irradiation, measured at different sites throughout Europe, he obtained *mean monthly* errors, expressed as:

$$\frac{\text{computed - observed values}}{\text{observed values}} \times 100, (\%)$$

which were not greater than ±4-5% for south-facing inclined and vertical surfaces, but were greater than 10% for east- and west-facing vertical surfaces. The errors were found to be of the same order for the annual totals.

Table 8-6

Survey of Various Methods for Computing the Irradiation of Inclined Surfaces

| | Instantaneous values, individual hourly totals | | Totals or averages[1] over periods ≥ 1 day | |
|---|---|---|---|---|
| | Applicable for | | Applicable for | |
| | General conditions | Only clear sky conditions | General conditions | Only clear sky conditions |
| Anisotropic models | Bugler (1977)<br>Dogniaux (1977)<br>Hay (1978a)<br>Loudon & Pethenridge (1965)<br>Loudon (1967) | Liebelt (1978)<br>Temps & Coulson (1977)<br>Souster et al (1978) | Dogniaux (1977)<br>Page (1975, 1978, 1979)<br>Rodgers et al (1978) | Tricaud (1976) |
| Isotropic models | Schüepp (1966)<br>Hocevar & Rakovec (1977)<br>Kusuda & Ishii (1977) | Basnett (1975) | Klein (1977)<br>Liu & Jordan (1961)<br>Perrin de Brichambaut (1978a)<br>DeVos & DeMay (1977) | |

[1] e.g., also hourly values averaged over a month

Apart from monthly means, the *individual daily* totals have been tested earlier by Norris (1966). He subdivided the different methods into two main categories: the diffuse radiation was assumed to be either mainly concentrated around the sun (and was therefore treated like the direct beam), or distributed isotropically. As prototypes he chose a proposal of Morse and Czarnecki (1958) for representing the first category and the method of Liu and Jordan (1961) for the second. To check the models, he used measurements of global irradiation for a south-facing surface inclined at 60° to the horizontal. He found errors of up to 30% and a mean error of 8% for the circumsolar (directional) model and corresponding errors of 22 and 7% for the Liu and Jordan isotropic model. However, using his own 1-year set of records and relating $G_{60}$ to G by months, he obtained a better fit and could reduce the mean error to 2%.

With respect to *individual hourly* data, Hay (1978b) tested his anisotropic model (1978a) (see discussion below in Section 8.5.4.3) along with the isotropic and the directional models, and a so-called "combination model". The latter assumes that half the diffuse radiation is circumsolar and half is distributed isotropically. As reference data he chose the global irradiation of south-facing surfaces inclined at 30°, 60° and 90°, recorded at Toronto and Vancouver (see Table 8-2). The number of observations of one-minute data was of the order of 2000 for each inclination and station. He obtained the following root-mean-square errors:

Table 8-7

Extract from the Results Obtained by Hay (1978b) for Verifying the Techniques used to Calculate Short-Wave Irradiation on Inclined Surfaces

| Inclined angle - s | Station | RMSE (%) Isotropic | Directional | Combination | Anisotropic |
|---|---|---|---|---|---|
| 30 | Toronto | 7.4 | 19.8 | 8.8 | 4.9 |
| | Vancouver | 8.3 | 15.5 | 9.1 | 7.1 |
| 60 | Toronto | 12.9 | 33.9 | 15.3 | 8.7 |
| | Vancouver | 10.5 | 25.0 | 13.6 | 9.0 |
| 90 | Toronto | 18.1 | 48.1 | 22.1 | 13.3 |
| | Vancouver | 10.4 | 28.9 | 18.9 | 13.3 |

As expected, the error increases with inclination angle and, for the combination approach, it lies between those of the isotropic and directional as-

sumptions. The anisotropic model shows a marked improvement compared with commonly used isotropic approximation. A further comparison showing the advantage of the anisotropic model can be made using the absolute values of the RMSE. Hay's value for south 60°, as averaged for the two sites, amounts to 0.13 MJ $m^{-2}$ $h^{-1}$, while Bugler's verification of his own method (1977) yielded 0.16 MJ $m^{-2}$ $h^{-1}$ for a 38° south-facing surface.

Although the different measures of goodness of fit are not strictly comparable, the influence of the time scale on the accuracy of estimation can be shown for typical methods. For south-facing surfaces inclined at 60°, the magnitude of the mean error in % are:

| Year | Month | Day | Hour | |
|---|---|---|---|---|
| 2.2 | 2.5 | 7 | 12 | 9 |
| (Page)[1] | (Page)[1] | (Norris/Liu-Jordan) | (Hay/Isotropic) | (Hay/Anisotropic) |

[1] Average of all values in Page (1979) for south-facing surfaces inclined at between 40° and 90° to the horizontal; the tests on the monthly and yearly scales showed no significant dependence on tilt angle.

### 8.5.4.3 Testing Computed Diffuse Irradiances

In the preceding section the suitability of the computational methods was judged by testing the *total* short-wave irradiation received by the inclined surface. Although this is the decisive quantity, the goodness of fit is nevertheless masked, especially for clear skies, since no assumption is needed to compute the direct component. Therefore, in the following, the agreement of the computed instantaneous diffuse irradiance values with those measured is checked separately. In this way only the essential assumption which characterizes each model is tested.

For this purpose, two sets of data have been chosen:

1. Hourly measurements of horizontal global (G), diffuse ($G_d$) and global south-facing inclined at 90° ($G_{90}$) were available at Locarno-Monti for July 1 for 5 years. Corresponding hours of data were summed. The days included clear skies with varying turbidity and varying amounts of clouds. The global diffuse ($G_{d,90}$) for the south-facing vertical surface was computed by:

$$G_{d,90} = G_{90} - \frac{G - G_d}{\cos\Theta} \cos i$$

with the solar zenith angle, Θ, and the incident angle, i, valid at the middle of each hourly interval.

2. Instantaneous diffuse irradiances measured by the mobile equipment (see Section 8.5.3) in Carpentras, on 39°, 60° and 90° inclined surfaces oriented towards the east, south, west and north. Three sets of measurements were chosen for different times of the day from three days with different turbidities.

Because of time limitations only computations following Hay (1978a), Loudon and Petherbridge (1965), Loudon (1967) and Temps and Coulson (1977) were made; the values for the isotropic case were obtained as interim results.

Common to all three models are corrections applied to the isotropic model to allow for anisotropy.

$$G_i = \frac{G - G_d}{\cos\Theta} \cos i + G_d \frac{1 + \cos s}{2} + \rho G \frac{1 - \cos s}{2}$$

$G_i$ denotes the global irradiance of an inclined surface. The models of Loudon and Hay treat diffuse irradiance as the sum of circumsolar and background components. For the horizontal surface this may be written as

$$G_d = G_d^{\odot}\cos\Theta + G_d^{b},$$

where the circumsolar term $G_d^{\odot}$ is treated geometrically in the same way as the direct beam; the background diffuse part $G_d^{b}$ is assumed to be uniformly distributed over the sky.

Loudon gives tabulated values for two empirical functions

$$G_d^{b} = f_1(\cos\Theta) \quad \textit{and} \quad G_d^{b} = f_2(\overline{\cos\Theta})$$

where $f_1$ is valid for cloud-free skies and $f_2$ for partially cloudy skies.

Using these functions, $I + G_d^{\odot} = G - G_d^{b}/\cos\Theta$ may be computed if G is measured; similarly $G_d^{\odot} = G_d - G_d^{b}/\cos\Theta$ if $G_d$ (or G and I) is measured.

Hay, on the other hand, postulates that the direct beam transmissivity normalized to air mass m = 1 is a good measure of the degree of anisotropy. This gives

$$G_d^{\circledcirc} = \frac{G_d}{\cos\Theta}\left(\frac{I}{I_o}\right)^{1/m}$$

and consequently

$$G_d^b = G_d\left[1 - \left(\frac{I}{I_o}\right)^{1/m}\right]$$

with $I_o$ being the extraterrestrial value of I.

Therefore, for numerical computations the formulas are:

$$G_{d,i} = \frac{G_d - G}{\cos\Theta}\cos i + G_d^b\,\frac{1+\cos s}{2} + \rho G\,\frac{1-\cos s}{2}$$

(Loudon),

and

$$G_{d,i} = G_d\left\{\left(\frac{I}{I_o}\right)^{1/m}\cos i + \cos\Theta\,\frac{1+\cos s}{2}\left[1 - \left(\frac{I}{I_o}\right)^{1/m}\cos i\right]\right\} + \rho G\,\frac{1-\cos s}{2}$$

(Hay).

From their measurements mentioned in 8.5.3.2 Temps and Coulson have derived three corrections for anisotropy:

$C_1 = 1 + \sin^3\frac{s}{2}$, for the increased radiance near the horizon;

$C_2 = [1 + \cos^2 i]\ \sin^3(\Theta)$, for the increased radiance around the sun; and

$C_3 = [1 + \sin^2(\frac{\Theta}{2})] \cdot |\cos a|$, for the anisotropy of reflection.

Using these, one can compute

$$G_{d,i} = Gd\,\frac{1+\cos s}{2}\cdot C_1 \cdot C_2 + \rho G\,\frac{1-\cos s}{2}\cdot C_3,$$

but this expression is only applicable to clear skies.

Although not used in the computations, it should be mentioned that in a very recent paper Klucher (1979) gives empirically obtained corrections for $C_1$ and $C_2$ allowing extension of the Temps-Coulson model to cloudy skies.

For the sky diffuse part they introduced

$$C_1' = 1 + F\sin^3\frac{s}{2} \text{ and } C_2' = [1 + F\cos^2 i]\ \sin^3(\Theta)$$

with $F = 1 - (\frac{G_d}{G})^2$.

The formulas of Loudon, Hay and Klucher for $G_d$ are reduced to the isotropic case for overcast skies, i.e., I = 0, if $G_d = G$.

Results of the computations, giving the relative percentage errors

$$\Delta D\% = \frac{G_{d,i,\text{Computed}} - G_{d,i,\text{Measured}}}{G_{d,i,\text{Measured}}} \times 100,$$

are summarized along with the corresponding reference data $G_{dM}$ in Tables 8-8 and 8-9 for Locarno-Monti and Carpentras, respectively. The ground albedo was assumed to be $\rho = 0.2$ at both sites (concrete roof). At Locarno values of B were obtained from pyrheliometer readings for every daylight hour of 1971 and as hourly values between 1340 and 1700 during 1964; for the other sunny hourly intervals B was determined from $G_d$ through the relationship formulated in Section 8.5.3.4 (see Valko, 1966). In Table 8-8 the daily ranges of B were entered.

Skimming over Table 8-8 it appears, that for the three days with 100% sunshine, the models of Hay and Loudon as well as the isotropic model are markedly sensitive to turbidity. $\Delta D = f(B)$ for hours with $\cos i > 0$ show the same tendency throughout. This is also valid for the Temps-Coulson model but to a lesser extent. The latter seems to underestimate in all cases (some values for overcast hours were computed only as a check) at both sites, except for surfaces oriented away from the sun when at small solar elevation angles (most pronounced for west inclines, Carpentras, 12 July). Since Temps and Coulson developed their $C_3$ term for grass turf, possibly this correction diminishes the goodness of fit when applied to the sites in question.

Neither the models of Hay and Loudon nor the terms $C_1$ and $C_2$ in the Temps-Coulson model take into account the azimuth dependence of the sky diffuse component; this might essentially contribute to the daily variations (Locarno) and the differences

Table 8-8

Percentage Deviations $\Delta G_d$ of Computed Versus Measured Diffuse Irradiances for a South-Facing Vertical Surface. The Hourly Were Selected From Five Different Calendar Years Always for July 1. (h, $\gamma$) are the Angular Coordinates of the Sun Valid at the Middle of Each Hourly Interval.

| Year<br>Turbidity Coefficient<br>Clouds | True Solar Time<br>h°<br>\|γ°\| | 6-7<br>21.4<br>101.4 | 7-8<br>31.8<br>91.1 | 8-9<br>42.1<br>79.7 | 9-10<br>52.0<br>65.5 | 10-11<br>60.6<br>45.9 | 11-12<br>66.1<br>17.3 | 12-13<br>66.1<br>17.3 | 13-14<br>60.6<br>45.9 | 14-15<br>52.0<br>65.5 | 15-16<br>42.1<br>79.7 | 16-17<br>31.8<br>91.1 | 17-18<br>21.4<br>101.4 |
|---|---|---|---|---|---|---|---|---|---|---|---|---|---|
| 1961 | [1] $D_{measured}$ [W m$^{-2}$] | 100 | 169 | 224 | 278 | 279 | 298 | 290 | 279 | 250 | 197 | 149 | 81 |
| B = 0.250-0.360<br>a.m. (2-3)/10 Sc<br>p.m. 1/10 Sc | Sunshine [%] | 82 | 100 | 100 | 100 | 100 | 100 | 100 | 100 | 100 | 100 | 100 | 87 |
| | ΔD% Hay | -10 | -22 | -23 | -28 | -31 | -30 | -28 | -28 | -28 | -25 | -26 | -1 |
| | ΔD% Loudon | 4 | -7 | -39 | -35 | -33 | -31 | -29 | -31 | -32 | -36 | -9 | 15 |
| | ΔD% Temps & Coulson | -2 | -40 | -59 | -71 | -73 | -68 | -67 | -71 | -70 | -61 | -45 | 6 |
| | ΔD% Isotropic | 4 | -7 | -12 | -22 | -27 | -27 | -25 | -24 | -21 | -13 | -9 | 15 |
| 1962 | $D_{measured}$ [W m$^{-2}$] | 0 | 15 | 36 | 85 | 202 | 314 | 258 | 186 | 157 | 127 | 114 | 100 |
| a.m. overcast Ac,Sc<br>1330-1600:<br>B = 0.90-0.110<br>(3-4)/10 Cu cong | Sunshine [%] | 0 | 0 | 0 | 0 | 0 | 43 | 80 | 100 | 100 | 100 | 78 | 45 |
| | ΔD% Hay | - | 76 | 47 | 21 | 23 | 7 | 7 | -8 | -9 | -8 | -7 | -4 |
| | ΔD% Loudon | - | 76 | 47 | 21 | 23 | -9 | 10 | -7 | 7 | -24 | 16 | 13 |
| | ΔD% Temps & Coulson | - | (26) | (-26) | (-57) | (-67) | (-76) | (-56) | -56 | -61 | -66 | (-33) | (5) |
| | ΔD% Isotropic | - | 81 | 47 | 21 | 23 | -5 | 11 | -3 | -1 | -14 | 16 | 13 |
| 1964 | $D_{measured}$ [W m$^{-2}$] | 66 | 99 | 112 | 170 | 184 | 184 | 182 | 185 | 174 | 151 | 123 | 67 |
| a.m. (1-5)/10 Ci<br>p.m. B = 0.110-0.135<br><1/10 Ci, Cu hum. | Sunshine [%] | 100 | 100 | 100 | 100 | 100 | 100 | 100 | 100 | 100 | 100 | 100 | 100 |
| | ΔD% Hay | -14 | -18 | 12 | 1 | 9 | -14 | -14 | -19 | -22 | -26 | -32 | -13 |
| | ΔD% Loudon | 2 | 1 | 8 | -6 | -8 | -13 | -12 | -4 | -20 | -24 | -15 | -3 |
| | ΔD% Temps & Coulson | -24 | -55 | -47 | -59 | -56 | -47 | -46 | -59 | -66 | -67 | -60 | -19 |
| | ΔD% Isotropic | 2 | 1 | 29 | 9 | -3 | -11 | -11 | -14 | -15 | -15 | -15 | 3 |
| 1965 | $D_{measured}$ [W m$^{-2}$] | 88 | 142 | 170 | 213 | 228 | 213 | 51 | 91 | 233 | 141 | 43 | 93 |
| a.m. (7-9)/10 Ac, Sc<br>p.m. 8/10 overcast Sc | Sunshine [%] | 45 | 48 | 65 | 83 | 100 | 55 | 7 | 25 | 73 | 30 | 0 | 97 |
| | ΔD% Hay | 6 | 8 | 20 | 3 | 3 | 1 | 77 | 32 | -0 | 4 | 35 | 17 |
| | ΔD% Loudon | 24 | 23 | 3 | 3 | -1 | 4 | 77 | (*) | -13 | 4 | 35 | 44 |
| | ΔD% Temps & Coulson | | | | | -59 | | | | | | | 26 |
| | ΔD% Isotropic | 24 | 23 | 23 | 7 | 10 | 3 | 77 | 35 | 9 | 9 | 35 | 44 |
| 1971 | $D_{measured}$ [W m$^{-2}$] | 65 | 98 | 83 | 100 | 109 | 114 | 127 | 137 | 140 | 124 | 114 | 63 |
| B = 0.050-0.070<br>completely cloudless<br>only early p.m.<br>≤1/10 Sc | Sunshine [%] | 100 | 100 | 100 | 100 | 100 | 100 | 100 | 100 | 100 | 100 | 100 | 100 |
| | ΔD% Hay | -13 | -22 | 19 | 22 | 26 | 28 | 16 | 2 | -10 | -17 | -7 | -15 |
| | ΔD% Loudon | 1 | -6 | 35 | 31 | 31 | 32 | 18 | 6 | -4 | -7 | -15 | -1 |
| | ΔD% Temps & Coulson | -33 | -67 | -56 | -46 | -27 | -6 | -16 | -42 | -60 | -68 | -69 | -35 |
| | ΔD% Isotropic | -88 | -6 | 32 | 29 | 30 | 31 | 18 | 6 | -4 | -6 | -15 | -1 |

[1] For this table ΔD% is diffuse radiation calculated minus that measured times 100 divided by diffuse radiation measured ($D_{measured}$), i.e., $\Delta D\% = \frac{D_c - D_m}{D_m} \times 100$.

*Since Loudon's table yielded $G_d^b > G_{measured}$, *no ΔD was therefore computed (1965, 13-14).*

( )Values not considered in computing mean deviation because of clouds.

Table 8-9

Percentage Deviations ΔD of Computed Versus Measured Diffuse Irradiances for East-, South-, West- and North-Facing Surfaces Inclined at 39°, 60° and 90° to the Horizontal

| Date | Orientation | East | | | South | | | West | | | North | | |
|---|---|---|---|---|---|---|---|---|---|---|---|---|---|
| Characteristic Data | Inclination s° | 39 | 60 | 90 | 39 | 60 | 90 | 39 | 60 | 90 | 39 | 60 | 90 |
| 5 July | | | | | | | | | | | | | |
| TST: 9:33 I = 749 W m⁻² | $D_{measured}$ W m⁻² | 188 | 193 | 179 | 166 | 162 | 163 | 123 | 111 | 114 | 126 | 109 | 118 |
| h = 53.6° $G_H$ = 767 W m⁻² | Hay | 1 | -2 | -3 | 2 | 0 | -13 | -3 | -10 | 4 | 10 | 9 | 0 |
| \|γ\| = 66° $D_H$ = 164 W m⁻² | Loudon | -3 | -5 | -8 | 1 | 0 | -11 | 4 | 2 | 11 | 14 | 18 | 8 |
| B = 0.151 $D_{bH}$ = 100 W m⁻² | Temps & Coulson ΔD% | -56 | -50 | -36 | -65 | -66 | -65 | -59 | -38 | -4 | -62 | -55 | -51 |
| completely cloudless | Isotropic | -10 | -13 | -6 | -3 | -2 | -5 | 27 | 46 | 40 | 33 | 53 | 35 |
| 12 July | | | | | | | | | | | | | |
| TST: 6:15 I = 323 W m⁻² | $D_{measured}$ W m⁻² | 171 | 173 | 151 | 83 | 68 | 60 | 55 | 49 | 49 | 104 | 89 | 74 |
| h = 17.3° $G_H$ = 202 W m⁻² | Hay | -21 | -20 | -17 | 3 | 7 | 3 | 46 | 50 | 27 | 2 | 10 | 6 |
| \|γ\| = 104° $D_H$ = 105 W m⁻² | Loudon | 8 | 16 | 28 | -15 | -22 | -19 | 3 | 9 | 0 | 11 | 21 | 15 |
| B = 0.183 $D_{bH}$ = 58 W m⁻² | Temps & Coulson ΔD% | -16 | -42 | -10 | 5 | 17 | 18 | 82 | 148 | 186 | -8 | -2 | -6 |
| completely cloudless | Isotropic | -44 | -68 | -53 | 20 | 30 | 20 | 79 | 80 | 48 | -7 | 2 | -4 |
| 17 July | | | | | | | | | | | | | |
| TST: 15:32 I = 856 W m⁻² | $D_{measured}$ W m⁻² | 100 | 95 | 128 | 85 | 107 | 145 | 101 | 125 | 132 | 84 | 108 | 127 |
| h = 40.0° $G_H$ = 627 W m⁻² | Hay | -49 | -35 | -35 | -3 | -20 | -39 | 5 | -6 | -5 | -12 | -32 | -35 |
| \|γ\| = 81° $D_H$ = 77 W m⁻² | Loudon | -12 | -1 | -18 | -2 | -14 | -29 | -24 | -34 | -23 | 0 | -15 | -17 |
| B = 0.058 $D_{bH}$ = 84 W m⁻² | Temps & Coulson ΔD% | -45 | -30 | -16 | -46 | -61 | -75 | -34 | -38 | -31 | -56 | -69 | -72 |
| completely cloudless | Istroptic | -4 | -6 | -21 | 1 | -13 | -28 | -29 | -39 | -35 | -6 | -21 | -20 |

for varying surface orientations (Carpentras). Effects of turbidity and cloudiness are reflected differently in the deviations, since only Hay's model allows for both, Loudon's functions for $G_d^b$ as well as the Temps-Coulson corrections $C_1$ and $C_2$ contain only angular terms. For overcast skies the isotropic model, and consequently the models of Hay and Loudon, yield positive deviations, probably due to overestimation of the ground reflection.

Considering the accuracy of the reference data, it should be mentioned that the measurements at Carpentras were made with pyranometers of high accuracy, specially developed at the World Radiation Centre at Davos. The absolute radiometer is also from this institute (type PMO 3/5, accuracy ±0.3%). On the other hand, at Locarno, the $G_d$-data from a pyranometer with shade ring have been used.[1] Nevertheless this could not be decisive for the test, since the averages of the deviations were of the same order for both places:

Table 8-10

Absolute Mean of Deviations Found for Locarno-Monti and Carpentras (± %)

| | Hay | Loudon | Temps-Coulson | Isotropic |
|---|---|---|---|---|
| Locarno-Monti | 18.6 | 18.4 | 44.5 | 19.2 |
| Carpentras | 15.1 | 12.3 | 47.7 | 26.4 |

In addition the fact that albedo was assumed and not measured might be of only secondary importance.

[1] Error analysis and quality control of all horizontal and vertical surface pyranometer data have been made by Schmid (1976). The overall mean error for the Locarno-Monti hourly $G_d$ values yields ±2% for clear skies, ±5% for partly cloudy skies and ±4% for overcast conditions.

It is planned to extend the test to a much larger amount of data than that of this small sample and also to evaluate other methods.

### 8.6 Combined Frequency Distribution

Weather sensitive systems, and solar energy applications specifically, are generally affected by several meteorological variables. Correspondingly, to understand their behavior, in many cases several meteorological parameters must be considered together. The probability of the simultaneous occurrence of two or more meteorological variables is used as an estimation of future occurrences. The usual statistics for independent variables do not apply because nearly all meteorological variables are dependent. Therefore, an empirical approach using past weather records is often used to count the past simultaneous occurrences of certain events. This past frequency of occurrences is projected as the probability that the events will occur in the future and may be applied to engineering design problems involving climatological loads.

With a two-variate cumulative frequency such as daily average temperatures and daily hours of sunshine, step intervals $\Delta T$ and $\Delta S$ respectively are arbitrarily established and the number of occurrences in each interval is expressed as a percentage of the overall total. Intervals may be summed from high to low and percentile curves, using temperature and hours of sunshine as arguments, yield the frequency of occurrence above and below certain criteria, see Figure 8-39. A third variable such as time may be added and a "carpet plot" similar to Figure 8-3 may be drawn. With the use of computers, wind speed and solar radiation on inclined surfaces have also been included. For more detailed information on this procedure and applications see Schmid (1976), Duppenthaler (1977), Kesselring and Duppenthaler (1979), Valko (1973a, 1975), Bray (1979) and Bahm (1978).

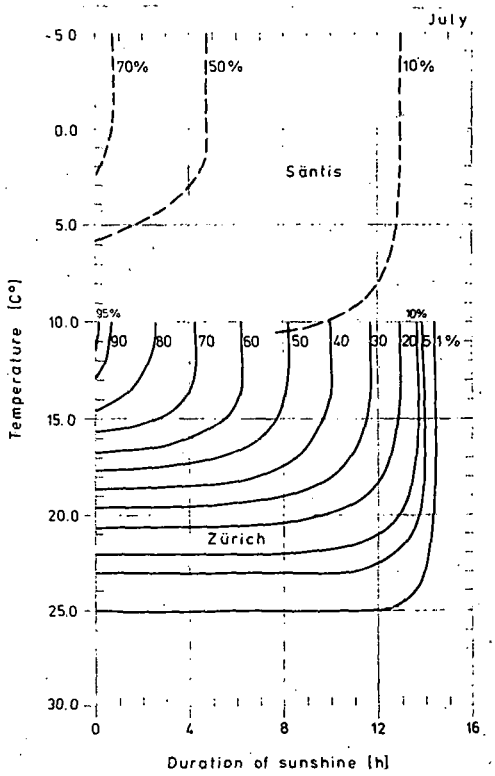


*Figure 8-39 Combined frequency distribution of daily mean temperature and daily total hours of sunshine for Zurich (continuous curves below) and Säntis (dashed curves above, drawn only for 10, 50 and 70%).*


### Acknowledgements

Part of the measurements and computations have been sponsored by the National Foundation for Energy Research; their helpful engagement is highly appreciated.

The author wishes to express his gratitude to Dr. Fritz Eggimann, Director of R&D Cerberus Ltd., Männendorf, for most useful discussions on statistical power spectra; to Alan Heimo for measurements with the mobile system and for developing various computer programs; as well as to Thomas Baumgartner, Anthony Korab and Francis Schubiger for their valuable work in supporting many numerical computations.

## References


Ambrosetti, F. and Thams, J. C. 1953. "Die Grösse der Globalstrahlung verschieden orientierter Flächen." *Geofisica pura e applicata.* No. 26, pp. 198-210.

Austrian Solar and Space Agency. 1977. *Meteorologische Messdaten für die Nutzung der Sonnenenergie.* 105 pp. Wien 1977.

Bahm, R. J. 1978. "Regional Differences in Solar Radiation Availability." *Solar Age.* June, 1978.

Basnett, P. 1975. "Estimation of Solar Radiation Falling on Vertical Surfaces from Measurements on a Horizontal Surface." *Electricity Council Research Centre Report M 846.* (Internal Report)

Baumgartner, T. 1978. "Die Schwellenintensität des Sonnenscheinautographen Campbell-Stokes an Wolkenlosen Tagen in Zürich." *Working Reports of the Swiss Meteorological Institute No. 82.* 21 pp., Zurich.

Bener, P., Frohlich, C. and Valko, P. 1973. "Mobile Station for Automatic Measurements of Spectral Solar and Sky Radiance and of the Fluxes of Global and Sky Radiation on Differently Oriented Planes." *International Solar Energy Society Conference.* Paper E 31. 10 pp. Paris.

Bener, P. 1979. *Survey and Comments on Various Methods to Compute the Components of Solar Irradiance of Horizontal and Inclined Surfaces.* (In preparation)

Bloomfield, P. 1976. *Fourier Analysis of Time Series: An Introduction.* New York: John Wiley & Sons. 258 pp.

Bray, R. 1979. *Solar-Climatic Statistical Study.* U. S. Department of Energy No. HCP/T4016 (2 vols.), Washington, DC. February 1979.

Bugler, J. W. 1977. "The Determination of Hourly Insolation on an Inclined Plane Using a Diffuse Irradiance Model Based on Hourly Measured Global Horizontal Insolation." *Solar Energy.* No. 19. pp. 477-491.

Collingbourne, R. H. 1975. "The United Kingdom Solar Radiation Network and the Availability of Solar Radiation Data from the Meteorological Office for Solar Energy Applications." *Proceedings, Solar Energy Society UK Section Conference.* pp. 2-17. London.

Dave, J. V. 1977. "Validity of the Isotropic-Distribution Approximation in Solar Energy Estimations." *Solar Energy.* No. 19. pp. 331-333.

Dave, J. V. 1979. "Isotropic Distribution Approximation in Solar Energy Estimations." *Solar Energy.* No. 22. pp. 15-19.

Davenport, A. G. 1961. "The Spectrum of Horizontal Gustiness Near the Ground in High Winds." *Quarterly Journal of the Royal Meteorological Society.* No. 87. pp. 194-211.

De Coster, M. and Schüepp, W. 1956. "La Variation Annuelle du Trouble Atmosphérique à Stanleyville." *Acad. Roy. Sci. Colon., Cl. Sci. Nat. et Méd. Mém. in -8: Nouv. Sér. Tome IV.* Fasc. 1, Bruxelles.

Dehne, K. 1974. "Entwicklung eines Sky-Scanners zur Schnellen Vermessung der räumlichen Verteilung Spektraler Himmelsstrahldichten." *Ber. Dt. Wetterd.* No. 134. pp. 39.

De Vos, A. and De May, G. 1977. "The Solar Energy Incident on a Plane at the Earth's Surface; Situation in Belgium." *Archiv. Met. Geoph. Biokl.* No. 25. pp. 135-150.

Dogniaux, R. 1977. "Computer Procedure for Accurate Calculation of Radiation Data Related to Solar Energy Utilization." *Proceedings UNESCO/WMO Solar Energy Symposium.* WMO No. 477, pp. 191-197. Geneva.

Dogniaux, R. 1978. "Compilation Within the Solar Radiation Data Acquisition Project of the EC Solar Energy Programme." Unpublished draft. November, 1978.

Dorno, C. 1919. "Himmelshelligkeit, Himmelspolororisation und Sonnenintensität in Davos 1911 bis 1918." *Veröff. d. Preuss. Meteor. Instituts Nr. 303.* Abhandlungen Bd. VI. 303 pp. Berlin.

Duppenthaler, A. 1977. "Die Berechnung des Bruttowärmeertrages von Solarkollektoren." Parts I and II. *Internal Report TM-IN-670, Swiss Federal Institute for Reactor Research.* pp. 34-55. Wurenlingen.

Funk, J. P. 1965. "Radiation Observations at Aspendale, Australia, and Their Comparison with Other Data." *Archiv. Meteor. Geoph. Biokl.* No. 13. pp. 52-70.

Garg, H. P., Rao, K. R. and Pal, R. S. 1974. "Measurement of Global Solar Radiation on Inclined Surfaces of any Orientation Under Overcast Sky Condition." *Indian J. Met. Geoph.* No. 25. pp. 295-300.

Garnier, B. H. and Ohmura, A. 1970. "The Evaluation of Surface Variations in Solar Radiation Income. *Solar Energy.* No. 13. pp. 21-34.

Gräfe, K. 1956. "Strahlungsempfang Vertikaler ebener Flächen: Globalstrahlung von Hamburg.' *Ber. Dt. Wetterd.* Vol. 5, No. 29. 15 pp.

Hay, J. E. 1978. "Measurement and Modelling of Shortwave Radiation on Inclined Surfaces." *Proceedings, Third Conference on Atm. Rad., AMS.* pp. 150-153.

Hay, J. E. 1978. "Shortwave Radiation on Inclined Surfaces." *Final Report, Department of Geography, The University of British Columbia, Vancouver.* 54 pp.

Heimo, A. and Valko, P. 1977. "First Results Obtained from the Swiss Mobile System for Solar Radiation Measurements." *Proceedings UNESCO/WMO Solar Energy Synposium.* WMO no. 477, pp. 144-152. Geneva.

Heywood, H. 1966. "The Computation of Solar Radiation Intensities. Part 2 - Solar Radiation on Inclined Surfaces." *Solar Energy.* No. 10. pp. 46-52.

Hocevar, A. and Rakovec, J. 1977. "General Models of Circum-global and Quasi-global Radiation on Hills of Simple Geometric Shapes." *Archiv. Met. Geoph. Biokl.* No. 25. pp. 151-176.

Josefsson, W. 1978. "Compilation to IEA V Data Source Catalogue." (Unpublished draft - June 1978)

Kesselring, P. and Duppenthaler, A. 1979. "The Layout of Solar Hot Water Systems, Using Statistical Meteo- and Heat Demand Data." *ISES Congress, Atlanta, GA, U.S.A.* May/June 1978. Reprint.

Klein, S. A. 1977. "Calculation of Monthly Average Insolation on Tilted Surfaces." *Solar Energy.* No. 19, pp. 325-329.

Klucher, T. M. 1979. "Evaluation of Models to Predict Insolation on Tilted Surfaces." *Solar Energy.* No. 23. pp. 111-114.

Kondratyev, K. Ya. 1969. *Radiation in the Atmosphere.* New York: Academic Press. 912 pp.

Kondratyev, K. Ya. and Fedorova, M. P. 1977. "Radiation Regime of Inclined Surfaces." *WMO Technical Note No. 152.* 82 pp. Geneva.

Kondratyev, K. Ya. and Manolova, M. P. 1959. "The Radiation Balance of Slopes." *The Reports at the Symposium on Radiation in Oxford.* pp. 3-20. Leningrad.

Kondratyev, K. Ya., Pivovarova, Z, I. and Fedorova, M. P. 1978. "Radiation Regime of Inclined Surfaces." (in Russian) 215 pp. Gidrometeoizdat, Leningrad.

Krochmann, J. 1973. "Quantities of Illuminating Engineering for Daylight. The Sun in the Service of Mankind." *Int. Solar Energy Society Conference.* Paper EH 52. Paris.

Krochmann, J. 1978. "Survey and Description of Papers in German Containing Methods of Estimating Radiation on Inclined Surfaces." *Solar Radiation Data Acquisition Project of the EEC Solar Energy Programme.* unpublished draft.

Kusuda, T. and Ishii, K. 1977. "Hourly Solar Radiation Data for Vertical and Horizontal Surfaces on Average Days in the United States and Canada." *National Bureau of Standards Building Science Series No. 96.*

Liebelt, C. 1978. "Leuchtdichte- und Strahldichtevertielung des Himmels." Thesis. 311 pp. Karlsruhe.

Liu, Y. H. and Jordan, R. C. 1961. "Daily Insolation on Surfaces Tilted Towards the Equator." *ASHRAE Journal.* No. 3. pp. 53-59.

Loudon, A. G. 1967. "The Interpretation of Solar Radiation Measurements for Building Problems." BRS Res. Papers No. 73. *Proceedings CIE Conf., "Sunlight in Buildings".* pp. 110-117. Rotterdam.

Loudon, A. G. and Petherbridge, P. 1965. "Solar Radiation on Inclined Surfaces." *BRS Note No. EN 5/65.* 5 pp.

May, B. R. 1978. "Survey and Description of Papers in English Containing Methods of Estimating Radiation on Inclined Surfaces." *Solar Radiation Data Acquisition Project of the EEC Solar Energy Programme.* (unpublished draft)

McArthur, L. B. and Hay, J. E. 1978. *Radiative and Photographic Determinations of the Distribution of Diffuse Shortwave Radiation over the Sky Hemisphere. Part I and Part II.* 20 pp.

McArthur, L. B. and Hay, J. E. 1979. "On the Anisotropy of Diffuse Solar Radiation." *Bull. Amer. Met. Soc.* No. 59. pp. 1442-1443.

Meinel, A. B. and Meinel, M. P. 1976. *Applied Solar Energy.* Reading, MA: Addison-Wesley Publ. Co. 651 pp.

Morse, R. N. and Czarnecki, J. T. 1958. "Flat Plate Solar Absorbers: The Effect on Incident Radiation of Inclination and Orientation." *CSIRO Eng. Section, Report E.D.6.* pp. 11-16. Melbourne.

Norris, D. J. 1966. "Solar Radiation on Inclined Surfaces." *Solar Energy.* No. 10. pp. 72-76.

Page, J. K. 1975. "The Estimation of Monthly Mean Values of Daily Shortwave Irradiation on Vertical and Inclined Surfaces from Sunshine Records for Latitudes 60°N - 40°S." *Report BS 32, Dept. of Building Science, University of Sheffield.* 42 pp.

Page, J. K. 1978. "Methods for the Estimation of Solar Energy on Vertical and Inclined Surfaces." *Report BS 46, Dept. of Building Science, Univ. of Sheffield.* 61 pp.

Page, J. K. 1979. "Predetermination of Irradiation on Inclined Surfaces for Different European Centres." *Interim Progress Report, Solar Radiation Data Acquisition Project of the EEC Solar Energy Programme.* (unpublished draft)

Parmelee, G. V. 1954. "Irradiation of Vertical and Horizontal Surfaces by Diffuse Solar Radiation from Cloudless Skies." *ASHVE Trans.* No. 60. pp. 341-357.

Perrin de Brichambaut, C. 1978. "Estimation du Rayonnement Solaire." *Publication de la Secrétariat d'Etat Auprès du Ministère de l'Equipement dt de l'Aménagement du Territoire.* Direction de la Météorologie.

Perrin de Brichambaut, C. 1978. "Survey and Description of Papers in French Containing Methods of Estimating Radiation on Inclined Surfaces." *Solar Radiation Data Acquisition Project of the EEC Solar Energy Programme.* (unpublished draft)

Puskas, J. 1973. "Evaluation of Diffuse Solar Radiation of Vertical Building Surfaces." *Int. Solar Energy Society Conference.* Paper E 121. 8 pp. Paris.

Rodgers, G. G., Page, J. K. and Souster, C. G. 1979. "Mathematical Models for Estimating the Irradiance Falling on Inclined Surfaces for Clear, Overcast and Average Conditions." *Proceedings Int. Solar Energy Society UK Section Conference on Meteorology for Solar Energy Applications.* pp. 48-62. London.

Rodgers, G. G., Page, J. K., Souster, C. G., and Sharples, S. 1978. "The Development of Interactive Computer Programs for Computing Energy Exchanges Between Sloping Surfaces and the Natural Environment." *Report BS 44, Dept. of Building Sciences, Univ. of Sheffield.* 21 pp.

Schmid, W. 1976. "Aufbereitung und Qualitätskontrolle langjähriger Messunterlagen der Globalstrahlung und Himmelsstrahlung." *Working Report No. 59, Swiss Meteorological Inst.* 47 pp.

Schram, K. and Thams, J. C. 1967a. "Die Kurzwellige Strahlung von Sonne und Himmel auf einen nach Süden Orientierten Würfel." *PAGEOPH 66.* pp. 183-200.

Schram, K. and Thams, J. C. 1967b. "Die Kurzwellige Strahlung von Sonne und Himmel auf Verschieden Orientierte und Geneigte Flächen." *Archiv. Meteor. Geoph. Biokl.* No. 15. pp. 99-126.

Schüepp, W. 1949. "Die Bestimmung der Komponenten der Atmospharischen Trubung aus Aktinometermessungen." *Archiv. Met. Geoph. Biokl.* No. 1. pp. 257-346.

Schüepp, W. 1955. *Bulletin Mensuel Serv. Met. Congo Belge 4.* No. 1 - 5, No. 8.

Schüepp, W. 1966. "Direct and Scattered Radiation Reaching the Earth as Influenced by Atmospheric, Geographical and Astronomical Factors." Chapter 4 in Robinson, N. *Solar Radiation.* Amsterdam: Elsevier. 347 pp.

Schulze, R. 1954. "Strahlungsempfang Geneigter Ebener Flächen." *Archiv. Meteor. Geoph. Biokl.* No. 6. pp. 128-138.

Souster, C. G., Rodgers, G. G. and Page, J. K. 1978. "The Development of an Interactive Computer Program SUN 3 for the Calculation of Solar Irradiances and Daily Irradiations Incident upon Surfaces of any Slope and Orientation on Cloudless Days for Given Conditions of Sky Clarity and Atmospheric Water Content." *Report BS 30, Dept. of Building Science, Univ. of Sheffield.* 69 pp.

Steven, M. D. 1977. "Standard Distribution of Clear Sky Radiance." *Quarterly Journal of the Royal Meteorological Society.* No. 103. pp. 457-465.

Steven, M. D. and Unsworth, M. H. 1979a. "The Diffuse Solar Irradiance of Slopes Under Cloudless Skies."*Quarterly Journal of the Royal Meteorological Society.* No. 105. pp. 593-602.

Steven, M. D. and Unsworth, M. H. 1979b. "The Radiance Distribution of Clear and Overcast Skies." *Proceedings, Int. Solar Energy Society UK Section Conference on Meteorology for Solar Energy Applications.* pp. 26-36. London.

Suckling, P. W. and Hay, J. E. 1976. "The Spatial Variability of Daily Values of Solar Radiation for British Columbia and Alberta, Canada." *Climatological Bulletin No. 20, McGill Univ. Montreal.*

Svendsen, D. A. 1979. "Some Results of the Measurements of Inclined Surface Irradiance at Cardiff." *Proceedings, Int. Solar Energy Society UK Section Conference on Meteorofor Solar Energy Applications.* pp. 37-47. London.

Temps, R. C. and Coulson, K. L. 1977. "Solar Radiation Incident Upon Slopes of Different Orientations." *Solar Energy.* No. 19. pp. 179-184.

Threlkeld, J. L. 1963. "Solar Irradiation of Surfaces on Clear Days." *ASHRAE Transaction 69.* pp. 24-36.

Tonne, F. 1967. Personal Communication.

Tricaud, J. -F. 1976. "Contribution à l'estimation des Ressources Énergétiques Solaires." Thesis presented at the University of Paris VII. April 22, 1976.

Valko, P. 1966. "Die Himmelsstrahlung in ihrer Beziehung zu Verschiedenen Parametern." *Archiv. Meteor. Geoph. Biokl.* No. 14. pp. 336-359.

Valko, P. 1967. "Strahlungsmeteorologische Unterlagen zur Berechnung des Kühlbedarfes von Bauten." *Schweiz. Bl. f. Heizung und Lüftung.* No. 34, pp. 9-21.

Valko, P. 1970a. "Das Kurzwellige Strahlungsfeld der Atmosphäre – Richtwerte für Ingenierue und Architekten." No. 1-4. *Schweiz. Blätter f. Heizung und Lüftung.* No. 37. pp. 24-32, 56-60, 115-119. No. 38. pp. 121-126. 1971.

Valko, P. 1970b. "On the Diffuse Irradiance of Non-Horizontal Plane Surface." *Proceedings, WMO/IUGG Symposium on Radiation Including Satellite Techniques.* Bergen, 1968. WMO Tech. Note. 104. pp. 191-195.

Valko, P. 1970c. "Radiation Load on Buildings of Different Shape and Orientation Under Various Climatic Conditions." *Proceedings, WMO/WHO Symposium on Urban Climates and Building Climatology.* Brussels, 1968. WMO Tech. Note 109. pp. 87-109.

Valko, P. 1973a. "Meteorologische Planung für die Klimatechnik." *"Promet" Meteorologische Fortbildung.* No. 4. pp. 15-20.

Valko, P. 1973b. "Probabilities of Sunshine Hours Accumulated Over Periods of $2 \leq N \leq 31$ Consecutive Days." *Proceedings, Intl. Solar Energy Society Conference. Paris, 1973. Working Reports of the Swiss Meteorological Institute.* No. 38. 15 pp.

Valko, P. 1975. "Das Informationsangebot der Strahlungsmeteorologie als Planungsgrundlage der Sonnenenergie-Nutzung." *Elektrizatätsverwertung.* No. 50. pp. 72-80.

Valko, P. 1975. "Sonnenbestrahlung von Gebäuden fur Verschiedene Bauformen und Fassadenrichtungen." *METEOPLAN No. 1.* Bern: Hallwag Verlag. 61 pp.

Valko, P. 1976. "Meteorologische Daten zur Sonnenenergienutzung." *Deutsche Gesellschaft f. Sonnenenergie. Conference Report "Grundlagen der Solartechnik I."* 43 pp.

Valko, P. 1977. "Meteorologische Strahlungsmessungen mit Fahrbarer Station." *Neue Zürcher Zietung.* No. 281.

Valko, P. 1979. *Sunshine Duration Statistics for Switzerland. METEOPLAN No. 3.* Bern: Hallwag Pub., Inc.

Van der Hoven, J. 1957. "Power Spectrum of Horizontal Wind Speed in the Frequency Range From 0.0007 to 900 Cycles per Hour." *Journal of Meteorology.* No. 14. pp. 160-164.

Van Deventer, E. N. and Dold, T. B. 1966. "Some Initial Studies on Diffuse Sky and Ground Reflected Solar Radiation on Vertical Surfaces." *Proceedings, 3rd Int. Biometeor. Congress. Pau, Sept. 1963.* Oxford: Pergamon Press. pp. 735-742.

Van Deventer, E. N. and Joubert, G. R. 1966. "An Automatic Sky Scanning Radiometer for Measuring the Distribution of Radiation From the Sky and Interpretation of the Measurements." *Proceedings, 3rd Int. Biometeor. Congress. Pau, Sept. 1963.* Oxford: Pergamon Press. pp. 730-734.

Volz, F. 1958. "Globalstrahlung auf Geneigte Hänge." *Meteor. Rundschau.* No. 11. pp. 132-135.

Volz, F. 1963. "Einige Häufigkeitsverteilungen des Trübungskoeffizienten und der Trübungstypen in Europa und Nordamerika." *Met. Rundschau.* No. 16 - 6. pp. 173-182.

CHAPTER 9

# DURATION OF SUNSHINE

**M. R. Riches**
**Office of Energy Research**
**U. S. Department of Energy**
**Washington, D. C. 20545**
**The United States of America**

## 9.1 Introduction

Duration of sunshine is defined as the time (hours or minutes) during which the sunshine is intense enough to cast a shadow. Sunshine duration measurements have been made for about 140 years, and have two main uses. First, it is a good climatic parameter for characterizing the general cloudiness of a region. The percentage of possible sunshine is often used by local commercial organizations as a selling point for their town. Generally, most people prefer an area with a high percentage of possible sunshine. Second, sunshine duration can be input into models to estimate the global irradiation. Each model is usually a variation of the one first suggested by Ångström (1924), i.e.,

$$G = G'(a' + b'\frac{S}{S_o})$$

where G is global irradiance, G′ is the clear day global irradiance (measured or estimated), a′ and b′ are constants for a given area, $S/S_o$ is the fraction of the possible sunshine on the given day. Such models are best used to compute monthly means. The final report for *IEA Solar Heating and Cooling Systems Task V* covers examples using this technique. (See Chapter 10, Section 10.5.1.)

## 9.2 Sensors

Four main types of sunshine duration sensors are in operational use: (1) the focusing type (Campbell-Stokes); (2) the differential thermometric (Maring-Marvin and Sumner); (3) the photographic (Jordan); and (4) the photoelectric (Foster, Haenni, Schlumberger, Helior and IAH).

The Campbell-Stokes sunshine recorder (Figure 9-1) consists of a glass sphere approximately 10 cm in diameter mounted concentrically in a section of a spherical bowl, whose diameter is such that the sun's rays can be focused on a card held in place by grooves in the bowl. This sensor is the WMO interim reference sunshine recorder (WMO, 1965) when built to the British Meteorological Office specifications and so certified by their office.

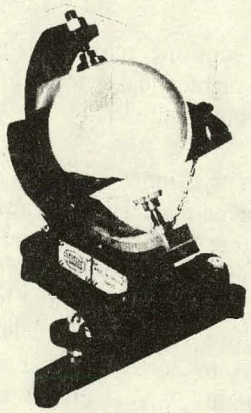

*Figure 9-1 The Campbell-Stokes sunshine recorder*

The record cards for the Campbell-Stokes recorder are available in three types. Long curved cards are required for summer; short curved cards for winter; straight cards for periods near the equinoxes. When using the long summer card, care must be taken so that the "tails" of the card do not shade out the early morning or evening sun. The French Meteorological Office is responsible for certification of the

cards. A major problem is humidity. In a dry atmosphere the burn can begin at about 70 W $m^{-2}$ (7 mW $cm^{-2}$) while in a very moist atmosphere the burn may not start until 280 W $m^{-2}$ (28 mW $cm^{-2}$). The average threshold value is approximately 210 W $m^{-2}$ (21 mW $cm^{-2}$) (WMO, 1965). These sensors are available from numerous dealers (see Appendix I).

The Maring-Marvin sunshine recorder is usually referred to as the Marvin, but was originally designed by Maring (Maring, 1898). It is essentially a differential air thermometer having a blackened bulb and a clear bulb mounted in an evacuated glass jacket. The temperature difference between the bulbs causes differential expansion of the alcohol separating the bulbs. This drives a column of mercury thereby closing an electric switch, which activates a suitable recording system such as a chronograph. The instrument must be set in the meridian plane at an angle, which is adjusted so that the mercury activates the electric circuit when the sun's disc can be just faintly seen through the clouds. This subjective procedure and the temperature dependence of the instrument are its weak points. Also, the instrument responds to diffuse as well as direct radiation. The device is no longer manufactured.

The Sumner-4 sunshine sensing element is composed of four to eight equal-spaced, bimetallic leaf elements, as shown in Figure 9-2.

Since the outer and inner leaves of each element are made of the same material, they absorb and lose heat at the same rate so they are, therefore, independent of large, rapid temperature chages. The inner leaf is shaded so that the differential heating of the exposed leaf relative to the shaded leaf causes the platinum contacts to come together and complete the electrical circuit. The electrical signal is then continuously recorded on a strip chart or integrated and digitally displayed and/or recorded.

When the sun is obscured, the diffuse radiation falling on the white glass base plate is reflected onto the blackened surface of the inner leaf element. This maintains the inner leaf at about the same temperature as the exposed outer leaf, thus keeping the contact open and preventing spurious recordings under strong diffuse radiation conditions. Ventilation of the housing maintains the instrument at ambient temperatures and provides cooling of the elements to insure rapid response.

The recording threshold of the instrument can be varied by changing the contact clearance. The leaves are adjusted to make contact at sunshine intense enough to cast a shadow–approximately 200 W $m^{-2}$ (20 mW $cm^{-2}$) at 15.6°C (60°F). The response time of the sensor ranges from 15 to 30 s. The sensor sensitivity tends to decrease as the temperature falls and wind speed increases. To overcome this, two models have been designed, one with deflector ventilation for temperatures between -6.7 and 48.9°C and the other with snow-proof chimney-type ventilation for operation in the range from -17.8 to 10.0°C. The records of daily sunshine totals for Aspendale, Australia compare well with daily totals obtained with a Campbell-Stokes instrument (Sumner, 1966).

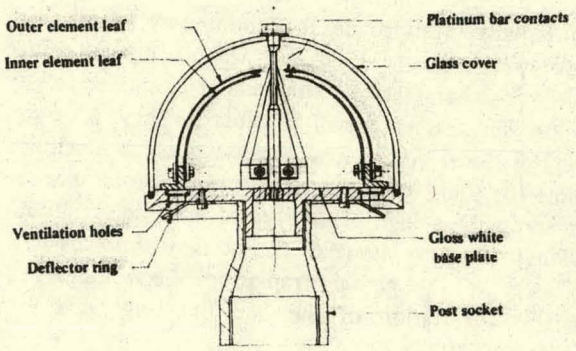


*Figure 9-2 Cross-section of sunshine sensing element (Sumner, 1966)*

The Sumner is manufactured and sold by Analite Pty. Ltd., Rauchfuss Instruments Division. [1]

The Jordan Photographic sunshine recorder consists of two semi-cylindrical cameras each having an aperture slit in its flat side through which photographic paper is exposed to the sun. The cameras are mounted side by side with one aperture facing

[1]Rauchfuss Instruments Divisions of Analite Pty. Ltd., Selby Scientific Ltd., 352-368 Ferntree Gully Road, Notting Hill, Melbourne, Victoria, Australia. Attn: Mr. Alan Prichard.

east and the other facing west. Although the simple design and permanency of records are attractive features, the daily adjustment required to prevent overlapping traces, and the special handling of the photographic paper cause operational problems. Much more uncertainty exists in these measurements than in the Campbell-Stokes measurements. This device is not in wide use.

The Foster sunshine switch was developed by Foster of the U. S. Weather Bureau[2] in 1953 (Foster and Foskett, 1953). The sensor is currently being used in the National Weather Service sunshine switch network (about 116 stations). The sensor consists of two selenium barrier-layer photovoltaic cells with one cell exposed to the direct solar radiation and the other cell shaded from it by a shade ring. The cells are connected in electrical opposition so that their response to diffuse light results in no output. Direct sunlight produces an output from the exposed cell which cannot be balanced by output from the shaded cell; the current actuates a recorder. The lag of the sensor is negligible, and its sensitivity allows reliable measurements from sunrise to sunset. This recorder is not commercially available.

The Haenni[3] Solar 110 and 111b Sunshine Recorders (Figure 9-3) and the Kunkis[4] Helior are examples of commercially available photoelectric sunshine recorders. Like the Foster, these devices have the advantage that their output can be recorded digitally, in contrast to the record of the Campbell-Stokes must be read manually.

These systems consist of two to six photovoltaic cells which receive solar radiation independent of the time of day and year. In order to distinguish between the direct and diffuse solar radiation components and thus register the duration of bright sunshine, a small

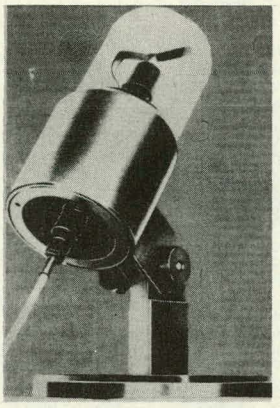

*Figure 9-3 The Haenni Solar 110 sunshine recorder*

rotor spins around a contact shaft alternately shading and exposing the cells. The shading element is small enough that on a cloudy day little signal change can result, but on a sunny day with bright sunshine a significant signal change results. The amplitude of the output signal is compared to a threshold value which can be adjusted. The duration (seconds or hours) above this threshold are recorded as the duration of bright sunshine. The manufacturer's specifications state that the sensitivity of these devices ranges from about 30 to 600 W $m^{-2}$ (3.0 to 60.0 mW $cm^{-2}$), which is a comparatively larger range than that of a Campbell-Stokes sensor. The Campbell-Stokes is often used by national meteorological services to record duration of sunshine; before these photoelectric devices are used a careful comparison should be made with a Campbell-Stokes sunshine recorder to establish a comparable threshold setting to allow direct comparison with historical records.

Another photoelectric sunshine recorder of unique design is that sold by Schlumberger[5]. The device is an octoganal arrangement of silicon photovoltaic cells as shown in Figures 9-4 and 9-5. It is tilted to the station latitude; four cell pairs allow for operation at all latitudes.

---

[2] Now the National Weather Service (NWS).

[3] Haenni and Cie. Ag. CH-3303 Jegenstorf b. Bern, Switzerland. (Also distributed by ENERCORP Instruments, Ltd., P.O. Box 20, Stn. U., Toronto, Ontario, M8F 5M4, Canada.)

[4] A. Kunkis, D-5100, Aachen-Oberforstback, Germany

[5] Enertec Schlumberger, 1 Rue Nieuport, Velizy-Villacoublay, F-78140, Paris, France.

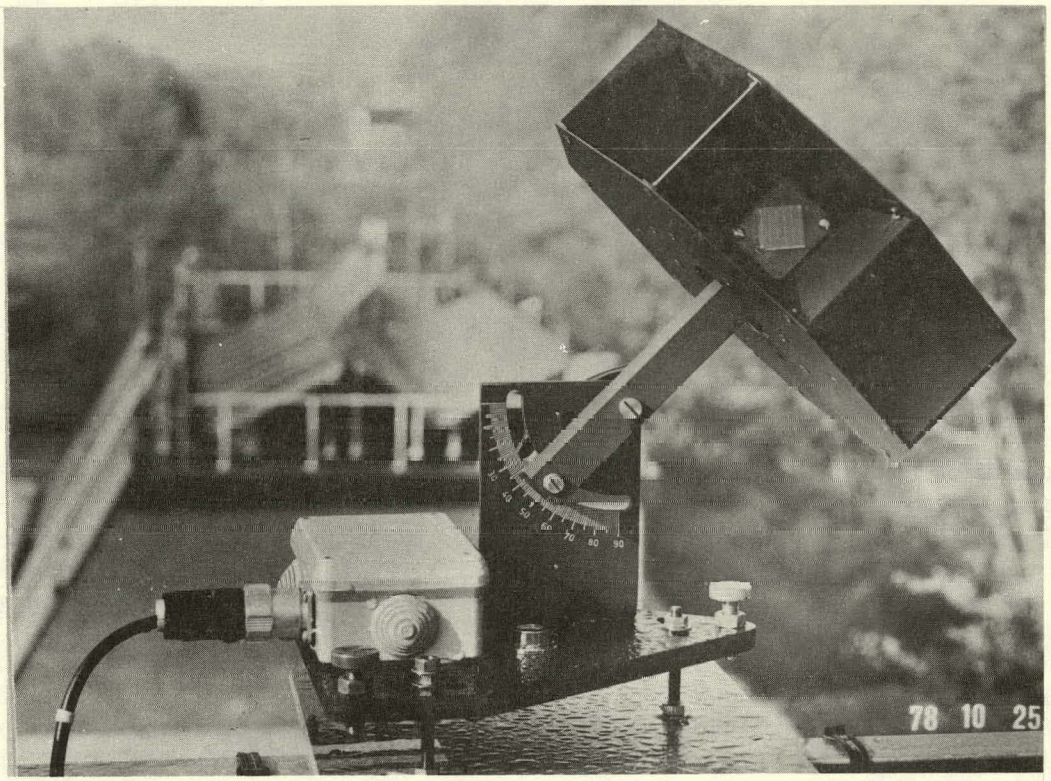


*Figure 9-4 Schlumberger sunshine recorder*

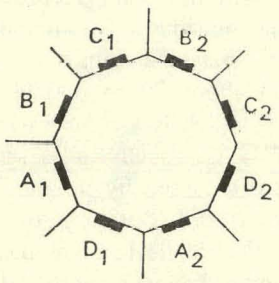


*Figure 9-5 Schlumberger sunshine recorder sensor arrangement. (Viton et al, 1978)*

The duration of sunshine is determined by comparing the outputs from the two cells, one exposed to the direct sunlight, and the other shaded (see Figure 9-6).

Viton et al (1978) found little difference between the records of the Schlumberger and Campbell-Stokes sunshine recorders over 18 months of comparisons.

A new prototype automatic sunshine recorder has been developed by the Deutscher Wetterdienst

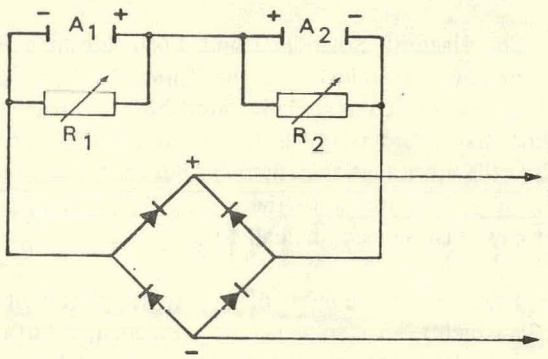


*Figure 9-6 Bridge circuit for comparing output of cell pairs (Viton et al, 1978).*

(German Weather Service) instrument development section in Hamburg (Dake and Linder, 1978). The design objectives of the device are:

- operation at a defined lower threshold independent of sun elevation and solar radiation received from sun and sky.
- electrical signal output.

- unattended operation.
- mean time between failure in excess of six months.
- simultaneous operation at several thresholds other than the basic threshold.

The basic components of the IAH receiver are mounted in a weather-tight box covered by a glass hemisphere (Figure 9-7). The solar radiation passes through the vertical slot guide and is picked up by the light conductor, which directs the radiation onto a silicon detector. The synchronous motor rotates the slot guide and light conductor around a vertical axis, twice per second. The conical head of the light conductor receives radiation with equal sensitivity independent of the sun's elevation. The output signal is chopped by means of the 180° diaphragm, and is rectified and supplied to go/no-go switches for the basic and three additional thresholds.

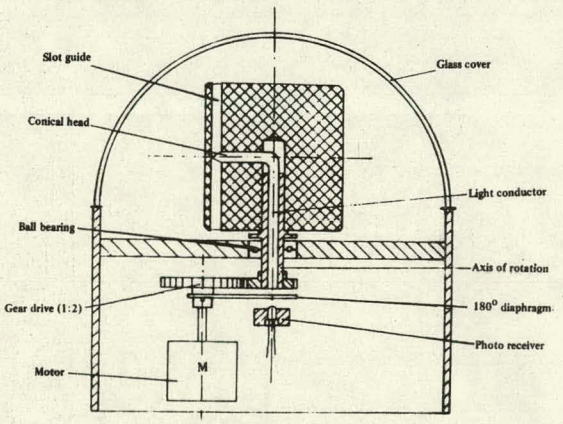


*Figure 9-7 Sectional view of the receiver unit (after Dake and Linder, 1978)*

Preliminary results compared with Campbell-Stokes and Helior recordings suggest that the design objectives have been met. Further testing is underway before field implementation.

### 9.3 Use of a Direct Beam Tracker and Compatible Data Acquisition System

It has been proposed and appears feasible that a solar tracking instrument such as a Normal Incident Pyrheliometer could serve a dual purpose. The data acquisition system would log the time that the direct beam is greater than 200 W $m^{-2}$ (20 mW $cm^{-2}$) (see discussion in section 9.2 where this value is quoted as the threshold to detect a shadow). The duration of sunshine could then easily be determined. Of course, as with the new systems described earlier, this method would need to be compared with others.

### 9.4 Correlation Between Sunshine Duration and Global Radiation

The daily sunshine duration correlates closely with global radiation. Coulson (1975) describes the relationship for estimating global radiation from measurements of sunshine duration. More information on solar radiation modelling in general will be provided by *IEA Solar Heating and Cooling Project Task V* to be published.

### 9.5 Maintenance of Sunshine Recorders

Sunshine recorders should receive daily care similar to that described in Chapter 4 of this handbook.

### References

Ångström, A. 1924. "Solar and Terrestrial Radiation." *Quarterly Journal of the Royal Meteorological Society*. Vol. 50. pp. 121-125.

Coulson, K. L. 1975. *Solar and Terrestrial Radiation: Methods and Measurements.* New York: Academic Press.

Dake, C. U. and Linder P. 1978. "A New Device for Measuring Sunshine Duration Adjustable in Accurately Known Thresholds." Personal Communication. Deutscher Wetterdienst. D-2000 Hamburg 65.

Foster, N. B. and Foskett, L. W. 1953. "A Photoelectric Sunshine Recorder." *Bulletin of the American Meteorological Society*. 34:212-215.

Maring, D. T. 1898. "An Improved Sunshine Recorder." *U.S. Department of Agriculture Misc. Publication.* Weather Bureau Circ. No. 148.

Sumner, C. J. 1966. "A Sunshine Sensing Device for Long Period Recording." *Quarterly Journal of the Royal Meteorological Society*. 92:567-569.

Viton, P., Godier, R. Plazy, J. L. and Pottier, H. 1978 *Capteurs Utilises en France Par Less Stations Automatiques.* To be published.

World Meteorological Organization. 1965. "Guide to Meteorological Instruments and Observing Practices." edition 4. WMO- No. 8, TP 3.

CHAPTER 10

# METEOROLOGICAL VARIABLES RELATED TO SOLAR ENERGY

B. B. Williams
Consulting Meteorologist
The Kenneth E. Johnson Environmental and Energy Center
The University of Alabama in Huntsville
Huntsville, Alabama 35807
The United States of America

## 10.1 Introduction

To obtain the full potential, understanding and application of solar radiation measurements, it is advisable to measure other meteorological phenomena at the solar radiation observation sites. One purpose of these measurements is to evaluate the effectiveness of the solar radiation for solar energy applications. Another purpose is to relate the climatological factors at the specific site to standard parameters measured throughout the world. Measurements for the latter purpose must conform to standard procedures for meaningful comparisons. Single measurements may meet both objectives in many situations, or it may be necessary to record more than one measurement of the same element, e.g., wind in an exposed location and on a building near collectors to satisfy both purposes. Data from nearby locations will be sufficient in most cases and additional measurements should be well justified.

The following sections briefly describe the meteorological phenomena related to solar radiation and the standard measurement requirements so that data collected will be compatible with those at other locations. Publications which give in detail the methods of observing and recording meteorological phenomena are listed in the references.

A list of the most commonly used meteorological instruments in any country may be obtained from its national meteorological service, whose office address is available from the Secretariat of the World Meteorological Organization (WMO), Geneva, Switzerland. Most manufacturers of radiation sensors listed in Chapter 9 and Appendix I also manufacture other meteorological equipment and will provide additional information upon request.

Although solar energy is not new, the increased use of solar energy is just evolving; the meteorological parameters discussed in this article will play an important role in this evolution and in the development of other energy sources.

## 10.2 Temperature

Temperature may be defined as a measure of the hotness or coldness of a body. In solar radiation measurements the temperature of the free air (ambient temperature) is required just above the surface of the earth. A height of between 1.25 and 2 m above ground level is recommended by the WMO (WMO, 1971) for measuring the surface air temperature.

The measurement of the ambient temperature is relatively simple remembering that heat can flow to or from the sensor, the thermometer, by conduction, radiation and convection. To obtain the true air temperature, the sensor should be isolated from all heat or cold sources except the air.

A shelter with a double top and louvered sides which permits air to circulate freely is the usual

housing for a mechanical-type thermometer, e.g., liquid expansion, vapor pressure or bimetallic strip. An electrical resistance or thermocouple thermometer normally includes the proper housing as an integral part of the unit.

The ground above which the thermometer is located should be representative of the surrounding area. A detailed discussion of shelters, including exposure and readings of maximum, minimum and regular liquid thermometers, is given in the *Weather Bureau Observing Handbook No. 2, Substation Observations* (1970).

The electrical type thermometer requires cleaning, routine maintenance and calibration. The operations manual for the instrument in use should be followed.

The temperature measurement scale generally used is Celsius (°C), related to the absolute thermodynamic Kelvin scale (K), t(°C) = T(K) - 273. The Celsius scale can be determined using a thermometer and interpolating between the ice point (0°C) and boiling point of water (100°C) at standard pressure (1013.25 mb, 101.32 kPa).

To convert from the Celsius to the Fahrenheit scale multiply degrees Celsius by 1.8 and add 32. Ambient air temperatures are generally recorded to tenths of a degree in any scale used. In some countries, including the United States, the Fahrenheit scale is still in use. Plans are underway in the U. S. A. to convert to the Celsius scale but it may be many years before historical records and summaries are converted.

Summaries of temperature data are straightforward and may be grouped by hours, days, months, seasons or years. The average temperature for a day is defined as the sum of the maximum and minimum temperatures divided by two.

The air temperature is an important meteorological parameter in most forms of energy conversion and in the application of energy. The temperatures applied often are the daily maximum and minimum and the computed mean (T) which is used in the computation of heating and cooling degree days.

Heating Degree Days (HDD) based on 18.3°C (65°F) are computed when the mean daily temperature (T) is below the base temperature by the formula:

$$HDD = \sum_{i}^{n}(T_n°C - 18.3) \quad or \quad \sum_{i}^{n}(T_n°F - 65).$$

and Cooling Degree Days (CDD) based on 18.3°C (65°F) are computed when the mean daily temperature (T) is above the base temperature by the formula:

$$CDD = \sum_{i}^{n}(T_n°C - 18.3) \quad or \quad \sum_{i}^{n}(T_n°F - 65)$$

To convert HDD and CDD as computed above from english units to metric units based on 18.3°C multiply by 0.556.

The ambient temperature per se does not affect the flux of radiation although, other elements remaining constant, the lower the temperature the more dense the air mass. As the amount of air mass penetrated by the solar beam increases, the greater the loss in the flux of radiation.

Hottel (1958) proposed that the approximate values of irradiance could be estimated using the equation:

$$\text{Total Solar Intensity} = 9.1\Delta + 1.26\Delta^2, \pm 50 \text{ W m}^{-2}$$

$$(1.6\Delta + 0.123\Delta^2, \pm 15 \text{ Btu/ft}^{-2} \text{ h}^{-1})$$

where $\Delta$ is the difference between the dry-bulb temperatures in the sun and the shade, expressed in deg C (F). Although the physical principles of this equation are correct, tests would have to be made at a site for the correct type of thermometer, that is, color of bulb exposed to sun and other properties. One must also account for the fact that the environment surrounding solar collector installations may be different from that where standard temperature measurements are made. However, as stated by Hottel (1958) tests of solar energy systems should be based on solar radiation measurements made in accordance with WMO recommendations concerning suitable equipment, and adequate installation and operating procedures.

## 10.3 Humidity

Water can exist in the atmosphere in three states: solid, liquid and vapor. The amount of water vapor present in the atmosphere can be expressed by several terms which are related: relative humidity, specific humidity and mixing ratio. If any one of these is known, along with the ambient temperature and pressure, the others may be calculated.

The term most commonly used is *relative humidity* which is the ratio, expressed as a percentage, of the amount of water vapor in the air to the amount of water vapor that the air, at the same pressure and temperature, could hold if saturated. When the word *humidity* is used alone it is generally accepted to mean relative humidity.

Four general types of sensors are used to measure air humidity: psychrometer (thermodynamic change), hair hygrometer (method using the dimensional change of a hygroscopic substance), electrical resistance hygrometer (method using the change of electrical resistance in an absorptive substance), and dew- or frost-point hygrometer (phase change, i.e., condensation or sublimation).

Psychrometers and hair hygrometers are most widely used, but the latter are not generally as accurate.

The general requirements for psychrometers as taken from WMO (1971), are:

(a) The wet and dry bulbs should be ventilated and protected from radiation by a minimum of two polished unpainted metal shields which are separated by insulating materials; or alternatively by a louvered screen plus one polished metal shield.

(b) At sea level, the air should be drawn past the bulb at a rate not less than 2.5 m $s^{-1}$ and not greater than 10 m $s^{-1}$, if the thermometers are of the types ordinarily used at meteorological stations. For appreciably different altitudes, these air-speed limits should be adjusted in inverse proportion to the density of the atmosphere.

(c) Separate ducts should be provided for the two thermometers.

(d) If the second of the alternatives (a) is used, the entrance of the ducts should be located so as to give the true ambient temperature, and the air should be delivered above the screen in such a position as to prevent recirculation.

(e) The greatest care should be taken to prevent significant amounts of heat from a motor being communicated to the thermometers.

(f) The water reservoir and wick should be so arranged that the water will arrive at the bulb with sensibly the wet-bulb temperature.

(g) Measurements should be taken at a height between 1.25 and 2 m above ground level.

To obtain accuracy with psychrometers the wet and dry bulbs should have approximately the same lag coefficient. With thermometers having the same size bulb the wet bulb has an appreciably smaller lag than the dry bulb. The fabric covering the wet bulb should fit snugly around the bulb and extend at least two centimeters below the bulb.

Psychrometric calculators, nomograms, or tables are used to obtain the relative humidity from measured values of the wet- and dry-bulb temperatures. The calculators, nomograms, and tables used must apply to the elevation of the observing sites.

The hygrothermometer is used extensively for obtaining the dew point and ambient air temperatures. This instrument may have dial indicators, recorder traces and remote sensors. A psychrometric calculator or table is then used to obtain the relative humidity from the temperatures indicated.

Detailed observing and operational procedures for various psychrometers and hygrothermometers are given in *Federal Meteorological Handbook No. 1, Surface Observations* (1970).

Psychrometers and hygrometers require the same precautions as to shelter, exposure site and maintenance as thermometers. The hygrometer should be cleaned at frequent intervals with distilled water and a soft, lint-free cloth.

The hygrothermometer requires weekly calibration checks which consist of comparing the readings

with simultaneous values from a ventilated shelter-mounted psychrometer. The hygrothermometer also requires fairly frequent servicing as described in its maintenance manual.

Generally, the data summaries which are used to determine the moisture in the air from historical records, contain the class intervals of temperature and an associated moisture parameter such as the relative humidity or dewpoint. Such data are recorded under standard conditions.

Water vapor plays a key role in the hydrologic cycle. Its molecular weight is 18 compared to the average molecular weight of about 28 for air. Thus, heating and evaporation near the surface of the earth results in water vapor being entrained in rising air and, with other atmospheric processes, transporting energy into the atmosphere. The energy is released as the water vapor condenses in the cooler air aloft.

The amount of water vapor in the air (the humidity) largely determines a person's comfort factor both in winter and summer. Humidity affects heating and cooling systems indirectly because of this comfort factor, but also directly because some systems with condensation and evaporation cycles depend on humidity.

The amount of water vapor in the atmosphere plays a major role in the penetration of solar radiation through the atmosphere. Chapter 3 lists eight wavelength regions where radiation is absorbed by $H_2O$ molecules.

## 10.4 Wind

The wind (movement of air) is the result of four forces: atmospheric pressure gradient, centrifugal, coriolis and frictional. The energy which produces the wind comes from the sun, either directly through uneven heating of the earth's surface or indirectly through condensation of water vapor.

Wind velocity, as defined by WMO (1971), is a three-dimensional vector quantity with small-scale random fluctuations in space and time superimposed upon a large-scale organized flow.

Wind, as used in this section, is taken to be the horizontal motion of the air past a given point about 10 m above open terrain. Open terrain is defined in WMO (1971) as an area in which the distance between the anemometer and any obstruction is at least ten times the height of the obstruction. Since the vertical wind component is small compared to the horizontal components, it is generally measured only for special studies. The absence of apparent motion of the air is termed *calm*.

Wind direction is defined as the true (not magnetic or grid) direction from which the wind is blowing and is reported in degrees to the nearest ten degrees using an 01 . . . 36 code; e.g., 36 will indicate wind from true north. The direction is determined by averaging the observed direction over a 1-, 5- or 10-min period. Of course, numerical averaging requires special treatment near 360 degrees, where large and small values of wind direction are adjacent.

Wind speed, the magnitude of the air motion, should be reported in meters per second ($m\ s^{-1}$) and should represent an average over a 1-, 5- or 10-min period.

The wind vane is the sensor for measuring wind direction. Middleton (1941) described a wind vane as being a body mounted unsymmetrically about a vertical axis, on which it is free to rotate. The end offering the greatest resistance to motion of the air goes to leeward. Self-synchronous motors may be used to display direction at one or more convenient locations, where continuous recordings of direction may be made.

Anemometers are instruments for measuring wind speed. Middleton (1941) classified them as: rotation anemometers, pressure-plate anemometers, bridled anemometers, pressure-type anemometers and cooling effect anemometers. Recently, more sensitive instruments have been developed for special studies, e.g., sonic anemometers detect variations in sound-wave transmission which is a function of the wind speed and is therefore a measure of its magnitude.

The rotating cup or propeller anemometer is most commonly used; it has two subassemblies, the rotor and the signal generator. A large number

of signal generators are commercially available so that the choice depends mainly on the type of data processor and readout system used.

The WMO (1971) lists the attainable and satisfactory characteristics for wind speed sensors as: range, 1 to 50 m $s^{-1}$; linearity, ±0.5 m $s^{-1}$; distance constant, 2 to 5 m. The distance constant varies directly with the moment of inertia of the rotor, inversely as the air density and depends on a number of geometric factors as indicated by MacCready and Jex (1964).

The maintenance and calibration of wind sensors depends on the operating system. Normally, very little maintenance on the direction sensor is required. A check can be made frequently on wind direction by visually comparing the wind vane with the direction dial or recorded value. The maintenance and calibration procedures contained in the operations manual of the wind speed sensor in use should be followed.

Wind speed should be recorded in m $s^{-1}$ to obtain a five-minute average preceding the time of observation. Presently some measurements are stored in km $h^{-1}$ and much archived data is in miles per hour.

Wind speed is generally summarized by frequency of occurrence in various class intervals. Such summaries are directly applicable for computing the power of the wind. Extreme wind speeds are frequently studied by applying statistical extremal theory to evaluate the return period and probability of occurrence of destructive winds within 5-, 10-, 50- or 100-year periods.

Wind direction is much more complex to present in summaries. Combinations of wind directions and speeds are generally displayed by *wind roses*—a specially constructed circular graph. A complete explanation is beyond the scope of this section. A meteorologist should be consulted to obtain data on wind direction and wind gusts.

Wind direction and speed are important parameters in many energy applications. The prevailing wind directions in summer and winter are factors to consider in locating and orienting a building. Proper design could diminish the effect of the cold winds and use the summer winds to advantage. The wind speed will be a major factor if a cooling tower, or an evaporation or drying process is involved in the energy application. Primary wind speed statistics used in designing wind power systems are: the average, the frequency of occurrence in various class intervals and the extreme values.

Although the wind per se does not affect the flux of radiation, the wind direction and speed are important factors affecting the amount of solar radiation received in many areas. This is especially true near large bodies of water and in mountainous regions. The winds bring the humid and cloudy weather which decrease the flux of solar radiation. Moist air, when lifted in mountainous regions, may condense and produce cloudiness.

## 10.5 Other Parameters

The following meteorological measurements are used mainly for the evaluation and application of solar radiation data.

### 10.5.1 Clouds

The amount of sky covered by clouds is referred to as cloudiness in this section. *The Federal Meteorological Handbook No. 1, Surface Observations* (1970) instructs cloud amount be measured in tenths, while WMO (1971) recommends that it be measured in eighths. The clouds do not have to be opaque.

For a complete description of cloud forms and methods of observation see WMO *International Cloud Atlas* (1956) and WMO No. 8, TP3 *Guide to Meteorological Instruments and Observing Practice* (1971).

The major factor depleting the solar beam is the cloudiness. Therefore, a rough estimate of cloudiness can be made from solar radiation measurements and vice versa. A sunshine recorder can also be used to obtain a gross estimate of cloud amount. Other instruments have been developed to provide such estimates, but at present acceptable values are only obtained in practice by visual observations. Under partly cloudy skies a brief increase in solar radiation intensity is caused by the reflection of the solar beam from cumulus type clouds.

Ångström (1924) assumed the following linear relationships:

$$G = G'(a' + b'\frac{S}{S_o}) \quad (1)$$

where:

G = Average horizontal solar radiation received during a certain period;

G′ = Clear day horizontal solar radiation for the same period;

S = Average daily hours of bright sunshine for the same period;

$S_o$ = Maximum daily hours of bright sunshine for the same period;

a′,b′ = Constants used with clear day horizontal solar radiation.

The values of a′ and b′ for several countries and stations are listed in Table 10-1. Values of G′ and day length can be obtained from Figures 10-1 and 10-2, respectively.

More recently, Page (1961, 1975) has modified the method based on extraterrestrial radiation on a horizontal surface:

$$G = G_o(a + b\frac{S}{S_o}) \quad (2)$$

where:

$G_o$ = Horizontal extraterrestrial radiation for the same period and location in question;

a,b = Modified constants used with horizontal extraterrestrial radiation.

$$a = \frac{G'}{G_o}a' \quad \textit{and} \quad b = \frac{G'}{G_o}b' \quad (3)$$

Sample values of a and b are listed in Table 10-2 and 10-3. $G_o$ can be obtained from Figure 10-3.

Löf et al (1966) developed a table from Prescott (1940) as suggested by Kimball (1919) using climatic

Table 10-1

a′ and b′ Values of the Formula $G = G'(a' + b'\frac{S}{S_o})$ for Several Countries and Stations

| COUNTRY / STATION | AUTHOR AND PUBLICATION DATE | ANNUAL MEAN a′ | ANNUAL MEAN b′ | SEASONAL OR MONTHLY MEANS OF a′ AND b′ |
|---|---|---|---|---|
| AUSTRALIA | HOUNAM (1958) | 0.34 | 0.66 | SUMMER a′ b′ / WINTER a′ b′ |
| ASPENDALE | FUNK (1965) | 0.38 | 0.62 | ASPENDALE 0.36 0.64 / ASPENDALE 0.40 0.60 |
| DENILIQUIN | FUNK (1965) | 0.345 | 0.655 | DENILIQUIN 0.32 0.68 / DENILIQUIN 0.37 0.63 |
| GREECE | | | | J F M A M J J A S O N D |
| ATHENS | MACRIS (1964) | 0.34 | 0.63 | a′ 0.39 0.39 0.29 0.37 0.34 0.29 0.29 0.25 0.32 0.30 0.41 0.44 |
| | | | | b′ 0.60 0.61 0.65 0.63 0.63 0.63 0.63 0.63 0.58 0.60 0.64 0.58 |
| INDIA | | | | JULY - SEPT. a′ b′ / REST OF THE YEAR a′ b′ |
| CALCUTTA | | 0.33 | 0.48 | 0.35 0.54 / 0.32 0.49 |
| DELHI | | 0.38 | 0.57 | 0.29 0.71 / 0.47 0.45 |
| MADRAS | RAMDAS (1964) | 0.37 | 0.49 | 0.39 0.49 / 0.37 0.49 |
| POONA | | 0.44 | 0.51 | 0.42 0.61 / 0.42 0.52 |
| INDONESIA | | | | J F M A M J J A S O N D |
| BANDUNG | DEE AND REESINEK (1951) | 0.35 | 0.65 | a′ 0.40 0.40 0.37 0.34 0.32 0.29 0.29 0.29 0.32 0.35 0.38 0.40 |
| | | | | b′ = 1 - a′ |
| THE NETHERLANDS | | | | J F M A M J J A S O N D |
| DE BILT | DE BOER (1961) | 0.32 | 0.68 | a′ 0.23 0.30 0.31 0.31 0.32 0.33 0.31 0.32 0.31 0.27 0.28 0.24 |
| | | | | b′ = 1 - a′ |
| SWEDEN | | | | SPRING SUMMER AUTUMN WINTER |
| STOCKHOLM | ÅNGSTRÖM (1956) | 0.25 | 0.75 | a′ 0.25 0.23 0.25 0.27 |
| | | | | b′ = 1 - a′ |

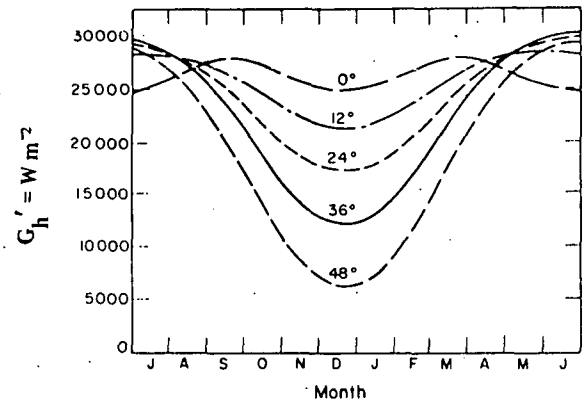


*Figure 10-1 Clear day solar radiation on a horizontal plane for various latitudes.*

classifications of Trewartha (1954), reproduced as Table 10-2. The coefficients a and b in this table may be used in Eq. (2). Table 10-3 gives values for a and b for Austria from Neuwirth (1979). $S/S_o$ may be obtained from local climatological services or from world cloud cover maps.

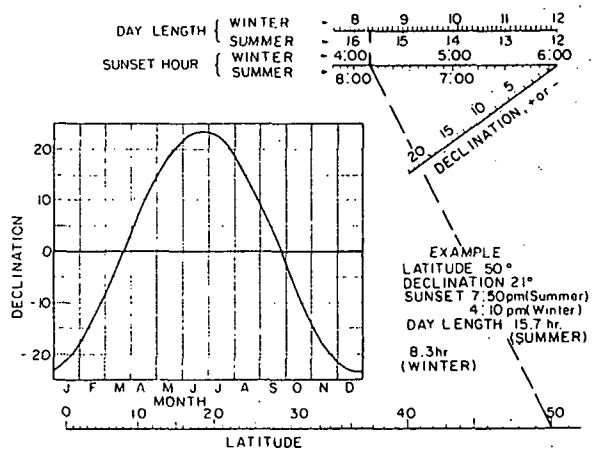


*Figure 10-2 Nomogram to determine time of sunset and day length (Whillier, 1965).*

Table 10-2

Constants a and b and Average Percent Possible Sunshine, $S/S_o$, for Various Locations and Climatic Types*

| Location | Type of Climate | a | b | $S/S_o$ (%) |
|---|---|---|---|---|
| Miami, Florida | Tropical rainy, winter dry | 0.42 | 0.22 | 65 |
| Honolulu, Hawaii | Tropical rainy, no dry season | 0.14 | 0.73 | 65 |
| Stanleyville, Congo | Tropical rainy, no dry season | 0.28 | 0.39 | 48 |
| Poona, India | Tropical rainy, no dry season | 0.30 | 0.51 | 37 |
| Malange, Angola | Tropical rainy, winter dry | 0.34 | 0.34 | 58 |
| Ely, Nevada | Dry, arid (desert) | 0.54 | 0.18 | 77 |
| Tamanrasset, Sahara | Dry, arid (desert) | 0.30 | 0.43 | 83 |
| El Paso, Texas | Dry, arid (desert) | 0.54 | 0.20 | 84 |
| Albuquerque, New Mexico | Dry, arid (desert) | 0.41 | 0.37 | 78 |
| Brownsville, Texas | Dry, semiarid (steppe) | 0.35 | 0.31 | 62 |
| Charleston, South Carolina | Humid mesothermal, no dry season | 0.48 | 0.09 | 67 |
| Atlanta, Georgia | Humid mesothermal, no dry season | 0.38 | 0.26 | 59 |
| Buenos Aires, Argentina | Humid mesothermal, no dry season | 0.26 | 0.50 | 59 |
| Hamburg, Germany | Humid mesothermal, no dry season | 0.22 | 0.57 | 36 |
| Nice, France | Humid mesothermal, dry summer | 0.17 | 0.63 | 61 |
| Madison, Wisconsin | Humid continental, no dry season | 0.30 | 0.34 | 58 |
| Blue Hill, Massachusetts | Humid continental, no dry season | 0.22 | 0.50 | 52 |
| Dairen, Manchuria | Humid continental, dry winter | 0.36 | 0.23 | 67 |

*After Löf, et al (1966)

Table 10-3

Values of a and b for Austria (48°N Lat) for Use in the Formula $G = G_o(a + b\ S/S_o)$ for the Range of Monthly Mean Values of $S/S_o$: 0.11-0.62

| Winter altitude | a | b | Spring | a | b |
|---|---|---|---|---|---|
| 100-300m | 0.18 | 0.49 | 100-300m | 0.21 | 0.49 |
| -500m | 0.22 | 0.48 | -500m | 0.21 | 0.49 |
| -1000m | 0.23 | 0.41 | -1000m | 0.24 | 0.45 |
| -1500m | 0.23 | 0.51 | -1500m | 0.25 | 0.48 |
| -2000m | 0.36 | 0.36 | -2000m | 0.38 | 0.36 |
| -3000m | 0.43 | 0.36 | -3000m | 0.44 | 0.32 |
| Summer altitude | a | b | Fall | a | b |
| 100-300m | 0.21 | 0.47 | 100-300m | 0.18 | 0.51 |
| -500m | 0.21 | 0.48 | -500m | 0.20 | 0.49 |
| -1000m | 0.22 | 0.46 | -1000m | 0.21 | 0.42 |
| -2000m | 0.22 | 0.54 | -2000m | 0.27 | 0.54 |
| -3000m | 0.33 | 0.46 | -3000m | 0.36 | 0.40 |

Source: Neuwirth 1971

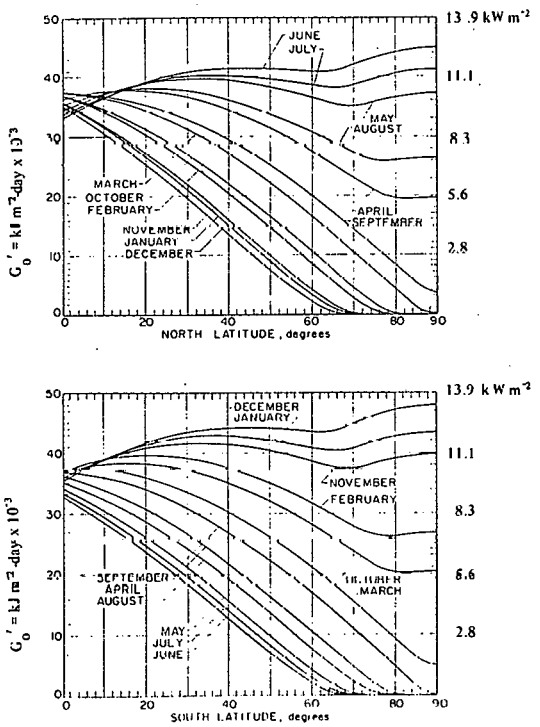


*Figure 10-3 Extraterrestrial daily solar radiation on a horizontal surface, for mid-point of each month.*

An analysis of the work done by Neuwirth (1979) shows that of 1,206 months of calculations ($Q_{cal}$) at 14 locations compared with global radiation measured ($Q_m$), the measure of error ($f = (1 - Q_{cal}/Q_m)\ 100$ yields the following generalization of the expected frequency of error:

99% of the calculations are within an error band of ±17%.

80% of the calculations are within an error band of ±10%.

57% of the calculations are within an error band of ±5%.

As stated by Coulson (1975), the use of sunshine duration measurements to estimate global solar radiation are empirical although based on sound physical principles and the results are valuable for areas with few available solar radiation measurements. However, these estimates are poor substitutes for the actual measurements.

### 10.5.2 Precipitation

Precipitation is water that either reaches the ground as liquid (rain or drizzle) or solid (snow, snow pellets, snow grains, ice pellets, hail or ice crystals) or freezes upon impact with the ground (freezing rain, freezing drizzle, rime or glaze).

The average raindrop diameter in light rain is near 1.3 mm; in heavy rain, near 2.0 mm. Seldom will raindrops over 6 mm occur as the rate of fall breaks such large drops into smaller ones (Daniels, 1976).

Measurements are made of the vertical depth of the water or water equivalent (liquid content) of all forms of solid precipitation which fall to the ground during a known period of time. The WMO (1971) recommends that the amount of precipitation be measured in millimeters, to the nearest 0.2 mm if the amount is 10 mm or less. Larger amounts of precipitation should be read to within 2% of the total. Precipitation less than 0.005 inch (.127 mm) is recorded as a *trace* in the United States. Snowfall is the depth of fresh snow covering a horizontal surface, measured in centimeters. One centimeter of fresh snow is equivalent to about one millimeter of rainfall, but this is only a rough approximation since the ratio depends on the snow texture.

Precipitation gauges essentially consist of an open cylinder having a fairly sharp upper edge for collecting and measuring all precipitation falling into it.

For non-recording gauges the area of the receiver should be known; a collector and a measuring cylinder or dip rod is required. The precipitation could also be measured by weighing.

Recording gauges can be divided into two main classes that record: (1) the accumulated amounts of precipitation which fall; (2) the instantaneous rate of rainfall.

Recording precipitation gauges can be classified into float, tipping bucket, drop counter and weighing types.

The following is an extract from *Weather Bureau Observing Handbook No. 2, Substation Observations* (1970) concerning precipitation gauges:

> "The exposure of a rain gauge is of primary importance in the accuracy of precipitation measurements, especially snowfall measurements. An ideal exposure would eliminate all turbulence and eddy currents near the gauge that tend to carry away the precipitation. The loss of precipitation in this manner tends to increase with wind speed. Obstructions which individually or in small groups, are numerous and so extensive that they reduce the prevailing wind speed, turbulence, and eddy currents near the gauge are usually beneficial in providing a more accurate catch. The best exposures are often found, therefore, in orchards, openings in a grove of trees, bushes or shrubbery, or where fences and other objects acting together serve as an effective windbreak. As a general rule in areas where objects and their distances from the gauge are generally uniform, their heights above the gauge should not exceed about twice their distances from it."

In open areas, individual or small groups of isolated objects near a gauge may generate vigorous eddies. As a general rule, the height of each object above the gauge should not exceed half the distance from it. Since it is not always possible to select sites which provide adequate protection from adverse wind effects, an open site away from isolated objects may be the only location available.

Wind shields help to minimize loss in precipitation catch. Wind effects or losses are much greater during snowfall than rainfall. Thus, wind shields are not generally installed at substations in locations where snowfall constitutes less than 20% of the mean annual precipitation.

Good exposures are not always permanent. The growth of vegetation, trees and shrubbery, and man-made alterations to the surroundings may change an excellent exposure to an unsatisfactory one in a relatively short time.

For the correct measurement of precipitation, the open end of the gauge (the receiver) must be in a horizontal plane.

The frequency and size of hail should be considered so that collectors can withstand the most severe conditions expected. Also the weight of snow in

conjunction with collector installations should be considered.

Precipitation, particularly snow, will change the albedo of the surrounding area and therefore affect both terrestrial and global radiation. During periods with precipitation the fluxes of direct and diffuse radiation will be near their lowest values; however, during periods with an unpolluted, cloudless and dry air mass these fluxes will be at a maximum and a minimum, respectively.

### 10.5.3 Atmospheric Pressure

Atmospheric pressure at a given level in the atmosphere is the weight of a vertical column of air of unit cross sectional area extending from that level to the outer limits of the atmosphere. Atmospheric pressure can be measured by mercury barometers, aneroid barometers or hypsometers. Hypsometers depend on the relationship between the boiling point of a liquid and the atmospheric pressure and have been of only limited application in meteorology. The mercury barometer is the most accurate instrument but the aneroid barometer has the advantage of portability and convenience. The aneroid barometer reading should be compared frequently with that from the mercury barometer which itself should be compared with a standard or another mercury barometer semi-annually.

The WMO (1971) recommends that the millibar (mb) be used for reporting pressure for meteorological purposes, (1 mb = 1000 dynes $cm^{-2}$). However, on the International System (SI) of units pressure should be reported in kilopascals (kPa), (1 Pa = 1 N $m^{-2}$).

Standard atmospheric pressure at sea level is defined as 101.32 kPa, 1013.2 mb, 29.92 in Hg., or 760.0 mm Hg.

Details as to the proper maintenance and reading of barometers are given in the *Federal Meteorological Handbook No. 1, Surface Observations* (1970).

Atmospheric pressure is generally converted to a hypothetical sea level pressure for synoptic comparison with pressures at other stations and for support of aircraft operations. For solar energy applications the atmospheric pressure at the station (station pressure) should be used in computations.

As the solar beam enters the atmosphere it is depleted by scattering, reflection and absorption. Therefore, the atmospheric pressure at a particular location is required to determine the total amount of atmosphere that the solar beam must penetrate before reaching the earth's surface.

### 10.5.4 Visibility

Visibility, as used here, is defined as the greatest distance at which an object can be identified when observed against a background of the sky or fog. At night, the visibility is defined as the greatest distance at which stationary lights of moderate intensity, unfocused, can be observed. Prevailing visibility as defined in *Federal Meteorological Handbook No. 1* (1970) is the greatest horizontal visibility prevailing throughout at least half of the horizontal circle which need not necessarily be continuous.

In the metric system visibility is reported in kilometers and decimal fractions. In the United States visibility is reported in miles and in selected fractional values if less than 3 miles.

The most practical means of obtaining the prevailing visibility is by visual observations. An instrument to measure visibility would be more practical for the nighttime or for occasions when suitable visibility markers are not present or for observations required in a special sector. An instrument for measuring visibility measures either the attenuation or extinction coefficient of a long, large cylinder of air, or the scattering of light from a small volume of air. The instrument most commonly used (transmissometer) measures the decrease in brightness of the beam from a small source located a few hundred meters distance by means of a photoelectric device situated at the focus of a condensing lens. This type of instrument requires frequent checks and calibration. A television camera and receiver can also be used to observe special reference lights.

Visibility measurements are valuable for evaluating solar radiation data from those stations which have no measurement of solar radaition transmission through the atmosphere, e.g., transmittance, turbidity

or clearness factors. The computation of the decrease in solar beam intensity as it penetrates the atmosphere is very complex. One depletion factor is atmospheric pollution; visibility gives a gross estimate of the impurities in the lower atmosphere.

An example of variability of atmospheric transmittance is indicated by records of the U. S. National Weather Service for Boston and Blue Hill, MA., located about 10 miles apart at the same altitudes. Mean values for the weeks including March 21, June 21, September 22 and December 21, are, respectively, 0.45, 0.43, 0.43, 0.39 for Boston, and 0.55, 0.51, 0.52, 0.50 for Blue Hill (Hottel, 1958).

### 10.5.5 Impurities in the Atmosphere

The effect of impurities on solar radiation passing through the atmosphere is discussed elsewhere in this handbook in terms of path length, turbidity and other factors. However, two effects of impurities must be considered by the engineer, because they interact with the collector materials and may accumulate on the collectors.

- The interaction with collector material requires a knowledge of the chemical composition of the impurities and measurements of their effects on exposed materials. Each case must be determined individually.

- The potential accumulation of impurities on the collectors is believed to decrease collector efficiency only slightly, however, because of very little experience, this effect should be considered. Other important items are the frequency of precipitation which may clean the collectors, and the tilt angle of the collectors. Although there may be an optimum tilt angle to take advantage of natural cleaning of the collector surfaces, other factors must be considered in determining the slope.

## 10.6 Concluding Remarks

The meteorological elements discussed are important, either directly or indirectly, for the performance of solar energy systems, energy conservation and other conversion systems. The instrumentation, installation and observation procedures of these elements must follow established standards. Some variation from these standards may be required for local testing of energy systems, but these should be kept to a minimum.

If an established meteorological station is nearby, generally within 35 km of the test site, the meteorological parameters of interest should be measured only for about one year. A correlation could be established between the parameters of the two locations; thereafter, the parameters at the permanent station would only be used.

Precise measurements of solar and terrestrial radiation in combination with standard measurements of other meteorological variables are important not only for developing solar and other energy systems but also for studying the transformation of energy within the earth-atmosphere system and for meeting the needs of biological, medical, agricultural and industrial activities. These measurements should increase in value in the future when conservation and conversion of energy become more critical.

### References


Ångström, A. K. 1924. "Solar and Terrestrial Radiation." *Quarterly Journal of the Royal Meteorological Society*. No. 50, pp. 121-125.

Coulson, K. L. 1975. *Solar and Terrestrial Radiation*. New York: Academic Press.

Daniels, G., ed. 1976. "Terrestrial Environment Criteria Guidelines for Use in Aerospace Vehicle Development." *NASA TM X-64757*. Marshall Space Flight Center, Huntsville, AL.

Hottel, H. C. 1958. "Solar Energy for Heating." *Mechanical Engineers' Handbook*. New York: McGraw-Hill.

Kimball, H. H. 1919. "Variations in the Total Luminous Solar Radiation with Geographical Position in the United States." *Mon. Weather Rev.* No. 47, pp. 769-793.

Löf, G. O. G., Duffie, J. A. and Smith, C. O. 1966. "World Distribution of Solar Radiation." *Solar Energy*. No. 10, pp. 27-37.

MacCready, P. B., Jr. and Jex, H. R. 1964. "Response Characteristics and Meteorological Utilization of Propeller and Vane Wind Sensors." *Journal of Applied Meteorology*. No. 3. pp. 182-193.

Middleton, W. E. 1941. *Meteorological Instruments.* Toronto, Canada: The University of Toronto Press.

Neuwirth, F. 1979. "Meteorological Research at Service of Solar Energy Utilization." Results of Research and Development work in Austria, 1979. pp. 11-21. ASSA Report.

Page, J. K. 1961. "The Estimation of Monthly Mean Values of Daily Total Short-Wave Radiation on Vertical and Inclined Surfaces from Sunshine Records for Latitudes 40°N-40°S." *Proceedings of the United Nations Conference on New Sources of Energy*. Vol. 4, p. 378.

Page, J. K. 1975. "The Estimation of Monthly Mean Values of Daily Total Short-Wave Irradiation on Vertical and Inclined Surfaces From Sunshine Records for Latitudes 60°N-40°S." Report BS32, Department of Building Science, University of Sheffield, p. 42.

Prescott, J. A. 1940. "Evaporation from a Water Surface in Relation to Solar Radiation." *Trans. Roy. Soc. So. Aust.* No. 64, pp. 114-125.

Trewartha, G. T. 1954. *An Introduction to Climate.* New York: McGraw-Hill.

U. S. Department of Commerce, et al. 1970. *Federal Meteorological Handbook No. 1, Surface Observations.* U. S. Department of Commerce, U. S. Department of Defense, U. S. Department of Transportation.

U. S. Department of Commerce, 1970. *Weather Bureau Observing Handbook No. 2, Substation Observations.* U. S. Department of Commerce, U. S. Weather Bureau.

Whillier, A. 1965. "Solar Radiation Graphs." *Solar Energy*. No. 9, pp. 164-165.

World Meteorological Organization. 1956. *International Cloud Atlas.* Geneva. Vols. I and II.

World Meteorological Organization. 1971. *Guide to Meteorological Instrument and Observing Practices.* No. 8, TP. 3.

**Bibliography**

Carter, E. A. Greenbaum, S. A. and Patel, A. M. 1976. *Listing of Solar Radiation Measuring Equipment and Glossary.* Prepared for ERDA Division of Solar Energy, Contract ERDA/NASA/3129317613. July, 1976.

deJong, B. 1973. "Net Radiation Received by a Horizontal Surface at the Earth." monograph published by Delft University Press. The Netherlands.

Duffie, J. A. and Beckman, W. A. 1974. *Solar Energy Thermal Processes.* New York: John Wiley & Sons, Inc.

EI & I Associates. 1975. "Determining the Availability of Solar Energy Within the Contiguous United States."

Hottel, H. C. and Woertz, B. B. 1942. "Performance of Flat Plate Solar Heat Collectors." Trans. *ASME*. No. 64, p. 91.

Houghton, G. 1951. "On the Physics of Clouds and Precipitation." *Compendium of Meteorology*. American Meteorological Society. Boston, Massachusetts. pp. 165-181.

Liu, B. Y. H. and Jordan, R. C. 1960. "The Interrelationship and Characteristic Distribution of Direct, Diffuse and Total Solar Radiation." *Solar Energy*. Vol. 4, No. 3, pp. 1-19.

Liu, B. Y. H. and Jordan, R. C. 1961. "Daily Insolation on Surfaces Tilted Toward the Equator." Trans. ASHRAE, No. 1762.

Rankins, W. H., III and Wilson, D. A. 1976. *The Solar Energy Notebook.* Lorien House, P. O. Box 1112, Black Mountain, North Carolina, 28711, U. S. A.

## APPENDIX I

# MANUFACTURERS AND DISTRIBUTORS OF SOLAR RADIATION MEASURING INSTRUMENTS

### Introduction

The development of solar radiation measuring instruments is not as advanced as many instruments used to sense atmospheric parameters. The instrument requirements are unique and have been discussed elsewhere in this handbook.

The purpose of this appendix is to identify manufacturers and distributors of solar radiation measuring instruments. Since this is the first attempt for such a list by an international organization, it may not be complete and it was difficult to differentiate between manufacturers and distributors. Some corrections may be necessary.

No attempt is made in this appendix to list types of instruments nor to evaluate performance. The manufacturers' performance data for many of the instruments are included in a U. S. Department of Energy report, *Catalog of Solar Radiation Measuring Equipment.*[1]

A format has been developed to list the primary performance considerations of instruments, either from manufacturers' specifications or from independent laboratory testing. The format is included in the appendix to assist in comparing and evaluating various instruments.

---

[1] Carter, E. A., Breithaupt, W. G. and Patel, A. M. 1977. *Catalog of Solar Radiation Measuring Equipment.* Energy Research and Development Administration (now U. S. Department of Energy), Division of Solar Energy, ORO/5362-1, April 1977.

## MANUFACTURERS AND DISTRIBUTORS OF

## SOLAR RADIATION MEASURING INSTRUMENTS

### Australia

Herbert A. Groise & Co.
Rear 1
Gordon Drive
Malvern, Australia

† Middleton Instruments
75-79 Crockford Street
Port Melbourne, Victoria 3207
Australia

Rauchfuss Instruments Division of Analite Pty., Ltd.
352-368 Ferntree Gully Road
Notting Hill
Melbourne, Victoria
Australia

† Solar Radiation Instruments
21-21A Rose Street
Altona, Victoria 3018
Australia

Swissteco Pty., Ltd.
Instrument Division
26 Miami Street
East Hawthorne
Melbourne, Victoria 3123
Australia

### Austria

* Philipp Schenk
Ges. M.B.H. Wien & Co., KG
Jedleseerstrasse 59
1212 Wien,
Austria

### Canada

† Enercorp Instruments, Ltd.
P. O. Box 20 Stn. U
Toronto, Ontario M8Z 5M4
Canada

### Denmark

* Siemen Ersking
Instrument Maker
Rørsangervej 7
Federikssund, DK 3600
Denmark

### Finland

* VAISALA Oy
PL 26
SF 00421 Helsinki 42
Finland

### France

* Enertic Schlumberger
1Rue Nieuport,
Velizy-Villacoublay F-78140
Paris, France
Tel. 1-946-9650
Telex SISVIL 698201

### Germany

* Adolf Thiess GmbH & Co., KG
Klima -, Mess-und Regeltechnik
3400 Gottingen - Geismar
Hauptstrasse 76
Federal Republic of Germany

* Dr. Bruno Lange GmbH
Königsweg 10
D-1000 Berlin 37
Federal Republic of Germany

Wilhelm-Lambrecht KG
Friedländerweg 65
D-34 Gottingen
Federal Republic of Germany

**Germany (cont.)**

Wolters U. Möhring
Lutzowstrasse 102-104
D-1000 Berlin 30
Federal Republic of Germany

**Italy**

* Assing
Ingegneri Associati
Via A. De Pretis, 70
00184 - Roma
Italy

* Italglas S. P. A.
Piazza Rossetti 4-18
16129 - Genova
Italy

* Montedel - Laben
Via E. Bassini, 15
20133 - Milano
Italy

* Sielco S. R. L.
Via Carlo Poma, 4
00195 - Roma
Italy

* Soc. Salmoiraghi
Piazzale Kennedy
16129 - Genova,
Italy

* Soc. Siap
Via Massarenti 412-2°
40138 - Bologna
Italy

* 3 G Electronics
Via del Perugino, 9
20135 - Milano
Italy

**Japan**

* EKO Instrument Trading Co., Ltd.
21-8 Hatagaya 1-chome
Shibuya-ku, Tokyo
151 Japan

**Japan (cont.)**

† Ishikawa Trading Co., Ltd.
4-6-13 Shinkawa
Mitaka, Tokyo, 181,
Japan

* Nekano Seisakusho Ltd.
Higashi Mita 1525
Ueno-City Mie prefecture
Japan (518)

**The Netherlands**

* Kipp and Zonen
P. O. Box 507
Delft, The Netherlands

**Sweden**

The Swedish Meteorological & Hydrological Inst.
SMHI, Fack
S-601 01 Nörrkoping
Sweden

**Switzerland**

Dr. C. Frolich
Physico-Meteorological Observatory
CH-7270
Davos-Platz, Switzerland

Haenni and Company
CH-3303 Jergenstorf b.
Bern, Switzerland

**U. S. S. R.**

* Mashpriborintorg
Smolenskaya - Sennaya Square 32-34
Moscow, U. S. S. R.

**United Kingdom**

* C. F. Casella and Co., Ltd.
Regent House
Britannia Walk
London, N1 7 ND, England

**United Kingdom (cont.)**

* Lintronic Limited
54-58 Bartholomew Close
London, ECIA 7 HB
England

**United States of America**

* Belfort Instrument Co.
1600 South Clinton Street
Baltimore, MD 21227, U. S. A.

* C. W. Thornthwaite Associates
Route 1, Centerton
Elmer, NJ 08318, U. S. A.

Devices & Services Co.
3501-A Milton
Dallas, TX 75205, U. S. A.

* Eppley Laboratory, Inc.
12 Sheffield Avenue
Newport, RI 02840, U. S. A.

* Gamma Scientific, Inc.
3777 Ruffin Road
San Diego, CA 92123, U. S. A.

* Hy-Cal Engineering
12105 Los Nietos Road
Santa Fe Springs, CA 90670, U. S. A.

* Kahl Scientific Instruments Corp.
P. O. Box 1166
El Cajon (San Diego), CA 92022, U. S. A.

* LI-COR, Inc.
4421 Superior Street
P. O. Box 4425
Lincoln, NE 68504, U. S. A.

† Matrix, Inc.
537 South 31st Street
Mesa, AZ 85204, U. S. A.

Molectron Corporation
177 N. Wolfe Road
Sunnyvale, CA 94086, U. S. A.

**U. S. A. (cont.)**

* Rho Sigma
15150 Raymer Street
Van Nuys, CA 91405, U. S. A.

† Science Associates, Inc.
230 Nassau Street
P. O. Box 230
Princeton, NJ 08540, U. S. A.

* Spectran Instruments
P. O. Box 891
La Habra, CA 90631, U. S. A.

* Spectrolab
12500 Gladstone Ave.
Sylmar, CA 91342, U. S. A.

† Sun Systems, Inc.
P. O. Box 347
Milton, MA 02186, U. S. A.

† Technical Measurements, Inc.
P. O. Box 838
La Canada, CA 91011, U. S. A.

† Teledyne Geotech
3401 Shiloh Road
Garland, TX 75041, U. S. A.

† WeatherMeasure Corporation
P. O. Box 41257
Sacramento, CA 95841, U. S. A.

† WEATHERtronics, Inc.
2777 Del Monte Street
P. O. Box 1286
West Sacramento, CA 95691, U. S. A.

† Yellow Springs Instrument Co.
Yellow Springs, OH 45387, U. S. A.

* = manufacturer
† = retail distributor
(no annotation = the manufacturing capability is unknown.)

## INSTRUCTIONS FOR INSTRUMENT

## DESCRIPTION AND PERFORMANCE FORM

1. **LETTERHEAD/LOGO**: In the space provided, attach a camera-ready mechanical of manufacturer or distributor letterhead or logo. This letterhead/logo must include the name, division, and mailing address. The left-hand edge of the mechanical should align with the left-hand guide line.

2. **CONTACT FOR FURTHER INFORMATION**: In the space provided, type the name of the person or office, telephone number and mailing address to be contacted for further information.

3. **PRODUCT DATA**: In the space provided, type answers to questions listed:

   a. **Model/Part No.**: Model or part number of the product on list of manufacturer or distributor.

   b. **Classification of the Instrument**:

      1. *Pyrheliometer:* An instrument for measuring the intensity of direct solar radiation at normal incidence.

      2. *Pyranometer:* An instrument for the measurement of the solar radiation received from the whole hemisphere.

      3. *Net Pyranometer:* An instrument for the measurement of the net flux of downward and upward solar radiation.

      4. *Pyrgeometer:* An instrument for the measurement of atmospheric radiation on a horizontal upward-facing black surface at the ambient air temperature.

      5. *Pyrradiometer:* An instrument for the measurement of both solar and terrestrial radiation (total radiation).

      6. *Net Pyrradiometer:* An instrument for the measurement of the net flux of downward and upward total (solar, terrestrial, surface and atmospheric) radiation.

   c. **Sensor Type**:

      1. *Calorimeter*

      2. *Thermocouples or thermopiles*

      3. *Bimetallic*

      4. *Photovoltaic, photo conductive or photoemissive cells*

      5. *Black Body*

      6. *Pyroelectric cell*

      7. *Others (specify)*

   d. **Sensor Surface Coating**: Coating applied on the surface of the sensing element.

   e. **Windows**: Declare the number of windows, the window material, the radii of windows (flat window: $r = \infty$), and the exchangeability.

   f. **Aperture**: Declare the full viewing angle in case of pyrheliometers (e.g., $6^\circ \times 3^\circ$).

4. **GENERAL FEATURES**: In the space provided, type answers to the questions listed:

   a. **Dimensions**: Declare the maximum dimensions (in cm).

   b. **Weight**: Declare the total weight (in kg).

   c. **Provision for Levelling**: Declare the indicator (e.g., spirit level) and the method of adjustment of the indicator (mechanical or optional).

   d. **Weatherproof**: Check mark "yes" if the instrument is suitable for long-time outdoor operation without any additional devices. Declare the desiccant used.

e. **Additional Equipment**: Declare available additional or optional equipment, e.g., filter glasses, blowers for ventilating the windows, shadow rings for measuring sky radiation, solar tracker for pyrheliometers.

5. **DEVELOPMENT STATUS**: Self explanatory.

6. **RESPONSE CHARACTERISTICS**: In space provided, type answers to the questions listed:

a. **Sensitivity** (mV/mW $cm^{-2}$): Absolute change in the output (millivolts) per unit change in the input (mW $cm^{-2}$) of the product described.

b. **Stability** (%/year): The stability of the calibration, i.e., the maximum expected change in this factor per cent per year.

c. **Impedance** (ohm): Impedance (ohm) of the product described.

d. **Spectral Response**: Declare the spectral range by the wavelength of 50% response. Provide, if available, a curve of the absolute or relative sensitivity of the receiver. Alternatively, provide the spectral transmittance of the used window and spectral absorptance of the used sensor surface coating (in case of normal incidence).

e. **Time Response** (seconds): Declare the time of 90% step response for increase *and* decrease.

f. **Temperature Dependence** (%/°C): Specify the temperature coefficient of change of response over the expected temperature working range (about 240 - 320 K). Provide a typical curve of the temperature dependence of the coefficient, if available. Alternatively, declare the coefficient for about 295 K and the total change over the whole range.

g. **Linearity** (%): Specify the dependence of sensitivity of the intensity in the range of 100 mW $cm^{-2}$ and 5 mW $cm^{-2}$, as percent deviation from the result in case of the upper limit. Provide a curve, if available. Alternatively, declare the maximum error and the limits of the corresponding intensity range and the inclination of the receiver.

h. 1. *Cosine Response:* Specify the deviation (in %) of response at a different angle of incidence i (related to response at normal incidence) from cos i. If possible, show the deviation as a function of $\alpha$ by a curve. Alternatively, declare the deviations for i = 20°, 40°, 60° and 80°.

2. *Azimuth Response:* Specify the deviation of response (in %) when the sensor rotated through 360° azimuth for radiation incident at i = 60° or 70°. If possible, provide a curve. Alternatively, declare the deviations at about 8 different azimuth angles.

3. *Attitude Response:* Specify the deviation of response (in %) when the receiver is tilted from horizontal (= 0°) to 45°, 90° and 180°; if possible for different constant radiation intensities (e.g., 100 mW $cm^{-2}$ and 20 mW $cm^{-2}$).

i. **Calibration Accuracy**: Specify the calibration standard and the calibration method (source of radiation intensity range, angle of incidence, angle of tilt). Declare the range of variation (in %) of the calibration factor delivered.

7. **QUALITY CONTROL**: Provide information on quality test routine, if available. Use for abbrev- item of quality in point 6, **RESPONSE CHARACTERISTICS**, (e.g., /-e stands for "control of time response").

8. **APPLICATION DATA**: In the matrix provided, check mark the space for which the product described is applicable in horizontal position and state the angular limit in degrees for which product described is applicable in tilted position.

**Radiation**:

a. **Global Solar**: Global solar radiation received on a horizontal surface direct from the solid angle of the sun's disc and also radiation that has been scattered or diffusely reflected in traversing the atmosphere.

b. **Diffuse Solar**: Downward scattered and reflected solar radiation coming from the whole hemisphere with the exception of the solid angle subtended by the sun's disc.

c. **Spectral Solar**: Radiation of selected wavelengths of the solar radiation.

d. **Direct Solar**: Solar radiation coming from the solid angle of the sun's disc on a surface perpendicular to the axis of this cone, comprising mainly unscattered and unaffected solar radiation.

e. **Solar and Infrared**: Global solar and infrared.

f. **Infrared**: Radiation with wavelength greater than 0.8 micron and less than 1 millimeter.

g. **Net**: Net radiation is the difference between downward and upward (total and terrestrial) radiation, net flux in all directions.

9. **ECONOMIC DATA**: In the space provided, type answers to the questions listed:

a. **Cost** ($/unit): The updated cost ($/unit) of the product described.

b. **Recalibration Cost** ($/unit): The updated cost ($/unit) to recalibrate the product described.

c. **Warranty** (months): The time period (months) during which the product described is under warranty after the date of purchase.

d. **Delivery Time** (days): The time period (days) required to deliver the product described after receiving the order.

10. **COMMENT**: In the space provided, type comments for the product described.

## INSTRUMENT DESCRIPTION AND PERFORMANCE FORM

Letterhead/Logo

Contact for Further Information

**Product Data**

| | |
|---|---|
| Model/Part No. | |
| Instrument Class. | |
| Sensor Type | |
| Sen. Sur. Coating | |

| | |
|---|---|
| Windows | No.: Materials: |
| | r = |
| | Exchangeability: |
| Aperture | |

**General Features**

| | |
|---|---|
| Dimensions (cm) | |
| Weight (kg) | |
| Prov. for Level. | Indicator: |
| | Method of Adjustment: |

| | |
|---|---|
| Weatherproof | yes no |
| Desiccant Used | |
| Additional Equipment | |
| | |

**Development Status**

| | yes | no |
|---|---|---|
| Proto. built & tested | | |
| In production | | |

**Response Characteristics**

| | |
|---|---|
| Sen. (mV/mW $cm^{-2}$) | |
| Stability (%/year) | |
| Impedance (ohms) | |
| Spectral Response | from: to: |

| | |
|---|---|
| Time Response (s) | |
| Temp. Depend. (%/°C) | |
| Linearity (%) | tilt ° |
| | range |

Relative Spectral Sensitivity (Spectral Transmittance, Spectral Absorptance)

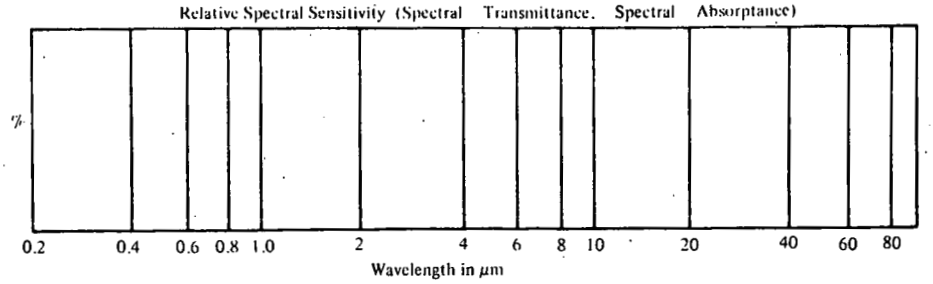


Temperature Coefficient

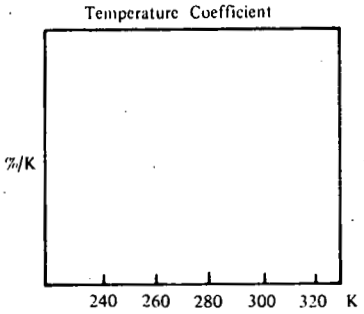


Error of Non-Linearity

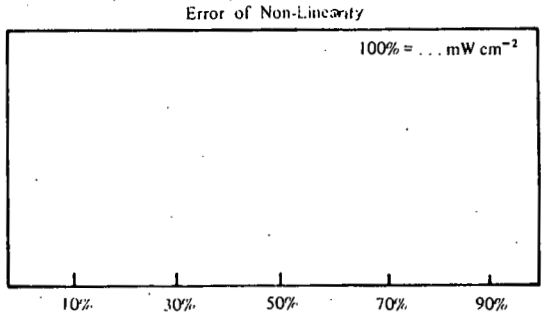


| Cosine $a$ | Degrees | | | | |
|---|---|---|---|---|---|
| | 20 | 40 | 60 | 80 | |
| Response % | | | | | |

| Azimuth A | Degrees | | | | | | | | |
|---|---|---|---|---|---|---|---|---|---|
| | 0 | | 90 | | 180 | | 270 | | |
| Response % | 0 | | | | | | | | |

Cosine Response

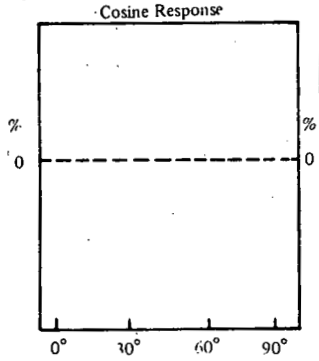


Azimuth Response

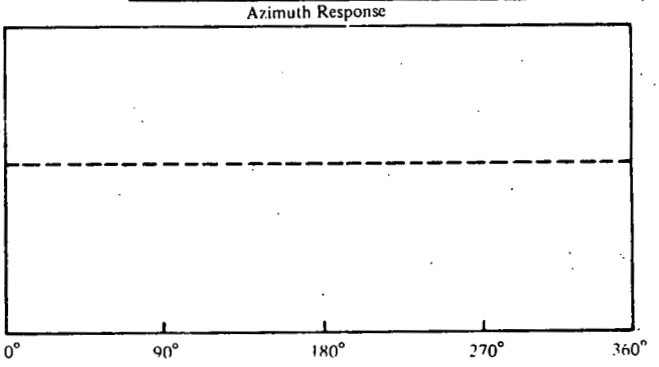


| Attitude $\delta$ | Degrees | | | | |
|---|---|---|---|---|---|
| | 0 | 45 | 90 | 180 | |
| Response % | 0 | | | | |

**Calibration Accuracy**

| | |
|---|---|
| Calibration Standard | |
| Source | |
| Angle of Incidence | |
| Angle of Tilt | |

**Quality Control**

| | |
|---|---|
| 7.a. | |
| 7.b. | |
| 7.c. | |
| 7.d. | |
| 7.e. | |
| 7.f. | |
| 7.g. | |
| 7.h. | |
| 7.i. | |

**Application Data**

| | Global Solar | Diffuse Solar | Spectral Solar | Direct Solar | Solar & Infrared | Infrared | Net |
|---|---|---|---|---|---|---|---|
| Horiz. | | | | | | | |
| Tilt | | | | | | | |

**Economic Data**

| | | | |
|---|---|---|---|
| Cost ($/unit) | | Warranty (months) | |
| Recalib. Cost ($/unit) | | Delivery time (days) | |

**Comments**

APPENDIX II

# AN APPROXIMATE METHOD FOR QUALITY CONTROL OF SOLAR RADIATION INSTRUMENTS

Lester Machta*
National Oceanic and Atmospheric Administration
8060 13th Street
Silver Spring, Maryland 20910
The United States of America

## FOREWARD

Calibration of instruments to measure solar radiation must be an essential ingredient to insure reliable data. The National Oceanic and Atmospheric Administration offers a series of methods for instrument calibration. The one selected by the user will depend on his needs and resource availability. In order of decreasing likely accuracy of calibration, one may use:

1. Calibration of field instrument against a standard in the controlled environment of the NOAA calibration facility, Boulder, Colorado, or in a controlled environment against another instrument which, in turn, has been calibrated in the NOAA calibration facility in Boulder. In European countries field instruments are calibrated against a standard instrument at a solar radiation center recognized by the World Meteorological Organization (WMO), or against another instrument which has been calibrated against such a standard. Such calibrations are directly traceable to the World Meteorological Organization standard. This is recommended procedure. The accuracy relative to the world standard for careful work can be less than one percent for readings in the normal range for solar radiation measurements.

2. The calibration service supplied by NOAA involves the shipment of a secondary calibrated sensor (with or without a recorder) to the organization or station wishing to perform the calibration. In some other countries a similar calibration service may be provided by the solar radiation centers recognized by WMO. Instructions for performing the calibration will also be supplied. After a reasonable time allotted for the calibration, the secondary standard will be returned and its calibration again checked. With careful work, this method should achieve an accuracy of less than one percent.

3. The third procedure, the subject of this appendix, attempts to estimate the solar radiation from certain readily available local observations and a set of tables and graphs. A prime source of potential error in this procedure is the correction factors of turbidity and precipitable water vapor; alternate methods for determining or estimating these atmospheric attenuaters appears in the workbook. A simple hand-held sunphotometer provides the atmospheric turbidity and water vapor in the vertical column. This method provides a calibration capability to an accuracy of within 5-10 percent for the prescribed conditions.

---

*Comments which apply to Europe provided by Brian May, U.K.

# AN APPROXIMATE SOLAR RADIATION QUALITY CONTROL PROCEDURE

## A WORKBOOK

### Introduction

The need to properly calibrate instruments which measure solar radiation is self evident. However, the technique and accuracy of the calibration varies with the kind of measurement, the data acquisition and instrumental capability, and the user needs. The spectrum of calibration requirements ranges from minimal accuracy to that needed for highly sophisticated scientific instruments. One can therefore envisage several alternative calibration procedures.

In Europe the regional and national radiation centers that have been recognized by the World Meteorological Organization (address: WMO, Case Postale No. 5, CH-1211 Geneva 20, Switzerland) are listed in Table 1. These centers are equipped with internationally calibrated reference pyrheliometers which are used to calibrate instruments for network use.

The NOAA maintains the internationally calibrated standard pyrheliometer for the U.S.A. in Boulder, Colorado. With support from the Department of Energy and the National Science Foundation, NOAA will calibrate selected instruments used for solar energy technology and for other users of solar radiation instruments. It is expected that one or more commercial firms will also provide a routine calibration service to the general public. However for some applications, the effort to perform direct intercomparisons between field instruments and primary or secondary standards is not justified. This workbook suggests an alternative, easy calibration procedure but one of only limited accuracy. Since the procedure calculates the direct and global solar radiation under clear skies, the predicted values in this workbook may also be used for applications to other than calibration provided the accuracy limitation is appreciated.

### General Description

Readings of solar radiation during clear weather, especially when the sun is close to the zenith (overhead), are the least "noisy" and most predictable. The variation of true solar noon readings between adjacent days and locations tends to be small. Second, theoretical calculations of the direct and diffuse components of the sun's radiation at the earth's surface best reproduce observations during such periods. These characteristics suggest that measurements of solar radiation during clear skies with the sun near zenith might be calibrated against other reliable measurements at nearby stations or against a calculated value.

This paper will *not* deal with procedures for interpolating between reliable, simultaneous nearby solar radiation measurements although this procedure, when available, may be preferred over that recommended below. Some cautions are in order, however, before accepting the value at a nearby station as the expected readings at the operating location. These cautions include: differences in station characteristics (such as altitude, ground reflectivity, or turbidity) or unexpected errors in observation at the "reliable" stations. Consultation with experts can generally clarify most if not all of such sources of error and may recommend, instead, the use of this comparison procedure. This workbook predicts solar radiation from such determinable parameters as zenith angle of the sun, ground reflectivity, turbidity, and precipitable water. The standard values are documented in Appendix II-A. The conversion from standard to actual conditions is based on the work of Braslau and Dave (1972).

As a general rule, observations with the least diffuse or scattered radiation will be the most reliable to predict. Thus, high turbidity, large zenith angle of the sun, and high ground reflectivity (e.g., snow cover) should be avoided.

It is necessary to select a daytime period at or very near true solar noon during which the sky is clear. If possible, clouds should be avoided even if they are near the horizon. The presence of any observable cloudiness may introduce two types of errors. First, clouds even remote from the sun's position in the sky enhance the diffuse or scattered solar radiation for which it is difficult to correct. Second, clouds in a remote part of the sky may indicate the presence of thin, invisible clouds elsewhere in the sky. Thus, measurements taken in the middle of an interval of "no clouds" rather than just before the appearance or just after the disappearance of clouds are preferred. In general, the bluer the appearance of the sky, the less likely that clouds, haze or excessive dust might be present. A whiter-appearing sky denotes larger particles including small water droplets that make for hazy conditions.

The basis for calculating the direct or global radiation are careful measurements obtained at Raleigh, North Carolina, by Mr. Edwin Flowers during clear skies with measured values of turbidity and precipitable water and an estimated value of ground reflectivity. The graphs which convert these observations to other environmental conditions than those for the above day and hour at Raleigh are derived from the work of Braslau and Dave. One graph, Figure 8, has been adjusted slightly to fit other observations taken by Mr. Flowers at Raleigh, North Carolina, and Boulder, Colorado.

**Calculation of Zenith Angle of the Sun**

The zenith angle is the angle between the vertical or zenith and the sun while the elevation angle (90° minus the zenith angle) is the angle which the sun makes with the horizontal or the horizon. A simple instrument which measures the sun angle with the vertical or horizontal is a clinometer. However, it is not commonly available and, if used, caution must be exercised to avoid viewing the sun with the naked eye. However, an equally reliable determination of the zenith angle may be found from the earth-sun geometry: the latitude and longitude of the measurement point, the day of the year and time of the day, as described in Appendix II-B.

**Altitude Correction**

The altitude of the measurement point must be known approximately. Locations at higher altitudes contain less air above them. This results in less atmospheric absorption and scattering.

The correction for direct solar radiation at altitudes above sea level assumes a single exponential pressure variation between the calculated sea level direct radiation and that at zero pressure, the top of the atmosphere. Thus, if D is the direct solar radiation and p is the atmospheric pressure, then it is assumed that as a first approximation

$$D(p) = D(o)e^{-bp} \qquad (1)$$

where b is an unknown constant. For sea level pressure, Eq (1) becomes

$$D(p_s) = D(o)e^{-bp_s} \qquad (2)$$

where $p_s$ is the sea level pressure, 1013.25 millibars (101.325 kilopascals). Since $D(p_s)$ and D(o) are known, one may solve for b in Eq. (2). Substituting for b in Eq. (1) and using only the first two terms in the expansion of $e^{-x} = 1 - x + x2/2 - \ldots$ leads to

$$D(p) = D(p_s)\left[1 + \left(1 - \frac{p}{p_s}\right)\frac{D(o) - D(p_s)}{D(o)}\right] \qquad (3)$$

This is the formula used to correct the calculated sea level direct solar radiation to that at an altitude where the pressure is "p". The quantity $p_s/p$ appears in Figure 3; the value of D(o), the solar constant, is taken as 1377 watts per square meter ($W\ m^{-2}$). The solar constant is the average amount of radiant energy per unit of time falling on a unit area normal to the sun's rays outside the earth's atmosphere. The quantity $D(p_s)$ is obtained by reference to other figures.

The global radiation is found by using different altitude corrections for the direct and diffuse components. The correction for direct solar radiation has already been given as Eq. (3). No altitude correction is applied to the diffuse component since the reduced number of scattering modules or particles with increasing altitude is approximately balanced by the greater amount of sunlight available for scattering.

This approximation may be poor at very high altitude locations. The other corrections for nonstandard zenith angle, ground reflectivity, precipitable water, turbidity, and earth-sun distance are applied to the global radiation rather than to each of the direct and diffuse components separately. The reason for this is the marked sensitivity of direct solar radiation to turbidity compared to the relatively insensitive dependence of global radiation to turbidity; that is, higher turbidity increases the diffuse radiation by approximately the amount lost in the direct solar beam.

Finally, Braslau and Dave's theoretical calculation of cloudless solar radiation apply to sea level conditions. The amount of precipitable water and number of particles producing the turbid atmosphere would be larger at sea level than reported at the elevated station. Hence both the precipitable water and the turbidity coefficients will be multiplied by $p_s/p$ or 1013.25/p in millibars before they are used to determine the correction factor for nonstandard environmental conditions.

**Earth-Sun Distance Correction**

The distance between the sun and earth varies over the course of the year. The resultant solar radiation falling at the outside of the atmosphere varies inversely with the square of the distance. Correction factors for the earth-sun distance appear in Figure 4.

**Precipitable Water**

Atmospheric water vapor is a major absorber of solar radiation. Precipitable water is the meteorological term for all of the water vapor molecules in a vertical column of air. The amount of precipitable water in the atmosphere varies from day to day, season to season, and place to place. The United States National Weather Service calculates and maps the amount of precipitable water vapor twice each day based on all balloon-borne measurements taken at about 60 locations in the United States. Interpolation between isolines on these maps which are transmitted by facsimile to the National Weather Service stations and other circuit outlets, probably constitutes the best estimate of the amount of precipitable water for the location and time of measurement. Consultation with a professional meteorologist may also be desirable since a variation in atmospheric water vapor during the course of a day is possible. The national weather services of many European countries make observations of the vertical humidity profile and hence the amount of precipitable water twice per day (at 00 h and 12 h UT). These observations are made with upper-air radiosondes at about 130 stations in Europe. Interpolation in space and time between these observations gives the best estimate that can be made of the amount of precipitable water for a given time and location. The addresses of the many national weather services in Europe responsible for making upper-air measurements may be obtained from the WMO Headquarters at Geneva, Switzerland. Appendix II-C discusses further aspects of the determination of and correction for precipitable water.

**Turbidity**

The diffuse or scattered radiation received at the ground depends on the dust or particle content of the air or turbidity, the reflectivity of the earth's surface (called the earth's albedo), and ordinary air molecules. The number of scattering molecules and dust particles is related to the zenith angle of the sun. A high value of the dust loading will increase the diffuse component of the solar radiation and reduce the direct component. Volz (1978) provides information about atmospheric turbidity for locations in Europe. Appendix II-D provides a way of estimating the atmospheric turbidity.

**Ground Reflectivity**

A higher ground reflectivity or albedo also allows dust as well as ordinary air molecules to scatter more solar radiation downward after being reflected upward to the atmosphere. Since measurements of the direct beam of solar radiation include no (or very little) scattered radiation, the direct solar radiation does not depend upon ground reflectivity. Table 3 permits the observer to estimate the ground reflectivity from ground conditions in the immediate area of the observation.

**Conversion of Units**

Table 5 lists the conversion factors to convert solar radiation W $m^{-2}$ to other units of energy per unit area and unit of time.

## WORKSHEET FOR SOLAR RADIATION CALIBRATION OR CHECK

### I. Geography and Time Information

1. Location identification:_____

2. Location latitude:_____ °

3. Location longitude:_____ °

4. Date of observation:_____

5. Observation time:_____
(See II below to determine the watch or clock time for local true solar noon.)

6. Time zone:_____
(For continental U.S.: Eastern, Central, Mountain, or Pacific.)

7. Station altitude:_____ ft., meters
(Strike out incorrect unit.)

### II. Time of True Solar Noon and Zenith Angle

1. Using the date of the observation, line 1.4., enter below the meridian passage of the sun (TSN) and declination of the sun (Dec) from Table 2. TSN is the time of true solar noon at the standard time meridian.

a. TSN_____ hour and minute

b. Dec _____ °,
(specify + (north) or - (south))

2. Find the difference in longitude between the standard time meridian for the time zone from Table 10, and location longitude, line 1.3. Specify whether the location longitude, line 1.3., is east or west of the standard time meridian.

3. Using the true solar noon time at the standard time meridian from line II. 1. a as the entry along the sloping lines of Figure 1 and the longitudinal difference between the standard time meridian and the location longitude from line II. 2. as the horizontal axis read off the local standard time or "clock" time from the vertical axis of Figure 1. This is the local standard time of true solar noon for your location.

Local Standard Time:____h____m_____
(hour and minute)

4. Subtract the declination, line II. 1. b., with due regard for sign, from the location latitude, line I. 2., to give the zenith angle of the sun at true solar noon.

Zenith angle_____ °

5. If observations are not taken at or very near true solar noon, consult Appendix II-B (a), "General Solution", for procedure to calculate zenith angle. After performing the calculations to find the zenith angle, enter below.

Zenith angle_____ °

**III. Ground Reflectivity**

1. Using Table 3 and the average ground cover within several meters or about a thousand feet of the observation point, estimate and enter below the ground reflectivity.

Ground reflectivity: _____

**IV. Precipitable Water**

1. If the precipitable water is obtained from local current weather, use that value in line 1. a. below in preference to a climatological value. The current numerical values for precipitable water from the U. S. National Weather Service network are given in inches (2.54 cm = 1 inch) from the ground to a pressure altitude of 500 millibars. The factor 1.15 converts precipitable water up to 500 millibars to total precipitable water in a column to the top of the atmosphere. The product of the two factors 2.54 X 1.15 = 2.92, appears in line 1. b. below.

a. Precipitable water as reported by the Nat. Weather Ser.: _____ inches to 500 millibars

b. Multiply IV. 1. by 2.92: _____ cm in total column

If a value of precipitable water is unavailable from current weather information, use a climatological value obtained from Figure 10. See Appendix II-C if line 1.3 lies west of 100°W. **Do not use if a number is already entered in line IV. 1. b.**

c. Precipitable water obtained from Fig. 2: _____ cm to 500 millibars all day

d. Multiply IV. 1. c. by 0.93: _____ cm in total column clear days

**V. Turbidity**

1. If a measured value for the turbidity coefficient is available, enter below. If not, use Table IV and/or Figure 2 (see Appendix II-D) to estimate turbidity coefficient and enter below.

Turbidity coefficient: _____

**VI. Calculation of Global Solar Radiation**

1. Enter station altitude, line I. 7., along the horizontal axis of Figure 3 and read the vertical axis at the point of intersection with the curve. This is the ratio of the average sea level to station pressure. Enter below:

Pressure ratio: _____

2. Enter the day of the year from line I. 4. along the horizontal axis of Figure 4 and read the vertical axis at the point of intersection. This is the earth-sun distance correction. Enter below:

Correction for earth-sun distance: _____

3. a. Multiply the value of precipitable water on line IV. b., if present, or line IV. 1. d., by VI. 1. to obtain the estimated precipitable water for an atmosphere beginning at sea level.

Estimated sea level precipitable water: _____

b. Enter the estimated sea level precipitable water, line VI. 3. a., along the horizontal axis of Figure 5, and read the value of the vertical axis along the appropriate sloping line, the zenith angle, line II. 4. or II. 5. (interpolation may be necessary). This is the precipitable water correction. Enter below:

Precipitable water correction: _____

4. Multiply the turbidity coefficient, line VI., by the pressure ratio, line VI. 1. This is the estimated sea level turbidity coefficient. Enter below:

Estimated sea level turbidity coefficient: _____

5. Enter the value of ground reflectivity from line III. 1. on the horizontal axis of Figure 6 and the estimated sea level turbidity coefficient, line V. 1. (interpolation may be necessary) as the sloping lines and read the values of the vertical axis. This is the correction for ground reflectivity. Enter below:

Ground reflectivity correction: _____

6. Enter the value for the zenith angle, line II. 4. or line II. 5. on the horizontal axis of Figure 7 and the turbidity coefficient, line VI. 4. (interpolation may be necessary) as the family of curves, and read the value of the vertical axis. This is the zenith angle correction. Enter below:

Zenith angle correction: _____

7. The correction for altitude for locations above sea level involves several steps. The global radiation for standard conditions other than altitude is composed of contributions of direct and diffuse solar radiation.

a. The standard direct solar radiation falling on a horizontal surface for locations above sea level is given by:

(Direct at altitude on a horizontal surface) = (Direct at sea level) X [1 + (1 - 1/pressure ratio) X solar constant - direct at sea level/solar constant] cos 30°
= 768 [1 + (1 - 1/1013.25/p) X 0.364)]

The quantity 1013.25/p is the pressure ratio, line VI. 1. Substitution in the above formula of the pressure ratio, line VI. 1., yields the contribution of direct solar radiation falling on a horizontal surface under standard conditions but at altitudes above sea level. Enter below:

Direct contribution: _____ $W\ m^{-2}$

b. The standard sea level global radiation is the sum of the direct solar radiation falling on a horizontal surface VI. 7. a., and the diffuse solar radiation 142.5 $W\ m^{-2}$. Enter below:

Standard global radiation: _____ $W\ m^{-2}$

8. Multiply line VI. 2. by VI. 3. b. by line VI. 5. by line VI. 6. Enter below:

Global correction factor: _____

9. Multiply standard global solar radiation, line VI. 7. b., by the global correction factor, line VI. 8. This is the calculated global solar radiation.

Calculated global solar radiation: _____

10. If units other than $W\ m^{-2}$ (watts per square meter) are desired, find the conversion in Table 5. Enter below:

Calculated global solar radiation: _____

**VII. Calculation of Direct or Normal Incidence Solar Radiation**

1. Enter the estimated sea level turbidity coefficient, line V. 1., along the horizontal axis of Figure 8 and read the turbidity correction factor along the vertical axis from the intersection on the curve. Enter below:

Turbidity coefficient correction: _____

2. Enter the zenith angle, line II. 4. or II. 5., along the horizontal axis of Figure 9, and the turbidity coefficient, line V. 1., from the family of curves (interpolation may be necessary) and read the vertical axis. This is the zenith angle correction for direct radiation. Enter below:

Zenith angle correction: _____

3. Multiply line VI. 2. by line VI. 3. b. by line VII. 1. by line VII. 2. This is the direct radiation correction factor. Enter below:

Direct radiation factor: _____

4. Multiply the direct solar radiation factor, line VII. 3. by 887 $W\ m^{-2}$. Enter below:

Direct solar radiation at sea level: _____

5. To obtain the direct radiation for a station at an altitude above sea level, use the formula:

Direct solar radiation at altitude = Direct solar radiation at sea level × [1 + (1 − 1/pressure ratio) solar constant − direct solar radiation at sea level/ solar constant] = value in line VII. 4. × [1 + 1 − 1/value in line VI.1.) 1377 − value in line VII.4./1377]

The value obtained by substitution in the above formula is the calculated direct solar radiation at altitude. Enter below:

Calculated direct solar radiation: _____ $W\ m^{-2}$

6. If units other than $W\ m^{-2}$ (watts per square meter) are desired, find the conversion in Table 5. Enter below:

Calculated direct solar radiation: _____

Table 1

European Regional and National Radiation Centers
Recognized by World Meteorological Organization

| Place | Country | Address |
|---|---|---|
| Bruxelles | Belgium | Institut Royal Météorologique de Belgique, 3 Avenue Circulaire, 1180 Bruxelles |
| Trappes/Carpentras | France | Centre Actinométrique Météorologique Hameau de Serres, 84200 Carpentras |
| Bracknell | Great Britain | Meteorological Office, London Road, Bracknell, Berkshire RG12 2SZ |
| Norrköping | Sweden | The Swedish Meteorological and Hydrological Institute, Fack, 60101 Norrköping |
| Davos | Switzerland | Physico-Meteorological Observatory World Radiation Center 7270 Davos-Platz |
| Leningrad | U. S. S. R. | Main Geophysical Observatory 7 Karbyshev Street, 194018 Leningrad |
| Vienna | Austria | Zentralanstalt für Meteorologie und Geodynamik, Hohe Warte 38, 1190 Wien |
| Hamburg | Federal Republic of Germany | Meteorologisches Observatorium Frahmredder 95, 2000 Hamburg 65 |
| Helsinki | Finland | Finnish Meteorological Institute Vuorikatu 24, 00101 Helsinki 10 |
| Potsdam | German Democratic Republic | Meteorological Main Observatory of the Met. Service of the GDR Telegrafenberg, 15-Potsdam |
| Budapest | Hungary | Meteorological Service of Hungarian People's Rep., II. Kitaibel Pal. u. 1 1675 Budapest 39 |
| Cahirciveen | Ireland | Valentia Observatory Cahirciveen, Co. Kerry |
| Bet Dagan | Israel | Meteorological Service, Division of Research and Development, Bet Dagan |
| Oslo | Norway | Norwegian Meteorological Institute Blindern, Box 320, Oslo 3 |

Table 2

True Solar Noon (TSN) and Solar Declination Angle (Dec)*

| | JAN. | | FEB. | | MAR. | | APR. | | MAY | | JUN. | | JUL. | | AUG. | | SEPT. | | OCT. | | NOV. | | DEC. | |
|---|---|---|---|---|---|---|---|---|---|---|---|---|---|---|---|---|---|---|---|---|---|---|---|---|
| | TSN | DEC | TSN | DEC | TSN | DEC | TSN | DEC | TSN | DEC | TSN | DEC | TSN | DEC | TSN | DEC | TSN | DEC | TSN | DEC | TSN | DEC | TSN | DEC |
| | H M | ° | H M | ° | H M | ° | H M | ° | H M | ° | H M | ° | H M | ° | H M | ° | H M | ° | H M | ° | H M | ° | H M | ° |
| 1 | 1204 | S23.0 | 1214 | S17.1 | 1212 | S 7.6 | 1204 | N 4.5 | 1157 | N15.0 | 1158 | N22.0 | 1204 | N23.1 | 1206 | N18.1 | 1200 | N 8.4 | 1150 | S 3.1 | 1144 | S14.4 | 1149 | S21.8 |
| 2 | 1204 | 22.9 | 1214 | 16.8 | 1212 | 7.3 | 1204 | 4.9 | 1157 | 15.3 | 1158 | 22.2 | 1204 | 23.1 | 1206 | 17.8 | 1200 | 8.0 | 1149 | 3.5 | 1144 | 14.7 | 1149 | 21.9 |
| 3 | 1204 | 22.8 | 1214 | 16.6 | 1212 | 6.9 | 1203 | 5.3 | 1157 | 15.6 | 1158 | 22.3 | 1204 | 23.0 | 1206 | 17.5 | 1159 | 7.6 | 1149 | 3.9 | 1144 | 15.0 | 1150 | 22.1 |
| 4 | 1205 | 22.7 | 1214 | 16.3 | 1212 | 6.5 | 1203 | 5.6 | 1157 | 15.9 | 1158 | 22.4 | 1204 | 22.9 | 1206 | 17.3 | 1159 | 7.2 | 1149 | 4.3 | 1144 | 15.3 | 1150 | 22.2 |
| 5 | 1205 | 22.6 | 1214 | 16.0 | 1212 | 6.1 | 1203 | 6.0 | 1157 | 16.2 | 1158 | 22.5 | 1204 | 22.8 | 1206 | 17.0 | 1159 | 6.9 | 1149 | 4.7 | 1144 | 15.6 | 1151 | 22.4 |
| 6 | 1206 | S22.5 | 1214 | S15.7 | 1211 | S 5.7 | 1203 | N 6.4 | 1157 | N16.5 | 1159 | N22.6 | 1205 | N22.7 | 1206 | N16.7 | 1158 | N 6.5 | 1148 | S 5.1 | 1144 | S15.9 | 1151 | S22.5 |
| 7 | 1206 | 22.4 | 1214 | 15.3 | 1211 | 5.3 | 1202 | 6.8 | 1157 | 16.8 | 1159 | 22.7 | 1205 | 22.6 | 1206 | 16.5 | 1158 | 6.1 | 1148 | 5.4 | 1144 | 16.2 | 1151 | 22.6 |
| 8 | 1207 | 22.3 | 1214 | 15.0 | 1211 | 4.9 | 1202 | 7.2 | 1156 | 17.1 | 1159 | 22.8 | 1205 | 22.5 | 1206 | 16.2 | 1158 | 5.7 | 1148 | 5.8 | 1144 | 16.5 | 1152 | 22.7 |
| 9 | 1207 | 22.1 | 1214 | 14.8 | 1211 | 4.5 | 1202 | 7.5 | 1156 | 17.3 | 1159 | 22.9 | 1205 | 22.4 | 1205 | 15.9 | 1157 | 5.4 | 1147 | 6.2 | 1144 | 16.8 | 1152 | 22.8 |
| 10 | 1208 | 22.0 | 1214 | 14.4 | 1210 | 4.2 | 1201 | 7.9 | 1156 | 17.6 | 1159 | 23.0 | 1205 | 22.3 | 1205 | 15.6 | 1157 | 5.0 | 1147 | 6.6 | 1144 | 17.1 | 1153 | 22.9 |
| 11 | 1208 | S21.8 | 1214 | S14.1 | 1210 | S 3.8 | 1201 | N 8.3 | 1156 | N17.8 | 1159 | N23.1 | 1205 | N22.1 | 1205 | N15.3 | 1157 | N 4.6 | 1147 | S 7.0 | 1144 | S17.4 | 1153 | S23.0 |
| 12 | 1208 | 21.7 | 1214 | 13.7 | 1210 | 3.4 | 1201 | 8.6 | 1156 | 18.1 | 1200 | 23.1 | 1205 | 22.0 | 1205 | 15.0 | 1156 | 4.2 | 1147 | 7.3 | 1144 | 17.7 | 1154 | 23.1 |
| 13 | 1209 | 21.5 | 1214 | 13.4 | 1210 | 3.0 | 1201 | 9.0 | 1156 | 18.4 | 1200 | 23.2 | 1206 | 21.9 | 1205 | 14.7 | 1156 | 3.9 | 1146 | 7.7 | 1144 | 17.9 | 1154 | 23.1 |
| 14 | 1209 | 21.3 | 1214 | 13.1 | 1209 | 2.6 | 1200 | 9.4 | 1156 | 18.6 | 1200 | 23.3 | 1206 | 21.7 | 1205 | 14.4 | 1156 | 3.5 | 1146 | 8.1 | 1144 | 18.2 | 1155 | 23.2 |
| 15 | 1209 | 21.1 | 1214 | 12.7 | 1209 | 2.2 | 1200 | 9.7 | 1156 | 18.8 | 1200 | 23.3 | 1206 | 21.6 | 1204 | 14.1 | 1155 | 3.1 | 1146 | 8.5 | 1145 | 18.5 | 1155 | 23.3 |
| 16 | 1210 | S21.0 | 1214 | S12.4 | 1209 | S 1.8 | 1200 | N10.1 | 1156 | N19.1 | 1201 | N23.3 | 1206 | N21.4 | 1204 | N13.8 | 1155 | N 2.7 | 1146 | S 8.8 | 1145 | S18.7 | 1156 | S23.3 |
| 17 | 1210 | 20.8 | 1214 | 12.0 | 1208 | 1.4 | 1200 | 10.4 | 1156 | 19.3 | 1201 | 23.4 | 1206 | 21.2 | 1204 | 13.5 | 1155 | 2.3 | 1145 | 9.2 | 1145 | 19.0 | 1156 | 23.4 |
| 18 | 1210 | 20.6 | 1214 | 11.7 | 1208 | 1.0 | 1159 | 10.8 | 1156 | 19.5 | 1201 | 23.4 | 1206 | 21.1 | 1204 | 13.2 | 1154 | 1.0 | 1145 | 9.6 | 1145 | 19.2 | 1156 | 23.4 |
| 19 | 1211 | 20.4 | 1214 | 11.3 | 1208 | 0.6 | 1159 | 11.1 | 1156 | 19.7 | 1201 | 23.4 | 1206 | 20.9 | 1204 | 12.8 | 1154 | 1.5 | 1145 | 9.9 | 1145 | 19.4 | 1157 | 23.4 |
| 20 | 1211 | 20.2 | 1214 | 11.0 | 1208 | 0.2 | 1159 | 11.5 | 1156 | 20.0 | 1201 | 23.4 | 1206 | 20.7 | 1203 | 12.5 | 1154 | 1.2 | 1145 | 10.3 | 1146 | 19.7 | 1157 | 23.4 |
| 21 | 1211 | S19.9 | 1214 | S10.6 | 1207 | N 0.2 | 1159 | N11.8 | 1156 | N20.2 | 1202 | N23.4 | 1206 | N20.5 | 1203 | N12.2 | 1153 | N 0.8 | 1145 | S10.6 | 1146 | S19.9 | 1158 | S23.4 |
| 22 | 1212 | 19.7 | 1214 | 10.2 | 1207 | 0.6 | 1159 | 12.2 | 1157 | 20.4 | 1202 | 23.4 | 1206 | 20.3 | 1203 | 11.9 | 1153 | 0.4 | 1145 | 11.0 | 1146 | 20.1 | 1158 | 23.4 |
| 23 | 1212 | 19.5 | 1213 | 9.9 | 1207 | 1.0 | 1158 | 12.5 | 1157 | 20.6 | 1202 | 23.4 | 1206 | 20.1 | 1203 | 11.5 | 1152 | S 0.0 | 1144 | 11.4 | 1146 | 20.3 | 1159 | 23.4 |
| 24 | 1212 | 19.2 | 1213 | 9.5 | 1206 | 1.4 | 1158 | 12.8 | 1157 | 20.7 | 1202 | 23.4 | 1206 | 19.9 | 1202 | 11.2 | 1152 | 0.4 | 1144 | 11.7 | 1147 | 20.5 | 1159 | 23.4 |
| 25 | 1212 | 19.0 | 1213 | 9.1 | 1206 | 1.8 | 1158 | 13.1 | 1157 | 20.9 | 1202 | 23.4 | 1206 | 19.7 | 1202 | 10.8 | 1152 | 0.8 | 1144 | 12.1 | 1147 | 20.7 | 1200 | 23.4 |
| 26 | 1213 | S18.7 | 1213 | S 8.8 | 1206 | N 2.1 | 1158 | N13.5 | 1157 | N21.1 | 1203 | N23.4 | 1206 | N19.5 | 1202 | N10.5 | 1151 | S 1.2 | 1144 | S12.4 | 1147 | S20.9 | 1200 | S23.4 |
| 27 | 1213 | 18.5 | 1213 | 8.4 | 1205 | 2.5 | 1158 | 13.8 | 1157 | 21.3 | 1203 | 23.3 | 1206 | 19.3 | 1202 | 10.1 | 1151 | 1.6 | 1144 | 12.7 | 1148 | 21.1 | 1201 | 23.3 |
| 28 | 1213 | 18.2 | 1213 | 8.0 | 1205 | 2.9 | 1157 | 14.1 | 1157 | 21.4 | 1203 | 23.3 | 1206 | 19.0 | 1201 | 9.8 | 1151 | 2.0 | 1144 | 13.1 | 1148 | 21.3 | 1201 | 23.3 |
| 29 | 1213 | 18.0 | 1213 | 7.8 | 1205 | 3.3 | 1157 | 14.4 | 1157 | 21.6 | 1203 | 23.2 | 1206 | 18.8 | 1201 | 9.4 | 1150 | 2.4 | 1144 | 13.4 | 1148 | 21.5 | 1202 | 23.2 |
| 30 | 1213 | 17.7 | | | 1205 | 3.7 | 1157 | 14.7 | 1157 | 21.8 | 1203 | 23.2 | 1206 | 18.6 | 1201 | 9.1 | 1150 | 2.7 | 1144 | 13.7 | 1149 | 21.6 | 1202 | 23.2 |
| 31 | 1213 | S17.4 | | | 1204 | N 4.1 | | | 1158 | N21.9 | | | 1206 | N18.3 | 1200 | N 8.7 | | | 1144 | S14.1 | | | 1203 | S23.1 |

*DOAN AND SANFORD (1970)

Table 3

Ground Reflectivity

| GROUND REFLECTIVITY | | |
|---|---|---|
| NATURE OF SURFACE | REFLECTIVITY (%) | REFERENCES |
| LAND | | |
| DESERT | 26 | LIST |
| SAND, DRY | 18 | LIST |
| SAND, WET | 9 | LIST |
| FIELDS, DRY PLOWED | 22 | LIST |
| FIELDS, GREEN | 12 | LIST |
| FIELDS, WHEAT | 7 | LIST |
| FIELD, MOIST PLOWED | 14 | ROBINSON, KONDRATIEV |
| GRASS, GREEN | 26 | ROBINSON |
| GRASS, DRIED IN SUN | 19 | ROBINSON, KONDRATIEV |
| GRASS, TALL AND DRY | 32 | LIST |
| GRASS, TALL AND WET | 22 | LIST |
| BARE GROUND | 15 | LIST |
| SNOW, FRESH | 81 | LIST |
| SNOW, SEVERAL DAYS OLD, WHITE & SMOOTH | 70 | LIST |
| SNOW, WHITE FIELD | 78 | LIST |
| URBAN DEVELOPMENTS | | |
| DOWNTOWN, CITY | 14 | PETERSON |
| OUTER CITY, ESTABLISHED SUBURBS | 19 | PETERSON |
| OLD RESIDENTIAL | 13 | PETERSON, DABBERDT & DAVIS |
| OLD RESIDENTIAL, SOME LIGHT COMMERCIAL | 12 | DABBERDT & DAVIS |
| OLD RESIDENTIAL, COMMERCIAL-INDUSTRIAL | 14 | DABBERDT & DAVIS |
| NEW RESIDENTIAL | 21 | PETERSON |
| URBAN SURFACES | | |
| CEMENT STREETS | 28 | DIRMHIRN |
| GRANITE PAVEMENT | 19 | DIRMHIRN |
| ASPHALT | 14 | DIRMHIRN |
| CRUSHED STONE PAVEMENT | 10 | DIRMHIRN |
| WOODLANDS | | |
| FOREST, GREEN | 12 | KUNG, ET.AL., LIST |
| FOREST, SNOW-COVERED GROUND | 18 | LIST |
| WATER (DIRECT BEAM ONLY) | | |
| ZENITH ANGLE, 0 - 40° | 2.5 | KONDRATIEV |
| 50° | 3.5 | KONDRATIEV |
| 60° | 6.2 | KONDRATIEV |
| 70° | 13.6 | KONDRATIEV |
| 80° | 35 | KONDRATIEV |
| 90° | 100 | KONDRATIEV |


REFERENCES

LIST, R.J., 1968: SMITHSONIAN METEOROLOGICAL TABLES, 6TH REVISED ED., WASHINGTON, DC, PP 527.

ROBINSON, N., 1966: SOLAR RADIATION. ELSEVIER PUB. CO., PP 347.

DIRMHIRN, I., 1964: DAS STRAHLUNGSFELD IM LEBENSTRAUM, ADAD. VERLAGGES., FRANKFURT, PP 426.

KUNG, E., R.A. BRYSON, D.H. LENSCHOW, 1964: "STUDY OF A CONTINENTAL SURFACE ALBEDO ON THE BASIS OF FLIGHT MEASUREMENTS AND STRUCTURE OF THE EARTH'S SURFACE OVER NORTH AMERICA, MWR, V. 92, PP 543-564.

KONDRATIEV, K.YA., RADIATION IN THE ATMOSPHERE, ACADEMIC PRESS, (INIT. GEOPH. SER. V. 12), PP 912.

PETERSON, J.T., PRIVATE COMMUNICATION.

DABBERDT, W. AND P.A. DAVIS, 1974: "DETERMINATION OF ENERGETIC CHARACTERISTICS OF URBAN-RURAL SURFACES IN THE GREATER ST. LOUIS AREA.", PRESENTED AT THE SYMP. ON ATMOS. DIFFUSION AND AIR POLL., SANTA BARBARA, CA, SEPT. 9-13, 1974, PP 133-141.

Table 4

Turbidity Estimation

| Description of Transparency of the Atmosphere | Turbidity Coefficient |
|---|---|
| Unusually blue sky; very transparent atmosphere; occurs in northern sites or Rocky Mountain regions; more likely in winter half of year; low humidity. | <0.02 |
| Blue sky, transparent atmosphere; more likely in northern states or Rocky Mountain region; more likely in winter half of year, low humidity.* | 0.05 |
| Ordinary unpolluted areas; northern U. S. or Rocky Mountains in summer; southern and coastal U. S. in winter, average humidity. | 0.10 |
| Ordinary urban areas with minimal pollution; slightly polluted or slight haze in non-urban locations. | 0.15 |
| Polluted or hazy conditions (not severe); visibility between about 2-10 miles. | 0.20 |

*Blue sky, transparent atmosphere, occurs with good visibility conditions (> 15 miles) in northern states and Rocky Mountain regions in all seasons and during winter season in southern U. S. A.

Table 5

Units and Conversions for Solar Radiation

| | |
|---|---|
| ENERGY | 1 Joule = $10^7$ ERG<br>= 1 W s (watt-second)<br>= $2.389 \times 10^{-4}$ Kcal (kilocalorie)<br>= $0.9480 \times 10^{-3}$ Btu (British thermal unit)<br>= $2.778 \times 10^{-7}$ kWh (kilowatt-hour) |
| RADIANT FLUX PER UNIT AREA | 1 W $m^{-2}$ = 0.3170 Btu $ft^{-2} hr^{-2}$<br>= 1141 Btu $ft^{-2}$ $min^{-1}$<br>= 1 Joule $m^{-2}$ $sec^{-1}$<br>= 2390 calories $cm^{-2}$ $sec^{-1}$<br>= $1.433 \times 10^5$ calories $cm^{-2}$ $min^{-1}$ |

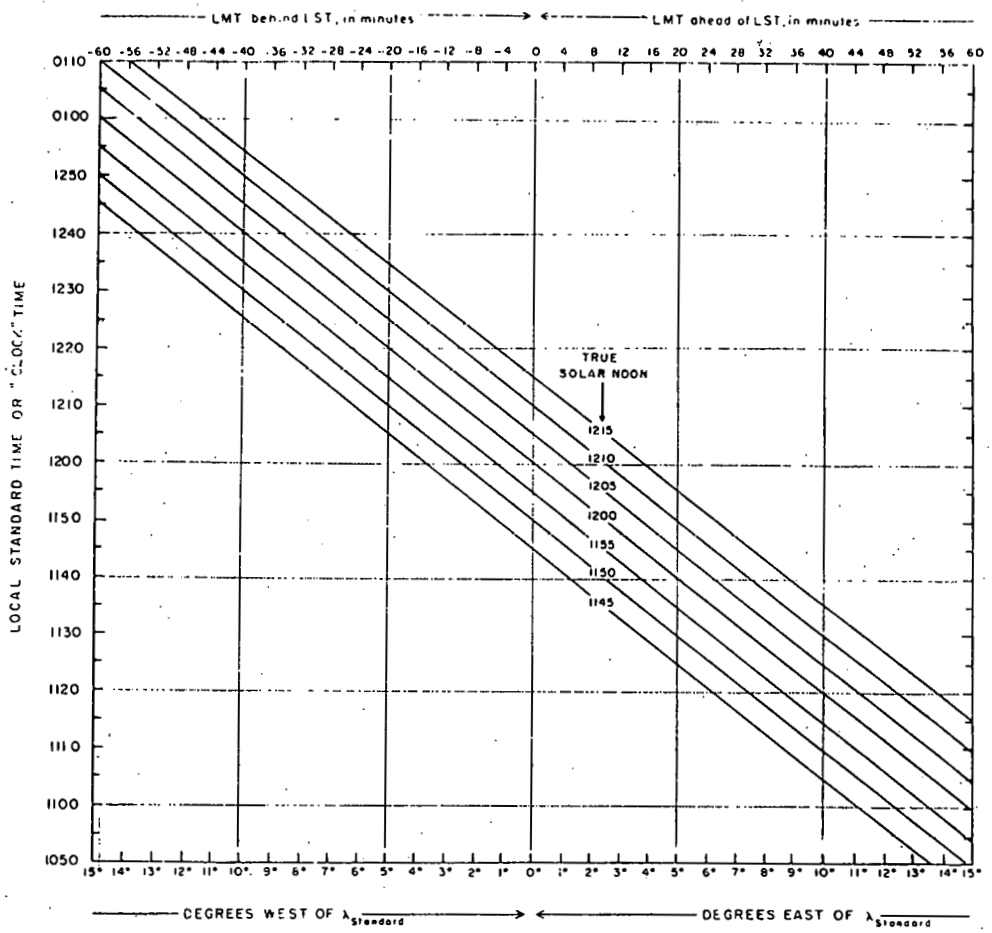


*Figure 1 Determination of Local Standard Time from True Solar Noon, TSN, and degrees of longitude east or west of standard latitude, $\lambda_{standard}$. For example, suppose a calculation is desired at the Greensboro, North Carolina, U. S. A. airport (79° 57' W) on March 28. The clock time is Eastern Standard Time and the standard meridian, $\lambda_{standard}$, is 75°W (Table 9). Greensboro is therefore almost 5° west of the standard meridian: 79° 57' - 75° = 4° 57'. On March 28, the TSN is 1205 from Table 2. Entering 1205 for True Solar Noon along the sloping lines and the longitudinal difference of just under 5° (west) as the horizontal axis. The corresponding Local Standard or "clock" Time is 1225. At 1225 local time at Greensboro airport the sun will be most direct overhead on March 28. Note that 5° difference is 20 minutes later at Greensboro than for a location on the 75th meridian (see top of figure and check: 1225 - 1205 = 20 min.). LMT stands for Local Mean Time, or the Local Standard Time at the 75th meridian. It takes 20 minutes for the sun to traverse the almost 5° of longitude between the 75th meridian and the approximately 80th meridian.*

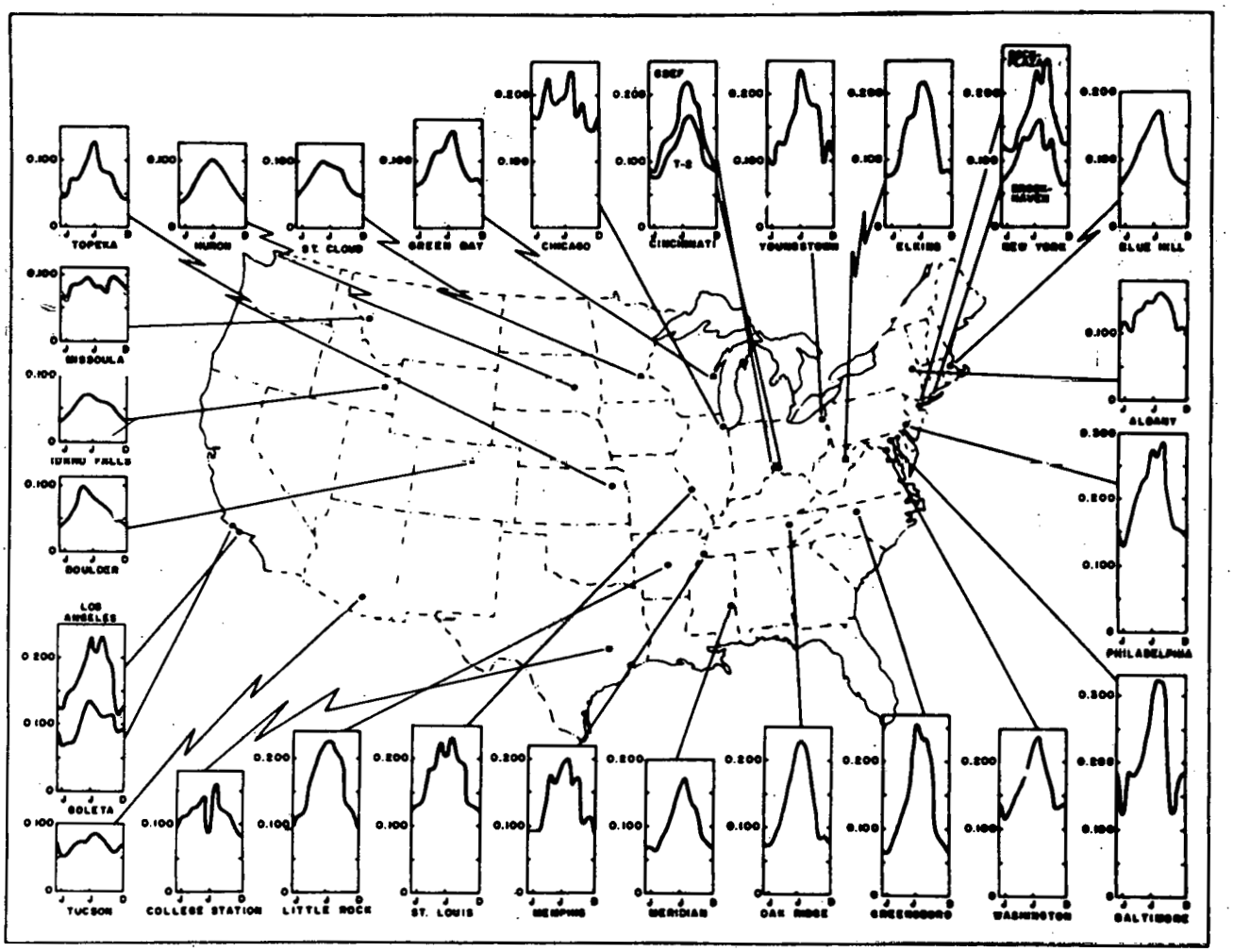


*Figure 2 Monthly average turbidity at network stations*

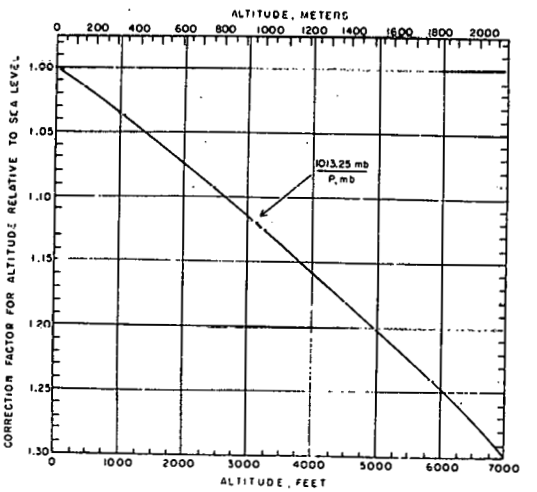


*Figure 3 Determination of pressure factor for altitude. For example, Greensboro, North Carolina airport is at an altitude of 273 m or 896 feet. The correction factor for altitude at Greensboro is 1.03.*

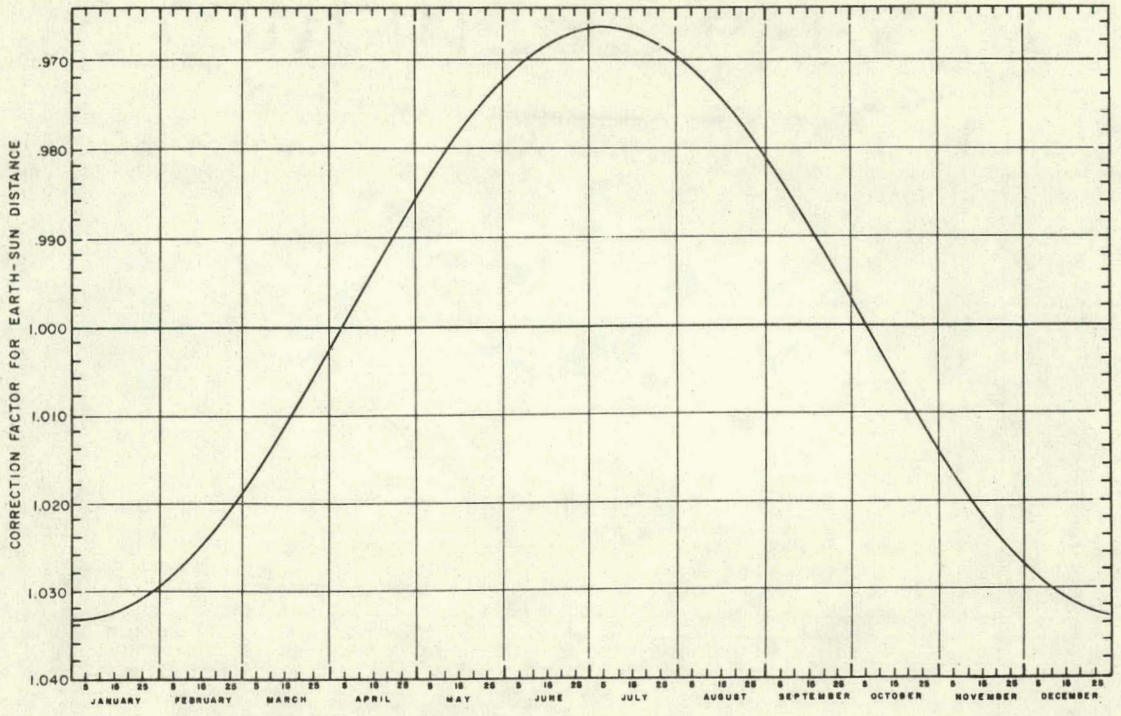


*Figure 4 Determination of the correction for earth-sun distance. For example, on March 28, the correction factor for the earth-sun distance is 1.005.*

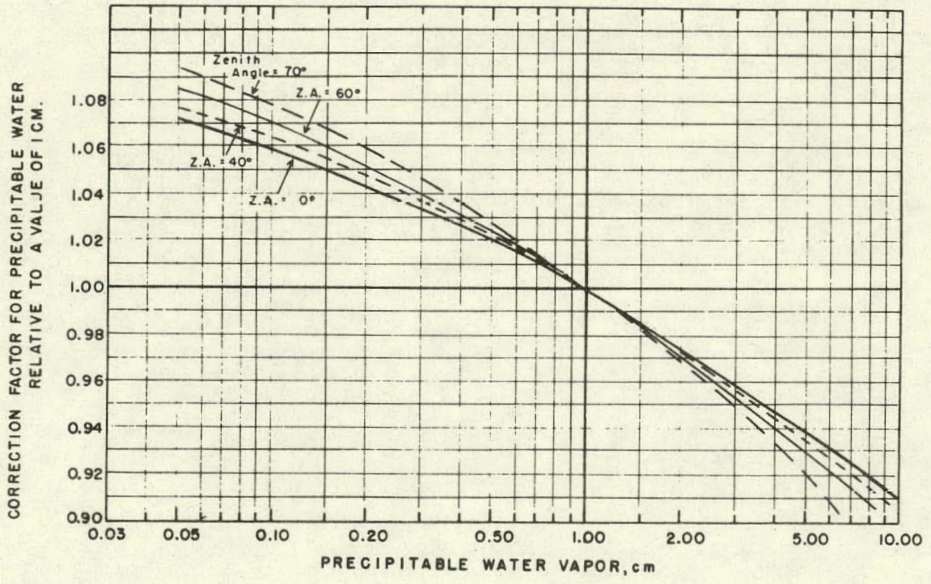


*Figure 5 Determination of correction factor for precipitable water. For example, if the precipitable water is 1.12 cm and the zenith angle 39°, then the correction factor for precipitable water is 0.98.*

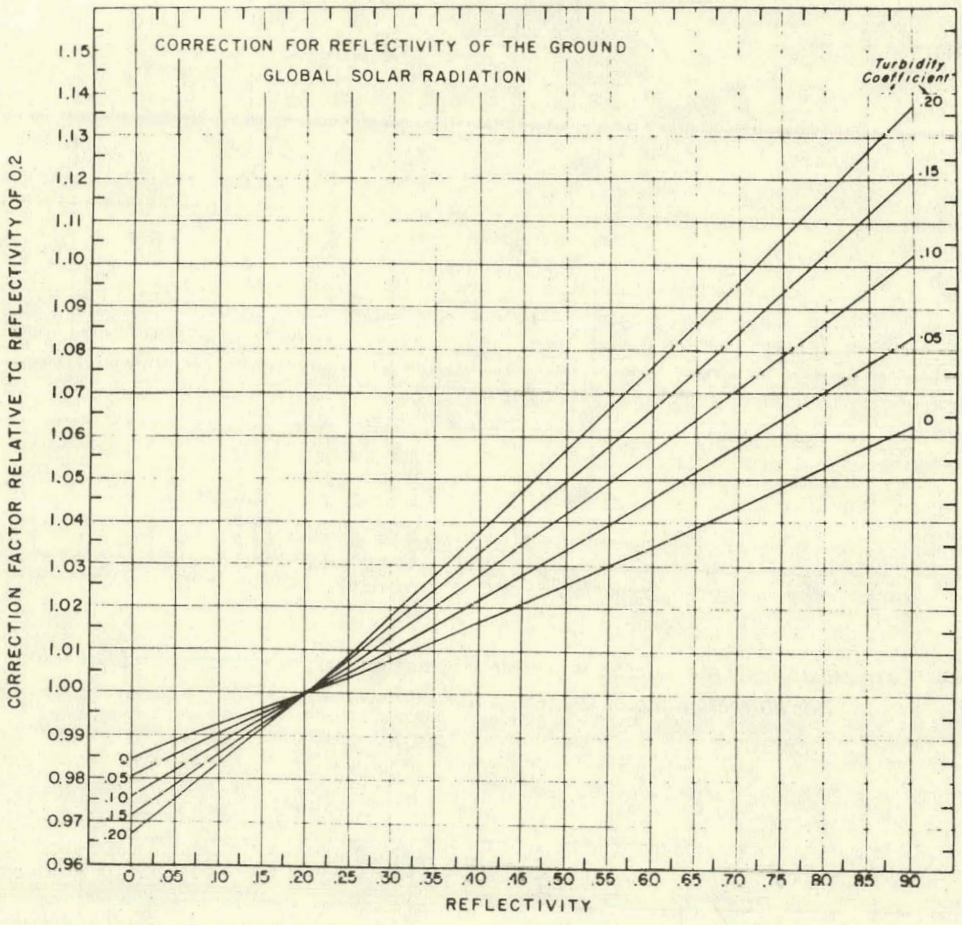


*Figure 6 Graph for determination of correction factor for ground reflectivity. For example, if the ground reflectivity is 0.3 and the turbidity coefficient 0.15, then the correction factor for reflectivity is 1.015.*

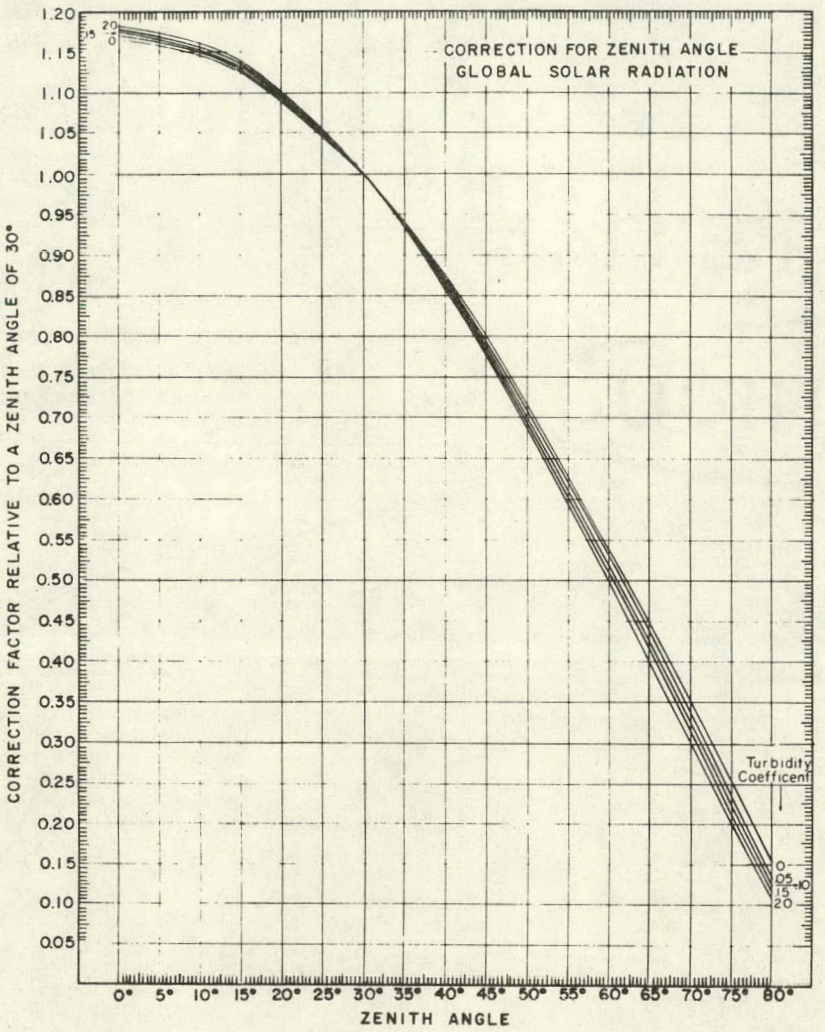


*Figure 7 Graph for determination of global radiation correction factor for zenith angle. For example, if the zenith angle is 39° and the turbidity coefficient 0.15, then the correction factor for zenith angle is 0.86.*

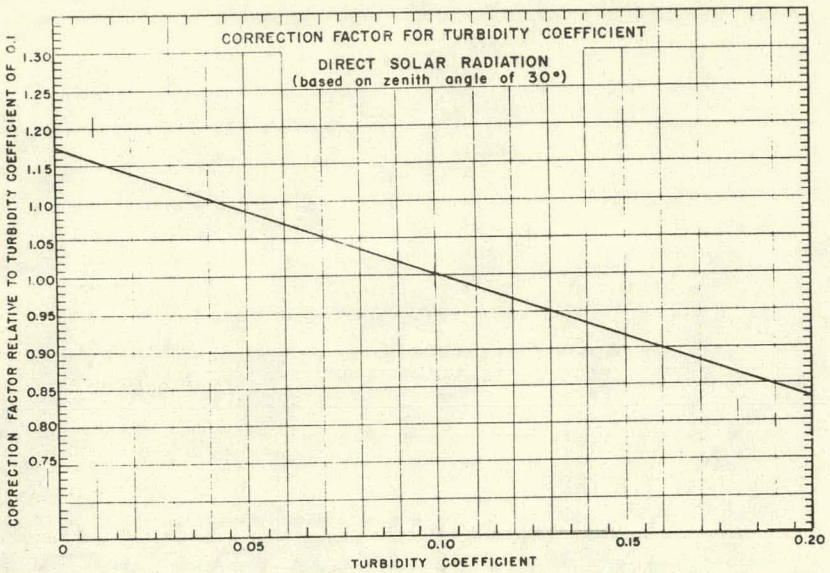


*Figure 8 Graph for determination of direct radiation correction factor for turbidity. For example, if the turbidity coefficent is 0.15 then the correction factor for turbidity is 0.92.*

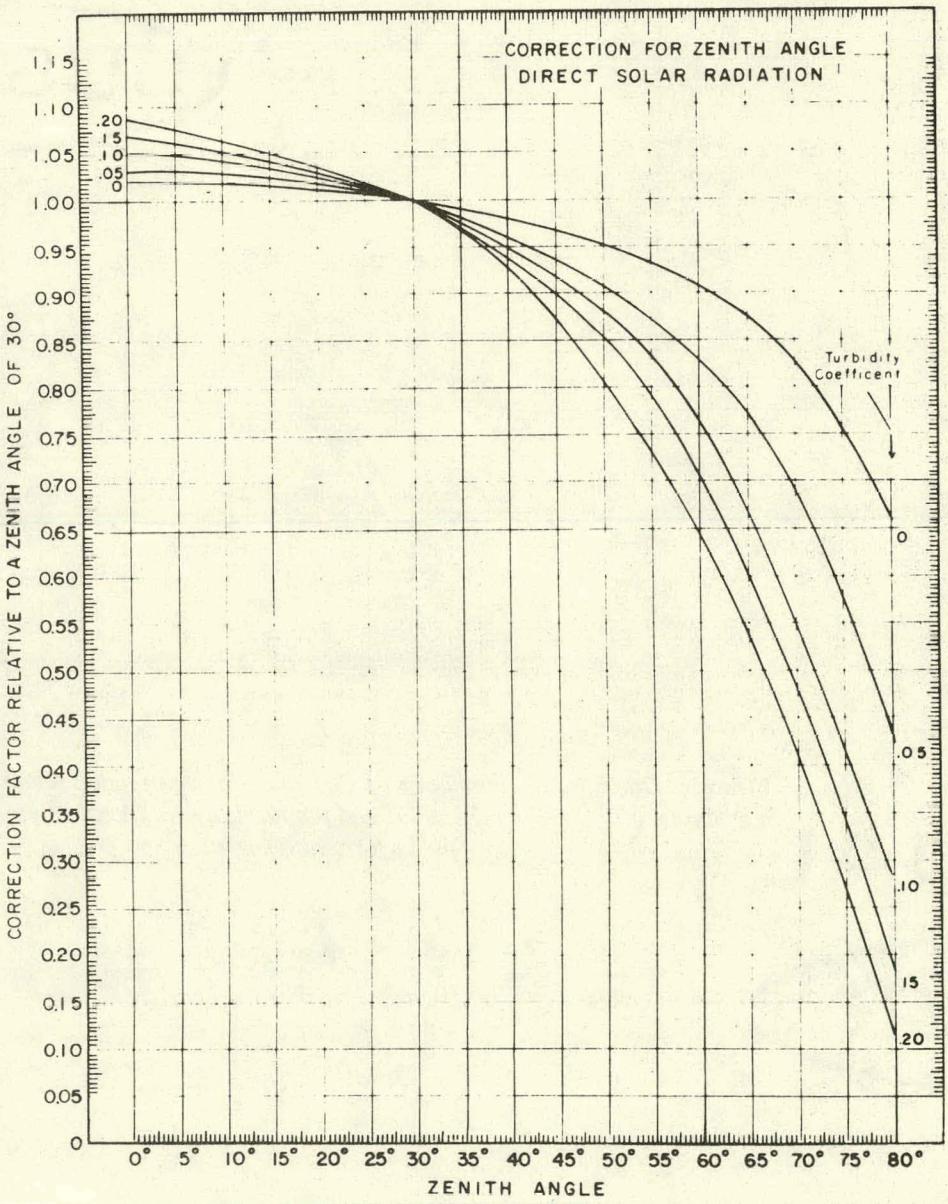


*Figure 9 Graph for determination of direct radiation correction factor for zenith angle. For example, if the zenith angle is 39° and the turbidity 0.15, then the correction factor for zenith angle is 0.94.*

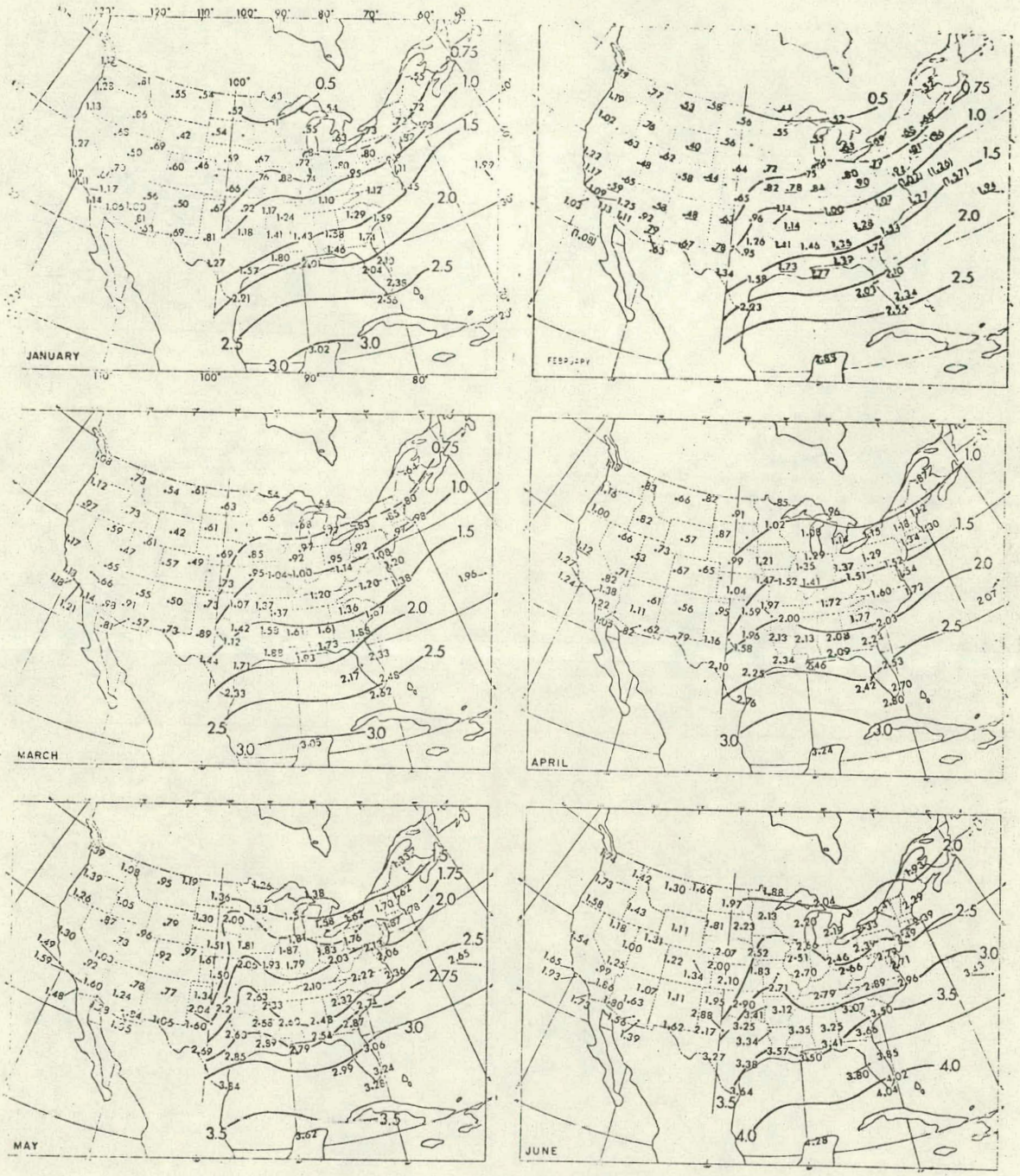


*Figure 10 Mean monthly precipitable water in the contiguous United States, surface to 500 mb, January – June (cm)*

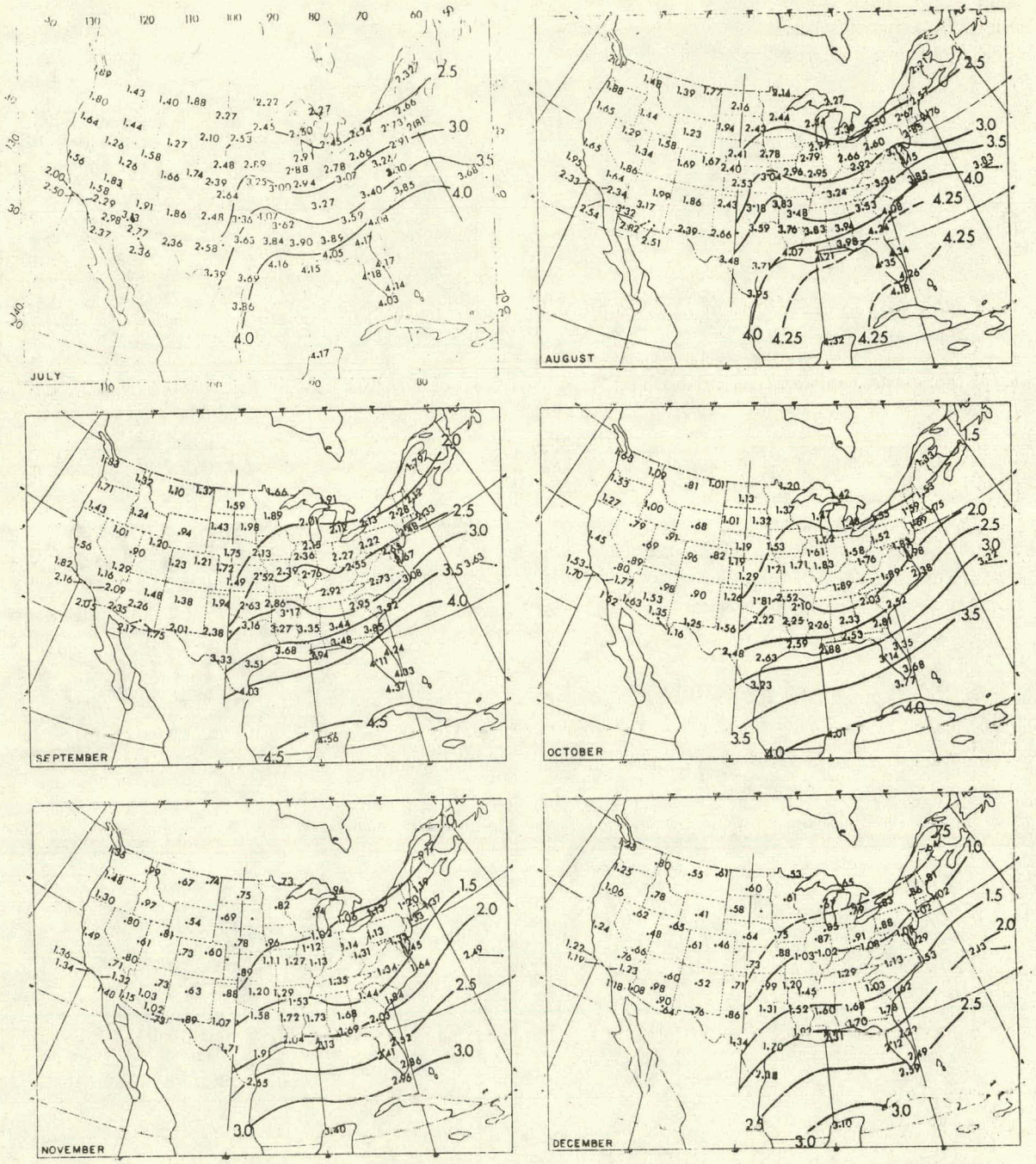


*Figure 10 (cont.) Mean monthly precipitable water in the contiguous United States, surface to 500 mb, July – December (cm)*
*(Lott, 1976)*

## APPENDIX II-A

## STANDARD VALUE OF DIRECT AND GLOBAL RADIATION

The standard values of solar radiation are arbitrarily taken from the following typical environmental conditions:

Table 6

Standard Environmental Values

| | |
|---|---|
| a. Zenith angle | cosine 30° = 0.866 |
| b. Turbidity coefficient | 0.10 |
| c. Precipitable water | 1.00 cm |
| d. Earth-sun distance | average annual |
| e. Altitude | sea level |
| f. Ground reflectivity | 0.20 |

Observations taken at Raleigh, North Carolina, (about 300 ft msl) near true solar noon on two clear days in April 1975 form the basis for the direct and global solar radiation. Table 7 lists the relevant quantities and some related values for each of the two days.

Table 7

Basis Data

| | 4/4/75 | 4/7/75 |
|---|---|---|
| Direct radiation, W $m^{-2}$ | 940 | 947 |
| Global radiation, W $m^{-2}$ | 935 | 931 |
| Zenith angle, degrees | 30.4 | 29.2 |
| Turbidity coefficient (measured) | 0.09 | 0.074 |
| Precipitable water, cm (measured) | 0.35 | 0.44 |
| Ground reflectivity (estimated) | 0.15 | 0.15 |
| Precipitable water to sea level (measured times 1.01) | 0.354 | 0.444 |

The precipitable water to sea level has been found from the measured precipitable water from the ground to the top of the atmosphere times the ratio of sea level pressure, 1013.25 millibars, to the pressure at station altitude. This ratio is given in Figure 3.

The derivation of the standard values of direct and global radiation follows.

### 1. Direct Solar Radiation

Table 8 lists the correction factors converting direct radiation from an as yet unknown standard value for environmental conditions in Table 6 to those in Table 7.

Table 8

Correction Factors for Direct Solar Radiation

| | 4/4/75 | 4/7/75 |
|---|---|---|
| a. Zenith angle (& turbidity) - Figure 9 | 1.00 | 1.00 |
| b. Turbidity - Figure 8 | 1.015 | 1.045 |
| c. Precipitable water - Figure 5 | 1.032 | 1.024 |
| d. Earth-sun - Figure 4 | 1.00 | 1.00 |
| e. Product of a through d | 1.048 | 1.070 |

If S is the standard value of direct solar radiation which should be associated with the observed solar radiation, then the altitude correction involves the following equations for each of the two days.

$$940 = 1.048S\left(1 + [1 - 0.99]\frac{1377 - 1.048S}{1377}\right) \qquad 4/4/75$$

$$947 = 1.070S\left(1 + [1 - 0.99]\frac{1377 - 1.070S}{1377}\right) \qquad 4/7/75$$

where the quantity 0.99 is the ratio of station pressure to sea level pressure (the reciprocal of the ordinate in Figure 3) and 1377 is the solar constant in W $m^{-2}$. Solution for S in each of the above leads to 894 W $m^{-2}$ for April 4, 1975 and 882 for April 7, 1975. The average value of 894 and 882 is 887 W $m^{-2}$ which is taken as the standard direct solar radiation. This average value produces an error on April 4 of 0.8% and on April 7 of 0.5%.

## 2. Global Solar Radiation

Table 9 lists the correction factors needed for the determination of the standard global radiation.

Table 9

Correction Factors for Global Solar Radiation

| | 4/4/75 | 4/7/75 |
|---|---|---|
| a. Zenith angle (& turbidity) - Figure 7 | .995 | 1.007 |
| b. Earth-sun - Figure 4 | 1.00 | 1.00 |
| c. Precipitable water - Figure 5 | 1.032 | 1.024 |
| d. Ground reflectivity (& turbidity) - Figure 6 | .992 | .993 |
| e. Product of a through d | 1.019 | 1.024 |

If Y is a standard value of the diffuse solar radiation which, when approximately added to the direct radiation, yields the global radiation then the formula to correct for altitude for each of the two days is as follows:

$$935 = (887(1 + [1 - 0.99]\frac{1377 - 887}{1377}).866 + Y)1.019 \qquad \text{April 4, 1975}$$

$$931 = (887(1 + [1 - 0.99]\frac{1377 - 887}{1377}).866 + Y)1.024 \qquad \text{April 7, 1975}$$

The solution of these equations leads to a diffuse radiation contribution of 146.7 W $m^{-2}$ on April 4 and 138.3 W $m^{-2}$ on April 7, 1975. The average of 146.7 and 138.3 is 142.5 W $m^{-2}$. The error introduced by using the average value of 142.5 W $m^{-2}$ for the diffuse radiation is about 1.1% on both days.

## 3. Summary

The standard value of direct solar radiation is 887 W $m^{-2}$. The standard value of diffuse solar radiation contributing to the global radiation is 142.5 W $m^{-2}$.

## APPENDIX II-B

## COMPUTATION OF THE SOLAR ZENITH ANGLE

**Prepared by P. Falconer**

### 1. General Solution

The zenith angle, $\Theta$, between the incident solar radiation and its projection with the local vertical depends upon the solar declination angle, $\delta$, the observer's latitude, $\lambda$, and the local hour angle, h. The general equation yielding the zenith angle is solved from spherical geometry considerations and is given by:

$$\cos\Theta = \sin\delta \sin\lambda + \cos\delta \cos\lambda \cos h$$

(all angles in degrees).

The solar declination angle, $\delta$, representing the angular inclination of the earth's equatorial plane to the solar radius vector, is slightly asymmetric, sinusoidal function of the day of the year. The values of $\delta$ are given in Table 2 under the heading Dec. (for declination). All entries prefixed with the letter "N" are understood to be positive; all entries prefixed with an "S" are negative.

The local hour angle is equivalent to the angle between the observer's longitude ($\lambda_{obs}$) and the longitude over which the sun is positioned. At true solar noon both are identical. Alternatively, because the earth is assumed to rotate through 360° during 24 hours, one can express the hour angle in terms of time differences as well. In particular, it may be shown that:

$$h(\text{deg}) = 15^\circ(\text{Local Mean Time} - \text{True Solar Noon}).$$

The Local Mean Time (LMT), not to be confused with Local Standard Time (LST, or "clock" time), is uniquely related to the longitude of the observer and is given as:

$$\text{LMT} = \text{LST} + 4^m(\lambda_{standard} - \lambda_{obs})$$

where $\lambda_{standard}$ is the 75th, 90th, 105th, etc. meridian. A simple table of the standard longitudes for each continental U. S. time zone is provided below.

Table 10

Time Zone Tabulation for the Contiguous United States with Standard Meridians to be Used for Calculation of Local Mean Times

| Time Zone of Observer | $\lambda_{standard}$ | $\lambda_{Daylight\ Savings\ Time}$ |
|---|---|---|
| Eastern | 75°W | 60°W |
| Central | 90°W | 75°W |
| Mountain | 105°W | 90°W |
| Pacific | 120°W | 105°W |

The Local Mean Time for observations at any time during the day may be found using this simple relationship and, in turn, the True Solar Noon value can be extracted from Table 2. Knowing the angle h, the formula for the zenith angle may be easily computed. An example of this method is now given for an observation made at 32.8°N, 80.1°W (near Charleston, South Carolina, U. S. A.) on 16 April at 0720 LST.

The $\lambda_{standard}$ is 75°W.

| | |
|---|---|
| 1. Local Standard Time | 07 h 20 min |
| 2. 4 min × ($\lambda_{standard} - \lambda_{obs}$) | − 20 min |
| 3. Local Mean Time | 07 h 0 min |
| 4. Local Mean Time − True Solar Time (From Table 1) | − 12 h 0 min |
| | 5 h 0 min |
| 5. 15° (Local Mean Time − True Solar Time) | = 75° (= h) |

By convention, negative angles refer to pre-noon observations and positive angles to post-noon observations. From Table 2 one substitutes the appropriate value of $\lambda$ (=32.8°N) into the zenith angle formula:

| | |
|---|---|
| 6. $\sin(32.8°N)\sin(10.0°)$ | 0.0950 |
| 7. $\cos(32.8°N)\cos(10.1°)(\cos(-75°))$ | 0.2142 |
| 8. $\cos\Theta$ | 0.3092 |
| 9. $\Theta$(zenith angle) | 71.99° |

**2. True Solar Noon Observations**

For the special case where true solar noon observations are required, the solution for the solar zenith angle is simplified because the cos h term becomes unity. Thus,

$$\cos\Theta = \sin\delta\sin\lambda + \cos\delta\cos\lambda$$

$$\cos\Theta = \cos(\lambda - \delta)$$

$$\Theta = \lambda - \delta$$

The solar zenith angle at true solar noon is the difference between the appropriate declination obtained from Table 2 and the observer's latitude. Furthermore, in order to assist the observer in determining the correct Local Standard Time at which true solar noon occurs, Figure 1 is provided and represents the relationship between local mean and local standard time for stations displaced from the standard meridian. One finds the true solar noon value (TSN in Table 2), enters this time as the slanting lines and using the appropriate longitude and reads off the corresponding Local Standard Time on the ordinate. An example of this computation follows:

Assume that an observation of solar radiation at 37.8°N, 100°W (near Dodge City, Kansas, U. S. A.) is required at True Solar Noon on 25 August. At what Local Standard Time must the observation be taken?

According to Table 2, on 25 August, $\delta$ = 10.8 and True Solar Noon arrives at 1202 LST at 90°W (the Standard Meridian for Central Time). Because our observation station is displaced 10° west of 90°W, the $\lambda_{standard}$ of the Central Time Zone, one enters Figure 1 at 10°W and proceed up this value until an intersection is made with the 1202 line. One then reads across the graph to the ordinate, 1242 LST, which is the "clock" time at Dodge City corresponding to true solar noon. Thus, at this time, the solar zenith angle as described in the first paragraph of this section becomes:

$$\Theta = (37.8° + 10.8°)$$

$$\Theta = 48.6°$$

For latitudes between 30N and 60N, it is not necessary to make an observation at precisely true solar noon if a tolerance of ±1° in $\Theta$ is allowed. It can be shown that, given any date from the spring equinox to the autumnal equinox, a leeway in time about true solar noon of approximately 30 minutes at the southern extreme up to 55-minutes at the northern extreme is permissible. Moreover, in the cool seasons between the equinoxes roughly ten additional minutes of leeway may be permitted.

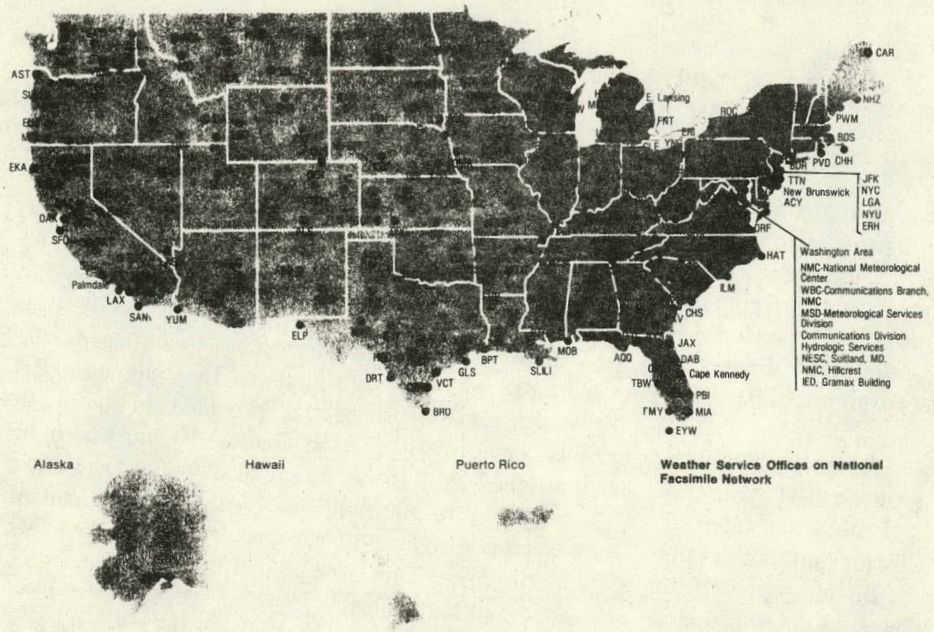


*Figure 11 Locations at which facsimile maps of precipitable water may be obtained twice a day.*

The value for precipitable water for the standard values of global and direct solar radiation is taken as 1 cm. Figure 5 provides corrections to the standard values of solar radiation when the amount of precipitable water differs from 1 cm. This figure has been prepared by Mr. P. Falconer based on a formula by Lacis and Hansen (1974).

$$R(m,w) = R_o\left(1 - \frac{2.9 \times m \times w}{(1 + 141.5 \times m \times w)^{0.635} + 5.925 \times m \times w}\right)$$

where R(m,w) is the solar radiation received at the ground for air mass m (air mass is the secant of the zenith angle), w is the precipitable water in cm, and $R_o$ is the extraterrestrial solar radiation, 1377 W $m^{-2}$.

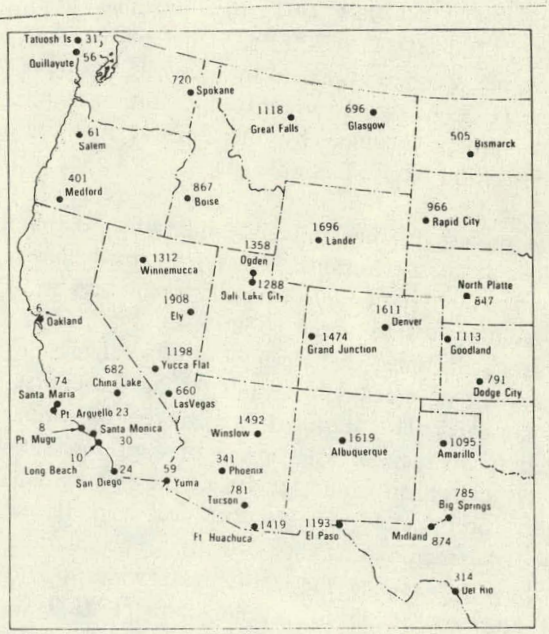


*Figure 12 Stations measuring precipitable water in the western United States. Station heights are given in meters.*

## APPENDIX II-C

## PRECIPITABLE WATER

Water vapor absorbs solar radiation thus reducing the amount of energy reaching the earth's surface. The term precipitable water or precipitable water vapor refers to the amount of water vapor in a vertical column in vapor form. In clear weather, precipitable water directly determines the extinction of solar radiation due to atmospheric water.

Precipitable water can be obtained in two ways: first, by measuring the energy received at the ground in those wavelengths at which the water vapor absorption occurs and, second, by integrating the water content in successive layers of the atmosphere from the ground to the top of the atmosphere as determined by balloon-borne hygrometers. There are too few stations using the spectral method to be useful. However, precipitable water by balloon-borne hygrometers is obtained at about 70 weather stations across the U. S. A. twice each day. The amounts of precipitable water from the observations taken at 0000 GMT (1900 EST the previous day) and at 1200 GMT (0700 EST) are plotted on weather maps and transmitted by facsimile throughout the U. S. A. (see Figure 11). In addition many airport stations manned by the Federal Aviation Administration receive facsimile charts.

The preferred value of precipitable water is that obtained from the National Weather Service balloon flights for the day of the solar radiation observation. Two points must be noted about these data. First, at infrequent times there can be a large change in the amount of precipitable water during the course of a day particularly during or immediately following a cold front passage. The advice of a professional meteorologist can indicate when these transient periods occur and perhaps advise on a preferred value of precipitable water to use. Second, the precipitable water is the amount of water up to 500 millibars or about 6 kilometers (18,000 ft) altitude msl. Small amounts of water vapor (about 15%) exist above these altitudes. Thus the precipitable water values up to 500 millibars supplied by the National Weather Service should be multiplied by 1.15 to obtain the water in the total column.

Interpolation can be made between stations reporting water east of about 100°W without difficulty. In the mountainous areas west of 100°W, please refer to the next to the last paragraph of this appendix.

If the precipitable water cannot be obtained from current weather information, the climatological average precipitable water is provided in Figure 10. The values derived from Figure 10 must also be multiplied by 1.15 since they also apply to the water content up to 500 millibars. Further, the amount of precipitable water on clear days is about 0.81 of that on all days. Thus, the climatological precipitable water values applicable to clear days in the total column should be multiplied by 0.93 (= 0.81 X 1.15).

The correction factors for nonstandard precipitable water are based on sea level conditions. A hypothetical additional layer of water is added to the existing column of water if the station lies above sea level. This addition is based on a simple pressure factor; that is, the extra water is proportional to the extra mass of air between station altitude and sea level.

Inspection of Figure 10 reveals no isolines of precipitable water west of the 100°W meridian. The reason for this omission is the strong dependence of the amounts of precipitable water on station elevation and the western regions of the U. S. A. is, of course, mountainous. Figure 12 shows the height of the observing stations at which the measurements of precipitable water are made. Thus, in addition to the general decrease of precipitable water northward and away from moisture sources in the Gulf of Mexico and the Pacific Ocean there is a dependence on station altitude. Thus, to estimate the precipitable water from Figure 10 interpolation between stations must take into account the altitude of both the point at which the precipitable water is desired and the locations on Figure 10 at which it is available.

## APPENDIX II-D

## TURBIDITY

Turbidity is the term describing the reduction in transparency of the atmosphere due to the presence of dust, smoke and haze. These nongaseous constituents of the atmosphere attenuate solar radiation. The direct beam is reduced more than the global radiation since the scattered solar energy due to particles in the atmosphere is primarily forward scattered which partially compensates for the loss in the direct solar beam.

Turbidity is often measured by the reduction in atmospheric transmission of solar radiation in certain portions of the solar spectrum. These spectral regions are selected so that typical particles will absorb and scatter their solar energy and contain little or no absorption by atmospheric gases. One such wavelength often used to measure turbidity is at 0.5 $\mu$m. The turbidity coefficient, is defined by the expression

$$R(m) = R(o)[10^{-B \text{ secant } \Theta}] - C$$

where R(m) is the direct solar radiation per unit area normal to the sun's rays at air mass, m, corresponding to zenith angle, $\Theta$, and R(O) is the solar radiation at the top of the atmosphere and C is the energy received by the sensor due to scattering by air molecules. A relatively simple instrument is used to measure the radiation of 0.5 $\mu$m and, hence, the turbidity coefficient, B, but the results of these observations are not normally available until many months later. Even the late numbers are from a limited number of places. Inexpensive sunphotometers costing as little as $100-200 are available. NOAA will lend these instruments to a user for short periods. As noted below, extrapolation or interpolation of the turbidity coefficient from place to place is not recommended. Thus, for the purpose of this workbook, the values of the turbidity coefficient, B, must be derived by other means.

If the station is not at sea level, an equivalent value of the turbidity coefficient should be derived accounting for the attenuation of the dust in the hypothetical layer between station altitude and sea level. The adjustment cannot be made rigorously since the nature of the hypothetical layer of air is unknown. For the purpose of this workbook the value of the turbidity coefficient should be multiplied by $p_s/p$, a quantity which can be found in Figure 3.

Table 4 provides estimates of B for various descriptions of atmospheric clarity. It is recommended that solar radiation instrument calibration be performed on days with as low a turbidity coefficient as possible; values of B greater than 0.2 should be avoided. Indeed, the figure providing corrections to a standard turbidity coefficient cuts off at 0.2.

Figure 2 provides climatological values of turbidity as derived from the actual measurements noted above. Unfortunately, there can be sharp variations in turbidity due in most part to variations in local pollution conditions. Thus, interpolation between the locations of Figure 2 or even using the value from Figure 2 for another part of the same city must be undertaken with caution. The figure does illustrate the seasonal variation in turbidity (greater in summer than winter), the effects of pollution, and the higher turbidity in humid locations. Climatological values in excess of 0.2 are common in many areas of the country in summer; however, days may be selected even in summer when the turbidity coefficient is below 0.2.

Fortunately as long as the turbidity coefficient does not exceed 0.2, the error in predicting global solar radiation due to an incorrect choice of the correct turbidity coefficient should be less than a few percent. The errors in the estimation of direct radiation due to uncertainties in the turbidity coefficient can be much larger.

**References**


Braslau, N. and Dave, J. V. 1972. "Effects of Aerosols on the Transfer of Solar Energy Through Realistic Model Atmospheres, Part 1: Non-absorbing Aerosols". RC-4114. "Part 2: Partly Absorbing". RC-4152. IBM Research.

Doan, L. R. and Sandford, B. P. 1970. "Solar Elevation, Depression and Azimuth Graphs." *Environmental Research Paper No. 313, Air Force Cambridge Research Laboratories.* Publ. No. AFCRL-7-0086, 291 pp.

Lacis, A. A. and Hansen, J. E. 1974. *Journal of Atmospheric Science*. Vol. 31, pp. 118-133.

Lott, G. A. 1976. "Precipitable Water Over the United States." Vol. 1: *Monthly Means, NOAA Technical Report, NWS 20.*

Volz, F. E. 1978. "Atmospheric Turbidity in Europe, 1963-1969." *U. S. Air Force Geophysics Environmental Laboratory Research Paper No. 631.* AFGL-TR-78-0108, April, 1978.